ROLE OF S6K1 IN REGULATING SELF-RENEWAL OF HEMATOPOIETIC STEM CELLS AND PROPAGATION OF LEUKEMIA

Joydeep Ghosh

Submitted to the faculty of the University Graduate School
in partial fulfillment of the requirements
for the degree
Doctor of Philosophy
in the Department of Microbiology and Immunology,
Indiana University

April 2016

Accepted by the Graduate Faculty, Indiana University, in partial fulfillment of the requirements for the degree of Doctor of Philosophy.

Reuben Kapur, Ph.D., Chairman

Doctoral Committee

Nadia Carlesso, MD, Ph.D.

Louis M. Pelus, Ph.D.

December 15, 2015

Edward F. Srour, Ph.D.

Acknowledgements

I would first like to thank my mentor, Dr. Reuben Kapur, for his guidance and support. His constant demand of excellence has helped me immensely to develop my knowledge about hematopoiesis. I would like to thank my committee members, Dr. Louis M. Pelus, Dr. Edward F. Srour and Dr. Nadia Carlesso for their continuous guidance, support and advice. Without the help of my committee members, my project would not have been as successful as it ended being towards the end. Their expert guidance helped me immensely to develop my project as well as advance my knowledge about the field. I would also like to thank Dr. Louis M. Pelus for his continuous support as the Graduate Student Advisor for the Department of Microbiology & Immunology. I would also like to thank Dr. Margaret Bauer for her feedback in the departmental seminars as well as her continuous support as the Graduate Student Advisor for the Department of Microbiology & Immunology. I would also like to thank Dr. Rebecca J. Chan and Dr. Yan Liu for their continuous advice and necessary reagents for experiments.

I would like to thank past and present members of Kapur laboratory, Dr. Peilin Ma, Dr. Ruchi Pandey, Dr. Baskar Ramdas, and Dr. Holly Martin for their help and support. A very special thanks goes to Dr. Michihiro Kobayashi who has been a great collaborator. I would also like to thank Marilyn Wales for her continuous support and patience.

A special thanks to Dr. Anindya Chatterjee who has been a great collaborator, friend and mentor. His experimental advice, thought-provoking questions and ideas have been key in developing my scientific ability.

I would like to thank Dr. Anirban Basu, Dr. Kallol Dutta and Dr. Soumya Ghosh for their advice and support in my research career. I would also like to thank a long-time friend Samriddhi Chatterjee for her continuous encouragement and support.

Finally, I would like to thank my parents for their love and support during my entire career. Their sacrifice and encouragement has been key to my growth as a person and as a student.

Joydeep Ghosh

ROLE OF S6K1 IN REGULATING SELF-RENEWAL OF HEMATOPOIETIC STEM CELLS AND PROPAGATION OF LEUKEMIA

The development and function of hematopoietic stem cells (HSCs) is regulated by numerous signaling pathways including Akt-mechanistic target of rapamycin complex1 (mTORC1) pathway. Dysregulation of this pathway results in impaired HSC function and contributes to the development of hematologic malignancies. Activated mTORC1 phosphorylates and subsequently activates ribosomal protein S6 kinase 1 (S6K1). To study the role of S6K1 in hematopoiesis as well as leukemogenesis, we used a genetic model of S6K1 deficient mice (*S6K1-/-*). We found that loss of S6K1 expression in HSCs results in reduction of absolute HSC number in bone marrow (BM). Following chemotherapy, cycling HSCs undergo apoptosis and quiescent HSCs are required to cycle to regenerate the hematopoietic system. S6K1 regulates the quiescence of HSCs and in the absence of S6K1, mice are more susceptible to repeated myeloablative stress. We also observed that loss of expression as well as gain of expression of S6K1 affects the self-renewal ability of HSCs. Interestingly, when we overexpressed S6K1, it also resulted in reduced self-renewal of HSCs. Next, we assessed the role of S6K1 in the propagation of acute myeloid leukemia (AML). The mixed-lineage leukemia *(MLL*) gene is required for the maintenance of adult HSCs. Translocations in *MLL* are detected in approximately 5-10% of adult acute leukemia patients and in approximately 70% of acute leukemias in infants. We

expressed MLL-AF9 fusion oncoprotein in WT and *S6K1-/-* hematopoietic stem and progenitor cells (HSC/Ps) and performed serial transplantation. Upon secondary transplantation, recipients of S6K1 deficient AML cells survived significantly longer compared to controls. *In vitro*, pharmacological inhibition of S6K1 activity resulted in reduced growth of primary human cells expressing MLL-AF9. Both human and murine HSC/Ps expressing MLL-AF9 showed reduced mTORC1 activity upon inhibition of S6K1 suggesting that loss of S6K1 activity results in reduced Akt-mTORC1 activation both upstream and downstream of mTORC1. Overall, our studies establish a critical role of S6K1 activity in the maintenance of HSC function and in the propagation of leukemia.

Reuben Kapur, Ph.D., Chairman

Table of Contents

List of Tables

List of Figures

Chapter 1

Chapter 3

Chapter 4

Chapter 6

Chapter 7

List of Abbreviations

4E-BP1	4E (eIF4E)-binding protein 1
5-FU	5-Fluorouracil
AID	Autoinhibitory domain
AGC	cAMP-dependent protein kinases A, cGMP-dependent protein kinases G, and phospholipid-dependent protein kinases C
ALL	Acute lymphoblastic leukemia
AML	Acute myeloid leukemia
ANOVA	Analysis of variance
APC	Allophycocyanin
APC-Cy7	Allophycocyanin cyanine7
Ara-C	Cytosine arabinoside
BFU-E	Burst forming unit-erythrocyte
BM	Bone marrow
BSA	Bovine serum albumin
BrdU	5′-bromo-2′-deoxyuridine
BV421	Brilliant Violet 421
BV450	Brilliant Violet 450
CAFC	Cobblestone-area forming cell
CDKI	Cyclin-dependent kinase inhibitors
CFC	Colony forming cell

CFU-E	Colony-forming unit-erythrocyte
CFU-GEMM	Colony-forming unit-granulocyte erythroid macrophage megakaryocyte
CFU-MEG	Colony-forming unit-megakaryocyte
CFU-S	Colony-forming unit-spleen
cGy	Centigray
CLP	Common lymphoid progenitors
CML	Chronic myelogenous leukemia
CMP	Common myeloid progenitors
COMPASS	Complex of proteins associated with SET1
CRA	Competitive repopulation assay
DiD	1,1'-dioctadecyl-3,3,3',3'-tetramethylindodicarbocyanine
DNA	Deoxyribonucleic acid
ER	Endoplasmic reticulum
FACS	Fluorescence activated cell sorter
FFA	Free fatty acid
FITC	Fluorescein isothiocyanate
FLT3	*fms*-related tyrosine kinase-3
Gfi1	Growth factor independence 1
GAP	GTPase-activating protein
GFP	Green fluorescent protein
GMP	Granulocyte-monocyte progenitors
HPC	Hematopoietic progenitor cells

HSC	Hematopoietic stem cells
IFN	Interferon
IGF	Insulin-like growth factor
IMDM	Iscove's modified Dulbecco's medium
Itpk	Inositol-trisphosphate 3-kinases
LIC	Leukemia initiating cells
LSK	$Lin^{-}c\text{-}Kit^{+}Sca1^{+}$
LT-HSC	Long-term hematopoietic cells
LTC-IC	Long-term culture-initiating cells
MAPK	Mitogen-activated protein kinase
MEF	Mouse embryonic fibroblasts
MEP	Megakaryocte-erythrocyte progenitors
MLL	Mixed lineage leukemia
MNC	Mononuclear cells
MPP	Multipotent progenitors
mTORC	Mechanistic target of rapamycin
PBS	Phosphate-buffered saline
PDK1	3-phosphoinositide-dependent protein kinase 1
PDK2	Pyruvate dehydrogenase kinase isozyme 2
PDK4	Pyruvate dehydrogenase kinase isozyme 4
PE-Cy7	Phycoerythrin cyanine7
PerCP-Cy5.5	Peridinin chlorophyll protein complex-cyanine5.5
PGC1	Peroxisome proliferator-activated receptor-γ coactivator

PI3K	Phosphoinositide 3-kinase
PIP2	Phosphatidylinositol (4,5)-biphosphate
PIP3	Phosphatidylinositol (3,4,5)-triphosphate
PTEN	Phosphatase and tensin homologue
RBC	Red blood cells
Rheb	Ras homolog enriched in brain
ROS	Reactive oxygen species
S6K1	Ribosomal protein S6 kinase 1
SCF	Stem cell factor
SCID	Severe combined immunodeficiency
SD	Standard deviation
SDS-PAGE	Sodium dodecyl sulfate polyacrylamide gel electrophoresis
SEM	Standard error of the mean
SLAM	Signaling lymphocyte activation molecule
SP	Side population
ST-HSC	Short-term hematopoietic stem cells
TBI	Total body irradiation
TGF	Transforming growth factor
TIMP	Tissue inhibitor of metalloproteinase
TSC	Tuberous sclerosis complex
UCB	Umbilical cord blood
WBC	White blood cells
WT	Wild type

Chapter 1: Introduction

The production of blood cells is a continuous process and is maintained throughout one's lifetime. It has been estimated that a man weighing 70 kgs may produce 1 trillion blood cells every single day, which include 200 billion red blood cells (RBC) and 70 billion neutrophilic leukocytes (Dancey et al., 1976; Ogawa, 1993). This continuous production of blood cells has been termed hematopoiesis, which derives from the Greek words *haima* (blood) and *poiein* (to make). The hematopoietic system has been considered the model paradigm to study the properties and functions of stem cells as well as understanding their contribution to diseases. The hematopoietic system is composed of a vast network of cells that are part of a definitive functional hierarchy. The hematopoietic cells contribute to different physiological processes as well as protect our body by mounting immune responses against different pathogens. To maintain hematopoiesis throughout lifetime, the hematopoietic stem cells (HSC) have to undergo self-renewal, differentiation and proliferation. These processes are regulated by a host of signaling networks and deregulation of these networks results in hematologic malignancies including acute myeloid leukemia (AML). Among different cellular signaling pathways, mechanistic target of rapamycin complex 1 (mTORC1) pathway has been identified as a critical regulator of HSC development and function. The focus of this chapter is to give a brief overview of development and function HSCs as well as to define the components of the mTORC1 pathway.

Hematopoietic stem cells:

In the early 20th century, the diversity in morphology of different hematopoietic cells at different states of differentiation was described. To account for this diversity, Maximow hypothesized that hematopoiesis is organized as a cellular hierarchy that originates from a common precursor, a hematopoietic stem cell (HSC) (Maximow, 1902). Later, the existence of HSCs was further established when transplantation of cells derived from bone marrow (BM) or spleen from non-irradiated donors rescued hematopoietic system of irradiated recipients (Jacobson et al., 1950a; Jacobson et al., 1950b; Lorenz et al., 1951). Studies by Till and McCulloch demonstrated that the regenerative potential of HSCs can be assayed using in vivo repopulation assays (Becker et al., 1963; Till and McCulloch, 1961). These studies revealed the existence of single clonogenic cells within the hematopoietic system. BM hematopoietic cells, upon transplantation, could create macroscopic colonies in spleens of lethally irradiated recipients in proportion to the number of cells transplanted (Becker et al., 1963; Siminovitch et al., 1963; Till and McCulloch, 1961; Wu et al., 1968). These data led to the hypothesis that the colony forming units-spleen (CFU-S) were derived from a single hematopoietic cell. These findings were followed by development of clonal *in vitro* assays, which along with immunophenotypic characterization of cell surface markers of different hematopoietic populations have resulted in establishment of a defined hematopoietic hierarchy. Multipotent HSCs are at the top of this hierarchy while terminally differentiated cells are at the bottom. The studies by Till and McCulloch also demonstrated the importance

of mouse as a model system to study hematopoiesis. Since then, assays based on mouse models have been indispensable to study both steady-state hematopoiesis as well as malignant hematopoiesis. Genetic approaches using mouse models involving loss or gain of gene functions in HSCs and hematopoietic progenitor cells (HPCs) have helped to identify genes involved in regulating the development and functions of HSCs (Rossi et al., 2012).

Immunophenotypic characterization of HPCs and HSCs:

HSCs and HPCs can be identified based on the presence or absence of certain markers on the cell surface of mouse BM hematopoietic cells. Initially, BM hematopoietic cells with long-term repopulating ability were identified by the absence of markers specific for mature lineage cells (Lin^-), low expression level of Thy1.1 and expression of stem cell antigen-1 (Sca1) on the cell surface. The lineage markers that were accounted for were B220 (B cells), Gr1 (granulocytes), Mac1 (myelomonocytic cells), CD4 and CD8 (T cells) (Spangrude et al., 1988). Transplantation of 40 $Thy1^{lo}Lin^-Sca1^+$ cells was sufficient to obtain donor-derived engraftment in irradiated hosts. Moreover, the donor cells were able to differentiate into myeloid and lymphoid cells in recipient hosts (Spangrude et al., 1988). Next, c-Kit was identified as another marker to identify HSCs. Okada et al. rescued hematopoiesis in lethally irradiated mice by transplanting $Lin^-Sca1^+c\text{-}Kit^+$ (LSK) cells (Okada et al., 1992). Later, Osawa et al. demonstrated that a single LSK cell expressing low or no CD34 ($CD34^{lo/-}$) can reconstitute the hematopoietic system of 21% of recipients (Osawa et al., 1996). Another cell surface marker that has been used to identify HSCs is fms-related tyrosine kinase-3 (Flt3).

Upregulation of Flt3 expression in HSCs was associated with reduced self-renewal ability (Adolfsson et al., 2001). Based on CD34 and Flt3 expression level and repopulating ability, $CD34^{-}Flt3^{-}$LSK cells were defined as long-term HSCs (LT-HSC) whereas short-term HSCs (ST-HSC) were $CD34^{+}Flt3^{-}$LSK cells and multi-potent progenitors (MPP) were $CD34^{+}Flt3^{+}$LSK cells (Yang et al., 2005).

Signaling lymphocyte activation molecule (SLAM) family of receptors, CD150, CD48 and CD244, along with LSK markers (SLAM-LSK) are another set of markers that have been used to identify HSCs. Initially, based on SLAM markers, HSCs and HPCs have been subdivided into three distinct populations: $CD150^{+}CD244^{-}CD48^{-}$ (HSC), $CD244^{+}CD150^{-}CD48^{-}$ (MPP) and most restricted progenitors $CD48^{+}CD244^{+}CD150^{-}$ (Kiel et al., 2005; Yilmaz et al., 2006a). Based on the expression level of CD229, the SLAM-LSK cells were further subdivided into the following populations: $CD150^{+}CD48^{-/low}CD229^{-/low}CD244^{-}$LSK (HSC-1), $CD150^{+}CD48^{-/low}CD229^{+}CD244^{-}$LSK (HSC-2), $CD150^{-}CD48^{-/low}CD229^{-/low}$ $CD244^{-}$LSK (MPP-1), $CD150^{-}CD48^{-/low}CD229^{+}CD244^{-}$LSK (MPP-2), $CD150^{-}$ $CD48^{-/low}CD229^{+}CD244^{+}$LSK (MPP-3), $CD150^{-}CD48^{+}$LSK (HPC-1), and $CD150^{+}CD48^{+}$LSK (HPC-2) (Oguro et al., 2013). When HSC-1 and HSC-2 populations were transplanted into lethally irradiated mice, HSC-1 cells showed increased long-term repopulating activity suggesting that HSC-1 cells have maximum HSC activity (Oguro et al., 2013).

Downstream of HSCs, the lineage restricted progenitor cells lack self-renewal ability. The lineage restricted progenitors can be subdivided into following populations: common myeloid progenitor (CMP), granulocyte-monocyte

progenitor (GMP), megakaryocyte-erythrocyte progenitor (MEP), and common lymphoid progenitors (CLP) (Akashi et al., 2000) (Figure 1). Akashi et al. have demonstrated that there are three important critical decision points in hematopoietic hierarchy: (i) LT-HSCs lose their self-renewal ability and undergo transition to ST-HSC, (ii) HSCs differentiate to either myeloid lineage (by generating CMP) or lymphoid lineage (by generating CLP), and (iii) the decision of CMPs to differentiate into either the granulocyte/macrophage lineage (by generating GMPs) or the megakaryocyte/erythrocyte lineage (by generating MEPs) (Akashi et al., 2000). From their model and other studies, it has been established that HSCs differentiate into MPPs, which do not possess self-renewal potential, but can differentiate into oligopotent progenitors, namely CLP and CMP (Akashi et al., 2000; Nakorn et al., 2003; Pronk et al., 2007). CMPs give rise to GMP and MEPs that in turn differentiate into lineage committed myeloid effector cells, whereas CLPs generate lymphoid cells.

Although the hematopoietic hierarchy in mouse has been well defined, recent studies have revealed the existence of HSCs with lineage bias. Following transplantation, HSCs display skewed myeloid to lymphoid ratios that has given rise to the hypothesis that HSCs have a bias to commit to a particular lineage (Muller-Sieburg et al., 2004). Myeloid biased HSCs are able to self-renew following serial transplantation. However, their differentiation into lymphoid cells is diminished (Muller-Sieburg et al., 2004). Challen et al., on the basis of CD150 and Hoechst dye efflux based side population (SP) cells, showed that there is a bias amongst HSCs to differentiate into distinct lineages (Challen et al., 2010).

Figure 1

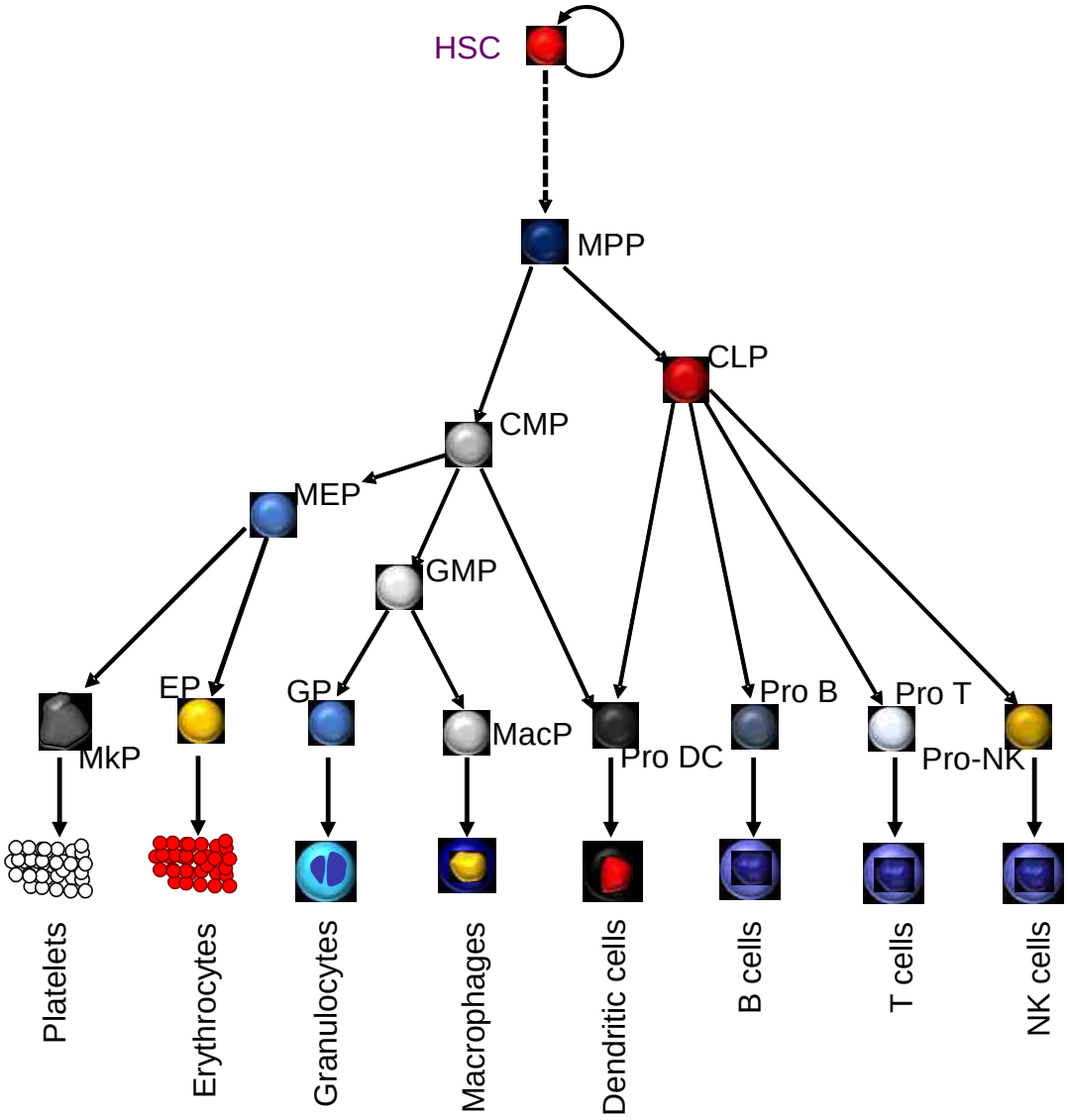
HSC
MPP
CLP
CMP
MEP
GMP
MkP
EP
GP
MacP
Pro DC
Pro B
Pro T
Pro-NK
Platelets
Erythrocytes
Granulocytes
Macrophages
Dendritic cells
B cells
T cells
NK cells

Figure 1: Hierarchy of the hematopoietic system.

Based on current knowledge and understanding of the hematopoietic system, a simplistic model of hematopoietic hierarchy has been shown. Hematopoietic stem cells (HSCs) are on top of the hierarchy and can self-renew as well as differentiate into multipotent progenitors (MPPs). MPPs have limited self-renewal potential and can differentiate into myeloid or lymphoid progenitors (common myeloid progenitors, CMP; and common lymphoid progenitors, CLP). The progenitor cells can further differentiate into oligopotent and lineage-restricted progenitors. The lineage-restricted progenitors finally differentiate into terminally differentiated mature blood cells. MEP, megakaryocyte-erythroid progenitor; GMP, granulocyte macrophage progenitor; MkP, megakaryocyte progenitor; EP, erythroid progenitor; GP, granulocyte progenitor; MacP, macrophage progenitor; Pro DC, dendritic cell progenitor; Pro NK, natural killer cell progenitor.

$CD150^+$ lower SP LSK cells have the highest self-renewal potential as well as bias to differentiate into myeloid lineage (Challen et al., 2010). However, these cells also have diminished proliferative capacity and lymphoid bias (Challen et al., 2010). On the other hand, $CD150^-$ SP LSK cells have maximum proliferative potential as well as lymphoid bias, but diminished self-renewal and myeloid bias (Challen et al., 2010). This study suggests that even among phenotypically defined HSC population, a functional diversity exists that skews the differentiation of HSCs towards a particular lineage.

In humans, the first marker that was used to identify HSCs was CD34 (Civin et al., 1984). By using anti-My-10 mouse monoclonal antibody, they have shown that My-10 (CD34) is specifically expressed on immature normal human marrow cells as well as on hematopoietic progenitor cells (Civin et al., 1984). CD34 is expressed on 0.5-5% of hematopoietic cells in fetal liver, cord blood and bone marrow (Civin et al., 1984; DiGiusto et al., 1994; Krause et al., 1996). Although CD34+ cells demonstrate multi-potency or oligo-potency, they are very heterogeneous in nature. Next, CD90 was identified as a marker for human HSCs. Human BM cells that are negative for T cell, B cell, natural killer (NK) cell, and myeloerythroid cell specific markers (Lin-) and positive for CD34 and CD90 ($Lin^-CD34^+CD90^+$) have been shown to generate both myeloid and lymphoid cells when transplanted into SCID mice, whereas $Lin^-CD34^+CD90^-$ cells fail to do so (Baum et al., 1992). HSCs have been further enriched based on differential expression of CD38 (Baum et al., 1992; Hao et al., 1996; Petzer et al., 1996). $CD34^+CD38^-$HSCs, and not $CD34^+CD38^+$ HSCs, are highly enriched with cells

capable of initiating long-term culture *in vitro* and repopulating transplanted recipients *in vivo*. Furthermore, most of the $Lin^-CD34^+CD90^+$ cells reside within the $CD38^-$ fraction (Uchida et al., 1998). This has led to the suggestion that in humans, $Lin^-CD34^+CD38^-CD90^+$ cells are highly enriched in HSCs. More recently, Notta et al. have demonstrated that a single $Lin^-CD34^+CD38^-CD45RA^-CD90^+Rho^{lo}CD49f^+$ cell is able to engraft in NSG mice and can self-renew upon serial transplantation (Notta et al., 2011).

Role of quiescence in maintenance of HSCs:

A key property of HSCs is their relatively low cell cycle rate, which in turn results in increased quiescence. Both in humans and in mice, HSCs mostly reside either in G0 or G1 phase of the cell cycle. Quiescence of HSCs is a protective mechanism that prevents their exhaustion. P21, a cyclin-dependent kinase inhibitor (CDKI), has been identified as a key regulator of quiescence of HSCs. P21 inhibits cyclin E-CDK2 activity and deficiency of p21 in HSCs results in reduced number of HSCs in G0 stage (Cheng et al., 2000). P21 deficient HSCs exhaust rapidly following serial transplantation and they are more susceptible to repeated myeloablaive stress (Cheng et al., 2000). Growth factor independent 1 (Gfi1) is a transcription factor that has been identified as a positive regulator of *p21* expression (Duan and Horwitz, 2003). In mice deficient in Gfi1, the number of HSCs is increased due to increased proliferation, but display reduced engraftment potential (Zeng et al., 2004). In *Gfi1-/-* HSCs, p21 expression level is markedly reduced compared to WT HSCs, which further demonstrates the importance of maintenance of quiescence in HSCs (Zeng et

al., 2004). Another key regulator of HSC quiescence is the Foxo group of proteins. Conditional deletion of Foxo1, 3 and 4 in HSCs results in increased cycling of the LSK population, but causes a reduction in LT-HSC number (Tothova et al., 2007). Foxo1/3/4 deficient mice are also more susceptible to repeated myeloablative stress suggesting a loss of quiescence in HSCs (Tothova et al., 2007). However, there are instances where increase in cell cycle does not result in exhaustion of HSCs. P18 deficient mice display increased HSC proliferation along with increase in functional HSCs that is maintained following serial transplantation (Yu et al., 2006; Yuan et al., 2004). Lack of p18INK4c is likely to result in rapid transition of HSCs to late G1 stage during which HSCs could be more susceptible to exhaustion.

The importance of HSC quiescence has been further illustrated by studying negative regulators of HSC quiescence. Deletion of myeloid Elf-1-like factor (MEF) in HSCs results in increased quiescence of HSCs along with an increase in HSC function (Lacorazza et al., 2006). Due to their increased quiescence, *MEF-/-* HSCs recover faster from myeloablative stress compared to controls (Lacorazza et al., 2006). HSCs deficient in lymphocyte-specific adapter protein (Lnk) have increased quiescence level (Bersenev et al., 2008). However, the number of functional HSCs are increased in *Lnk-/-* mice and they have increased engraftment potential when transplanted in a 1:1 dilution in lethally irradiated mice (Bersenev et al., 2008). Proliferative cells are also susceptible to acquiring genetic mutations that could cause senescence (Piacibello et al., 2005). In response to physiological stress like infection or chronic blood loss,

HSCs exit a quiescent state resulting in increase in proliferation and accumulation of DNA damage (Walter et al., 2015). Quiescence also protects HSCs from malignant transformation. Loss of PTEN in HSCs results in increased proliferation of HSCs, which subsequently results in hematologic malignancies (Yilmaz et al., 2006b).

5-Fluorouracil induced stress hematopoiesis:

The pyrimidine analog 5-fluorouracil (5-FU) has been used extensively as a myeloablative reagent. Administration of 5-FU results in ablation of cycling cells. 5-FU is incorporated into the DNA, which is propagated among dividing daughter cells and causes DNA damage and results in leukopenia (Busch et al., 2015; Lerner and Harrison, 1990). 5-FU treatment eliminates day 8 CFU-S population as well as BM colony-forming cells (CFC) (Randall and Weissman, 1997). However, the primitive blast CFC as well as long-term culture initiating cells (LTC-IC) are either spared or generated in the initial proliferation burst to repopulate the hematopoietic system (Harrison and Lerner, 1991; Randall and Weissman, 1997). To reconstitute the hematopoietic system following myeloablative stress, LT-HSCs start to proliferate and differentiate into ST-HSCs. Busch et al. demonstrated that following myeloablative stress in mice, 7-fold increase in LT-HSC differentiation and proliferation corresponds to a 16-fold increase in ST-HSC differentiation and proliferation (Busch et al., 2015). 5-FU also causes changes in the expression of cell surface markers of HSCs. Expression level of c-Kit has been reported to be about 10-fold downregulated after 2 days following 5-FU treatment (Randall and Weissman, 1997). After 5-FU

treatment, HSCs with long-term repopulating ability, expresses Mac1 on their cell surface (Cheshier et al., 1999; Randall and Weissman, 1997). Studies have shown that HSCs, in steady state, express very low or absolutely no Mac1 (Spangrude et al., 1988). However, following 5-FU treatment, HSCs with long-term repopulating ability are derived from Mac1 expressing cells only (Randall and Weissman, 1997). After 2nd day post 5-FU treatment, HSCs enter a stage where they reach a higher quiescent level compared to that seen under steady-state conditions (Venezia et al., 2004). This state correlates with an increase in anti-proliferative genes like *p21*, *Btg3*; anti-migratory genes *TIMP3*, *A-3g* and interferon-γ -induced genes (Venezia et al., 2004). On Day 3, post 5-FU treatment, HSCs enter active state of cycling and start proliferating, which also marks the increase in expression level of genes involved in DNA replication and repair (Venezia et al., 2004). The number of HSCs become maximum after day 6 post 5-FU administration. HSCs are cycling at the highest rate and this correlates with a significant increase in the expression of genes associated with metabolism and energy production (Venezia et al., 2004). Alpha4 (α4)-integrin is one of the key modulators of HSC proliferation at this stage (Venezia et al., 2004). Down-regulation of α4-integrin is one of the critical step in induction of HSC proliferation following 5-FU treatment (Venezia et al., 2004). This time marks the shifting of HSCs from the quiescent niche of the bone marrow to a niche that is supportive of proliferation. HSCs decrease their migration by increasing cell-cell adhesion, which is regulated by molecules like endoglin, whose expression is highest after day 6 of 5-FU administration, suggesting that the adhesion of HSCs decreases

during this period thereby increasing their migratory potential (Venezia et al., 2004). On day 10, HSCs migrate back to the quiescent niche within the bone marrow. HSCs proliferate at a reduced rate and express increased level of Endoglin and anti-proliferative genes such as *Btg1* (Venezia et al., 2004).

Competitive repopulation assay (CRA):

The ability of HSCs to home, engraft and self-renew within the bone marrow niche following transplant into lethally irradiated recipients has been used as a procedure to determine the functional potential of HSCs. Harrison first described the standard competitive repopulation assay (CRA) to determine HSC function (Harrison, 1980). In this assay, donor HSCs from test groups are mixed with competing HSCs derived from congenic wild type mouse and transplanted into lethally irradiated recipients. A standard number of competing HSCs are used against each test group (Harrison, 1980). Functional potential of test HSCs was determined by their relative ability to compete against the competitor HSCs. After hematopoietic reconstitution of the transplant recipients, the percentage of erythrocytes derived from donor and test HSCs were determined by the difference in electrophoretic mobility of donor and competitor hemoglobin (Harrison, 1980). Currently, the standard method to determine the functional potential of HSCs by competitive repopulation assay (CRA) uses distinct cell surface markers expressed by the test and competitor cells. C57BL/6 (CD45.2) mice and the B6.SJL-PtrcAPep3B/BoyJ (BOYJ) (CD45.1) mice differ from each other by the expression of CD45 on the cell surface (Shen et al., 1986). Test cells in different doses can be transplanted with competitor cells and following

transplantation contribution of the test cells and competitor cells in the peripheral blood of the recipients using fluorescence conjugated antibodies directed against cell surface antibodies can be assessed. The interpretation of this experiment depends on several factors including source of donor and competitor cells and the time of analysis after transplantation (Tothova et al., 2007). Szilvassy et al. used female HSCs that have undergone two round of transplantation as competitor cells against test cells derived from male mice (Szilvassy et al., 1990). However, as the competitor cells have undergone two rounds of transplantation previously, they became depleted of HSCs after a third round of transplantation and could not provide enough HSCs to compete against test cells. Freshly isolated bone marrow cells provide increased number of competitor HSCs as they have not undergone proliferative stress compared to previously transplanted HSCs (Janzen et al., 2006). It has been determined that in every $1X10^5$ bone marrow hematopoietic cells, there are 3-4 HSCs with multilineage repopulating ability (Abkowitz et al., 2000; Ema et al., 2005). Another critical factor in the analysis of CRA is the time point of analysis following transplant. Yang et al. have demonstrated that 50 ST-HSCs or 50 MPPs can reconstitute myeloid and lymphoid lineages after 16 weeks of transplant (Yang et al., 2005). In their studies, ST-HSCs reconstituted >0.01% myeloid cells and >1% of lymphoid cells (B lymphocytes and T lymphocytes) at 16 weeks post-transplant. MPPs could reconstitute B cells (>0.1%) and T cells (>0.01%) along with the myeloid compartment after 16 weeks post-transplant (Yang et al., 2005). These data indicate that 16 weeks post-transplant might not be an ideal time-point to

determine LT-HSC functions as ST-HSCs and MPPs can contribute to the hematopoietic system until this time-point. More recently, Benveniste et al. (Benveniste et al., 2010) have demonstrated that “intermediate-term” multipotent HSCs, which are different from ST-HSCs and LT-HSCs, can persist and sustain hematopoiesis for 6-8 months following transplantation.

The most stringent test to determine the functional potential of HSCs is to perform serial transplantation assays. The most immature HSCs in the hematopoietic hierarchy have the potential to regenerate the hematopoietic system of lethally irradiated hosts after serial transplantation and it can be sustained up to 4-5 rounds of transplantation (Ogden and Mickliem, 1976). In this assay, only HSCs with long-term repopulating ability will be able to self-renew and reconstitute the hematopoietic system of an irradiated host.

Mixed-lineage leukemia (*MLL*):

The mixed-lineage leukemia (*MLL*) gene encodes a DNA-binding protein that primarily acts as a component of the proteins associated with su(var)3-9, enhancer-of-zeste, trithorax (SET1) and complex of proteins associated with SET1 (COMPASS)-like complex (Yokoyama et al., 2004). COMPASS-like complexes methylate Lys4 on histone H3 (H3K4) through their conserved SET domain, and MLL associates with cofactors such as menin, a tumor suppressor, for chromatin localization and H3K4 trimethylation of genes including HOX genes (Yokoyama et al., 2004). In HSCs, MLL is required to maintain the quiescent state of HSCs. Deletion of MLL in HSCs results in reduced number of HSCs in G0/G1 phase of cell cycle (Jude et al., 2007). Deficiency of MLL in HSCs also

results in decreased engraftment of HSCs in competitive settings (Jude et al., 2007).

The functions of *MLL* gene are dysregulated due to translocation of genes encoding different proteins into the MLL gene. The most common translocation partner genes include AF4, AF6, AF9, AF10 and ENL (Eguchi et al., 2003). In leukemic cells, the major genomic breakpoints are clustered within an 8.3 kb BamHI fragment that encompasses the exon 5 to 11 of the MLL gene (Broeker et al., 1996a; Broeker et al., 1996b). This region has been termed as the breakpoint cluster region (bcr) (Broeker et al., 1996a; Broeker et al., 1996b). *MLL* translocations are identified in up to 10% of de novo acute lymphoblastic leukemias (ALL) and acute myeloid leukemias (AML) (Aoki et al., 2015). In children diagnosed with AML, rearrangements in MLL have been diagnosed in 35-50% of patients. In AML, translocation of MLL results in loss of function of catalytic SET domains. The new protein, as a result of acquired translocation, confers the ability to recruit a histone methyltransferase, DOT1L, to target genes determined by specific recognition elements in the remaining portion of *MLL*. Patients with *MLL* rearrangements have shorter event free survival as well as overall survival, which together contribute to poor prognosis (Muntean and Hess, 2012). The World Health Organization has classified leukemias with *MLL* rearrangement as a group with 4-year event-free survival of 24%-55% (Chessells et al., 2002; Raimondi et al., 1999; Stark et al., 2004).

AML cells have been shown to form a functional hierarchy in which the leukemia initiating cells (LICs), which are at the top of this hierarchy, have the

potential to initiate the disease. LICs are defined as cells that when transplanted into immunodeficient or lethally irradiated recipients have the potential to give rise to disease as well as differentiate into all the cells that constitute the malignancy. Lapidot et al. transplanted peripheral blood cells from AML patients into SCID mice and showed that the frequency of LIC was 1 in 250,000 cells (Lapidot et al., 1994). The same study also demonstrated that when CD34+ CD38+ cells and CD34+ CD38- cells were isolated from the same AML patient and transplanted into SCID mice, CD34+ CD38+ cells engraft poorly compared to CD34+ CD38- mice cells thus providing further evidence about the existence of a functional hierarchy within AML cells (Lapidot et al., 1994). Furthermore, CD34+ CD38- AML cells are more quiescent compared to CD34+ CD38+ AML cells (Ishikawa et al., 2007). Cytosine arabinoside (Ara-C) is a standard chemotherapeutic agent that is used to treat AML (Lowenberg et al., 1999; Momparler, 1974; Reese and Schiller, 2013). Ishikawa et al. transplanted NOD/SCID/IL2rϒnull (NSG) mice with cells derived from AML patients and treated the mice with Ara-C. CD34+ CD38- cells are more resistant to Ara-C treatment compared to CD34+ CD38+ AML cells (Ishikawa et al., 2007). Moreover, CD34+ CD38- cells from Ara-C treated mice were also able to engraft in secondary recipients (Ishikawa et al., 2007). These data indicate that the quiescent state of AML LICs appears to be responsible for their chemoresistance property and may contribute to disease relapse.

Upstream regulators and downstream substrates of mechanistic target of rapamycin complex 1 (mTORC1):

Mechanistic target of rapamycin (mTOR) is a serine/threonine complex that can be divided into two distinct complexes, mTOR complex1 (mTORC1) and mTOR complex2 (mTORC2) (Kaizuka et al., 2010). mTORC1 has six and mTORC2 has seven protein components. Both complexes share the catalytic mTOR subunit, mammalian lethal with sec-13 protein 8 (mLST8, GbL) DEP domain containing mTOR-interacting protein (DEPTOR) and the Tti1/Tel2 complex (Kaizuka et al., 2010; Yoon et al., 2015). Regulatory-associated protein of mammalian target of rapamycin (raptor) and proline-rich Akt substrate 40 kDa (PRAS40) are specific to mTORC1, whereas rapamycin-insensitive companion of mTOR (rictor), mammalian stress-activated map kinase-interacting protein 1 (mSin1), and protein observed with rictor 1 and 2 (protor1/2) are part of mTORC2 complex (Julien et al., 2010; Sancak et al., 2007; Yoon et al., 2015). mTORC1 activity is mainly regulated by Class IA phosphoinositide 3-kinases (PI3Ks) (Zhao and Vogt, 2008) (Figure 2). PI3Ks are dimers formed by regulatory (p85α, p85β, p55α, p55γ, and p50α) and catalytic (p110α, p110β, and p110δ) subunits. PI3K is recruited to the cell membrane where it converts phosphatidylinositol (4,5)-biphosphate (PIP2) to phosphatidylinositol (3,4,5)-triphosphate (PIP3) (Zhao and Vogt, 2008). Akt, a protein of AGC family kinases, has three isoforms, which are highly conserved in nature – Akt1, Akt2 and Akt3 (Cheng et al., 1992; Jones et al., 1991; Masure et al., 1999). Among them, Akt1 and Akt2 are expressed at high levels in hematopoietic cells (Juntilla et al., 2010). PIP3 recruits 3-

Figure 2

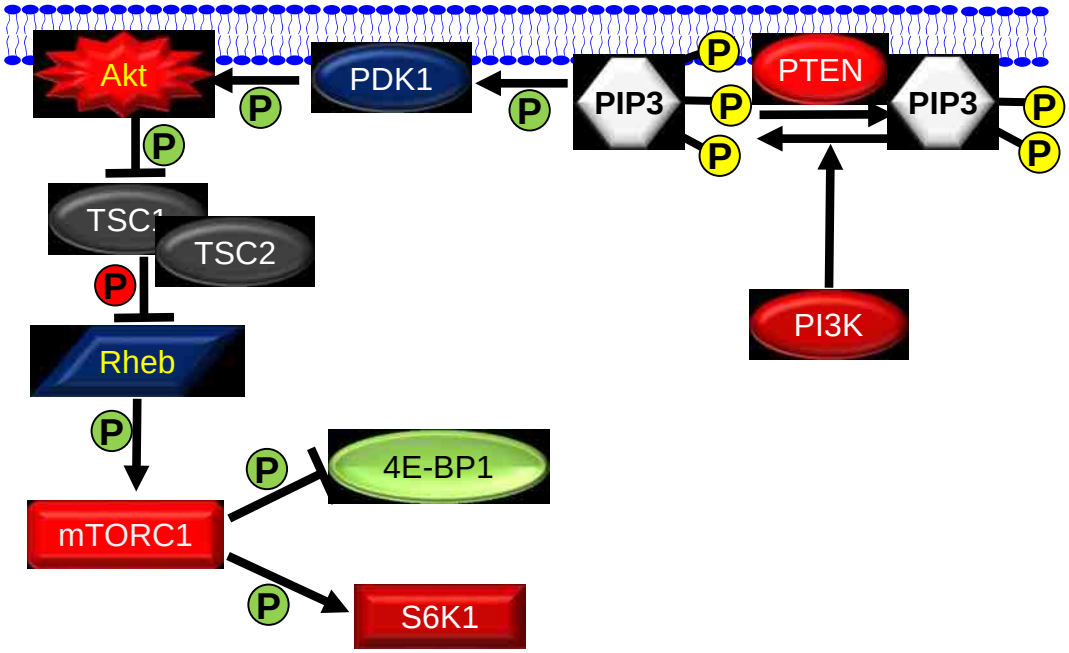
Akt
PDK1
PIP3
PTEN
PIP3
TSC1
TSC2
PI3K
Rheb
4E-BP1
mTORC1
S6K1
P

Figure 2: The mechanistic target of rapamycin 1 (mTORC1) signaling pathway.

In response to growth factors and mitogenic stimuli, phosphatidylinositol (4,5)-biphosphate (PIP2) is converted into phosphatidylinositol (3,4,5)-triiphosphate (PIP3) by phosphoinositide 3-kinases (PI3K) activity. Akt binds to phosphatidylinositol (3,4,5)-triphosphate (PIP3) allowing 3-phosphoinositide dependent protein kinase-1 (PDK1) to access activation sites of Akt. Following phosphorylation by PDK1, activated Akt phosphorylates and inhibits tuberous Sclerosis 2 (TSC2)-mediated inhibition of Rheb. Activated Rheb subsequently phosphorylates and activates mTORC1. Activated mTORC1 phosphorylates the translational regulators eukaryotic translation initiation factor 4E (eIF4E)-binding protein 1 (4E-BP1) and ribosomal protein S6 kinase 1 (S6K1).

phosphoinositidedependent protein kinase-1 (PDK1) and Akt to the plasma membrane where PDK1 phosphorylates and activates Akt (Kandel and Hay, 1999). The primary negative regulators of PI3K-mTORC1 pathway are Phosphatase and Tensin Homologue (PTEN), Tuberous Sclerosis 1 (TSC1 or tuberin) and Tuberous Sclerosis 2 (TSC2 or harmatin) (Figure 2). PTEN converts PIP3 to PIP2 (Das et al., 2003; Vazquez and Devreotes, 2006; Vazquez et al., 2006). TSC2 is a GTPase-activating protein and it is associated with TSC1 to form a complex, which inactivates the small G protein Ras homolog enriched in brain (Rheb) (Inoki et al., 2003). Akt phosphorylates TSC2, which results in binding of TSC2 to 14-3-3 and subsequent reduction in GAP activity of the TSC1/TSC2 complex (DeYoung et al., 2008; Inoki et al., 2002; Li et al., 2002). Withdrawal of TSC-mediated inhibition results in increased GTP-bound Rheb level (DeYoung et al., 2008; Inoki et al., 2003). GTP-bound Rheb phosphorylates and subsequently activates mTORC1. Activated mTORC1 phosphorylates the translational regulators eukaryotic translation initiation factor 4E (eIF4E)-binding protein 1 (4E-BP1) and ribosomal protein S6 kinase 1 (S6K1) (Yang et al., 2014).

Structure and functions of ribosomal protein S6 kinase 1 (S6K1):

S6K1 is a member of the cAMP-dependent protein kinases A, cGMP-dependent protein kinases G, and phospholipid-dependent protein kinases C (AGC) subfamily of serine-threonine kinases (Manning et al., 2002). S6K1 consists of 502 amino acids (Grove et al., 1991). The cellular localization of S6K1 has been shown to be dependent on cell cycle stage and regulated by mTORC1 (Rosner and Hengstschlager, 2011; Rosner et al., 2012). Rosner et al.

demonstrated that in primary human fibroblasts, S6K1 is primarily localized in the cytoplasm during most of the stages of cell cycle, but localizes into nucleus at mid G1 phase (Rosner and Hengstschlager, 2011).

S6K1 consists of an N-terminal catalytic kinase domain, C-terminal tail region and C-terminal auto-inhibitory domain (AID) (Alessi, 1997; Pullen et al., 1998). The catalytic kinase domain of S6K1 has a conserved phosphorylation site on the activation loop at Thr-229 (Alessi et al., 1997; Pullen et al., 1998). The C-terminal tail domain has two phosphorylation sites that have been termed as turn motif and hydrophobic motif (HM) site (Keshwani et al., 2011). On the HM site, the phosphorylation site is on Thr-389 (Burnett et al., 1998a; Isotani et al., 1999). The primary kinase that phosphorylates Thr-389 is mTORC1 (Burnett et al., 1998a; Isotani et al., 1999). The AID has 4 phosphorylation sites (Ser-411, Ser-418, Thr-421, Ser-424) and blocks the phosphorylation of the kinase domain by activators of S6K1 (Ferrari et al., 1992). The AID domain, which is basic in nature, interacts and binds with acidic kinase domain and creates an inactive conformation (Banerjee et al., 1990; Price et al., 1991). The initial steps required for S6K1 activation by upstream regulators are phosphorylation of four phosphorylation sites on the AID that leads to a conformational change of S6K1 and exposes the internal region of S6K1 (Burnett et al., 1998a; Burnett et al., 1998b; Dennis et al., 1998). Subsequently, S6K1 is phosphorylated on Thr-389 residue by mTORC1 followed by phosphorylation on Thr-229 by PDK-1 (Burnett et al., 1998a; Isotani et al., 1999; Pullen et al., 1998). The phosphorylation on Thr-389 is critical for S6K1 functions as mutation of threonine to alanine on 389

residue inhibits S6K1 activity (Dennis et al., 1998; Schalm and Blenis, 2002; Weng et al., 1998). However, for maximal activity of S6K1, phosphorylation on both Thr-229 and Thr-389 is required. S6K1 has been found to be inactive in *PDK1-/-* embryonic stem cells (Williams et al., 2000). Furthermore, S6K1 activity is abolished when the Thr-229 residue is mutated to prevent phosphorylation by PDK1 (Weng et al., 1998). These evidence establish that PDK1-mediated phosphorylation on Thr-229 is required for S6K1 activity.

S6K1 has been identified as a negative regulator of mTORC2 activity. SIN1 and Rictor are two components of the mTORC2 complex and both are required for mTORC2-dependent phosphorylation of Akt (Yang et al., 2006). In mouse embryonic fibroblasts (MEF), S6K1 phosphorylates SIN1 at Thr-86 and Thr-398 that leads to dissociation of SIN1 from mTORC2 complex thus impairing mTORC2 activity (Liu et al., 2013). mTORC2 phosphorylates and activates Akt and in the absence of mTORC2 activity, Akt phosphorylation is diminished (Liu et al., 2013). In MEFs, following mTORC1-dependent activation, S6K1 also phosphorylates Rictor, another component of mTORC2, at Thr-1135 (Julien et al., 2010). Phosphorylation of Rictor at Thr-1135 results in inhibition of Akt (Julien et al., 2010). Overall, these data demonstrate that activated S6K1 negatively regulates Akt activity by impairing the kinase activity of mTORC2.

S6 has been identified as the primary downstream substrate of S6K1 and phosphorylation of S6 by S6K1 has been considered as an indicator of S6K1 activity (Chauvin et al., 2014; Koh, 2013; Pende et al., 2004). As S6 is a critical regulator of protein synthesis and cell cycle progression, it has been postulated

that S6K1 regulates protein synthesis and cell cycle stages. However, a recent study by Garelick et al. demonstrated that S6K1 deficiency did not affect the global translational activity in muscle and liver of mice (Garelick et al., 2013).

S6K1 also regulates cytoskeletal reorganization by binding to F-actin in ovarian cancer cells (Ip et al., 2011). Furthermore, in ovarian cancer cells, S6K1 also activates Rac1, Cdc42 and PAK1 – three critical regulators of cytoskeletal reorganization and cellular migration (Ip et al., 2011). However, evidence suggests S6K1 might regulate Rac1 and Cdc42 activity in a cell dependent manner. In fibroblasts, S6K1 acts downstream of Rac1 and Cdc42 (Chou and Blenis, 1996; Martin et al., 2001). On the other hand, in ovarian cancer cells, both Rac1 and Cdc42 are downstream substrates of S6K1 (Ip et al., 2011).

S6K1 has also been identified as a regulator of apoptosis by controlling the activity of different downstream substrates. S6K1 binds to and phosphorylates Mdm2 preventing its nuclear translocation (Lai et al., 2010). Mdm2 regulates ubiquination of nuclear p53 and in the absence of nuclear Mdm2, increased p53 level results in cell cycle arrest and cellular apoptosis (Lai et al., 2010). In contrast, S6K1 can also phosphorylate glycogen synthase kinase 3 beta (GSK-3β) and pro-apoptotic protein Bcl-2 associated agonist of cell death (BAD) thus inhibiting apoptosis. In *S6K1-/-* hepatocytes, expression level of pro-apoptotic protein caspase-8 and BH3-interacting domain death agonist (Bid) were significantly downregulated compared to wild-type (WT) controls (Gonzalez-Rodriguez et al., 2009). In response to apoptotic signals, *S6K1-/-* hepatocytes have reduced cytochrome C release and reduced capase-3 activation –

hallmarks of apoptosis (Gonzalez-Rodriguez et al., 2009). It has been shown that in absence of S6K1, S6K1-dependent phosphorylation of insulin receptor substrate-1 (IRS-1) diminishes and results in increased IRS-1 activity (Gonzalez-Rodriguez et al., 2009). The increase in IRS-1 activity correlates with increased activation of PI3K and Erk mediated pro-survival pathways (Gonzalez-Rodriguez et al., 2009). S6K1-deficient hepatocytes undergo apoptosis when treated with either PI3K or Erk inhibitor (Gonzalez-Rodriguez et al., 2009). In human colon adenocarcinoma cells and breast cancer cells, inhibition of S6K1 activity induces apoptosis (Hong et al., 2013; Song et al., 2014). Taken together, it appears that S6K1 can regulate different functions in different cell types utilizing distinct substrates. Thus, it is essential to assess the role of S6K1 in a cell dependent manner.

Summary and significance:

Conventional chemotherapeutic measures to treat AML are beneficial for a minority of patients (Buchner et al., 2012). Furthermore, due to toxic effects, chemotherapies have limited use to treat elderly and patients with comorbidities (Buchner et al., 2012). Following treatment with chemotherapeutic agents like mitoxantrone, etoposide, and cytarabine, patients show signs of drug-induced toxicities including diarrhea, neutropenic infection and transaminase elevation (Greenberg et al., 2004; Tallman et al., 1999). Treatment with mTORC1 inhibitor, sirolimus, causes toxicities which include headache, stomatitis, hyperlipidemia and mild thrombocytopenia in patients (MacDonald and Group, 2001; Saunders et al., 2001). In view of the above facts, it is imperative to identify a downstream target of mTORC1 to develop pharmacological inhibitors that will show minimal toxicities in patients. Previously, different studies have identified that upstream effectors of S6K1 are critical regulators of hematopoiesis and leukemogenesis (Guo et al., 2013; Haneline et al., 2006; Juntilla et al., 2010; Kharas et al., 2010; Lee et al., 2010; Magee et al., 2012; Yilmaz et al., 2006b). In response to growth factors and other mitogenic stimuli, S6K1 is phosphorylated and activated by mTORC1 (Burnett et al., 1998a; Fang et al., 2003). Multiple line of evidences have shown that mTORC1 is expressed in HSCs as well as in AML cells and critical for their functions (Guo et al., 2013; Sujobert et al., 2015; Zeng et al., 2012). However, the exact role of S6K1 in both hematopoiesis and leukemogenesis is not known yet. The main objective of this study was to determine the role of S6K1 in development and function of HSCs as well as

Figure 3

A

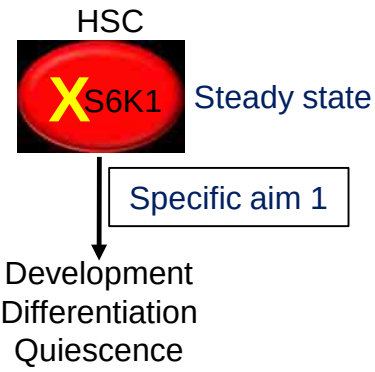

B

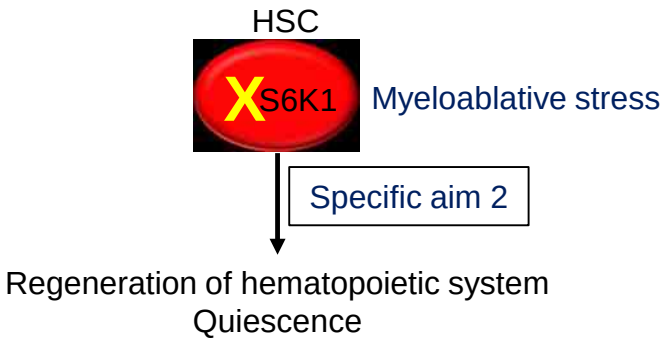

C

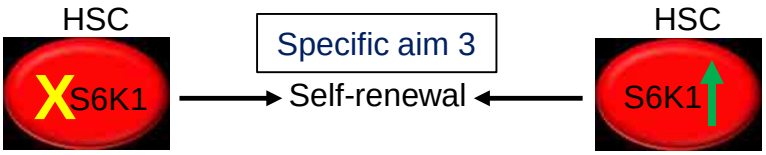

D

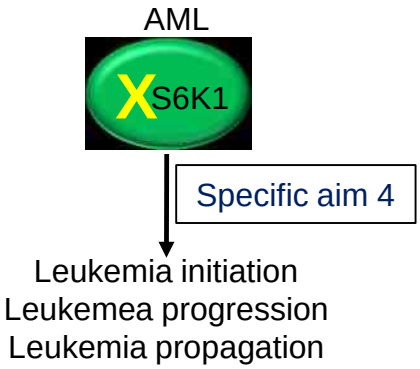

Figure 3: Schematic models of proposed specific aims in the study.

(A) Determining the role of S6K1 on development, differentiation and quiescence of HSCs using a genetic model of S6K1-deficient (*S6K1-/-*) mouse. (B) Determining the role of S6K1 on regeneration of hematopoiesis and quiescence of HSCs following myeloablative stress. (C) Determining the effect of modulation of S6K1 expression level on self-renewal of HSCs using loss-of-expression and overexpression approaches. (D) Determining the role of S6K1 on initiation, progression and propagation of leukemia.

initiation, development and propagation of AML.

Our studies specifically address the following aims:

Specific aim 1: We hypothesized that S6K1 regulates development and differentiation of HSCs to maintain steady-state hematopoiesis. We have determined the role of S6K1 in regulation of HSC as well as HSC/P frequency and number using a genetic approach (Figure 3A).

Specific aim 2: We hypothesized that S6K1 regulates quiescence of HSCs and the recovery of hematopoietic system following myeloablation. We have determined the role of S6K1 in regulation of regeneration of hematopoietic system following myeloablative stress (Figure 3B).

Specific aim 3: We hypothesized that S6K1 expression level regulates engraftment, differentiation and self-renewal potential of HSCs. We have determined the effect of S6K1 deficiency as well as hyperactivation of S6K1 on HSC function using genetic approaches and serial transplantation models (Figure 3C).

Specific aim 4: We hypothesized that S6K1 is a key regulator of initiation, development and propagation of AML. We have determined the role of S6K1 in a MLL-AF9 translocation driven leukemia model using genetic approaches and serial transplantation models (Figure 3D).

Overall our studies revealed that S6K1 regulates self-renewal of HSC as well as AML cells. Deficiency of S6K1 results in reduced quiescence of HSCs. Following myeloablative stress, S6K1 deficiency delays HSCs return to the quiescent state. Using genetic approaches, we have also

demonstrated that S6K1 expression level is critical for maintenance of HSC function. In our studies, dysregulation of S6K1 expression level results in reduced self-renewal of HSCs. Furthermore, we have also shown that S6K1 is a positive regulator of *p21* expression and deficiency of S6K1 results in reduced *p21* level in HSCs. We have also identified S6K1 as a therapeutic target to delay the propagation of AML. Our studies have provided compelling evidence that loss of expression of S6K1 in AML cells results in delayed propagation of AML in secondary recipients. Furthermore, our studies also revealed that pharmacological inhibition of S6K1 activity causes inhibition of growth of human leukemic cells.

Chapter 2: Materials and Methods

Mice:

C57BL/6 (CD45.2) mice were purchased from Jackson Laboratories (Bar Harbor, ME). B6.SJL-PtrcAPep3B/BoyJ (BOYJ) (CD45.1) and C57BL/6 X BOYJ-F1 (CD45.1/CD45.2) mice were obtained from the In Vivo Therapeutics (IVT) Core of Indiana University School of Medicine (Indianapolis, IN). *S6K1-/-* mice were obtained from University of Cincinnati (Cincinnati, OH) and were bred and maintained in-house. Mice used in transplantation studies received doxycycline feeds for 30 days post-irradiation. All protocols were approved by the Institutional Animal Care and Use Committee (IACUC) of Indiana University School of Medicine.

Antibodies, cytokines and other reagents:

Antibody against S6K1 was purchased from BD Biosciences (San Jose, CA). Antibodies against phosphorylated forms of S6K1, S6, 4E-BP1, mTOR and Akt were purchased from Cell Signaling Technology (Danvers, MA). Antibody against β-actin was purchased from Sigma (St. Louis, MO). Murine interleukin-6 (mIL-6), murine thrombopoietin (mTPO), murine interleukin-3 (mIL-3), murine stem cell factor (mSCF), murine FLT3 ligand (mFLT3L), human insulin-like growth factor-2 (hIGF2), human fibroblast growth factor-acidic (hFGF), human interleukin-6 (hIL-6), human thrombopoietin (hTPO), human interleukin-3 (hIL-3), human stem cell factor (hSCF) and human FLT3 ligand (hFLT3L) were purchased from Peprotech (Rocky Hill, NJ). PF-4708671, S6K1 inhibitor, was

purchased from Tocris (Bristol, UK). 5-FU was purchased from APP Pharmaceuticals (Schaumburg, IL). The fluorochrome conjugates and clones of antibodies used for flow cytometry are described in Table 1. Fluorochrome conjugated antibodies against CD150 and CD48 were purchased from BioLegend (San Diego, CA). Fluorochrome conjugated antibodies against CD34 and CD16/32 were purchased from eBioscience (San Diego, CA). Fluorochrome conjugated antibodies against c-Kit, Sca1, B220, Ter119, CD11b, Ly6C and 6G, CD3, CD4, CD8, CD19, CD45.1 and CD45.2 were purchased from BD Biosciences. Iscove's Modified Dulbecco's Medium (IMDM) was purchased from Thermo Fisher Scientific. StemSpan serum-free expansion medium (StemSpan-SFEM) was purchased from StemCell Technologies (Vancouver, BC, Canada). Fetal Bovine Serum (FBS) was purchased from GE Healthcare Life Sciences (Pittsburgh, PA). Rat serum and bovine serum albumin (BSA) was purchased from Sigma. Human umbilical cord blood (UCB) derived CD34+ cells were obtained from Indiana University Melvin and Bren Simon Cancer Center Angio BioCore with Institutional Review Board's (IRB) approval.

Cell culture:

Human leukemic cell line MA9-3 was obtained from University of Cincinnati (Cincinnati, OH). Cells were cultured in IMDM in the presence of 20% FBS and supplemented with hSCF, hIL-3, hIL-6, hFlt-3L, and hTPO (10 ng/ml of each cytokine). UCB derived CD34+ cells were cultured in StemSpan-SFEM in presence of 10 ng/ml hSCF, 20 ng/ml hTPO, 20 ng/ml hIGF-2 and 10 ng/ml hFGF.

Thymidine incorporation assay:

Cells were washed with IMDM containing 0.2% BSA and cultured in serum-free media for 6 hours. After 6 hours, cells were collected, centrifuged and resuspended in IMDM containing 20% FBS. $5X10^4$ cells were plated in each well of a 96-well plate. Cells were incubated for 42 hours and subsequently pulsed with 1.0 µCi (0.037 MBq) [3H] thymidine (Perkin Elmer, Waltham MA) for 6 hours. Cells were harvested using an automated 96-well cell harvester (Brandel, Gaithersburg, MD) and thymidine incorporation was determined as counts per minute (CPM).

Apoptosis assay:

MA9-3 cells were washed with IMDM containing 0.2% BSA and cultured in serum-free IMDM for 6 hours. After 6 hours, cells were collected, centrifuged and resuspended in IMDM containing 20% FBS. $2X10^5$ cells were plated in each well of a 24-well plate at a final volume of 1 ml. Cells were incubated for 18 hours in presence or absence of PF-4708671. After 18 hours, cells were collected, centrifuged and resuspended in Annexin V binding buffer (BD Biosciences). Cells were incubated with APC-conjugated Annexin V (BD Biosciences) for 20 minutes on ice. Cells were washed and incubated with 7-Aminoactinomycin D (7-AAD; BD Biosciences). Cells were acquired in LSR II flow cytometer machine (BD Biosciences). Data analysis was performed using FlowJo software (FlowJo, Ashland, OR).

Isolation of bone marrow mono nuclear cells:

Mice were humanely euthanized and two femurs, two tibias and two iliac crests were surgically removed. Whole BM cells were flushed using IMDM with a 23G syringe, centrifuged at 1500 r.p.m. for 5 minutes and the supernatant was discarded. To obtain mono nuclear cells (MNCs), RBC lysis was performed using RBC lysis buffer (eBioscience). Whole BM cells were incubated in 1 ml of RBC lysis buffer for 5 minutes at room temperature. After 5 minutes, cells were centrifuged at 1500 r.p.m. for 5 minutes. The supernatant was discarded and cells were resuspended in PBS containing 0.2% BSA to obtain a single cell suspension.

Analysis of murine hematopoietic stem and progenitor cells:

For detection of HSCs and HPCs, BM MNCs were resuspended in blocking buffer (10% rat serum and 0.2% BSA in PBS) and incubated on ice for 30 minutes to prevent non-specific binding. To detect SLAM LSK cells, we used Gr1, Mac1, B220, Ter119, CD3, CD4 and CD8 as lineage markers along with CD150, CD48, c-Kit and Sca1. For GMP, CMP and MEP, CD34, CD16/32, c-Kit and Sca1 were used along with lineage markers as described above. Cells were incubated with antibodies on ice for 30 minutes. Cells were washed with 0.2% BSA in PBS and analyzed using LSRII flow cytometer machine. Data analysis was performed using FlowJo software.

To detect Ki-67 positive cells in SLAM LSK cells, BM MNCs were stained for surface markers as described above. After staining, cells were washed with 0.2% BSA in PBS, permeabilized and fixed using Cytofix/Cytoperm buffer (BD

Biosciences, Franklin Lakes, NJ) and incubated with antibody against Ki-67 for 30 minutes on ice. Cells were washed, incubated with 4′,6-diamidino-2-phenylindole (DAPI) (Sigma) and acquired using LSR II flow cytometer machine. Data analysis was performed using FlowJo software.

Sorting of HSCs and HSC/Ps:

Whole BM cells were aseptically isolated from WT and *S6K1-/-* mice and single cell suspension of MNCs were obtained as described above. MNCs were incubated with biotin-conjugated B220, CD11b, CD3, Ter119, Ly6G and 6C for 30 minutes on ice. Streptavidin Microbeads (Miltenyi Biotec, San Diego, CA) were added into the cell solution at a concentration of 10 µl/10^7 cells and incubated for 15 minutes on ice. Tubes containing labelled cells were inserted into a magnet block and cell suspension was collected. Cell suspension was centrifuged at 1500 r.p.m. for 5 minutes and the supernatant was discarded. Cells were resupended in blocking buffer and stained for cell surface markers as described above. Cells were washed and resuspended in PBS containing 0.2% BSA. Cells were sorted based on the cell surface markers using BD FACSARIA III (BD Biosciences). Cells, which were sorted for RNA isolation, were sorted into tubes containing 350 µl of Buffer RLT plus (Qiagen, Hilden, Germany). Cells used for transplantation studies were sorted into tubes containing PBS-BSA.

Quantitative polymerase chain reaction:

Cells were loaded on QIAshredder (Qiagen) and centrifuged at 13500 r.p.m. for 2 minutes. The flow through was collected and total RNA was isolated from cells using RNeasy Plus Micro kit (Qiagen) according to manufacturer's

instructions. Isolated RNA was reverse transcribed using random hexamers and SuperScript III First-Strand Synthesis System (Life Technologies, Carlsbad, CA) according to manufacturer's instructions. Primers for SYBR Green qRT-PCR were designed to produce an amplicon size of 80-150 base pairs (Table 2). qRT-PCR was performed using FastStart Universal SYBR Green Master with ROX (Roche, Basel, Switzerland) using a 7500 Real-Time PCR System (Applied Biosystems, Foster City, CA) for 40 cycles. All samples were run in either triplicates or quadruplicates. *Actb* (encoding β-actin) was used for normalization of samples.

Competitive repopulation assay with BM MNCs:

Whole BM cells were aseptically isolated from WT and *S6K1-/-* mice and single cell suspension of MNCs were obtained as described above. Freshly isolated $5X10^5$ BM MNCs from either WT or *S6K1-/-* mice were mixed with freshly isolated $5X10^5$ competitor BM MNCs from BoyJ mice. C57BL/6 X BOYJ-F1 recipients were lethally irradiated at 1100 cGy from a cesium source using a split dose of 700 cGY and 400 cGy at an interval of 4 hours. Cells were injected intravenously into the recipients. Engraftment of donor-derived cells (CD45.2+) was monitored in the peripheral blood of recipients at 4 week intervals. Data analysis was performed using FlowJo software. For secondary transplants, BM MNCs were isolated aseptically from primary transplant recipients at 24 weeks after primary transplant and $1x10^6$ MNCs were injected intravenously into lethally irradiated C57BL/6 X BOYJ-F1 recipients. For all the transplantation experiments, cells were resuspended in PBS containing 0.2% BSA. For both

primary and secondary transplants, cells were resuspended at a final concentration of $5X10^6$ cells/ml and 200 µl of cell solution was used for transplantation into each individual mouse.

Competitive repopulation assay with SLAM LSK cells:

Whole BM cells were aseptically isolated from WT and *S6K1-/-* mice and single cell suspension of MNCs were obtained as described above. SLAM LSK cells were sorted as described above. For primary transplant, 250 SLAM LSKs from either WT or *S6K1-/-* mice were mixed with freshly isolated $3X10^5$ competitor BM MNCs from BoyJ mice. C57BL/6 X BOYJ-F1 recipients were lethally irradiated as described above. Cells were injected intravenously into the recipients. For secondary transplants, BM MNCs were isolated aseptically from primary transplant recipients on 24 weeks post-transplant and one million cells were injected intravenously into lethally irradiated C57Bl/6 X BOYJ-F1 recipients. For tertiary transplants, BM MNCs were isolated aseptically from secondary transplant recipients on 24 weeks post-transplant and $2.5x10^6$ cells were injected intravenously into lethally irradiated C57BL/6 X BOYJ-F1 recipients. Engraftment of donor-derived cells (CD45.2+) were monitored in the peripheral blood of the recipients at 4 week intervals. Data analysis was performed using FlowJo software. 200 µl of cell solution was used for transplantation into each individual mouse.

Analysis of peripheral blood from transplant recipients:

Peripheral blood from the transplant recipients was collected by tail-vein bleeding into heparinized microcapillary tubes (Fisher Scientific, Waltham, MA).

RBCs were lysed by treating with RBC lysis buffer (eBioscience). Cells were washed with PBS and resuspended in blocking buffer (10% rat serum and 2% BSA in PBS). Cells were incubated on ice for 30 minutes for blocking. Cells were stained with the following antibodies: FITC conjugated anti-CD45.1, APC conjugated anti-CD45.2, Pacific Blue conjugated anti-B220, PE-conjugated Mac1, APC-Cy7-conjugated Gr1 and PerCpCy5.5-conjugated CD3. Cells were incubated with antibodies on ice for 30 minutes. Cells were washed with 0.2% BSA in PBS and acquired using LSR II flow cytometry machine. Data analysis was performed using FlowJo software.

Homing assay:

Whole BM cells were aseptically isolated from WT and *S6K1-/-* mice and single cell suspension of MNCs were obtained as described above. MNCs were resuspended at a concentration of $1X10^6$ cells/ml in 0.2% BSA in IMDM. DiD (1,1'-dioctadecyl-3,3,3',3'-tetramethylindodicarbocyanine) cell-labeling solution (Life Technologies, Carlsbad, CA) was added to the cell suspension at a concentration of 4 µl/ml and incubated for 30 minutes at 37^{o}C. Labelled cells were centrifuged at 1500 r.p.m. for 5 minutes and supernatant was discarded. Cells were resuspended at a concentration of $50X0^6$ cells/ml in PBS containing 0.2% BSA. Lethally irradiated Boy/J mice were injected intravenously with 10^7 Did-labeled MNCs. After 18 hours, recipient mice were euthanized and BM MNCs were isolated as described above. MNCs were stained for lineage markers as well as for c-Kit and Sca1 as described above. Homing of DiD+ LSK

cells were acquired using LSRII flow cytometry machine. Data analysis was performed using FlowJo software.

5-FU treatment:

Eight to twelve weeks old WT and *S6K1-/-* mice were injected intra-peritoneally with 5-FU (150 mg/kg body wt.) on day zero of the experiment. On day 6, 9, and 15 after 5-FU treatment, mice were euthanized and BM MNCs were isolated as described above. BM MNCs were stained for lineage markers as well as c-Kit and Sca1 as described above. BM MNCs were analyzed by flow cytometry as described above.

BrdU incorporation assay:

WT and *S6K1-/-* mice were injected with 1mg of BrdU (BD Biosciences) intraperitoneally after day 8 following 5-FU injection. Injected mice were euthanized after 16 hours. BM MNCs were isolated as described above. BM MNCs were resuspended in blocking buffer (10% rat serum and 0.2% BSA in PBS) and incubated on ice for 30 minutes for blocking. To detect LSK cells, we used Gr1, Mac1, B220, Ter119, CD3, CD4 and CD8 as lineage markers along with c-Kit and Sca1. Cell surface staining was done as described before and cells were washed by resuspending in 2% BSA in PBS followed by centrifugation at 1500 r.p.m. for 5 minutes. The supernatant was discarded and cells were resuspended in Cytofix/Cytoperm buffer (BD Biosciences) for 30 minutes on ice. Cells were washed with BD Perm/Wash buffer and resuspended in Cytoperm Permeabilization Buffer Plus. Cells were incubated for 10 minutes on ice and washed with BD Perm/Wash buffer. Cells were resuspended in Cytofix/Cytoperm

buffer for 5 minutes on ice and washed with Perm/Wash buffer. Cells were resupended in 100 µl of DPBS containing 300 µg/ml of DNase. Cells were incubated in 37^{o}C for 30 minutes and washed with BD Perm/Wash buffer. Cells were incubated with APC-conjugated anti-BrdU antibody for 30 minutes on ice. Cells were washed with BD Perm/Wash buffer. Cells were incubated with 7-AAD and were aacquired by LSR II flow cytometry machine. Data analysis was performed using FlowJo software.

Transplantation of HSC/Ps following 5-FU treatment:

Eight to twelve weeks old WT and *S6K1-/-* mice were injected intraperitoneally with 5-FU (150 mg/kg body wt.) on day zero of the experiment. After 6 days post 5-FU treatment, mice were euthanized and WBM cells were aseptically isolated as described above. Following RBC lysis, 0.1 million BM MNCs from either WT or *S6K1-/-* mice were mixed with freshly isolated competitor cells from BoyJ mice. BoyJ recipients were lethally irradiated as described above. Cells were injected intravenously into the recipients. Engraftment of donor-derived cells (CD45.2+) were monitored in the peripheral blood of the recipients at 1, 2, 3, and 4 months post-transplant as described previously. Data analysis was performed using FlowJo software.

Generation of retroviral supernatants and retroviral transduction:

Retroviral supernatants for the transduction of BM MNCs were generated using the Phoenix ecotropic packaging cell line transfected with retroviral vector plasmids using a calcium phosphatase transfection kit (Promega, Madison, WI). After 48 hours of transfection, supernatants were collected and filtered through

0.45 µm membrane (GE Healthcare Life Sciences). BM MNCs were isolated as described above and cultured in IMDM supplemented with FBS, mIL-6 (10 ng/ml), mFLT3L (10 ng/ml), mTPO (50ng/ml) and mSCF (50 ng/ml) for overnight. For transduction, cells were cultured for 48 hours in the presence of retroviral supernatant on tissue culture plates coated with retronectin (Takara Bio Inc, Otsu, Japan). After 48 hours, cells were withdrawn from retroviral supernatants and sorted based on GFP expression using FACS ARIA III.

Leukemogenesis assay:

8-12 weeks old WT and *S6K1-/-* mice were injected intraperitoneally with 5-FU (150 mg/kg body wt.). After 5 days, BM MNCs were aseptically isolated as described above. Cells were incubated overnight in IMDM containing 20% FBS along with mIL-3 (10 ng/ml), mIL-6 (10 ng/ml) and mSCF (100 ng/ml). Cells were transduced with MLL-AF9 as described above. Cells were sorted to homogeneity based on GFP expression using FACS. One million sorted cells were injected intravenously into lethally irradiated C57/BL6 mice. For secondary transplant, MNCs were isolated from the spleens of primary transplant recipients with AML. One million MNCs were injected intravenously into lethally irradiated C57/BL6 mice.

Western blotting:

WT and *S6K1-/-* BM MNCs were transduced with either retroviral empty vector or retrovirus encoding MLL-AF9 as described above. Sorted cells were starved in serum and growth factor free IMDM containing 0.2% BSA for 6 hours. Cells were lysed using CelLytic buffer (Sigma) supplemented with

protease inhibitor (Roche) as per manufacturer's instructions. Cell lysates were cleared by centrifugation at 13500 r.p.m. for 12 minutes and the supernatant was collected. Protein was quantified by bicinchoninic acid assay (BCA assay) by using Pierce BCA Protein Assay Kit (Thermo Fisher Scientific, Waltham, MA) according to manufacturer's instructions. Equal amount of protein was boiled in 4X Laemmli sample buffer (Bio-Rad, Hercules, CA) at 95^{o}C for 5 minutes. Proteins were separated by SDS-PAGE using Novex Tris-Glycine gels (Thermo Fisher Scientific) and transferred electrophoretically onto a nitrocellulose membrane. Membranes were incubated with blok-CH (Millipore, Norwood, OH) to prevent non-specific binding. Membranes were incubated with primary antibodies followed by horseradish peroxidase-conjugated secondary antibodies. Blots were developed using Luminata Forte (Millipore) and images were captured using Universal Hood II imager (Bio-Rad).

Statistical analysis:

The means of two groups were compared by two-tailed *t* tests. The means of multiple groups were compared by one-way ANOVA with Bonferroni post-hoc analysis. *P* values less than 0.05 were considered statistically significant.

Table 1: Antibodies used for flow cytometry

Antibody	Clone	Conjugate
CD150	TC15-12F12.2	APC
CD48	HM48-1	APC-Cy7
c-Kit	2B8	BV421
c-Kit	2B8	BV450
c-Kit	2B8	Pacific Blue
c-Kit	2B8	APC
Ly-6A/E	E13-161.7	FITC
Ly-6A/E	E13-161.7	PE-Cy7
Ly-6G and Ly-6C	RB6-8C5	APC-Cy7
Ly-6G and Ly-6C	RB6-8C5	PE
B220	RA3-6B2	PE
CD11b	M1/70	PE
TER-119	TER-119	PE
CD3	17A2	PE
CD4	GK1.5	PE
CD8	53-6.7	PE
CD16/CD32	93	PerCP-Cy5.5
CD34	RAM34	Pacific Blue
CD19	1D3	APC
CD45.1	A20	FITC
CD45.2	104	APC
CD3	17A2	PerCP-Cy5.5

Table 2: Primer sequences used for qRT-PCR

Target	Sequence
S6K1 fwd	TCTGAGGATGAGCTGGAGGAG
S6K1 rev	TCACAATGTTCCATGCCAAGT
p21 fwd	AACATCTCAGGGCCGAAAAC
p21 rev	TCCTGACCCACAGCAGAAGA
p27 fwd	CAGTGTCCAGGGATGAGGAAG
p27 rev	TTCGGGGAACCGTCTGAAA
p130 fwd	TGGCATGGAAAACCAAGTCC
p130 rev	CAAGTCCTCCAGCATCAGCA
Hoxa9 fwd	CTTCAGTCCTTGCAGCTTCCA
Hoxa9 rev	TCCTTCTCAGTTCCAGCGTCT
Bmi1 fwd	CAGGTTCACAAAACCAGACCAC
Bmi1 rev	TGACGGGTGAGCTGCATAAA
Foxo3 fwd	ACTCCAAGACCTGCTTGCTTC
Foxo3 rev	AAGGACATCATTGGATCGTTG
PTEN fwd	GATTACAGACCCGTGGCACT
PTEN rev	ATCACCACACACAGGCAATG
PU1 fwd	GGATCTGACCAACCTGGAG
PU1 rev	CTACTACTCCTTCGTGGGCAG
Cyclin B2 fwd	GTGAAACCAGTGCAGATGGAG
Cyclin B2 rev	GCAGAGCAGAGCATCAGAGAA
Cyclin D1 fwd	CCAGAGGCGGATGAGAACA
Cyclin D1 rev	TGCGGTAGCAGGAGAGGAAG

Cyclin D3 fwd	TGCGTGCAAAAGGAGATCAAG
Cyclin D3 rev	AGTTCATAGCCAGAGGGAAGACA
Cyclin E1 fwd	GATTGGCTGATGGAGGTGTG
Cyclin E1 rev	TGGTGCAACTTTGGAGGGTA
Cyclin G1 fwd	CGGAGACATTTTCCCTAGCTGT
Cyclin G1 rev	CCTTTCCTCTTCAGTCGCTTTC

Chapter 3: Role of S6K1 in regulation of steady-state hematopoiesis

Introduction:

Activation of S6K1 in response to different stimuli including growth factors is mediated through PI3K, Akt and mTORC1. PI3K is the upstream regulator of Akt and mTORC1 activation. Deficiency of p85α, but not p85β, subunit of PI3K results in reduced cellularity in fetal liver (Haneline et al., 2006). The reduction in cellularity is further increased when both p85α and p85β subunits are deleted. The deficiency of p85α subunit results in reduced BFU-E, CFU-E, CFU-GM and CFU-MEG formed by fetal liver hematopoietic cells compared to WT fetal liver hematopoietic cells. Fetal liver HPCs deficient in either p85α subunit or both p85α and p85β subunit showed reduced proliferation in response to SCF compared to WT controls (Haneline et al., 2006).

Downstream of PI3K, deficiency of Akt1 and Akt2 results in increased frequency of HSCs in fetal liver and bone marrow. However, in mice deficient in Akt1 and Akt2, myeloid, B and T cells are markedly reduced compared to WT mice (Juntilla et al., 2010). Akt1 and Akt2 deficient HSCs show increased quiescence level whereas the apoptosis level in MPPs are increased (Juntilla et al., 2010). It has also been shown that Akt1 and Akt2 help to maintain a critical balance of ROS level in HSCs, which in turn regulates differentiation and proliferation of HSCs (Juntilla et al., 2010).

Deletion of mTOR in adult mice results in reduced count in neutrophils and monocytes, which contributes to an overall decrease in WBCs when compared to

controls (Guo et al., 2013). Furthermore, the platelet count as wells as RBCs and hemoglobin level were decreased in the peripheral blood of *mTOR-/-* mice (Guo et al., 2013). The absolute number of HSCs were increased in *mTOR-/-* mice, which was associated with increased cell cycling (Guo et al., 2013). Bone marrow cellularity as well as absolute number of myeloid cells and different subsets of B lymphocytes (pre/pro B cells, immature B cells and mature B cells) were significantly reduced in the BM of *mTOR-/-* mice (Guo et al., 2013). This reduction in absolute number was associated with an increase in apoptosis of myeloid and lymphoid cells in mTOR deficient mice (Guo et al., 2013). Furthermore, the absolute number of CMPs was decreased in *mTOR-/-* mice along with an increase in CLPs (Guo et al., 2013). Lineage negative cells derived from bone marrow of *mTOR-/-* mice showed reduced activation of S6K1 (Guo et al., 2013). These data suggest that mTOR mediated S6K1 activation might play a critical role in development and maintenance of HSCs and HPCs. In another study, treatment with rapamycin increased the number of LSK cells when murine HSCs were cultured ex-vivo (Luo et al., 2014). Rapamycin also increases the CAFC number of ex-vivo cultured murine HSCs. However, although the roles of PI3K, Akt and mTOR in development and maintenance of HSCs and HPCs are known, the role of S6K1 in this aspect is hitherto unknown.

In this chapter, we show that deficiency of S6K1 results in reduced overall BM cellularity and phenotypically defined HSC number. We also show that S6K1 is a regulator of HSC quiescence and following deficiency of S6K1, HSCs have reduced expression of *p21*. We further provide evidence that the reduction in the

absolute hematopoietic cell number in *S6K1-/-* mice is not due to the loss of expression of S6K1 in the hematopoietic niche.

Results:

***S6K1* is expressed in HSCs and HPCs:**

Previous studies have demonstrated that S6, a downstream substrate of S6K1, is expressed and activated in HSCs and HPCs (Magee et al., 2012). However, as S6 can be activated by S6K2 too (Pende et al., 2004), activation of S6 is not an appropriate indicator of S6K1 activity and expression. We sorted HSCs, HPCs and mature hematopoietic cells based on cell surface expression of markers and analyzed the expression level of *S6K1* in these subsets by qRT-PCR. We found that *S6K1* is expressed in HSCs as well as in MPPs and mature hematopoietic cells (Figure 4A). However, when *S6K1* expression is normalized relative to the expression level of HSCs, GMPs and MEPs have significantly increased *S6K1* expression whereas *S6K1* expression in mature myeloid cells is significantly decreased (Figure 4A). We did not observe any significant change in expression level of S6K1 in MPPs, CLPs, CMPs and B lymphocytes relative to HSCs (Figure 4A).

***S6K1-/-* mice have reduced BM MNCs and HSCs:**

Previous studies have linked mTORC1 activity with absolute hematopoietic cell numbers (Guo et al., 2013). To determine the effect of S6K1 deficiency on absolute hematopoietic cell numbers, we isolated BM MNCs from age-matched and sex-matched WT and *S6K1-/-* mice. *S6K1-/-* mice had significantly reduced BM MNCs compared to WT controls (Figure 4B). Based on expression of CD150 and CD48, LSK cells can be broadly divided into HSCs and MPPs (Figure 5A). In *S6K1-/-* mice, there was no change in the frequency of

Figure 4

A

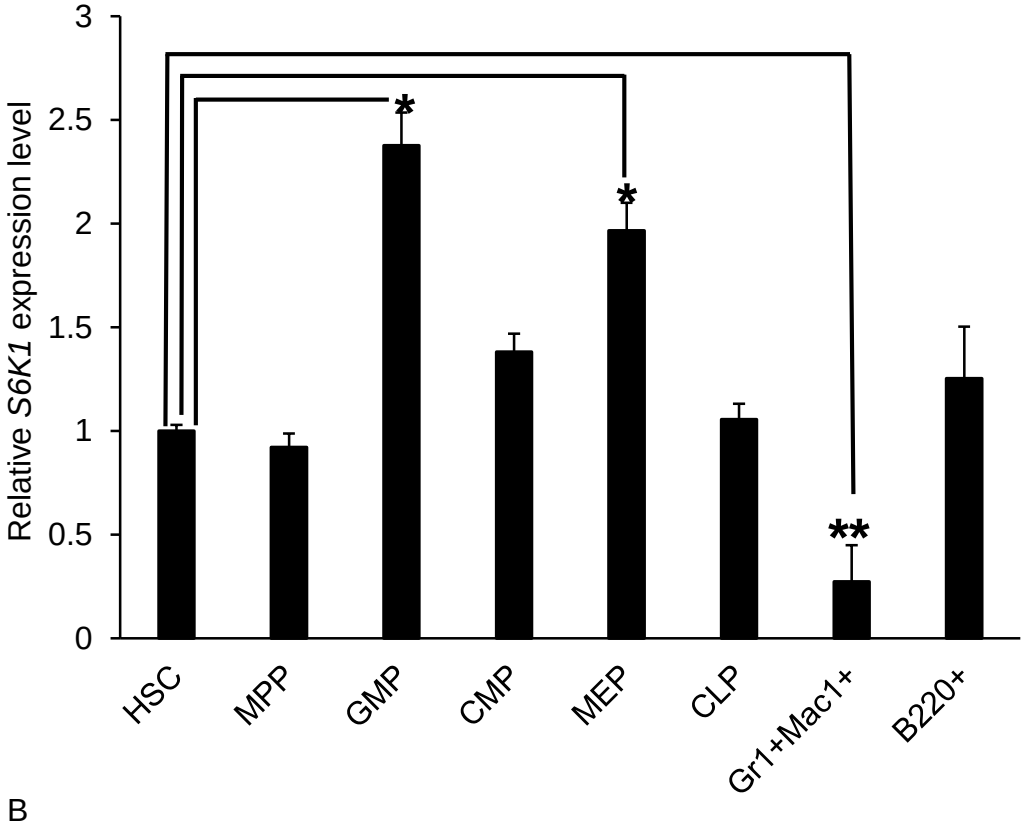
Relative S6K1 expression level
3
2.5
2
1.5
1
0.5
0
*
*
**
HSC
MPP
GMP
CMP
MEP
CLP
Gr1+Mac1+
B220+

B

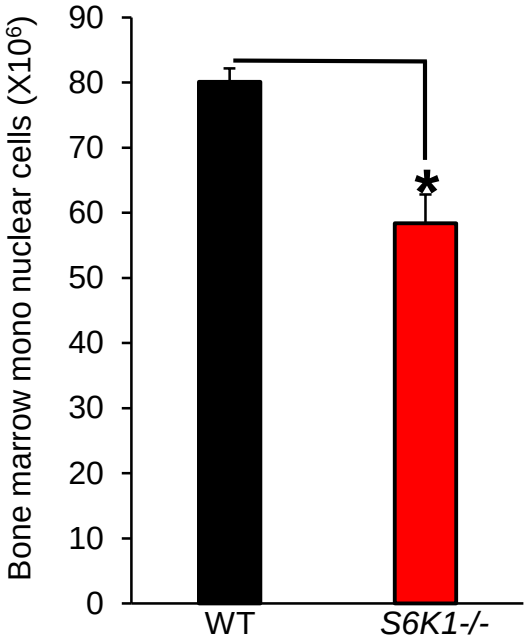
Bone marrow mono nuclear cells (X10⁶)
90
80
70
60
50
40
30
20
10
0
*
WT
S6K1-/-

Figure 4: Expression level of *S6K1* in HSCs and HPCs and effect of S6K1 deficiency on absolute number of mono nuclear cells in bone marrow.

(A) Expression of S6K1 in HSCs, HPCs and mature effector cells as determined by qRT-PCR. BM MNCs were isolated from WT mice and stained for cell surface markers to identify HSC, MPP, GMP, CMP, MEP, CLP, mature myeloid cells and B cells. Cells were sorted using flow cytometry and total RNA was isolated. cDNA was synthesized from total RNA using reverse transcriptase. Using SYBR Green Master mix and primers designed to specifically amplify murine *S6K1*, expression level of *S6K1* in each subset was determined. *S6K1* expression level in each subset was normalized to β*-actin* expression and expressed as values relative to HSCs. Experiment was performed in quadruplicate. Data are expressed as mean ± SD; *p<0.05. (B) BM MNCs were isolated from WT and *S6K1-/-* mice and total number of MNCs in two femurs, two tibias, and two iliac crests was determined. n=4-5 mice in each group. Data are expressed as mean ± SEM; *p<0.05.

Figure 5

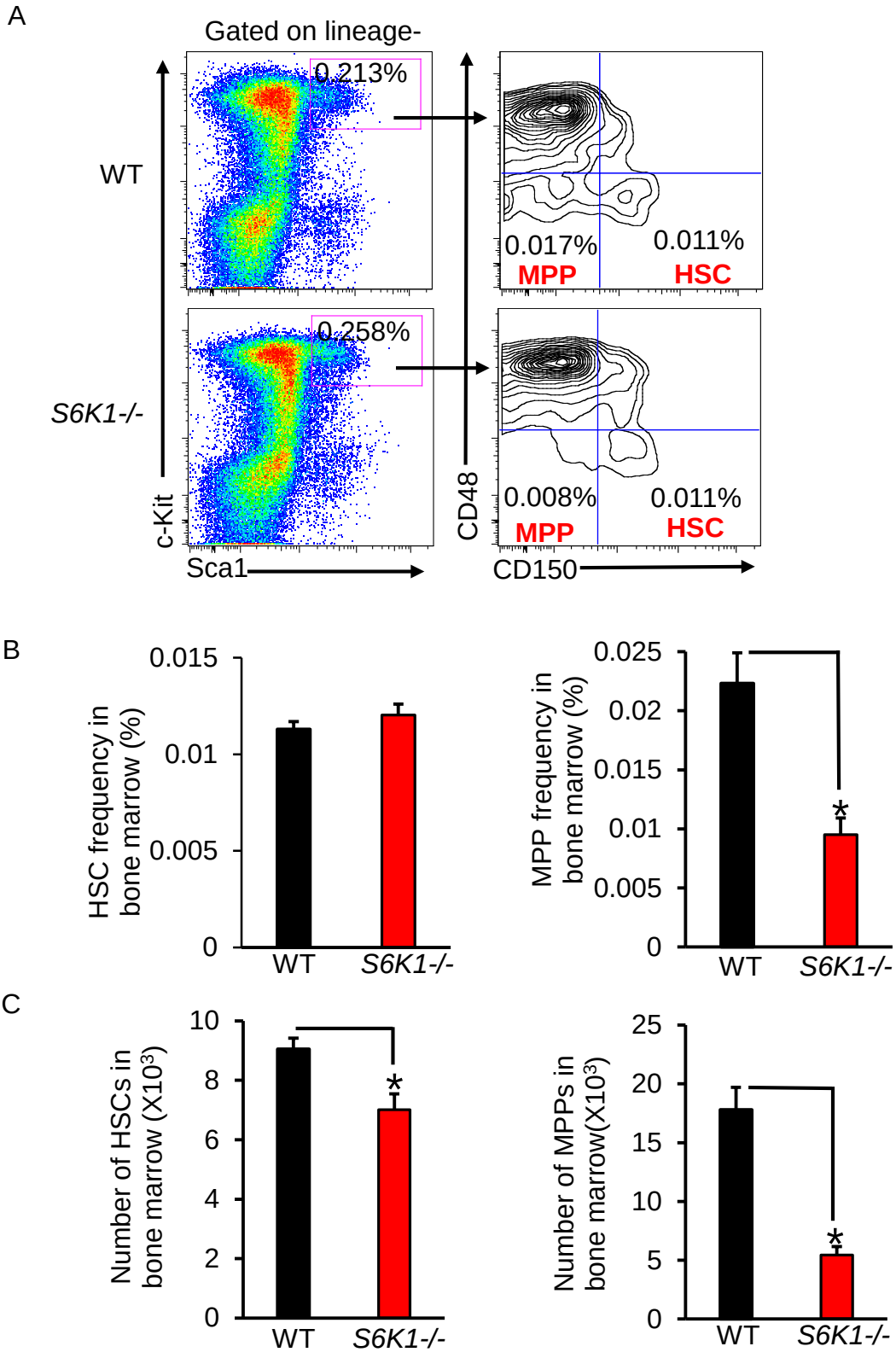
A
Gated on lineage-
WT
S6K1-/-
0.213%
0.258%
0.017%
MPP
0.011%
HSC
0.008%
MPP
0.011%
HSC
c-Kit
Sca1
CD48
CD150
B
HSC frequency in bone marrow (%)
0.015
0.01
0.005
0
WT
S6K1-/-
MPP frequency in bone marrow (%)
0.025
0.02
0.015
0.01
0.005
0
WT
S6K1-/-
C
Number of HSCs in bone marrow (X10³)
10
8
6
4
2
0
WT
S6K1-/-
Number of MPPs in bone marrow(X10³)
25
20
15
10
5
0
WT
S6K1-/-

Figure 5: *S6K1-/-* mice have reduced HSCs.

(A) Representative dot plot of BM HSCs (CD150+ CD48- LSK cells) gated on LSK cells of WT and *S6K1-/-* mice. (B) Frequency of HSCs (CD150+ CD48- LSK), MPPs (CD150- CD48- LSK) populations in WT and *S6K1-/-* mice were determined by flow cytometry. (C) Absolute numbers of HSCs and MPPs in two femurs, two tibias and two iliac crests of WT and *S6K1-/-* mice. n=4-5 mice in each group. Data are expressed as mean ± SEM; *p<0.05.

HSCs compared to WT (Figure 5B). However, the frequency of MPPs were significantly reduced in *S6K1-/-* mice compared to WT controls (Figure 5B). In terms of absolute cell numbers, *S6K1-/-* mice have significantly reduced HSCs and MPPs compared to WT controls (Figure 5C).

S6K1 is a positive regulator of HSC quiescence:

Ki-67, a nuclear nonhistone protein, is present in the nuclei of cells in the G1, S and G2 phase of cell cycle and absent in the cells that are in G0 phase (Gerdes et al., 1984; Gerdes et al., 1991). This unique property of this protein has been used to identify quiescent cells in the bone marrow. We stained HSCs from WT and *S6K1-/-* mice to determine the effect of S6K1 deficiency on quiescence of HSCs. The frequency of Ki-67 negative cells in *S6K1-/-* HSCs was significantly decreased compared to WT LT-HSCs (Figure 6A). As these data indicate that the HSCs in *S6K1-/-* mice were less quiescent, we next examined expression level of different genes known to regulate quiescence in HSCs. The expression of *p21* was significantly reduced in *S6K1-/-* HSCs compared to WT controls (Figure 6B). However, we did not find any change in mRNA expression level of *p27, p130, PTEN, Bmi1* and *Hoxa9* expression in *S6K1-/-* HSCs.

S6K1 regulates frequency and absolute number of HPCs and terminally differentiated cells:

Previous studies on *mTOR-/-* mice have shown that mTOR deficiency results in reduced number of CMPs as well as myeloid and B cells in bone marrow (Guo et al., 2013). These data indicate that S6K1 activity might be a critical regulator of hematopoietic progenitor and terminally differentiated cell

Figure 6

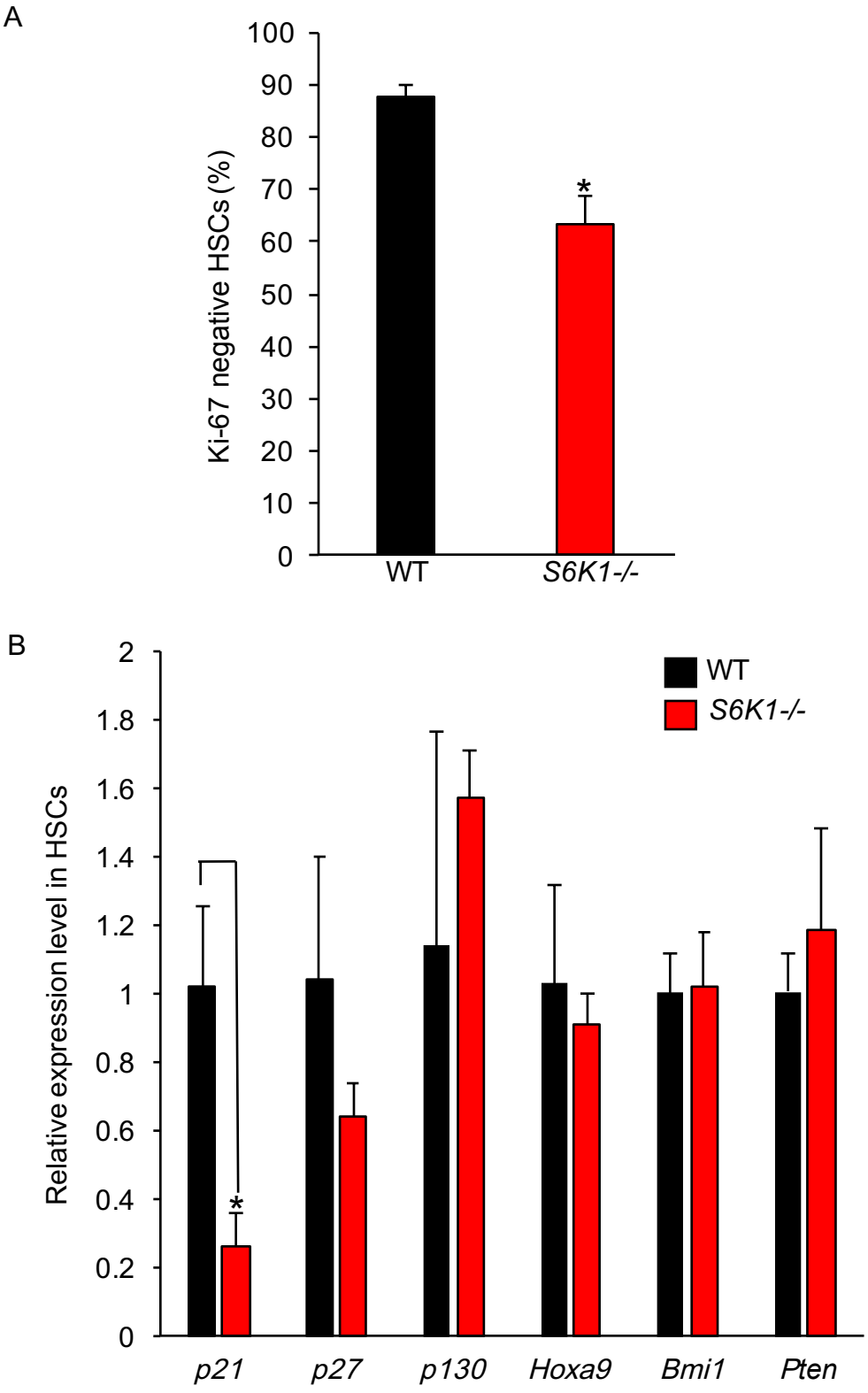
A
Ki-67 negative HSCs (%)
100
90
80
70
60
50
40
30
20
10
0
*
WT
S6K1-/-
B
Relative expression level in HSCs
2
1.8
1.6
1.4
1.2
1
0.8
0.6
0.4
0.2
0
WT
S6K1-/-
*
p21
p27
p130
Hoxa9
Bmi1
Pten

Figure 6: S6K1 deficiency results in reduced quiescence of HSCs.

(A) Quantitative representation of frequency of Ki-67 negative BM HSCs (CD150+ CD48- LSK cells) in WT and *S6K1-/-* mice. n=4-5 mice in each group. Data are expressed as mean ± SEM; *p<0.05. (B) Expression levels of genes regulating quiescence in HSCs were determined in HSCs isolated from BM of WT and *S6K1-/-* mice. Expression level of each gene was normalized with respect to *β-actin*. Experiment was performed in triplicates. Data are expressed as mean ± SEM; *p<0.05.

numbers. To determine the effect of S6K1 deficiency on hematopoietic progenitor and terminally differentiated cells, we analyzed the frequency and absolute number of HPCs along with mature myeloid cells and B lymphocytes in WT and *S6K1-/-* mice. The frequency of GMP was significantly increased in *S6K1-/-* mice while the frequency of MEP was significantly decreased compared to WT controls (Figure 7A). The absolute number of CMP and MEP was significantly decreased in *S6K1-/-* mice compared to WT controls, although we did not observe any difference in absolute GMP number between two genotypes (Figure 7B). We observed a significant increase in the frequency of mature myeloid cells whereas the frequency of mature B lymphocytes was significantly reduced in *S6K1-/-* compared to WT controls (Figure 8A and B). However only the absolute number of B lymphocytes in BM of *S6K1-/-* mice was significantly reduced (Figure 8C). There was no difference in absolute number of mature myeloid cells between *S6K1-/-* mice and WT controls.

The decrease in BM MNC number in *S6K1-/-* mice is cell intrinsic:

Previous studies have shown that *S6K1-/-* mice have reduced body size compared to WT mice (Pende et al., 2004; Selman et al., 2009). To determine whether the reduced BM cellularity in *S6K1-/-* mice is due to deficiency of S6K1 in BM microenvironment, we transplanted lethally irradiated WT and *S6K1-/-* mice with WT BM MNCs (Figure 9A). We analyzed the absolute number of BM MNCs at 16 weeks following transplant. We found that there were no significant differences in the BM MNC numbers between two groups of WT BM MNC recipients (Figure 9B). To further determine whether the decrease in the BM

Figure 7

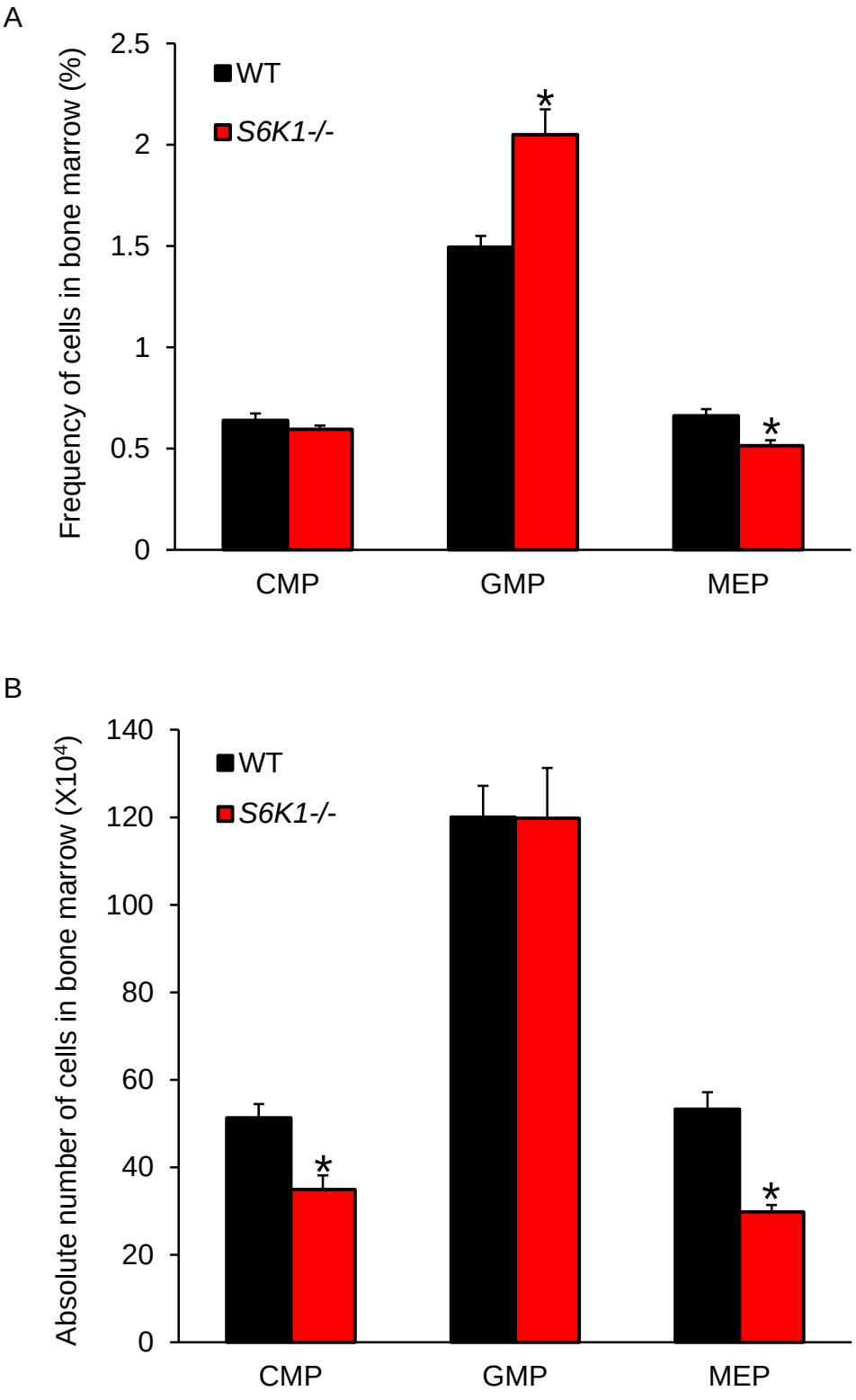
A
Frequency of cells in bone marrow (%)
2.5
2
1.5
1
0.5
0
WT
S6K1-/-
*
*
CMP
GMP
MEP
B
Absolute number of cells in bone marrow (X10⁴)
140
120
100
80
60
40
20
0
WT
S6K1-/-
*
*
CMP
GMP
MEP

Figure 7: *S6K1-/-* mice have altered HPC population in bone marrow.

(A) Quantitative representation of frequency of CMP, GMP and MEP in BM of WT and *S6K1-/-* mice. n=4-5 in each group. Data are expressed as mean ± SEM; *p<0.05. (B) Absolute numbers of CMP, GMP and MEP in two femurs, two tibias, and two iliac crests of WT and *S6K1-/-* mice; n=4-5 mice in each group. Data are expressed as mean ± SEM; *p<0.05.

Figure 8

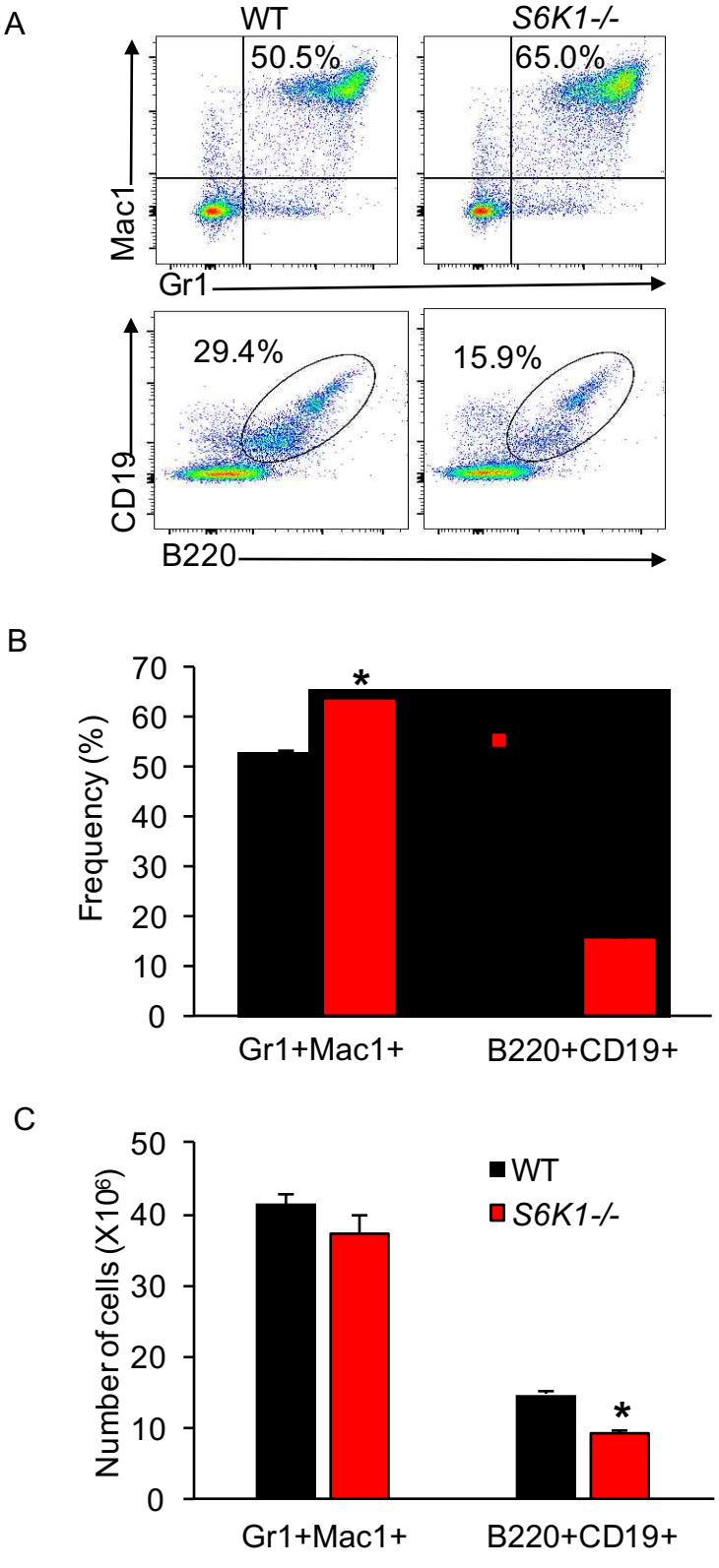
A
WT
S6K1-/-
50.5%
65.0%
Mac1
Gr1
29.4%
15.9%
CD19
B220
B
Frequency (%)
70
60
50
40
30
20
10
0
*
Gr1+Mac1+
B220+CD19+
C
Number of cells (X10⁶)
50
40
30
20
10
0
WT
S6K1-/-
*
Gr1+Mac1+
B220+CD19+

Figure 8: *S6K1-/-* mice have altered mature hematopoietic population in bone marrow.

(A) Representative dot plot of mature myeloid cells (Gr1+ Mac1+) and B lymphocytes (B220+ CD19+) in BM of WT and *S6K1-/-* mice. (B) Frequency of mature myeloid cells and B lymphocytes in BM of WT and *S6K1-/-* mice. (C) Absolute number of mature myeloid cells and B lymphocytes in two femurs, two tibias, and two iliac crests of WT and *S6K1-/-* mice; n=4-5 mice in each group. Data are expressed as mean ± SEM; *p<0.05.

cellularity was cell intrinsic, we transplanted lethally irradiated WT mice with either WT or *S6K1-/-* BM MNCs (Figure 10A). We analyzed the absolute number of BM MNCs at 16 weeks following transplant. We found that WT recipients of *S6K1-/-* BM MNCs showed significant reduction in BM MNCs compared to recipients of WT BM MNCs (Figure 10B). Taken together, these data suggest that the decreased number of BM MNCs seen in *S6K1-/-* mice is cell-intrinsic, and not dependent on the expression of S6K1 in the BM microenvironment.

Figure 9

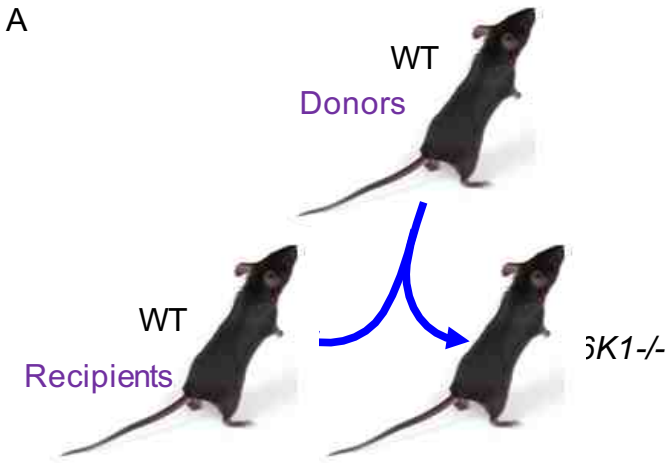
A
WT
Donors
WT
Recipients
6K1-/-

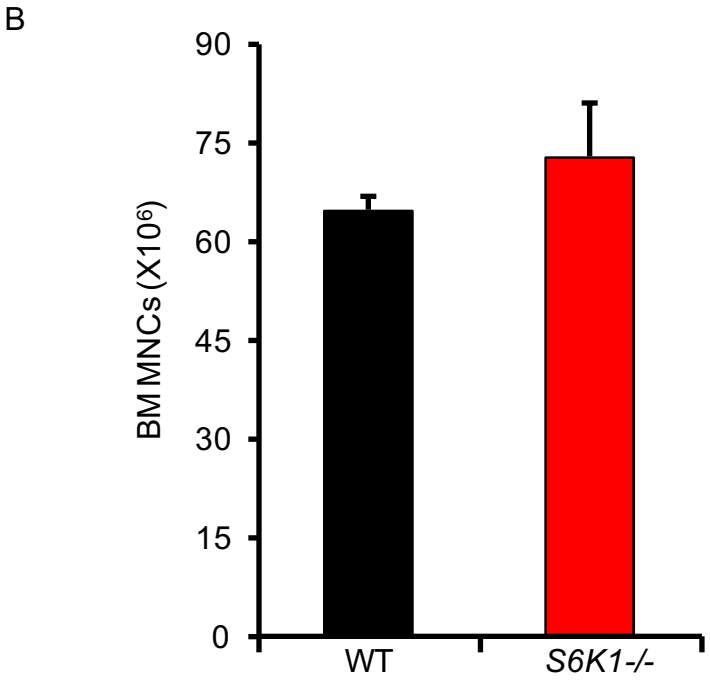
B
90
75
60
45
30
15
0
BM MNCs (X10⁶)
WT
S6K1-/-

Figure 9: The decrease in BM MNCs in *S6K1-/-* mice is not microenvironment dependent.

(A) Model of transplantation assay to determine the effect of S6K1 deficiency in BM microenvironment on absolute number of BM MNCs. BM MNCs were isolated from WT mice and transplanted into lethally irradiated WT and *S6K1-/-* mice. BM MNC number was determined at 16 weeks post-transplant. (B) Absolute number of BM MNCs isolated from two femurs, two tibias, and two iliac crests of transplant recipients at 16 weeks post-transplant. Data are expressed as mean ± SEM; n=4-5 mice in each group.

Figure 10

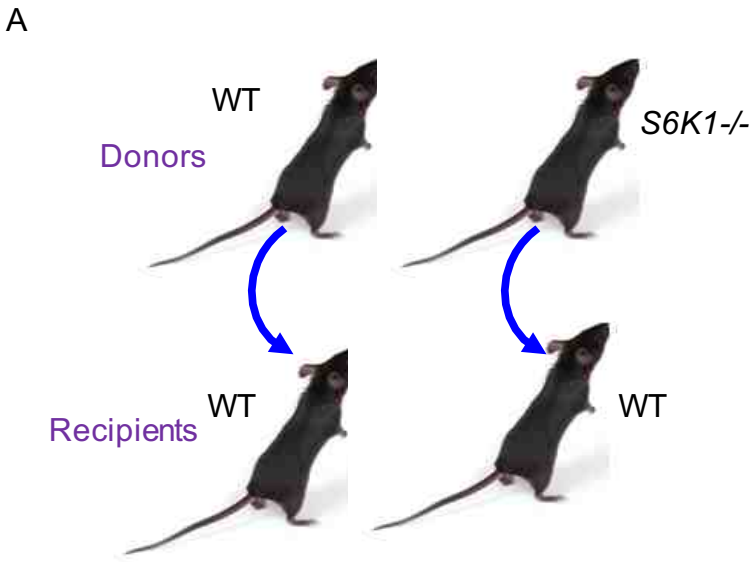
A
WT
Donors
S6K1-/-
WT
Recipients
WT

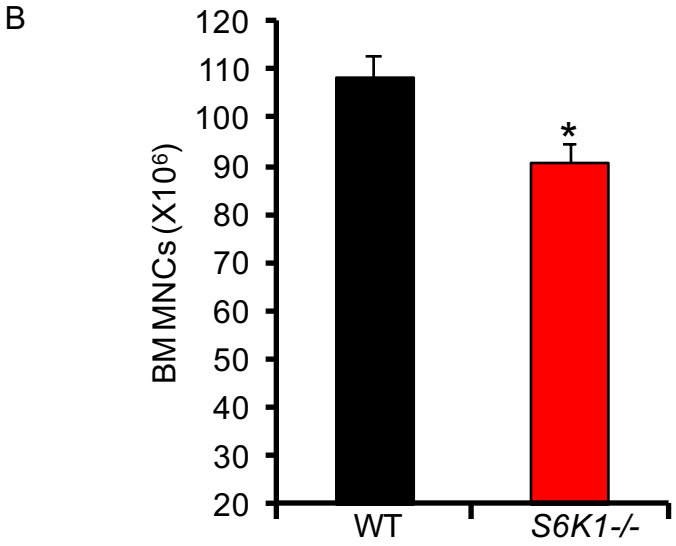
B
BM MNCs (X10⁶)
120
110
100
90
80
70
60
50
40
30
20
*
WT
S6K1-/-

Figure 10: The decrease in BM MNCs in *S6K1-/-* mice is cell-intrinsic.

(A) Model of transplantation assay to determine the effect of S6K1 deficiency in HSCs on absolute number of BM MNCs. BM MNCs were isolated from WT and *S6K1-/-* mice and transplanted into lethally irradiated WT mice. BM MNC number was determined at16 weeks post-transplant. (B) Absolute number of BM MNCs isolated from two femurs, two tibias, and two iliac crests of transplant recipients in (A) at 16 weeks post-transplant. n=4-5 mice in each group. Data are expressed as mean ± SEM; *p<0.05.

Discussion:

The role of mTORC1 activation on steady state hematopoiesis has been well characterized (Guo et al., 2013; Juntilla et al., 2010; Magee et al., 2012). However, following activation of mTORC1, 4E-BP1 is inactivated and S6K1 is activated. Downstream of mTORC1 how these two molecules regulate steady state hematopoiesis has not been explored. We found that *S6K1* is expressed in all the hematopoietic subsets in mice, including HSCs and HPCs. However, the expression level of *S6K1* is significantly elevated in GMPs and downregulated in mature myeloid cells relative to HSCs (Table 3). Interestingly, in *S6K1-/-* mice, the frequency of GMP and mature myeloid cells were both upregulated. These data suggest that S6K1 might play a role in differentiation and maturation of myeloid cells. In *mTOR-/-* mice, GMP frequency was also elevated compared to WT. Along with our data, it can be concluded that S6K1 negatively regulates GMP frequency in hematopoietic compartment. Although S6K1 is expression is relatively low in mature myeloid cells compared to HSCs, our data suggests that S6K1 is a negative regulator of maturation of myeloid cells. However, this study has not assessed whether the increase in GMP frequency in *S6K1-/-* mice corresponds to an increase in functional potential or not. Further studies are required to determine the effect of S6K1 deficiency on the functional potential of GMPs. *In vitro* CFU assay with sorted GMP population from WT and *S6K1-/-* mice could further elucidate the role of S6K1 on the functional ability of GMPs.

Our data establishes S6K1 as critical regulator of absolute number of hematopoietic cells. These findings also corroborate previous studies where loss

Table 3: Effect of S6K1 deficiency on different hematopoietic subsets in bone marrow compared to WT controls.

Population	Frequency	Absolute number
HSC	No change	Decreased
MPP	Decreased	Decreased
CMP	No change	Decreased
GMP	Increased	No change
MEP	Decreased	Decreased
Gr1+Mac1+	Increased	No change
B220+CD19+	Decreased	Decreased

of expression of upstream effectors of S6K1 results in reduced hematopoietic cellularity in fetal liver and bone marrow. We also provide evidence that the reduced cellularity in *S6K1-/-* mice is not because of deficiency of S6K1 in hematopoietic niche. Our findings are in line with study with *mTOR-/-* mice. *mTOR-/-* mice have reduced number of absolute hematopoietic cells despite having less quiescent HSC/Ps (Guo et al., 2013). Further studies are required to determine the exact mechanism underlying reduced cellularity in *S6K1-/-* mice. S6K1 could also regulate HSC/P number by also regulating glycolysis. S6K1 has been shown to be a positive regulator of glycolysis in hematopoietic cells. Recently Takubo et al. had shown that regulation of glucose metabolism is critical for HSC functions (Takubo et al., 2013). HSCs deficient in PDK2 and PDK4 have reduced glucose metabolism. Mice transplanted with PDK2 and PDK4 HSCs have reduced BM MNCs (Takubo et al., 2013). A study by Liu et al. had shown that PDK4 is an activator of mTORC1 (Liu et al., 2014b). Overexpression of PDK4 upregulates mTORC1 activity in murine fibroblasts. It is probable that in *S6K1-/-* HSCs PDK4 mediated glycolysis has been downregulated, which resulted in reduced number of hematopoietic cells in BM. Further studies are required to determine if S6K1 deficiency affects steady state hematopoiesis by altering their metabolic profile.

In our studies, we observed reduced quiescence in *S6K1-/-* HSCs as there was a decrease in number of HSCs in G0 phase of cell cycle compared to WT controls. In a previous study, HSCs deficient in mTOR, an activator of S6K1 activity, showed reduced quiescence in HSCs (Guo et al., 2013). Decrease in

quiescence has been associated with functional defects and exhaustion of HSCs. One of the key regulator of HSC quiescence is p21. P21 is a member of wild-type p53-activated fragment (WAF1), and Cdk-interacting protein (Cip1) family of protein (Harper et al., 1993) and acts as a cyclin dependent kinase (CDK) inhibitor (Brugarolas et al., 1998; Brugarolas et al., 1999). E2 factor (E2F) family of transcription factors are positive regulators of genes required for cell cycle progression into and through S phase (Johnson et al., 1993; Lukas et al., 1996; Qin et al., 1994). E2Fs are negatively regulated by p107 and p130, two members of retinoblastoma (Rb) family (Woo et al., 1997). CDK2 phosphorylates Rb proteins and promotes E2F-dependent gene transcription (Akiyama et al., 1992; Woo et al., 1997). P21 binds to CDK2 and disrupts the interaction between CDK and Rb proteins (Shiyanov et al., 1996; Zhu et al., 1995). This disruption in binding with Rb proteins inhibits CDK2 activity, thus resulting in inhibition of E2F-dependent gene transcription (Brugarolas et al., 1999; Shiyanov et al., 1996). CDK2–cyclin A interaction is required for progression through S and G2 phase (Gu et al., 1992; Hu et al., 2001). P21 inhibits the kinase activity of CDK2 thus inhibiting cell cycle progression. Furthermore, p21 has also been shown to be an inhibitor of the kinase activity of CDK1, which results in inhibition of cell cycle progression through G2 and G2/M phase (Satyanarayana et al., 2008). P21 can also associate with E2F1 directly and suppress cellular growth (Dimri et al., 1996). In response to notch1 activation, p21 inhibits E2F1-dependent Wnt4 expression (Devgan et al., 2005). P21 has also been demonstrated as both necessary and sufficient to mediate p53-dependent repression of genes that

promotes cell cycle progression (Gottifredi et al., 2001; Lohr et al., 2003; Shats et al., 2004). *P21-/-* HSCs undergo increased cycling and exhaust upon serial transplantation (Cheng et al., 2000). We show that *S6K1-/-* HSCs have reduced *p21* expression level compared to controls. Thus, *S6K1-/-* HSCs could be less quiescent due to decrease in p21 expression. However, further studies are required to determine the exact mechanism of how S6K1 regulates p21 expression in HSCs.

In summary, we have established the role of S6K1 in steady state hematopoiesis. We have demonstrated that S6K1 is expressed in HSCs and deficiency of S6K1 results in reduced HSC number (Table 3) as well as a decrease in overall HSC/P number. Deficiency of S6K1 results in altered HPC and mature effector cells in BM (Table 3). Moreover, we also provide evidence that S6K1 is a positive regulator of HSC quiescence. We also provide evidence suggesting that S6K1 is a positive regulator of *p21* expression in HSCs.

Chapter 4: Role of S6K1 in stress hematopoiesis

Introduction:

Following exposure to effectors that induce cellular stress, cells respond in multiple ways in order to defend against the stress as well as to recover following the stress (Kultz, 2005). The responses include activation of pro-survival pathways and initiating programmed cell death to eliminate damaged cells. Previous studies have established S6K1 as a critical regulator of cellular responses to stress. Treatment with doxorubicin, a chemotherapeutic agent, upregulates S6K1 phosphorylation in mouse embryonic fibroblasts in a p38α MAPK dependent manner (Lai et al., 2010). Activated S6K1 inhibits Mdm2 – mediated ubiquitination and degradation, which results in increased apoptosis in cells following Doxorubicin treatment (Lai et al., 2010).

In another model of cellular stress, free fatty acids (FFA) induce endoplasmic reticulum (ER) stress in hepatocytes in a S6K1-dependent manner (Pardo et al., 2015). Inhibition of S6K1 activity results in reduced FFA induced ER stress in murine hepatocytes (Pardo et al., 2015). A recent study showed that the response to ER stress is critical for HSC function. In hematopoietic system, 5-FU has been used extensively to study stress hematopoiesis. In HSC/Ps, 5-FU treatment results in increased S6K1 activity (Basu, 2014). Peroxisome-proliferator-activated-receptor γ coactivator 1 beta (PGC1β) is required for an efficient ER stress response in mouse brain in response to high fat diet (HFD). Deficiency of PGC1β results in apoptosis of neurons following administration of

HFD. In PGC1β deficient neurons, reduced stress response is associated with reduced mTORC1 activity. PGC1α is another member of PGC family and is expressed in HSCs. In *PGC1α-/-* mice, S6K1 phosphorylation level, mitochondrial membrane potential and ROS level are elevated in HSC/Ps following 5-FU treatment (Basu, 2014). Rapamycin treatment reduces S6K1 phosphorylation in 5-FU treated *PGC1α-/-* HSCs, which resulted in reduced ROS level and mitochondrial membrane potential (Basu, 2014). Overall, these data suggest that S6K1 plays a critical role in stress response in different cells. However, the exact role of S6K1 in the regeneration of HSCs following myeloablative stress is not well defined.

In this chapter, we show that following myeloablative stress, S6K1 deficient HSC/Ps increase in frequency. We also show that the increased frequency of HSC/P is in part due to increase in cell cycle of S6K1 deficient HSC/Ps. Competitive transplantation using 5-FU treated HSC/Ps showed reduced functional potential of *S6K1-/-* HSC/Ps compared to controls following exposure to chemotherapeutic agent. We also demonstrate that myeloablative stress results in reduced quiescence of S6K1 deficient HSC/Ps that renders them susceptible to repeated myeloablative stress.

Results:

S6K1 regulates recovery of HSC/Ps following myelotoxic stress:

Following 5-FU injection, cycling HSCs and HPCs acquire DNA damage and undergo apoptosis. Quiescent HSCs undergo self-renewal and differentiation for recovery of the mature hematopoietic cells as well as to replenish the HSC pool (Harrison and Lerner, 1991; Venezia et al., 2004). To determine the role of S6K1 in the recovery of hematopoietic system following myelotoxic stress, we injected WT and *S6K1-/-* mice with a single dose of 5-FU. We monitored the recovery of peripheral blood WBCs at different time points post 5-FU treatment. No significant change in WBC counts in the peripheral blood of *S6K1-/-* mice were seen compared to WT controls after 5-FU treatment (Figure 11A).

To determine the effect of 5-FU on S6K1 deficient BM HSC/Ps, we determined the bone marrow cellularity of WT and *S6K1-/-* mice after 5-FU injection at different time points (Figure 11B). As described in the previous chapter, there was a significant reduction in the BM MNC number of *S6K1-/-* mice at day 0 (Figure 11B). However, the difference in BM cellularity did not persist on day 6 and day 9 post 5-FU treatment. We observed a significant difference in the BM cellularity on day 15 post 5-FU injection (Figure 11B). In the hematopoietic hierarchy, LSK cells are a heterogeneous population that are enriched in HSCs having long-term repopulating potential as well as MPPs (Uchida et al., 1994). We analyzed the LSK frequency in BM of WT and *S6K1-/-* mice at different time point after 5-FU treatment. In the BM of *S6K1-/-* mice, there was a significant increase in LSK frequency on day 9 after 5-FU treatment

Figure 11

A

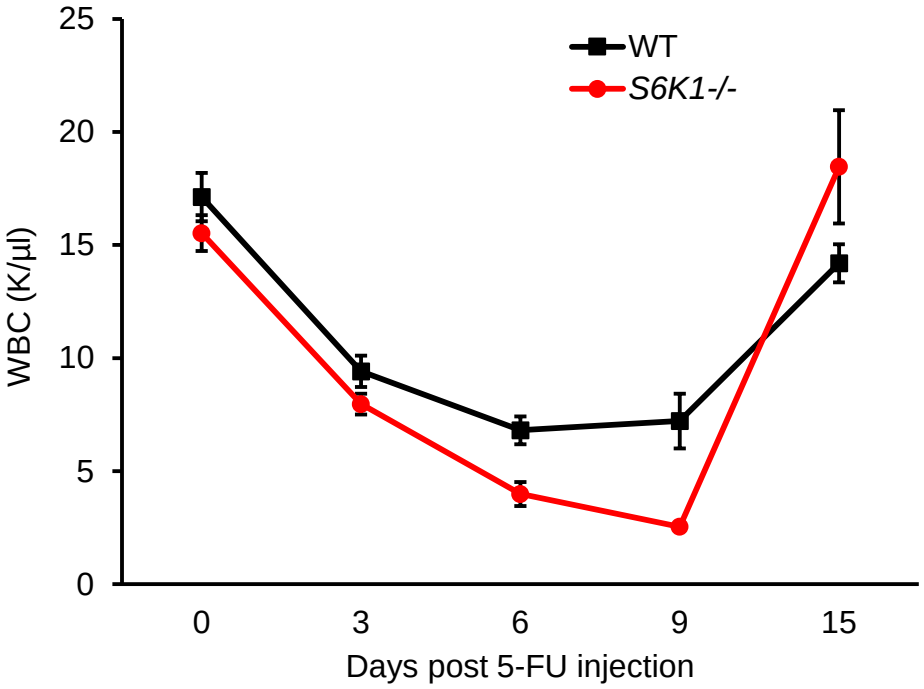
25
20
15
10
5
0
WBC (K/µl)
WT
S6K1-/-
0
3
6
9
15
Days post 5-FU injection

B

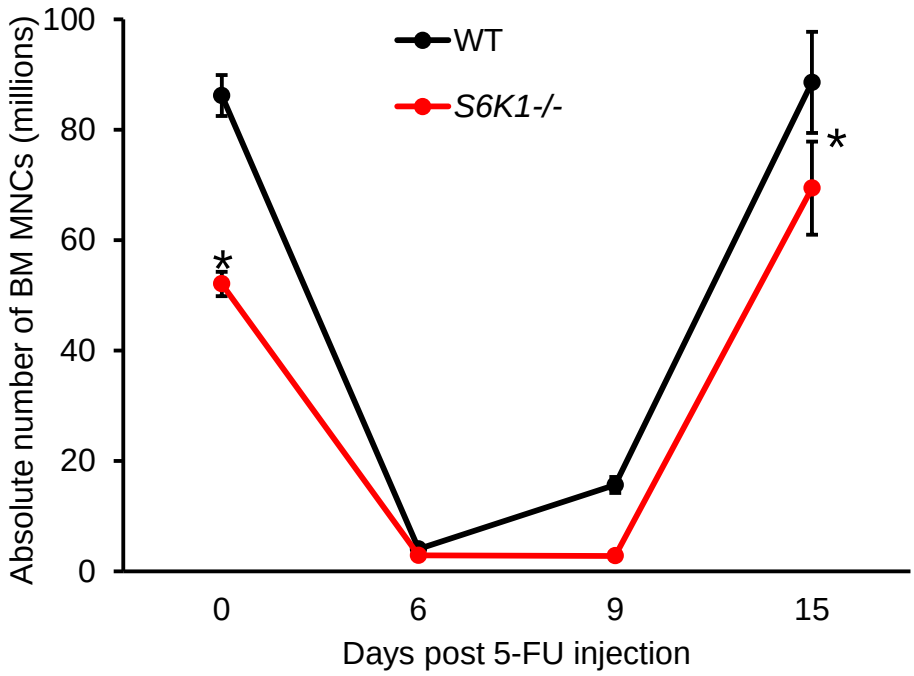
100
80
60
40
20
0
Absolute number of BM MNCs (millions)
WT
S6K1-/-
*
*
0
6
9
15
Days post 5-FU injection

Figure 11: Effect of loss of expression of S6K1 on recovery of hematopoietic system following myeloablative stress.

(A) Quantitative representation of WBC count in peripheral blood of WT and *S6K1-/-* mice at different time points following 5-FU treatment. Data are expressed as mean ± SEM; n=4-12 mice in each genotype. (B) Quantitative representation of BM MNC number isolated from two femurs, two tibias, and two iliac crests of WT and *S6K1-/-* mice at different time points following 5-FU treatment; n=12-19 mice in each group. Difference between the group means was analyzed by one-way ANOVA with Bonferroni post-hoc analysis. Data are expressed as mean ± SEM; *$p<0.05$.

Figure 12

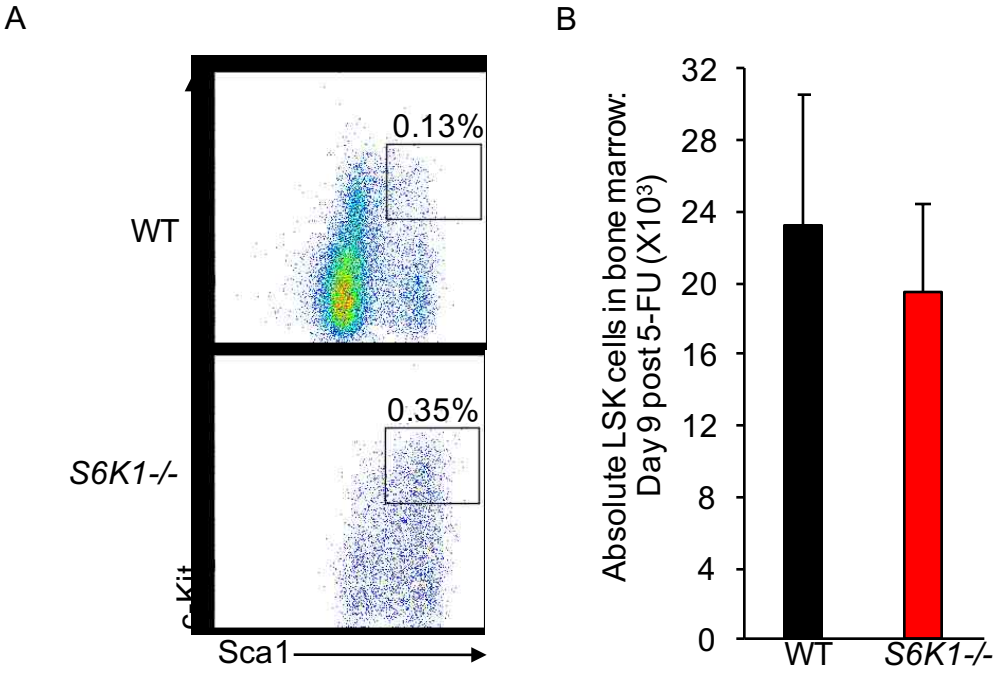
A
B
0.13%
WT
0.35%
S6K1-/-
c-Kit
Sca1
Absolute LSK cells in bone marrow:
Day 9 post 5-FU (X10³)
32
28
24
20
16
12
8
4
0
WT
S6K1-/-

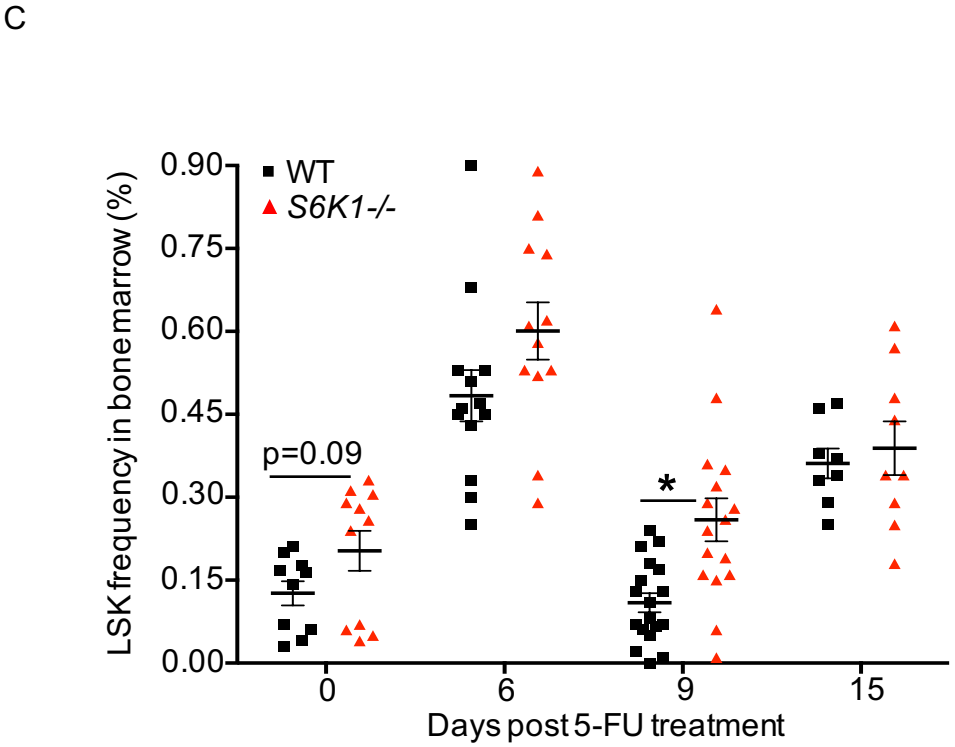
C
LSK frequency in bone marrow (%)
0.90
0.75
0.60
0.45
0.30
0.15
0.00
WT
S6K1-/-
p=0.09
*
0
6
9
15
Days post 5-FU treatment

Figure 12: Increased frequency of LSK cells in BM of *S6K1-/-* mice after 5-FU treatment.

(A) Representative dot plot of LSK cells in BM of WT and *S6K1-/-* mice after 9 day following a single dose of 5-FU. Cells are gated on linage negative population. (B) Quantitative representation of absolute number of LSK cells in the BM of WT and *S6K1-/-* mice at 9 days after 5-FU treatment; n=16-19 mice in each group. Data are expressed as mean ± SEM. (C) Quantitative representation of frequency of LSK cells in the BM of WT and *S6K1-/-* mice at different time points following a single dose of 5-FU; n=8-19 mice in each group in each time point. Difference between the group means was analyzed by one-way ANOVA with Bonferroni post-hoc analysis. Data are expressed as mean ± SEM; *$p<0.05$.

(Figure 12A and C). However, there was no difference in LSK frequency between the two groups at steady state and on day 6 and day 15 after 5-FU treatment (Figure 12C). Furthermore, there was no change in the absolute BM LSK number in *S6K1-/-* mice compared to WT controls after day 9 following 5-FU injection (Figure 12B). These data suggest that S6K1 deficiency results in a transient increase in the frequency of LSK cells during the recovery of the hematopoietic system following myelotoxic stress.

S6K1 deficiency results in increased cycling of HSC/Ps following myeloablative stress:

5′-bromo-2′-deoxyuridine (BrdU) is a DNA analog that is incorporated into the DNA of proliferating cells (Nowakowski et al., 1989). BrdU substitutes for thymidine residues within DNA during replication (Nowakowski et al., 1989). Analysis of BrdU incorporation into the DNA of replicating cells within a defined period can reveal what proportion of cells have undergone cell cycle in that period. BrdU incorporation over a short-term period has been previously used to identify the cycling status of HSCs (Cheshier et al., 1999; Fleming et al., 1993; Goodell et al., 1996). We hypothesized that the increase in frequency of LSK cells in the bone marrow of *S6K1-/-* mice on day 9 following 5-FU treatment could be due to increased cycling of the LSK population. We injected WT and *S6K1-/-* mice with BrdU on day 8 post 5-FU injection. After 16 hours, mice were euthanized, BM MNCs were isolated and stained for LSK cells. After staining, cells were washed and BrdU incorporation assay was performed. LSK cells in *S6K1-/-* mice displayed a significant increase in BrdU positive cells compared to WT controls

Figure 13

A

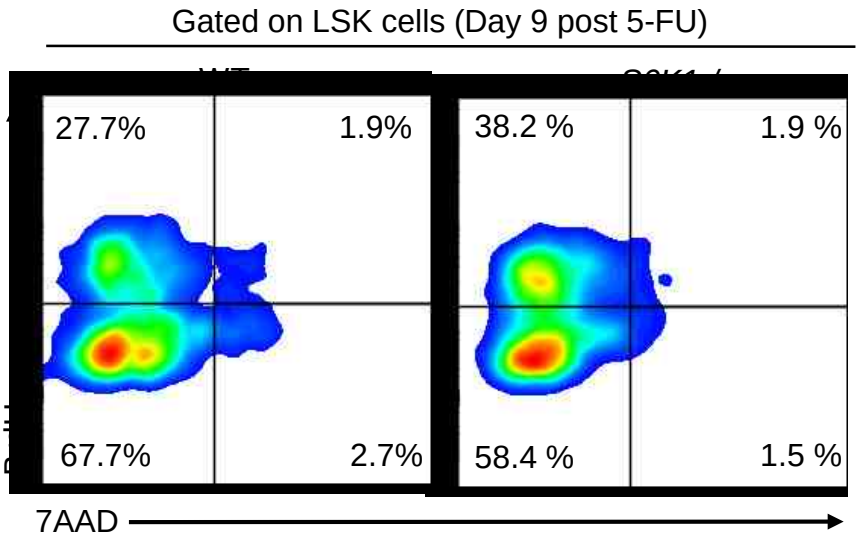
Gated on LSK cells (Day 9 post 5-FU)
27.7%
1.9%
67.7%
2.7%
38.2 %
1.9 %
58.4 %
1.5 %
7AAD

B

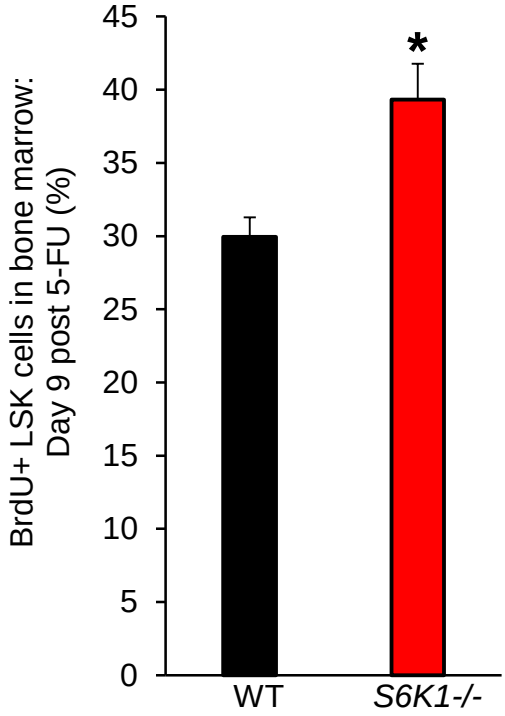
BrdU+ LSK cells in bone marrow:
Day 9 post 5-FU (%)
45
40
35
30
25
20
15
10
5
0
*
WT
S6K1-/-

Figure 13: *S6K1-/-* HSC/Ps undergo increased cycling following 5-FU treatment.

(A) Representative dot plot of BrdU+ LSK cells in BM of WT and *S6K1-/-* mice after 9 day following a single dose of 5-FU. Cells are gated on LSK population. (B) Quantitative representation of frequency of BrdU+ LSK cells in the BM of WT and *S6K1-/-* mice after 9 day following 5-FU treatment; n=3-4 mice in each group. Data are expressed as mean ± SEM; *p<0.05.

Figure 14

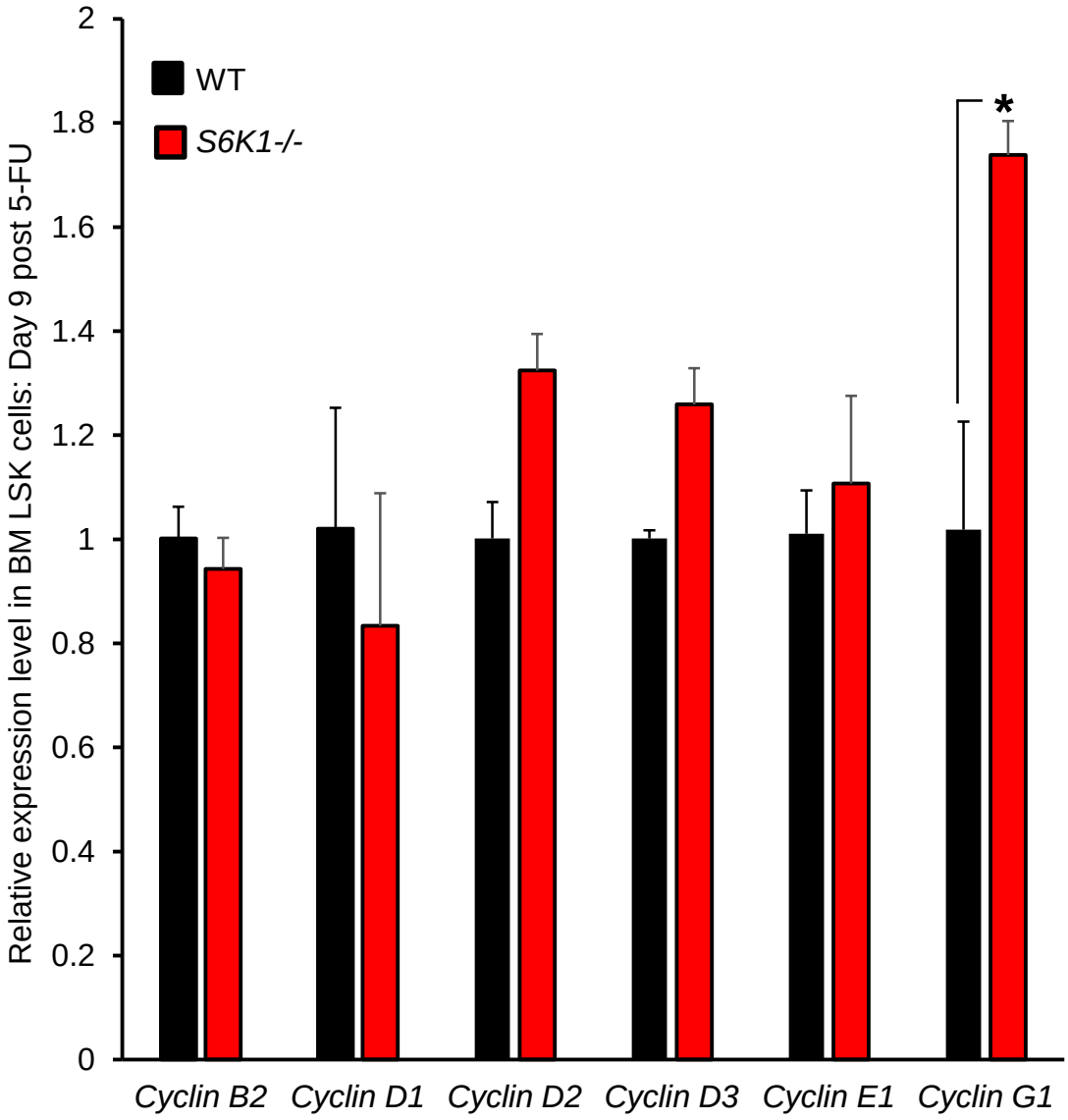
WT
S6K1-/-
Relative expression level in BM LSK cells: Day 9 post 5-FU
2
1.8
1.6
1.4
1.2
1
0.8
0.6
0.4
0.2
0
*
Cyclin B2
Cyclin D1
Cyclin D2
Cyclin D3
Cyclin E1
Cyclin G1

Figure 14: *Cyclin G1* expression is increased in *S6K1-/-* LSK cells following 5-FU treatment.

Expression level of genes regulating cell cycle in BM LSK cells isolated from WT and *S6K1-/-* mice 9 days following a single dose of 5-FU. Expression level in each gene was normalized to β *-actin* expression and expressed as values relative to WT. Experiment was performed in quadruplicates. Data are expressed as mean ± SD; *p<0.05.

(Figure 13A, B). This result suggests that following myelotoxic treatment, the HSC/P enriched population within the bone marrow undergoes increased cycling in the absence of S6K1. We next analyzed genes involved in regulating different phases of cell cycle. We isolated BM MNCs from WT and *S6K1-/-* mice on day 9 after 5-FU treatment and sorted LSK cells using FACS. We analyzed expression level of genes by qRT-PCR. Expression level of *Cyclin G1* was increased in the LSK population derived from *S6K1-/-* mice compared to WT control (Figure 14). This suggests that *Cyclin G1* might contribute to the increased cycling of LSK cells in absence of S6K1 following 5-FU treatment.

***S6K1-/-* mice are susceptible to repeated myeloablative stress:**

Quiescent HSCs within the bone marrow are protected from myeloablative treatment because of their low cell cycle status. Increase in cell cycle progression renders HSCs more susceptible to myeloablative stress (Miyamoto et al., 2007). Since we observed increased cycling of *S6K1-/-* LSK cells following myelotoxic stress, we hypothesized that loss of S6K1 expression in HSCs will result in increased susceptibility to such stress. For our studies, we have used a previously described model of repeated myeloablative stress (Miyamoto et al., 2007). WT and *S6K1-/-* mice were injected with weekly doses of 5-FU (Figure 15A). As 5-FU ablates the proliferating HSCs, quiescent HSCs are forced to proliferate and reconstitute the hematopoietic system. However, due to repeated doses of 5-FU, the quiescent HSCs that started proliferating after previous dose of 5-FU is depleted and a new pool of quiescent HSCs is required to reconstitute the hematopoietic system and mice with reduced number of quiescent HSCs succumb

Figure 15

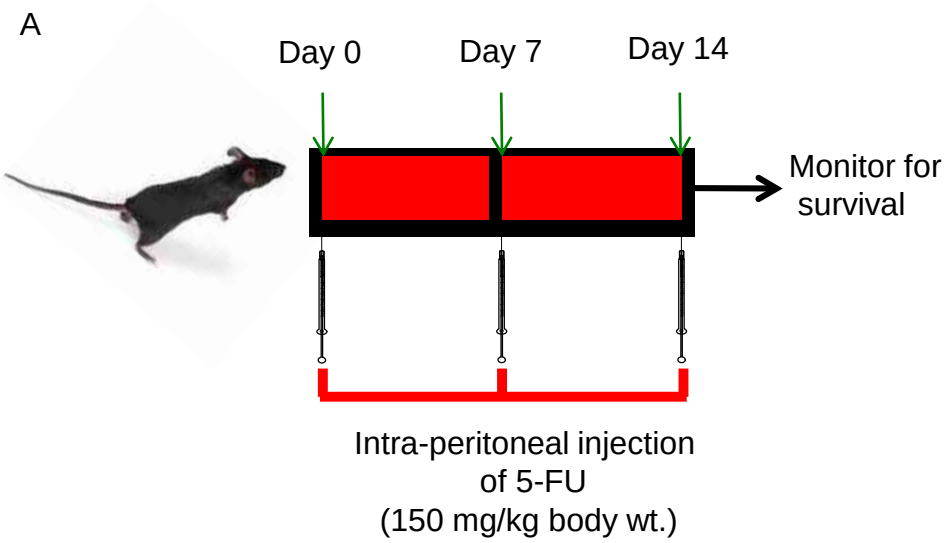
A
Day 0
Day 7
Day 14
Monitor for survival
Intra-peritoneal injection of 5-FU (150 mg/kg body wt.)

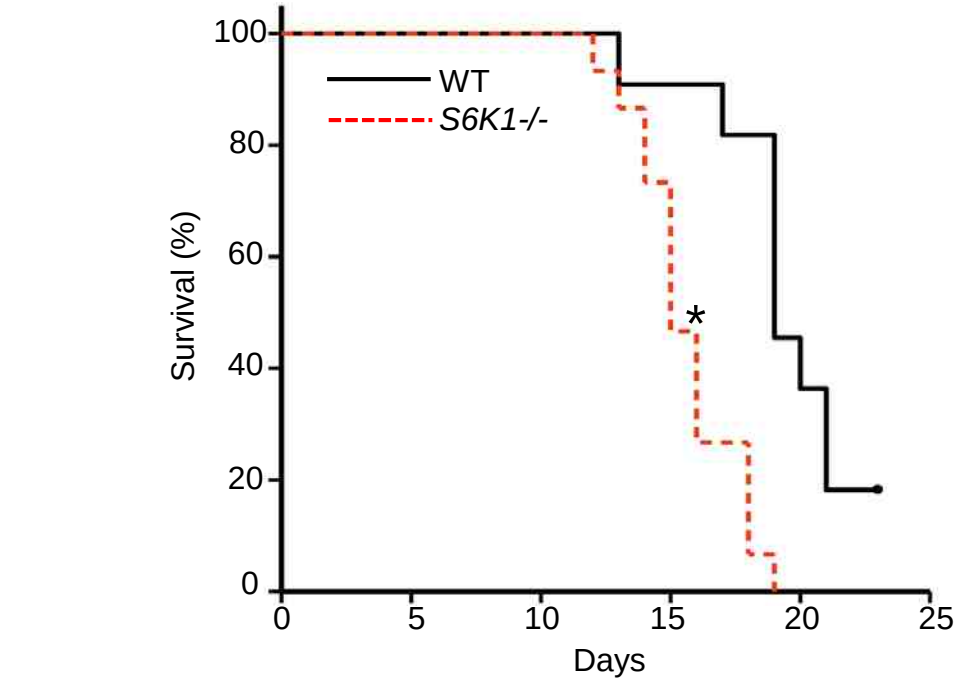
B
100
80
60
40
20
0
Survival (%)
WT
S6K1-/-
*
0
5
10
15
20
25
Days

Figure 15: S6K1 deficiency renders mice susceptible to repeated myelotoxic stress.

(A) Model of repeated myeloablative stress using 5-FU. WT and *S6K1-/-* mice were treated with 5-FU at an interval of 7 days and the mice were monitored for survival. (B) Kaplan-Meier survival curve of WT and *S6K1-/-* mice after repeated doses of 5-FU. Statistical significance between the survival of two groups were analyzed by the log-rank (Mantel-Cox) test; n=11 WT & 15 *S6K1-/-*;*$p<0.01$.

earlier to repeated myelotoxic stress due to hematopoietic exhaustion. Following weekly doses of 5-FU, *S6K1-/-* mice succumbed to death significantly earlier compared to WT mice. The median survival time of *S6K1-/-* mice was 17 days while the median survival time for WT controls was 21 days (Figure 15B). This suggests that S6K1 deficiency results in loss of quiescence in HSCs leading to hematopoietic exhaustion following repeated myelotoxic stress.

S6K1 deficient HSC/Ps have reduced engraftment potential following myelotoxic stress:

Previous studies have shown that in the BM of WT mice, phenotypically defined HSCs reach maximum frequency on day 6 post 5-FU administration (Venezia et al., 2004). To determine whether 5-FU administration affect the functional ability of S6K1 deficient HSCs, we performed CRA with cells derived from WT and *S6K1-/-* mice after 6 days following 5-FU injection. We mixed the test cells with competing Boy/J BM MNCs at two different doses and transplanted them into lethally irradiated mice. When mice were transplanted with cells at a ratio of 1:8 (test: competitor), we observed a significant decrease in donor-derived cells in the peripheral blood of recipients of *S6K1-/-* BM MNCs (Figure 16A). The decrease in the engraftment persisted until 16 weeks following transplant. However, when recipients were transplanted with 1:4 (test: competitor) cell dilution, there were no difference in the contribution of donor-derived cells in the peripheral blood of recipients of *S6K1-/-* BM MNCs (Figure 16B). These results suggest that following genotoxic stress, S6K1 protects the functional potential of

Figure 16

A

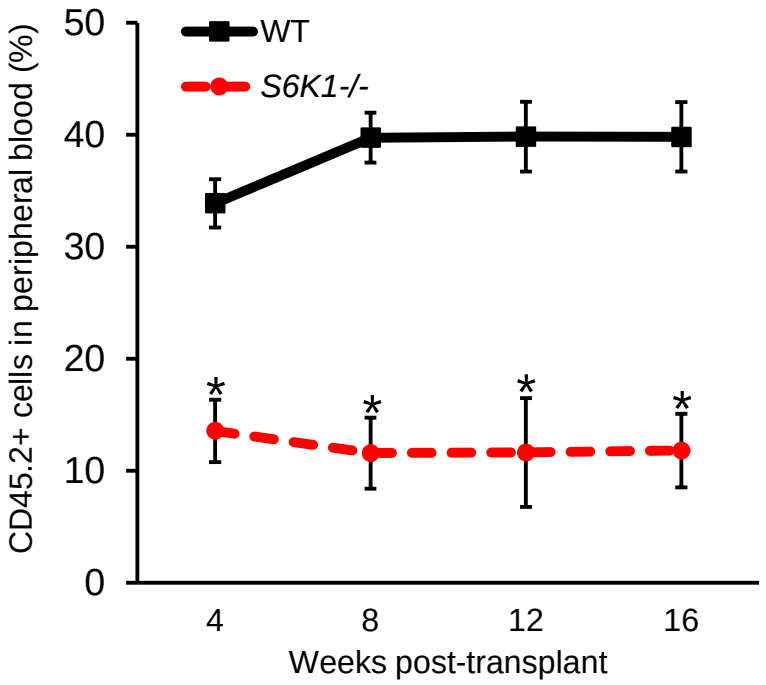
WT
S6K1-/-
CD45.2+ cells in peripheral blood (%)
50
40
30
20
10
0
*
*
*
*
4
8
12
16
Weeks post-transplant

B

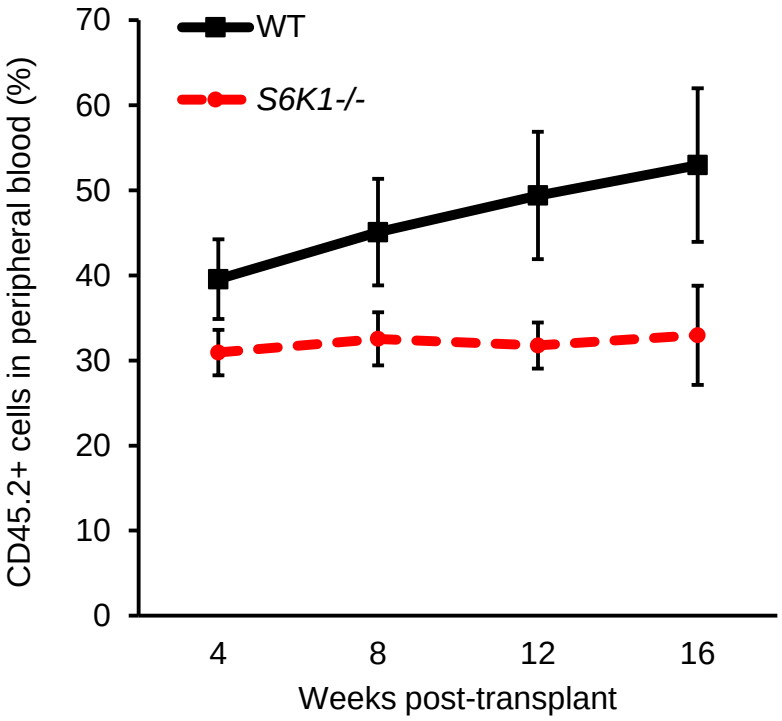
WT
S6K1-/-
CD45.2+ cells in peripheral blood (%)
70
60
50
40
30
20
10
0
4
8
12
16
Weeks post-transplant

Figure 16: *S6K1-/-* HSCs have reduced engraftment after exposure to chemotherapeutic agents.

(A) WT and *S6K1-/-* mice were treated with a single dose of 5-FU. On 6th day following 5-FU treatment, BM MNCs were isolated, mixed with competitor BM MNCs isolated from Boy/J mice and transplanted into lethally irradiated hosts. Donor-derived (CD45.2+) cells in peripheral blood of recipients of cells in ratio of 1:8 (test:competitor) was determined at different time points following transplantation. (B) Donor-derived (CD45.2+) cells in peripheral blood of recipients cells in ratio of 1:4 (test:competitor) was determined at different time points following transplantation. n=3-4 mice in each recipient group. Data are expressed as mean ± SEM. Difference between the group means was analyzed by one-way ANOVA with Bonferroni post-hoc analysis; *$p<0.05$.

HSC/Ps and the deficiency of S6K1 results in reduced engraftment of HSC/Ps following 5-FU treatment.

Discussion:

Chemotherapeutic agents like 5-FU cause DNA damage and induces apoptosis in proliferating HSCs. Quiescent HSCs undergo rapid proliferation and rapid cycling during the recovery of hematopoietic system. Previous studies found S6K1 to function as a repressor of cell cycle progression (Henriques et al., 2013). We found that HSC enriched population in the bone marrow undergo increased cycling following 5-FU treatment. Our data suggests that S6K1 is required for HSCs to re-enter their quiescent state after they have undergone proliferation following myeloablative stress. Our studies find that *S6K1-/-* HSC/Ps increase in frequency on 9^{th} day post 5-FU treatment. Our data revealed no significant difference on day 6 and day 15 post 5-FU treatment on HSC/P frequency between *S6K1-/-* and control HSC/Ps. *S6K1-/-* mice display similar hematopoietic response like *CD81-/-* mice in response to stress. Lin et al. had shown that in HSCs, CD81 is required for re-entering quiescence following 5-FU induced proliferation (Lin et al., 2011). Similar to *S6K1-/-* mice, *CD81-/-* mice had increased HSC frequency at a single time point following myeloablative stress. On day 8 following myeloablative stress, the HSC frequency in *CD81-/-* mice was increased. However, there were no significant changes in the frequency of *CD81-/-* HSCs on day 4, day 7 and day 12 post 5-FU treatment. Our studies observed an increase in *S6K1-/-* HSC-enriched population at similar time point following myeloablative stress when compared to *CD81-/-* HSCs. It is possible that S6K1 regulates the return of quiescence state of HSCs in a similar mechanism like CD81, which causes increase in LSK frequency at a single time point after

myeloablative stress. CD81 inhibits Akt activity in HSCs, which results in nuclear translocation of Foxo1a (Lin et al., 2011). S6K1 has been revealed as negative regulator of Akt activation. S6K1 acts in a negative feedback loop to repress mTORC2-dependent and IRS-1 dependent Akt activation (Um et al., 2004. Um et al. have shown that in *S6K1-/-* mice maintained on high-fat diet, insulin-induced Akt activity is significantly upregulated compared to controls (Um et al., 2004). Additionally, S6K1 mediated phosphorylation of Rictor, a component of mTORC2, inhibits mTORC2 and Akt activation (Julien et al., 2010; Treins et al., 2010). It is possible that in the absence of S6K1, Akt activity is upregulated in HSCs following myeloablative stress, which might have prevented *S6K1-/-* HSCs from re-entering quiescence by regulating Foxo1a activity. To further elucidate the signaling mechanism, expression and activation level of Akt, CD81 and Foxo1A is required in *S6K1-/-* HSCs following myeloblative stress.

Autophagy has also been identified as an important factor in response to stress induced by chemotherapeutic agents. Li et al. showed that inhibition of autophagy increases 5-FU induced apoptosis in human colon cancer cells (Li et al., 2010). A recent study by Hac et al. showed that S6K1 does not play a role in autophagy under normal growth condition (Hac et al., 2015). However, under stress conditions, S6K1 activity is required for digestion of autophagosome interior by lysosomal proteases, which is the final stage of autophagy (Hac et al., 2015). Autophagy activity has been shown to be active in HSCs, but not in committed myeloid progenitors, which suggests that HSCs require the autophagy protective mechanism. In our model, S6K1 deficiency could result in reduced

autophagy in HSCs and along with loss of quiescence, could contribute to increased susceptibility of *S6K1-/-* mice to repeated myeloablative stress. *S6K1-/-* mice also mirrors the phenotype of *p21-/-* mice in response to stress. *P21-/-* mice survive significantly shorter time compared to WT mice when exposed to repeated myeloablative stress (Cheng et al., 2000). In previous chapter, we have shown that in steady-state, *p21* expression to be significantly reduced in *S6K1-/-* HSCs compared to controls. The increased susceptibility of *S6K1-/-* mice to myeloablative stress could be due to reduced p21 levels in HSCs. We also provide evidence to suggest that deficiency of S6K1 results in reduced engraftment of HSC/Ps following myeloablative stress. Quiescent HSCs have better homing and repopulating ability compared to actively cycling HSCs (Orschell-Traycoff et al., 2000). Since S6K1 deficiency results in increased cycling of HSC/Ps following myeloablative stress, this could contribute to their reduced engraftment in lethally irradiated recipients. However, we did not observe a statistically significant difference when we used a lower dilution for the transplantation studies. It could be possible that at a lower dilution, the number of functional HSC/Ps in *S6K1-/-* mice is higher to overcome the competitive disadvantage.

In summary, we have established S6K1 as a critical regulator of recovery of the hematopoietic system following myeloablative stress and regulator of quiescence of HSCs. Loss of S6K1 expression in HSC/Ps results in increased cycling following myeloablative stress and S6K1 protects HSCs from repeated myeloablative stress. Additionally, we have also provided evidence that S6K1

deficiency causes reduced engraftment of HSC/Ps following myeloablative stress.

Chapter 5: Modulation of S6K1 expression results in reduced self-renewal of HSCs

Introduction:

Previous studies have established a role for the PI3K-mTORC1 pathway in regulating the function of HSCs. Deficiency of p85α subunit of PI3K complex in fetal liver HSCs results in reduced long-term engraftment of HSCs when transplanted into lethally irradiated recipients (Haneline et al., 2006). Furthermore, differentiation of HSCs into myeloid and lymphoid lineages in peripheral blood of transplanted mice was also reduced in comparison to controls (Haneline et al., 2006). Deficiency of Akt1 and Akt2 in fetal liver HSCs as well as in adult young HSCs also results in reduced engraftment in peripheral blood of recipients following serial transplantation (Juntilla et al., 2010). Myeloid and lymphoid lineages were reduced in Akt1 and Akt2 deficient HSC recipients compared to control (Juntilla et al., 2010). mTOR deficient HSCs have significantly reduced engraftment potential in lethally irradiated transplant recipients (Guo et al., 2013). In contrast, pharmacological inhibition of mTORC1 by rapamycin has yielded opposite results compared to genetic approaches. Inhibition of mTORC1 activity in old HSCs by administering rapamycin results in increased long-term engraftment of HSCs (Chen et al., 2009). Treatment of ex-vivo expanded HSCs by rapamycin results in increase in long-term engraftment of HSCs (Luo et al., 2014).

Figure 17

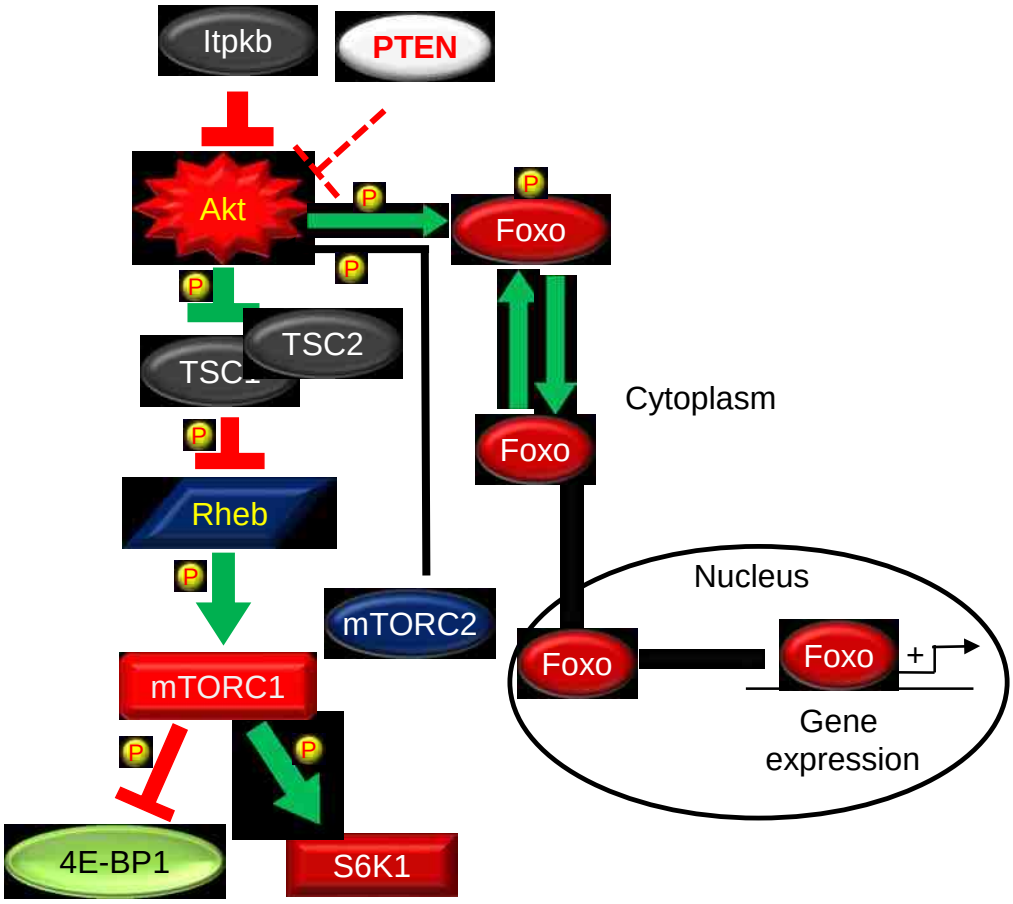
Itpkb
PTEN
Akt
P
Foxo
TSC2
Cytoplasm
Rheb
Nucleus
mTORC2
mTORC1
Foxo
Foxo
+
Gene
expression
4E-BP1
S6K1

Figure 17: Schematic model of Akt-mTORC1 signaling in HSCs.

A schematic of Akt-mTORC1 signaling pathway in HSCs based on curren literature. Following phosphorylation, activated Akt phosphorylates and inhibits tuberous Sclerosis 2 (TSC2)-mediated inhibition of Rheb. Activated Rheb subsequently phosphorylates and activates mTORC1. Activated mTORC1 phosphorylates the translational regulators eukaryotic translation initiation factor 4E (eIF4E)-binding protein 1 (4E-BP1) and ribosomal protein S6 kinase 1 (S6K1). Foxo family of transcription factors translocate to nucleus and regulate gene expression. Akt phosphorylates Foxo group of transcription factors and inhibits their nuclear translocations by sequestering them within the cytoplasm. On the other hand, Itpkb acts as an inhibitor of Akt activity and subsequently represses mTORC1 activation.

Interestingly, hyperactivation of mTORC1, which is the major activator of S6K1, also affect HSC function. Increase in Akt activity, a positive regulator of S6K1 (Figure 17), causes dysfunction in HSCs and mice develops myeloproliferative disorders as well as T-cell lymphoma (Kharas et al., 2010). HSCs bearing constitutively active Akt also display reduced engraftment following transplantation (Kharas et al., 2010). Inositol-trisphosphate 3-kinases (Itpk) phosphorylate IP4 that results in subsequent inhibition of Akt activity (Jia et al., 2007). Among three isoforms of Itpk, HSCs express only Itpkb isoform and deficiency of Itpkb results in increased absolute number of LT-HSCs and MPPs within the bone marrow (Siegemund et al., 2015). The increase in LT-HSC number is associated with a subsequent decrease in quiescent HSCs in *Itpkb-/-* mice (Siegemund et al., 2015). Itpkb deficiency also results in deficiency of long-term self-renewal ability of HSCs (Siegemund et al., 2015). *Itpkb-/-* mice develop hematopoietic disorders with progressive ageing, which includes reduced LT-HSCs, MPPS and HPCs in bone marrow and succumb to anemia (Siegemund et al., 2015). Itpkb deficient LT-HSCs display increased cytokine induced Akt activation. Rapamycin treatment reduces hyperproliferation of *Itpkb-/-* LT-HSCs as well as decreases mTORC1 activity (Siegemund et al., 2015). These data suggest that Itpkb is a negative regulator of Akt-mTORC1 activity in HSCs (Figure 17).

In vivo inflammation also results in increased mTORC1-S6K1 activity in HSCs, which causes reduced bone marrow cellularity and reduction in the functional potential of HSCs (Chen et al., 2010). Treatment with rapamycin can

revert the defects in HSCs caused by inflammation, which suggests that hyperactivation of mTORC1 negatively regulates HSC function (Chen et al., 2010). IFNα, a mediator of inflammation, causes loss of quiescence followed by increased cycling of HSCs (Essers et al., 2009). IFNα also reduces PTEN expression in HSCs along with an increase in Akt phosphorylation. PTEN, a negative regulator of mTORC1-S6K1 activity (Figure 17), itself is a critical mediator of HSC function. Deletion of PTEN results in reduced engraftment of HSCs and expansion of myeloid population following transplant (Yilmaz et al., 2006b; Zhang et al., 2006). Interestingly PTEN differentially regulates functional potential of neonatal and adult HSCs. Neonatal HSCs deficient in PTEN show multilineage differentiation potential from 16 to 24 weeks post-transplant (Magee et al., 2012). However, their reconstitution capability diminishes after 24 weeks (Magee et al., 2012). In contrast, adult HSCs fail to reconstitute hematopoiesis up to 16 weeks post-transplant (Magee et al., 2012). The differential functional capability could be attributed to the maturation of neonatal HSCs to adult HSCs over the period. Similarly, in adult HSCs, PTEN deletion results in activation of PI3K-mTORC1 pathway but not in neonatal HSCs. In PTEN-deficient adult HSCs increased mTORC2 activity results in increased Akt activation (Figure 17) (Magee et al., 2012). Deletion of Rictor, a component of mTORC2, results in restoration of long-term functional potential of PTEN deficient HSCs (Magee et al., 2012).

The Foxo group of transcription factors regulate transcription of genes involved in cell-cycle arrest, apoptosis, and reactive oxygen species (ROS)

detoxification. Activated Akt phosphorylates Foxo group of proteins thus facilitating their removal from the nucleus and suppressing Foxo dependent gene transcription (Figure 17). PTEN deletion results in activation of Akt and mTORC1 in adult HSCs but does not alter Foxo1 or Foxo3a expression level nor does it affect Foxo3a nuclear localization (Lee et al., 2010). Treatment of HSCs with rapamycin also results in increased Akt activation, which suggests that there is a negative feedback loop in HSCs that is downstream of mTORC1 (Lee et al., 2010). Downstream of PTEN, constitutive activation of Akt results in increased phenotypic expansion of HSCs as a consequence of increased cycling, which gradually results in apoptosis of HSCs and reduced engraftment ability (Kharas et al., 2010). Mice bearing constitutively active Akt in HSCs develop MPD, AML and T cell lymphoma along with an accumulation of immature myeloid cells in bone marrow (Kharas et al., 2010). However, a recent study has shown that HSCs and MPPs undergoing cell cycle progression do not require increased Akt activation (Magee et al., 2012).

TSC1 and TSC2 are negative regulators of mTORC1-S6K1 activity and TSC1 deletion in HSCs results in increased mTORC1 activity (Chen et al., 2008). Conditional deletion of TSC1 in HSCs results in increased cycling and apoptosis (Chen et al., 2008). However, the cycling rate of TSC1 deficient HSCs is higher compared to their apoptosis rate. Functionally, TSC1 deficient HSCs have reduced self-renewal potential. TSC1 deficiency results in increased mitochondria biogenesis along with increased ROS production in HSCs. In another study, deletion of TSC1 in HSCs also resulted in reduced quiescence

and decreased self-renewal potential that was regulated by a mTORC1 dependent pathway.

Rheb2 is a direct activator of mTORC1 activity (Figure 17) and overexpression of Rheb2 results in hyperactivation of mTORC1 in hematopoietic cells (Campbell et al., 2009). Overexpression of Rheb2 in HSCs causes phenotypic expansion of HSCs along with a reduction in self-renewal ability (Campbell et al., 2009).

Overall, previous works from different groups involving both deficiency and hyperactivity of mTORC1 have demonstrated that maintenance of an optimal mTORC1 activity level is key for the HSC function. Modulation of mTORC1 activity level can result in reduced long-term engraftment and self-renewal of HSCs. However, the exact role of S6K1 expression and activity level in regulation of HSC function has not been investigated. We hypothesized that as S6K1 is a downstream substrate of mTORC1, it acts as a main effector of mTORC1 signaling in HSCs and HSCs functional ability depend on an optimal level of S6K1 activity.

In this chapter, we show that modulation of S6K1 expression level in HSCs results in reduced self-renewal. Our studies demonstrate that deficiency of S6K1 results in reduced self-renewal of HSCs. Our studies also reveal that S6K1 deficiency does not affect differentiation and homing ability of HSCs. We show that decreased self-renewal of S6K1 deficient HSCs corresponds to a decrease in *p21* level. Overexpression of S6K1 in HSCs results in reduced short-term and long-term engraftment as well as decreased self-renewal potential. Overall, our

studies establish that expression level of S6K1 in HSCs is a key regulator of their self-renewal potential. Both deficiency of S6K1 and its overexpression results in decreased self-renewal of HSCs.

Results:

S6K1 deficiency does not affect homing, engraftment or multi-lineage differentiation of HSCs:

Given the critical role of upstream effectors of S6K1 in the regulation of HSC function, we hypothesized that S6K1 might be a critical regulator of engraftment and self-renewal of HSCs. To determine the role of S6K1 on HSC function, competitive repopulation assay was performed with MNCs isolated from adult WT or *S6K1-/-* mice (Figure 18). *S6K1-/-* HSC/Ps showed reduced engraftment in the peripheral blood of recipients compared to controls as determined by engraftment of CD45.2+ cells in peripheral blood after 5 weeks of transplant compared to control group transplanted with WT HSC/Ps. The reduced engraftment of *S6K1-/-* HSC/Ps persisted until week 16 post-transplant (Figure 19A and B). However, from week 16 to week 24 post-transplant, there were no significant differences between the engraftment of CD45.2+ cells in peripheral blood of the recipients of either WT or *S6K1-/-* HSC/Ps (Figure 19A and B). At 8, 16 and 24 weeks post-transplant, there was no difference in the differentiation of *S6K1-/-* cells into myeloid (Gr1+, Mac1+, Gr1+Mac1+), B cells (B220+) and T cells (CD3+) in the peripheral blood of recipients as compared to WT controls (Figure 20A and B). The differentiation of WT and *S6K1-/-* HSC/Ps were also similar at 8 weeks 16 weeks and 24 weeks post-transplant (Figure 20B), which suggests that the decrease in engraftment was not due to reduced differentiation of *S6K1-/-* cells. These results suggest that S6K1 deficiency in HSCs does not affect long-term engraftment and differentiation of HSCs in

Figure 18

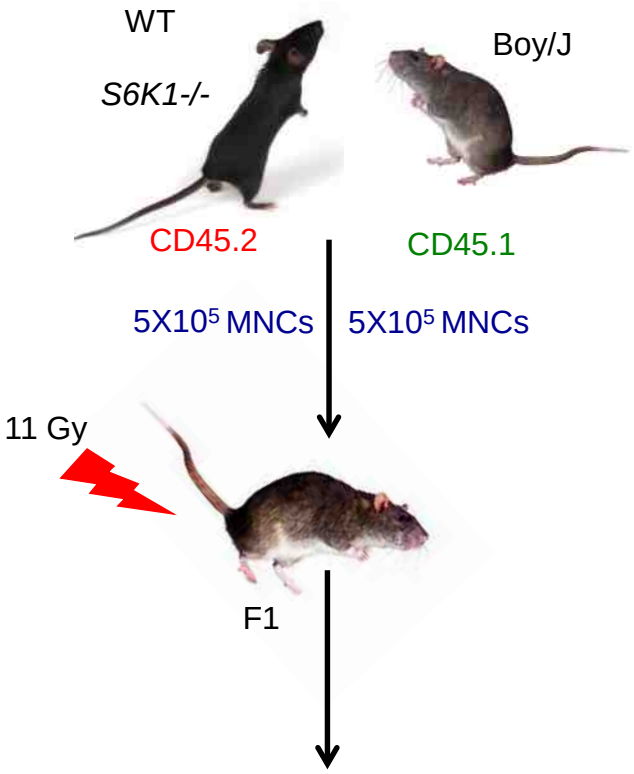
WT
S6K1-/-
Boy/J
CD45.2
CD45.1
5X10^5 MNCs
5X10^5 MNCs
11 Gy
F1
Analysis of donor-derived chimerism in peripheral blood

Figure 18: Model of CRA for primary transplant using unfractionated BM MNCs.

Model of CRA for primary transplant using unfractionated BM MNCs. Aseptically isolated $5X10^5$ WT or *S6K1-/-* MNCs (CD45.2+) were mixed with $5X10^5$ MNCs isolated from Boy/J mice (CD45.1+) and transplanted into lethally irradiated F1 recipients. Peripheral blood was obtained from the recipients at different time points and analyzed for engraftment of donor-derived cells (CD45.2+) by flow cytometry.

Figure 19

A

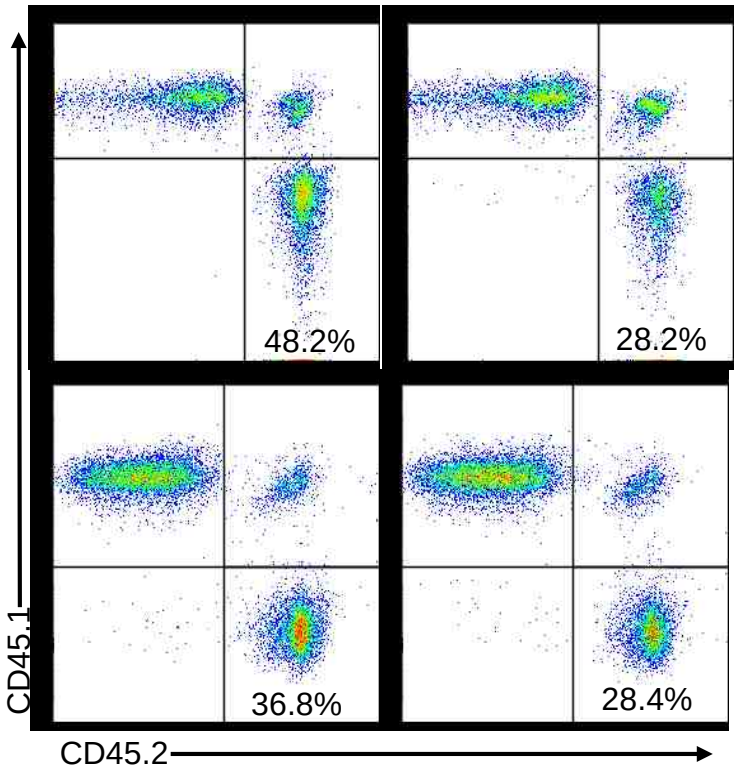
5 weeks
24 weeks
48.2%
28.2%
36.8%
28.4%
CD45.1
CD45.2

B

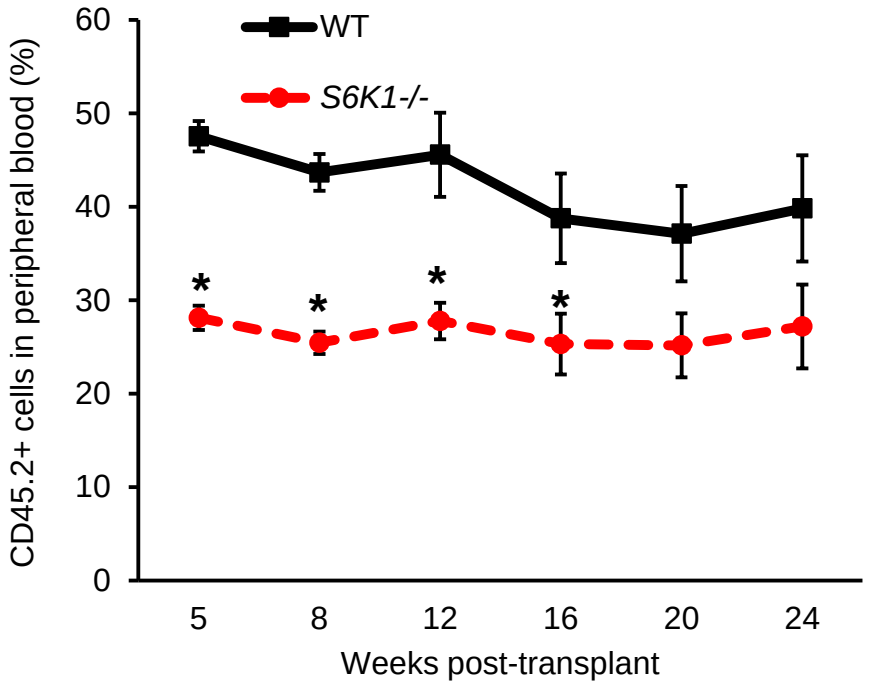
WT
S6K1-/-
CD45.2+ cells in peripheral blood (%)
60
50
40
30
20
10
0
5
8
12
16
20
24
Weeks post-transplant
*
*
*
*

Figure 19: Effect of loss of expression of S6K1 on engraftment of HSCs in primary transplant recipients.

(A) Representative flow plot of peripheral blood of primary transplant recipients of either WT or *S6K1-/-* MNCs at 4 weeks and 24 weeks of transplantation. Peripheral blood was obtained from the recipients at different time points and analyzed for engraftment of donor-derived cells by flow cytometry. (B) Quantitative representation of donor-derived cells in peripheral blood of primary transplant recipients of either WT or *S6K1-/-* MNCs; n=7 mice in each group. Data are expressed as mean ± SEM. Difference between the group means was analyzed by one-way ANOVA with Bonferroni post-hoc analysis; *$p<0.05$.

Figure 20

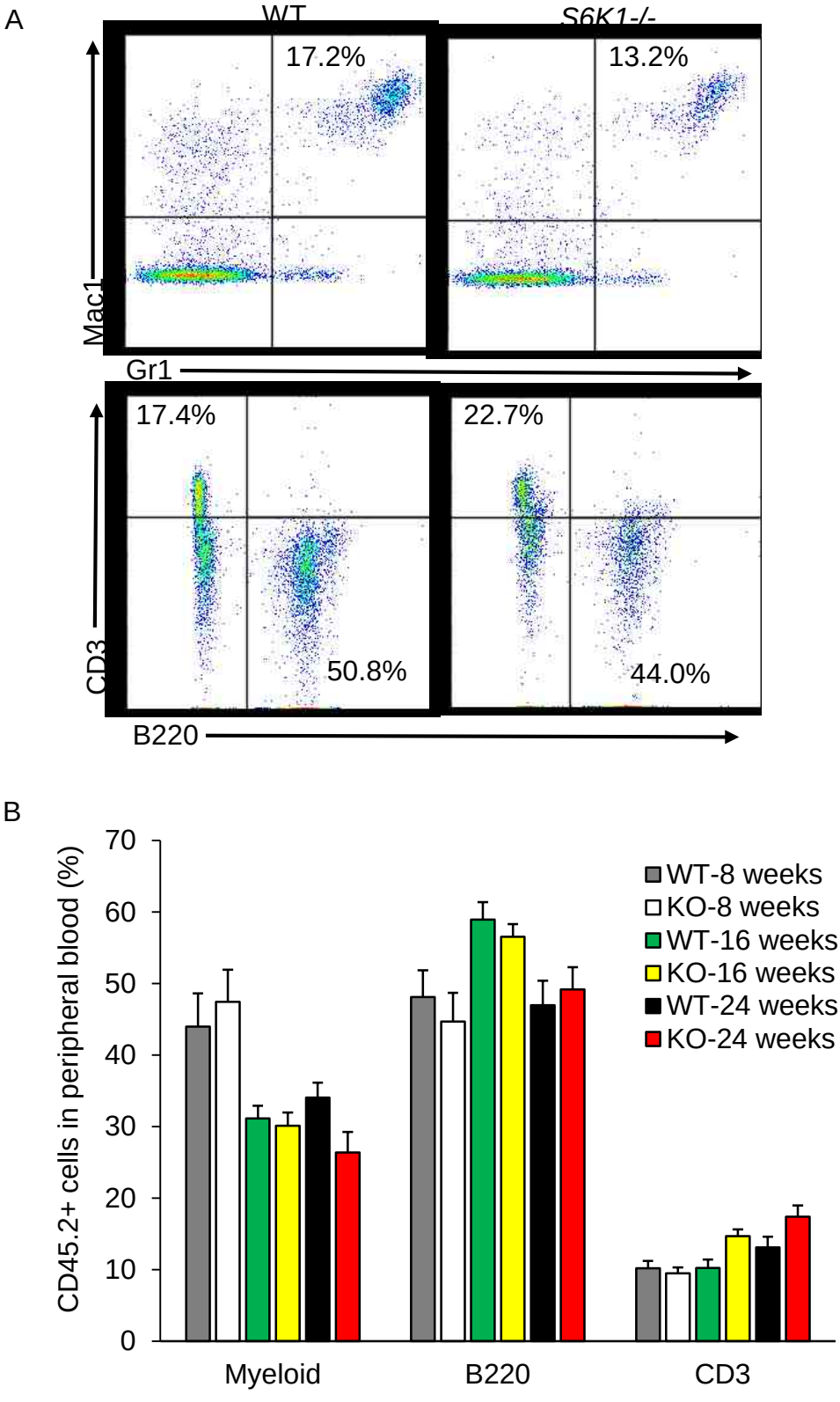
A
WT
S6K1-/-
17.2%
13.2%
Mac1
Gr1
17.4%
22.7%
50.8%
44.0%
CD3
B220
B
CD45.2+ cells in peripheral blood (%)
70
60
50
40
30
20
10
0
WT-8 weeks
KO-8 weeks
WT-16 weeks
KO-16 weeks
WT-24 weeks
KO-24 weeks
Myeloid
B220
CD3

Figure 20: S6K1 deficiency does not affect differentiation of HSCs.

(A) Representative flow plot of donor-derived (CD45.2+) myeloid (Gr1+ Mac1+) and lymphoid cells (B220+; CD3+) in peripheral blood of primary transplant recipients of either WT or *S6K1-/-* MNCs at 24 weeks post-transplant. Peripheral blood was obtained from the primary transplant recipients at 24 weeks post-transplant and analyzed for engraftment and differentiation of donor-derived cells by flow cytometry. (B) Quantitative representation of donor-derived myeloid (Gr1+, Mac1+, Gr1+Mac1+) and lymphoid cells in peripheral blood of primary transplant recipients of WT or *S6K1-/-* MNCs at 8, 16 and 24 weeks post-transplant; n=7 mice in each group. Data are expressed as mean ± SEM. Difference between the group means was analyzed by one-way ANOVA with Bonferroni post-hoc analysis.

primary recipients. Following intravenous transplantation, HSCs have to cross blood-bone marrow endothelium barrier in order to engraft into the bone marrow compartment (Lapidot et al., 2005). The process, known as homing, is a rapid process and the initial event following bone marrow transplant (Lapidot et al., 2005). Given the importance of homing on engraftment of HSCs, we hypothesized that the initial defect in engraftment of *S6K1-/-* HSCs could be due to reduced homing. To test this hypothesis, we performed homing experiments with WT and *S6K1-/-* HSC/Ps. DiD is a lipophilic carbocyanine dye which is photostable when incorporated in to the cell membrane and has very low cytotoxicity (Sipkins et al., 2005; Sutton et al., 2008). Following incubation with the cells, DiD diffuses laterally through the cellular plasma membrane and stains the cell (Sipkins et al., 2005; Sutton et al., 2008). BM MNCs were isolated from WT and *S6K1-/-* mice and labeled with DiD. We transplanted DiD labelled WT or *S6K1-/-* MNCs into lethally irradiated mice. Deficiency of S6K1 did not affect the homing of DiD+ LSK cells that are enriched in HSCs (Figure 21A and B), which suggests that S6K1 deficiency does not affect homing of HSCs into bone marrow.

In order to determine whether the defect in short-term engraftment is HSC specific or not, we sorted HSCs (CD150+ CD48- LSK), mixed them with syngenic competitor bone marrow cells and transplanted into lethally irradiated mice (Figure 22). In the primary transplant recipients, there were no differences in the engraftment of HSCs in the peripheral blood between the two groups (Figure 23A and B). After 24 weeks post-transplant, there were no difference in the

Figure 21

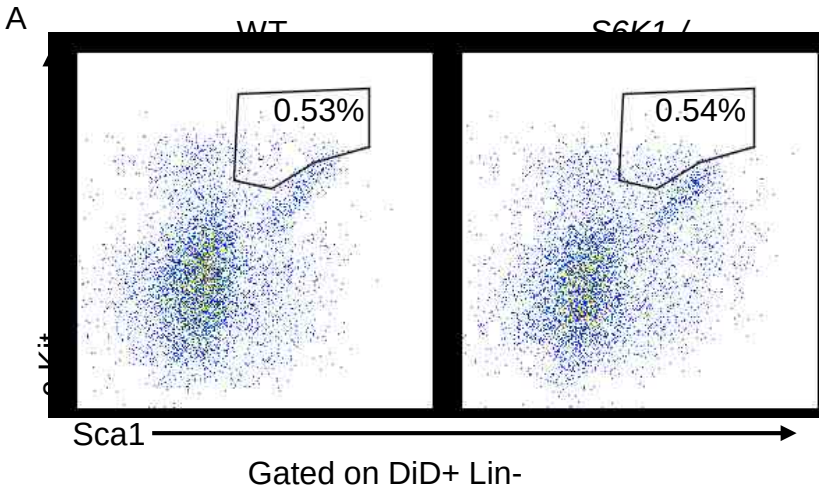
A
WT
S6K1-/-
0.53%
0.54%
c-Kit
Sca1
Gated on DiD+ Lin-

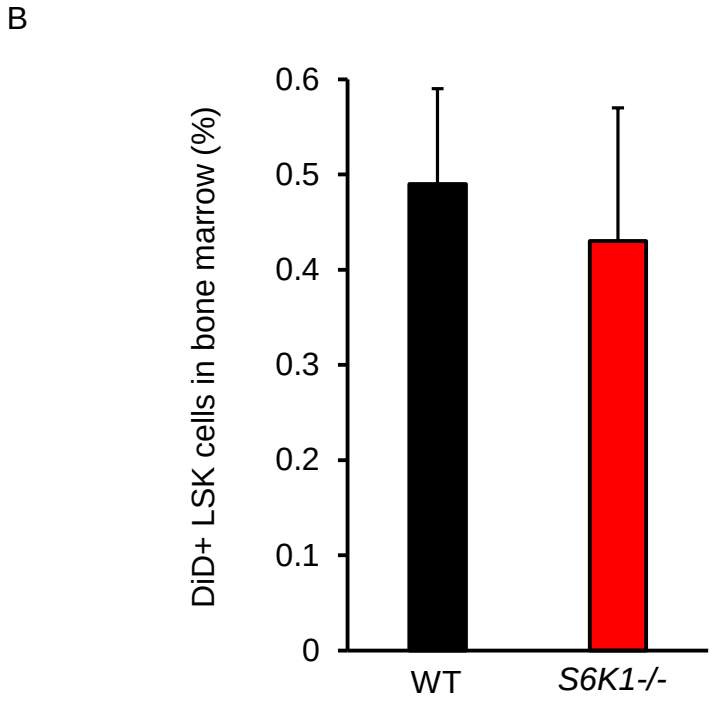
B
DiD+ LSK cells in bone marrow (%)
0.6
0.5
0.4
0.3
0.2
0.1
0
WT
S6K1-/-

Figure 21: S6K1 deficiency does not affect homing of HSCs.

(A) Representative flow plot (gated on DiD+ Lin- cells) of DiD+ LSK cells in bone marrow of lethally irradiated hosts transplanted with either WT or *S6K1-/-* MNCs. MNCs isolated from either WT or *S6K1-/-* mice were labelled with DiD and $1X10^7$ MNCs were injected intravenously into lethally irradiated Boy/J mice. The recipients were euthanized after 18 hours and MNCs were isolated. Cells were stained with antibodies against lineage markers, Sca1 and c-Kit and acquired using FACS. (B) Quantitative representation of DiD+ LSK cells in bone marrow of lethally irradiated hosts transplanted with either WT or *S6K1-/-* MNCs; n=6-7 mice in each group. Data are expressed as mean ± SEM.

Figure 22

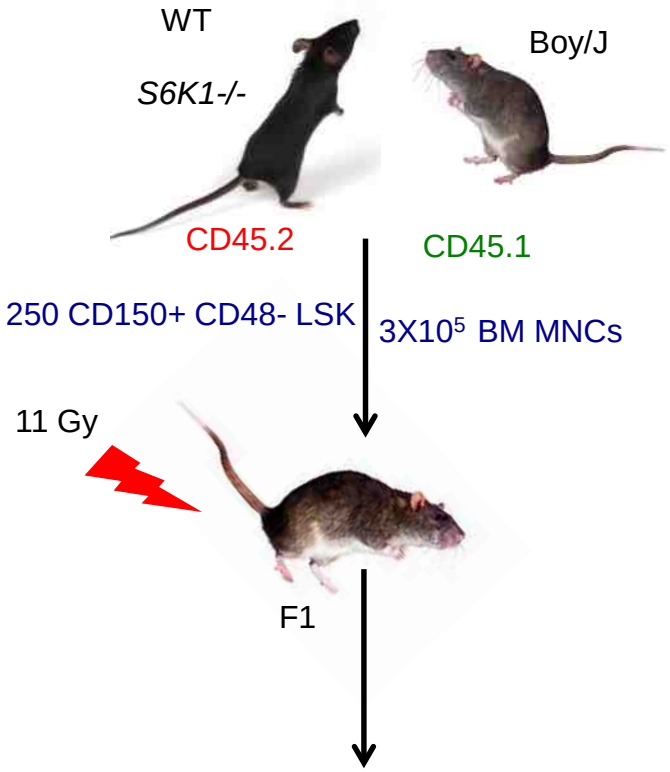
WT
S6K1-/-
Boy/J
CD45.2
CD45.1
250 CD150+ CD48- LSK
3X10^5 BM MNCs
11 Gy
F1
Analysis of donor-derived chimerism in peripheral blood

Figure 22: Model of CRA for primary transplant using LT-HSCs.

Model of CRA for primary transplant using LT-HSCs. 250 WT or *S6K1-/-* LT-HSCs (CD45.2+ CD150+ CD48- LSK) were mixed with $3X10^5$ MNCs isolated from Boy/J mice (CD45.1+) and transplanted into lethally irradiated F1 recipients. Peripheral blood was obtained from the recipients at different time points and analyzed for engraftment of donor-derived cells by flow cytometry.

Figure 23

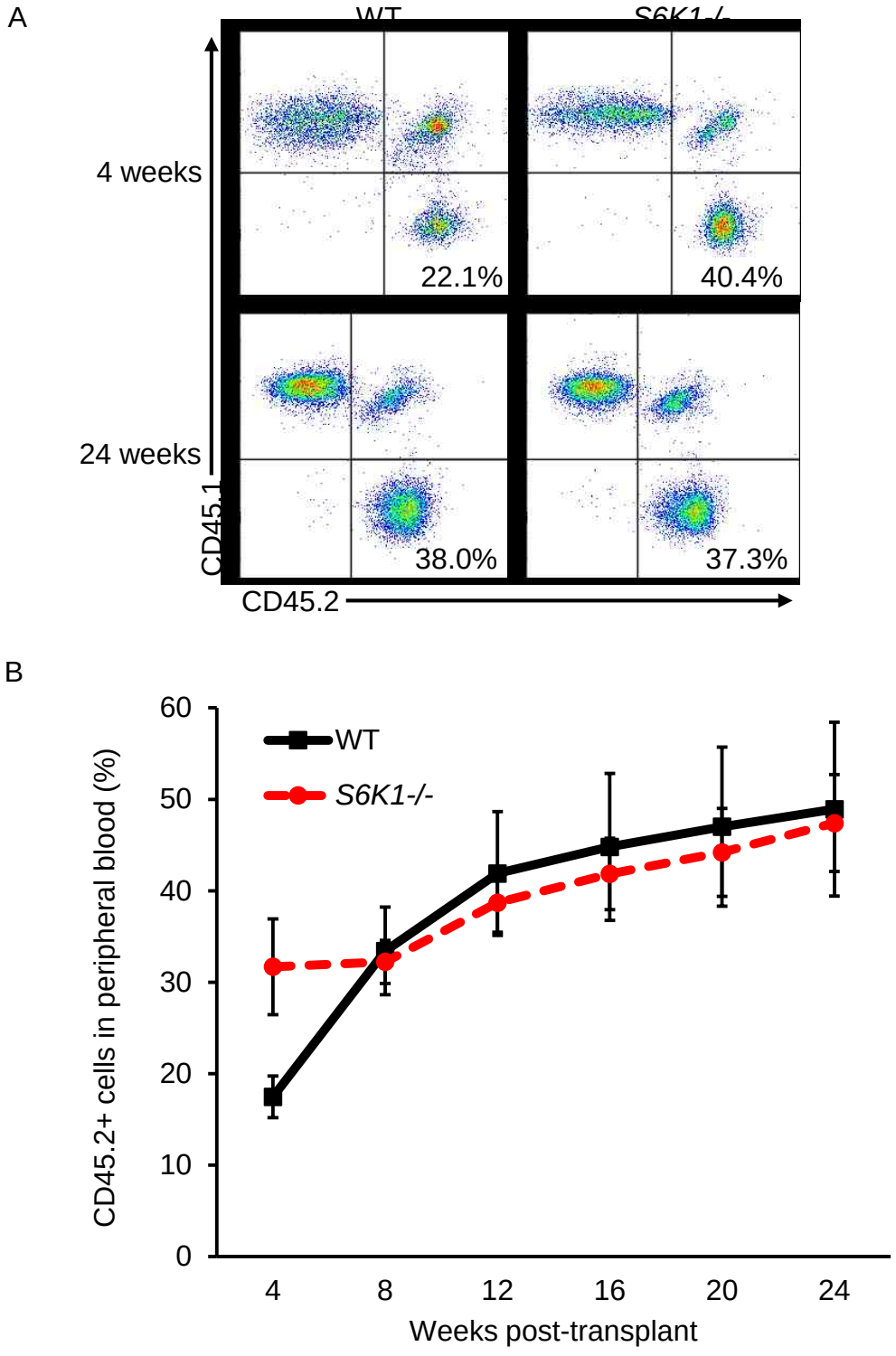
A
WT
S6K1-/-
4 weeks
24 weeks
CD45.1
CD45.2
22.1%
40.4%
38.0%
37.3%
B
WT
S6K1-/-
CD45.2+ cells in peripheral blood (%)
Weeks post-transplant
0
10
20
30
40
50
60
4
8
12
16
20
24

Figure 23: Loss of expression of S6K1 does not affect engraftment of HSCs in primary transplant recipients.

(A) Representative flow plot of peripheral blood of primary transplant recipients of either WT or *S6K1-/-* MNCs after 4 weeks and 24 weeks of transplantation. 250 WT or *S6K1-/-* LT-HSCs (CD45.2+ CD150+ CD48- LSK) were mixed with $3X10^5$ MNCs isolated from Boy/J mice (CD45.1+) and transplanted into lethally irradiated F1 recipients. Peripheral blood was obtained from the recipients at different time points and analyzed for engraftment of donor-derived cells by flow cytometry. (B) Quantitative representation of donor-derived cells in peripheral blood of primary transplant recipients of either WT or *S6K1-/-* LT-HSCs; n=6-7 mice in each group. Data are expressed as mean ± SEM. Difference between the group means was analyzed by one-way ANOVA with Bonferroni post-hoc analysis.

differentiation of *S6K1-/-* cells into myeloid (Gr1+-Mac1+), B cells (B220+) and T cells (CD3+) in the peripheral blood of recipients (Figure 24A and B). Overall, these data suggest that S6K1 deficiency in HSCs does not affect long-term engraftment, homing and differentiation of HSCs.

S6K1 deficiency results in reduced self-renewal of HSCs:

The functional activity of HSCs *in vivo* can be determined by their ability to sustain hematopoiesis through serial transplantation (Purton and Scadden, 2007). To determine whether S6K1 is a regulator of self-renewal of HSCs, we performed secondary transplant with cells derived from primary transplant recipients. At 24 weeks after primary transplant, we isolated MNCs from WT or KO primary recipients and transplanted them into lethally irradiated recipients (Figure 25). We observed a significant reduction in the engraftment of *S6K1-/-* recipients in the peripheral blood of recipients from week 4 to week 16 post-transplant (Figure 26A and B).

In order to determine whether this defect in engraftment is HSC specific or not, we isolated BM MNCs from primary recipients of either WT or *S6K1-/-* HSCs and transplanted them into lethally irradiated recipients (Figure 27). The donor-derived cells in the peripheral blood of the secondary recipients bearing *S6K1-/-* HSCs was significantly decreased compared to WT controls (Figure 28A and B). The difference persisted from week 4 to week 24 post-transplant (Figure 28A and B). The engraftment of CD45.2+ cells in the BM of secondary recipients bearing *S6K1-/-* cells was significantly decreased compared to WT controls (Figure 29A and B). To determine whether the reduction in engraftment of *S6K1-/-* HSCs

Figure 24

A

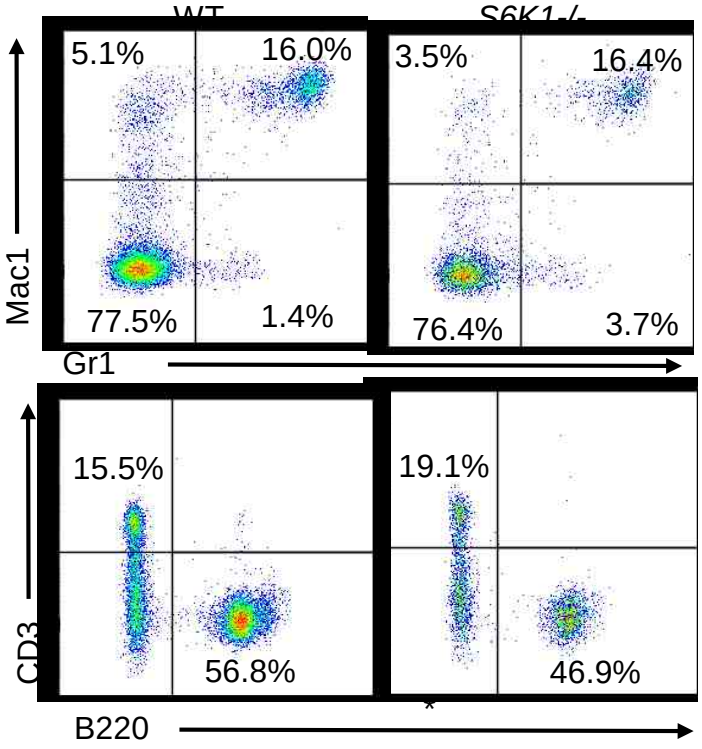
WT
S6K1-/-
5.1%
16.0%
3.5%
16.4%
Mac1
77.5%
1.4%
76.4%
3.7%
Gr1
15.5%
19.1%
CD3
56.8%
46.9%
B220

B

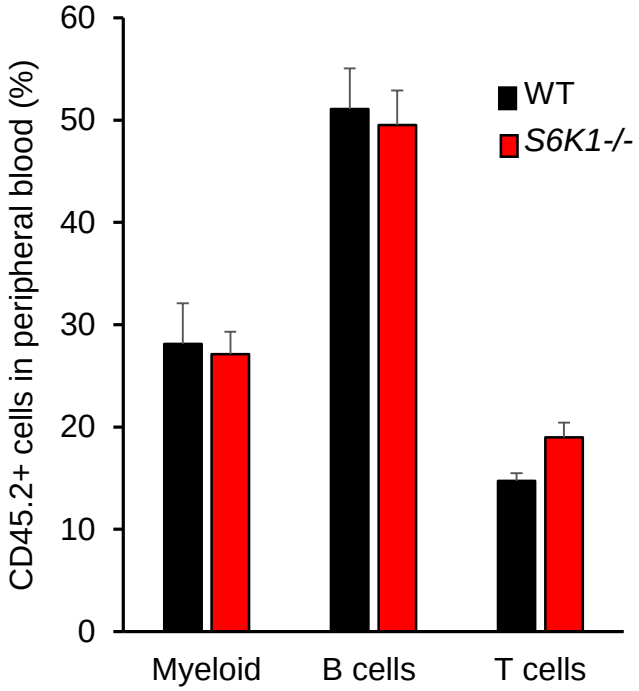
60
50
40
30
20
10
0
CD45.2+ cells in peripheral blood (%)
WT
S6K1-/-
Myeloid
B cells
T cells

Figure 24: S6K1 deficiency does not affect differentiation of HSCs.

(A) Representative flow plot of donor-derived (CD45.2+) myeloid (Gr1+ Mac1+) and lymphoid cells (B220+; CD3+) in peripheral blood of primary transplant recipients of either WT or *S6K1-/-* LT-HSCs after 24 weeks post-transplant. Peripheral blood was obtained from the primary transplant recipients after 24 weeks post-transplant and analyzed for engraftment and differentiation of donor-derived cells by flow cytometry. (B) Quantitative representation of donor-derived myeloid and lymphoid cells in peripheral blood of primary transplant recipients of either WT or *S6K1-/-* LT-HSCs after 24 weeks post-transplant; n=6-7 mice in each group. Data are expressed as mean ± SEM. Difference between the group means was analyzed by one-way ANOVA with Bonferroni post-hoc analysis.

Figure 25

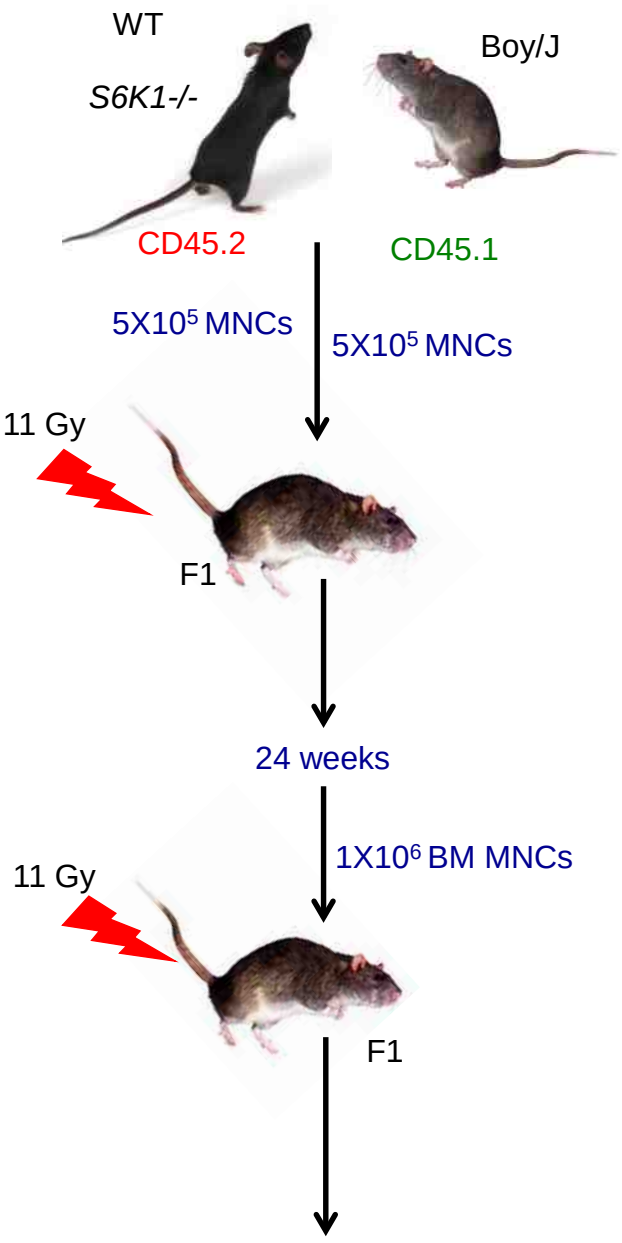
WT
S6K1-/-
Boy/J
CD45.2
CD45.1
5X10^5 MNCs
5X10^5 MNCs
11 Gy
F1
24 weeks
1X10^6 BM MNCs
11 Gy
F1
Analysis of donor-derived chimerism in peripheral blood

Figure 25: Model of secondary transplant with BM MNCs as primary donor cells.

After 24 weeks of primary transplant, $1X10^6$ MNCs isolated from the recipients of either WT or *S6K1-/-* BM MNCs and transplanted into lethally irradiated F1 recipients. Peripheral blood was obtained from the secondary recipients at different time points and analyzed for engraftment of donor-derived cells by flow cytometry.

Figure 26

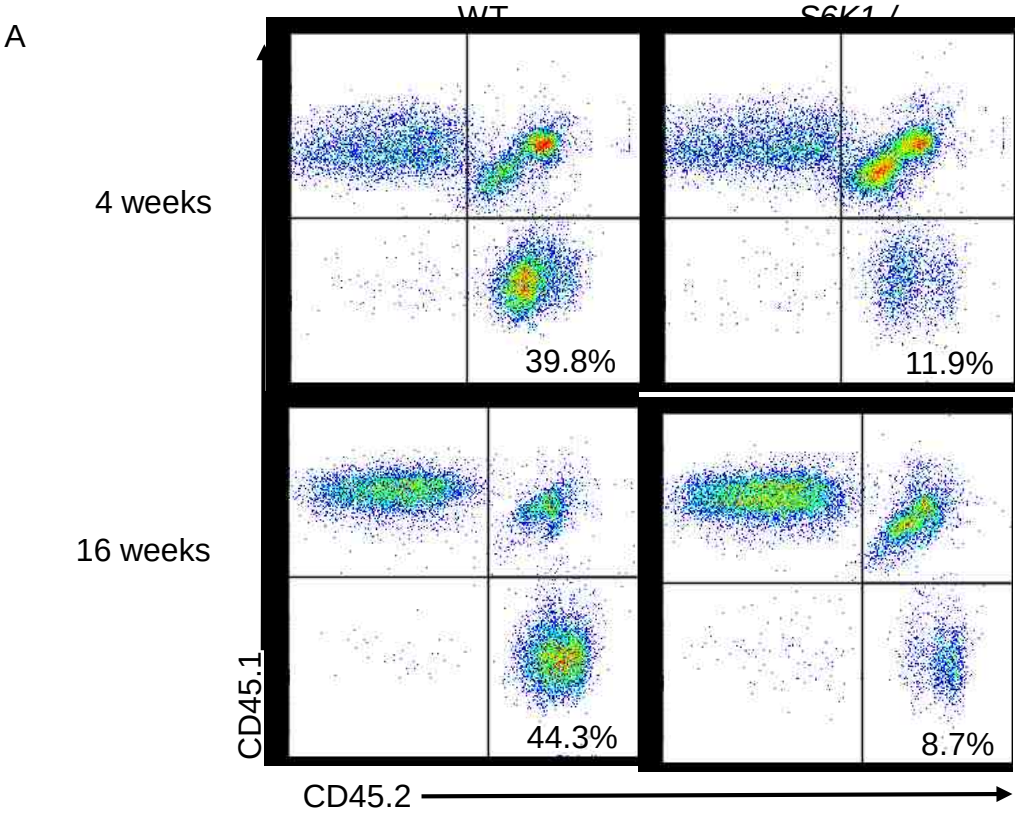
A
WT
S6K1-/-
4 weeks
16 weeks
39.8%
11.9%
44.3%
8.7%
CD45.1
CD45.2

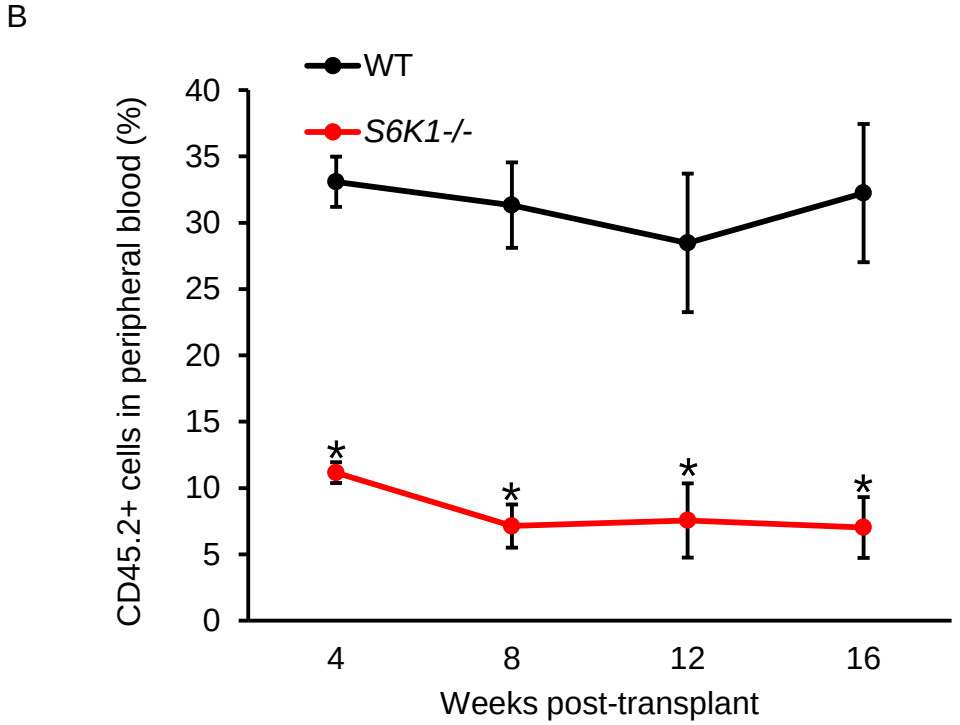
B
WT
S6K1-/-
CD45.2+ cells in peripheral blood (%)
40
35
30
25
20
15
10
5
0
4
8
12
16
Weeks post-transplant
*
*
*
*

Figure 26: S6K1 deficiency causes reduced self-renewal of HSCs.

(A) Representative flow plot of peripheral blood of secondary transplant recipients of either WT or *S6K1-/-* MNCs after 4 and 16 weeks of transplantation. After 24 weeks of primary transplant, $1X10^6$ MNCs were isolated from the recipients of either WT or *S6K1-/-* MNCs and transplanted into lethally irradiated F1 recipients. Peripheral blood was obtained from the secondary recipients at different time points and analyzed for engraftment of donor-derived cells by flow cytometry. (B) Quantitative representation of donor-derived cells in peripheral blood of secondary transplant recipients with cells derived from primary transplant recipients of either WT or *S6K1-/-* MNCs; n=6-7 mice in each group. Data are expressed as mean ± SEM. Difference between the group means was analyzed by one-way ANOVA with Bonferroni post-hoc analysis; *$p<0.05$.

Figure 27

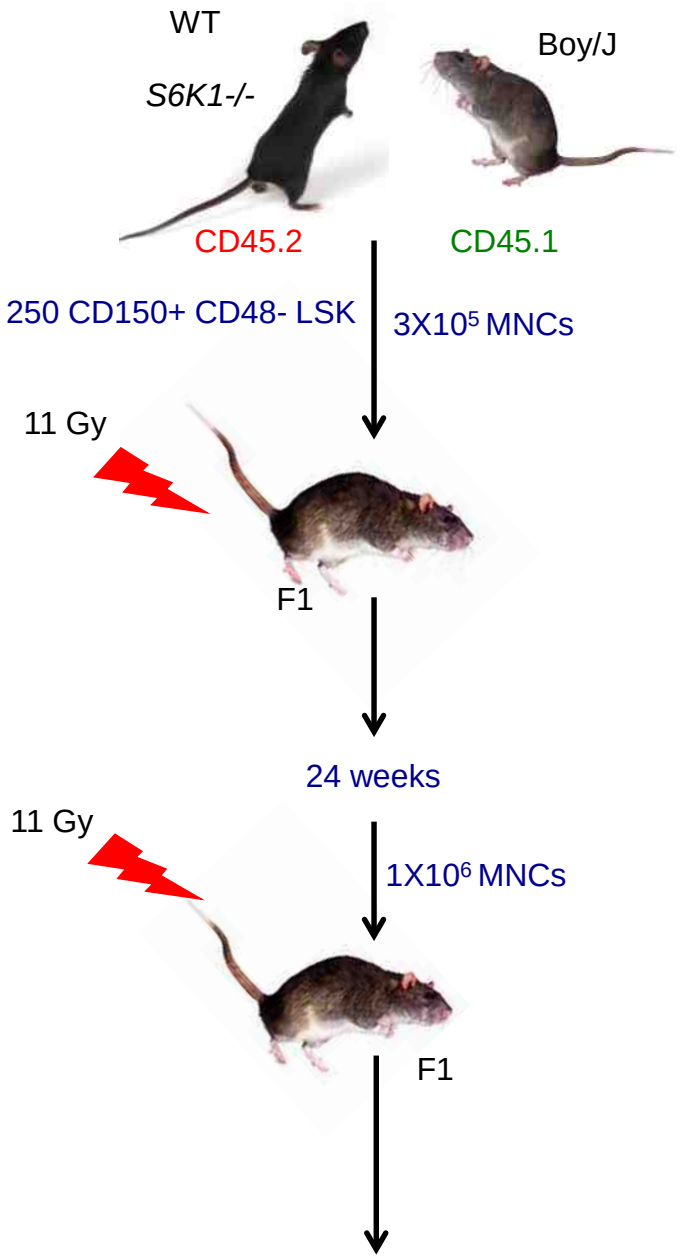

Analysis of donor-derived chimerism in peripheral blood

Figure 27: Model of secondary transplant with LT-HSCs as primary donor cells.

After 24 weeks of primary transplant, $1X10^6$ MNCs isolated from the recipients of either WT or *S6K1-/-* LT-HSCs and transplanted into lethally irradiated F1 recipients. Peripheral blood was obtained from the secondary recipients at different time points and analyzed for engraftment of donor-derived cells by flow cytometry.

Figure 28

A

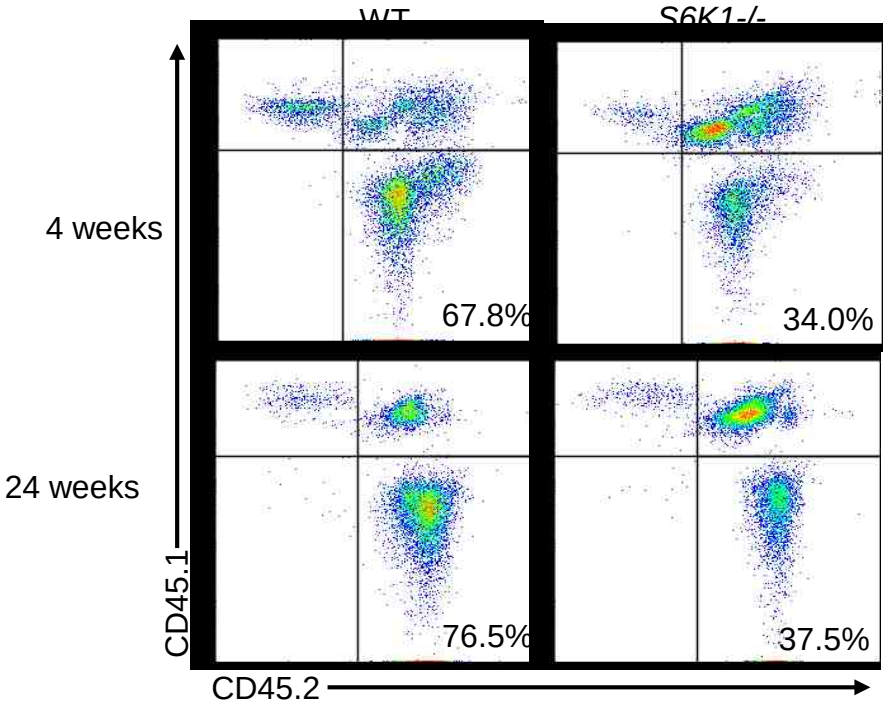
WT
S6K1-/-
4 weeks
24 weeks
67.8%
34.0%
76.5%
37.5%
CD45.1
CD45.2

B

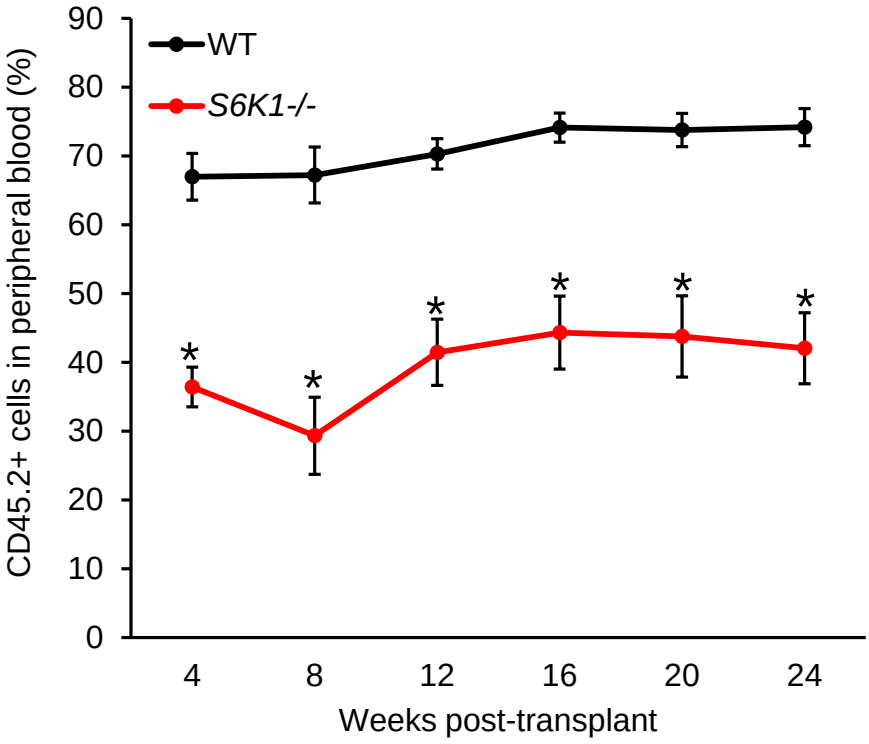
WT
S6K1-/-
CD45.2+ cells in peripheral blood (%)
Weeks post-transplant
0
10
20
30
40
50
60
70
80
90
4
8
12
16
20
24
*

Figure 28: S6K1 deficiency causes reduced self-renewal of HSCs.

(A) Representative flow plot of peripheral blood of secondary transplant recipients of either WT or *S6K1-/-* LT-HSCs after 4 weeks and 24 weeks of transplantation. After 24 weeks of primary transplant, $1X10^6$ MNCs isolated from the recipients of either WT or *S6K1-/-* LT-HSCs and transplanted into lethally irradiated F1 recipients. Peripheral blood was obtained from the secondary recipients at different time points and analyzed for engraftment of donor-derived cells by flow cytometry. (B) Quantitative representation of donor-derived cells in peripheral blood of secondary transplant recipients with cells derived from primary transplant recipients of either WT or *S6K1-/-* LT-HSCs; n=9-10 mice in each group. Data are expressed as mean ± SEM. Difference between the group means was analyzed by one-way ANOVA with Bonferroni post-hoc analysis; *$p<0.05$.

Figure 29

A

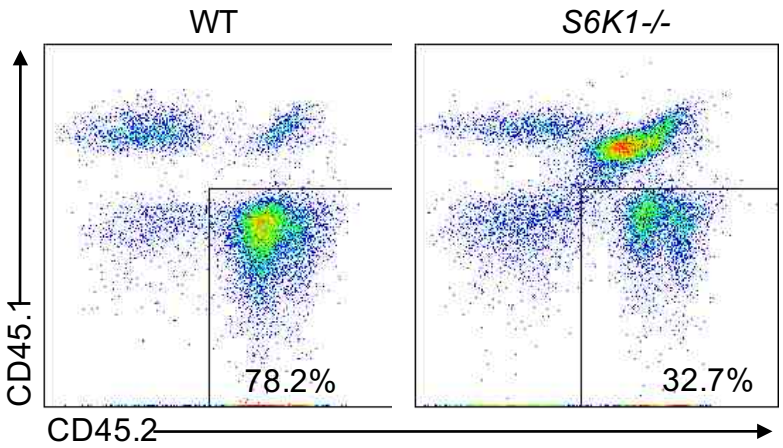
WT
S6K1-/-
CD45.1
CD45.2
78.2%
32.7%

B

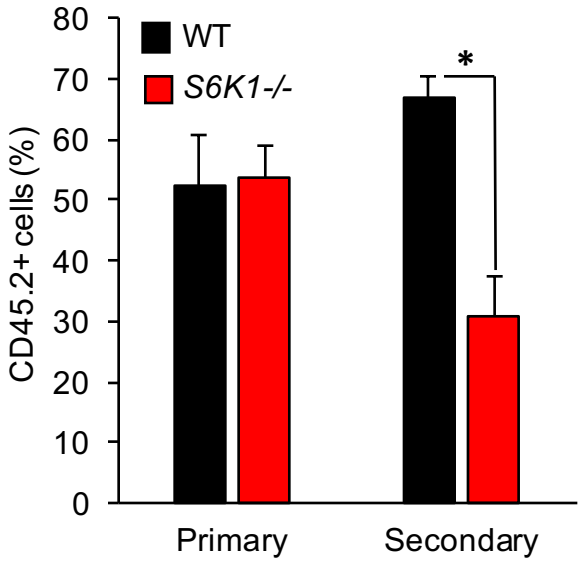
80
70
60
50
40
30
20
10
0
CD45.2+ cells (%)
WT
S6K1-/-
*
Primary
Secondary

Figure 29: S6K1 deficiency causes reduced engraftment of HSCs into BM of secondary transplant recipients.

(A) Representative dot plot of CD45.2+ cells in bone marrow of secondary recipients after 24 weeks. (B) Quantitative representation of donor-derived cells in BM of primary and secondary transplant recipients of either WT or *S6K1-/-* LT-HSCs after 24 weeks of transplantation; n=6-10 mice in each group. Data are expressed as mean ± SEM. Difference between the group means was analyzed by one-way ANOVA with Bonferroni post-hoc analysis; *p<0.05.

persists upon another round of serial transplant, we performed tertiary transplant with BM MNCs derived from secondary transplant recipients. The donor-derived cells in the peripheral blood of the tertiary recipients bearing *S6K1-/-* HSCs was also significantly reduced compared to WT controls (Figure 30A and B). P21 has been identified as a key regulator of HSC self-renewal and deficiency of p21 impairs the self-renewal ability of HSCs (Cheng et al., 2000). We sorted donor-derived LSK cells (CD45.2+ LSK) cells from bone marrow of WT and *S6K1-/-* secondary recipients and analyzed the expression level of genes regulating the self-renewal of HSCs. The expression of *p21* was significantly reduced in LSK cells isolated from *S6K1-/-* recipients of secondary transplant (Figure 31). We did not observe any change in *Pten*, *Bmi1*, *PU1*, *Foxo3* and *Meis1* expression in LSK cells isolated from *S6K1-/-* recipients (Figure 31).

Overexpression of S6K1 in HSC/Ps:

Multiple studies had demonstrated that both hyperactivation of mTORC1 (Chen et al., 2008; Kharas et al., 2010; Yilmaz et al., 2006b) and inhibition of mTORC1 (Guo et al., 2013; Haneline et al., 2006; Juntilla et al., 2010) activity results in defect in HSC functions. Given the importance of maintenance of critical level of activation of upstream effectors of S6K1 in regulation of functions of HSC functions, we hypothesized that S6K1 expression and activity level might be a critical regulator of engraftment and self-renewal of HSCs. We overexpressed murine S6K1 in WT HSC/Ps and determined the expression and activation level of S6K1. WT HSC/Ps were transduced with either MIEG3 or S6K1 and sorted to homogeneity by FACS according to GFP expression. As

Figure 30

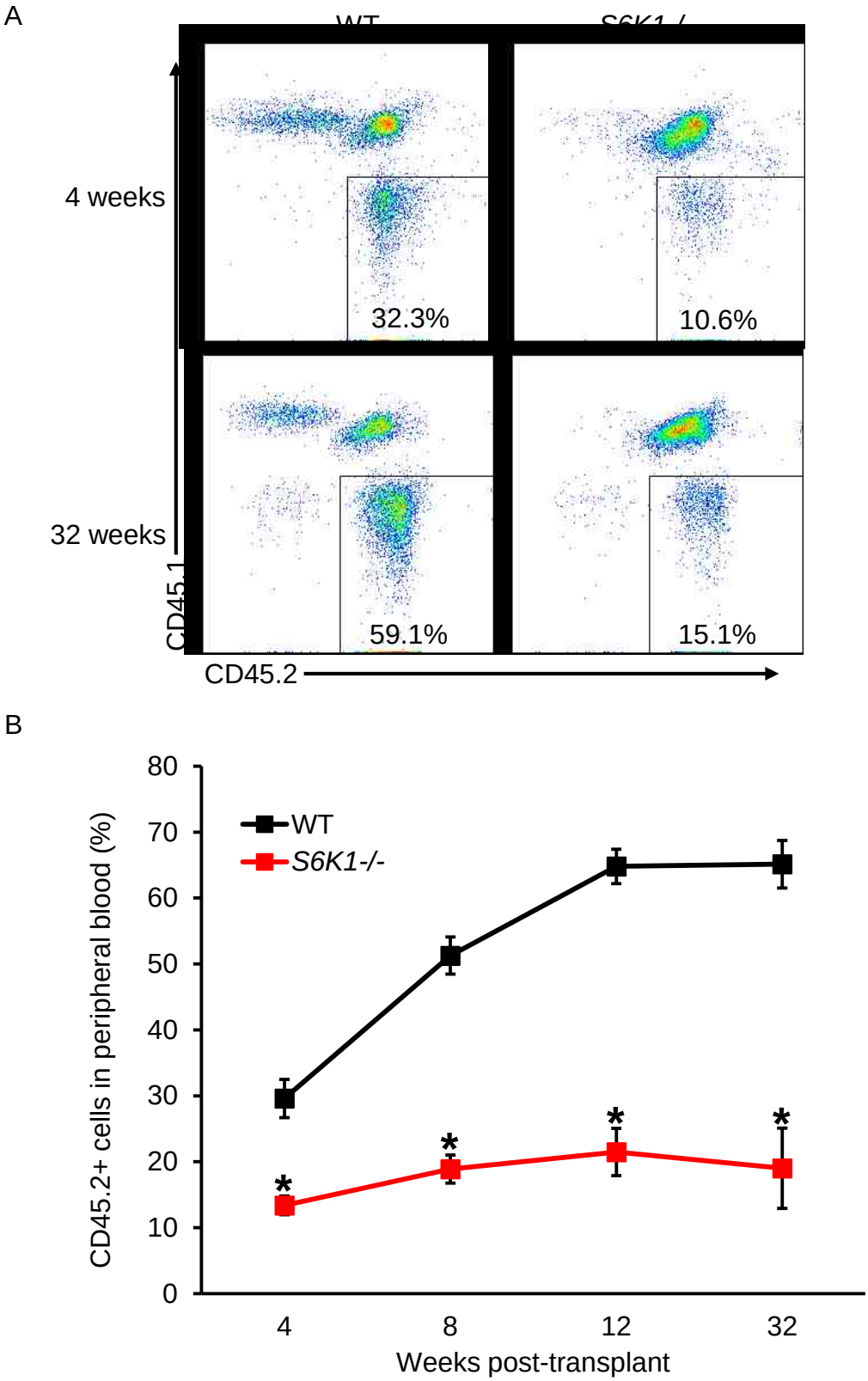
A
WT
S6K1-/-
4 weeks
32 weeks
32.3%
10.6%
59.1%
15.1%
CD45.1
CD45.2
B
WT
S6K1-/-
CD45.2+ cells in peripheral blood (%)
0
10
20
30
40
50
60
70
80
4
8
12
32
Weeks post-transplant
*
*
*
*

Figure 30: S6K1 deficiency causes reduced self-renewal of HSCs in tertiary recipients.

Quantitative representation of donor-derived cells in peripheral blood of tertiary transplant recipients with cells derived from secondary transplant recipients of either WT or *S6K1-/-* LT-HSCs. After 24 weeks of secondary transplant, $1X10^6$ MNCs isolated from the recipients of either WT or *S6K1-/-* LT-HSCs and transplanted into lethally irradiated F1 recipients. Peripheral blood was obtained from the tertiary recipients at different time points and analyzed for engraftment of donor-derived cells by flow cytometry. n=8-10 mice in each group. Data are expressed as mean ± SEM. Difference between the group means was analyzed by one-way ANOVA with Bonferroni post-hoc analysis; *$p<0.05$.

Figure 31

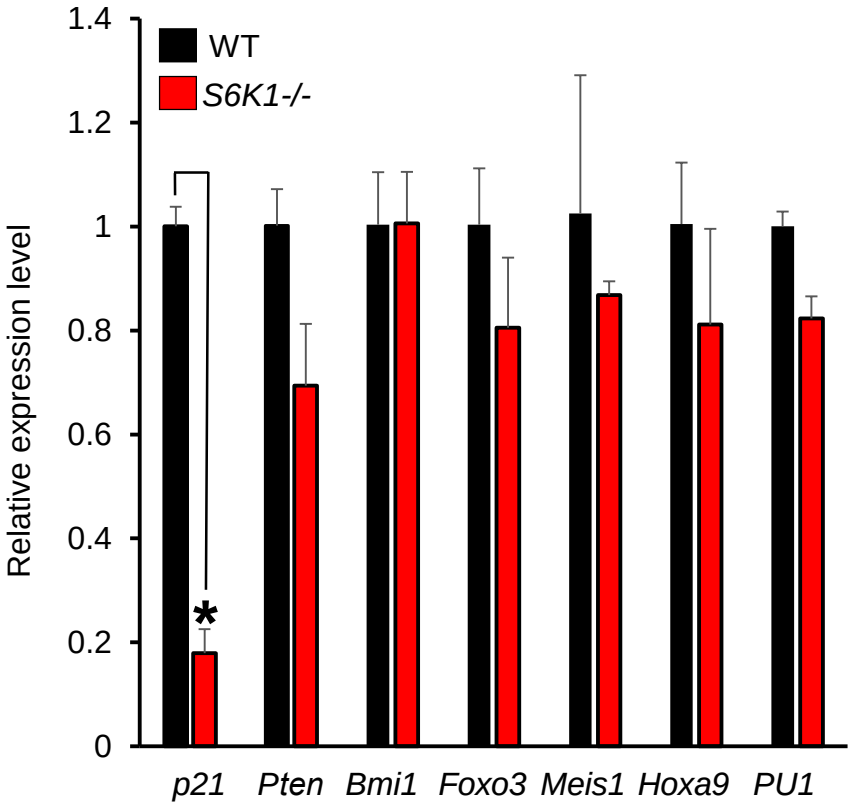
1.4
1.2
1
0.8
0.6
0.4
0.2
0
Relative expression level
WT
S6K1-/-
*
p21
Pten
Bmi1
Foxo3
Meis1
Hoxa9
PU1

Figure 31: S6K1 deficiency causes reduction in *p21* expression in LSK cells in secondary recipients.

Quantitative representation of expression level of genes in of donor-derived BM LSK (CD45.2+ LSK) cells isolated from secondary transplant recipients. Experiment was performed in quadruplicates. Data are expressed as mean ± SD; *p<0.05.

compared to empty vector expressing HSC/Ps (MIEG3), cells transduced with MIEG3-S6K1 (Figure 32A, Lane2) expressed significantly higher level of S6K1 as well as increased activation level compared to cells transduced with empty vector (Figure 32A, Lane1).

We next determined if overexpression of S6K1 renders any proliferative advantage to HSC/Ps. We transduced WT HSC/Ps with either MIEG3 or MIEG3-S6K1 and sorted to homogeneity by FACS according to GFP expression. The cells were starved in serum-free media and thymidine incorporation assay was performed as described in the materials and methods section. Overexpression of S6K1 does not have any effect on proliferation of WT HSC/Ps in presence of growth factors (Figure 32B). To determine if the overexpressed protein functions similarly like endogenous protein *in vitro*, we transduced *S6K1-/-* HSC/Ps with either MIEG3 or MIEG3-S6K1 and sorted to homogeneity by FACS according to GFP expression. *S6K1-/-* HSC/Ps transduced with empty vector have significantly increased proliferation in presence of growth factors. However, the increase in proliferation of *S6K1-/-* HSCP/s was abrogated when S6K1 is overexpressed in S6K1 deficient cells (Figure 32B). Overall, these data suggest that overexpression of S6K1 in HSC/Ps result in hyperphosphorylation of S6K1. However, the increase in S6K1 activity does not result in increased proliferation of HSC/Ps in presence of growth factors.

Overexpression of S6K1 in HSCs results in reduced self-renewal:

To determine the functional significance of overexpression of S6K1 in HSCs, we performed competitive repopulation assay (Figure 33). Lethally

Figure 32

A

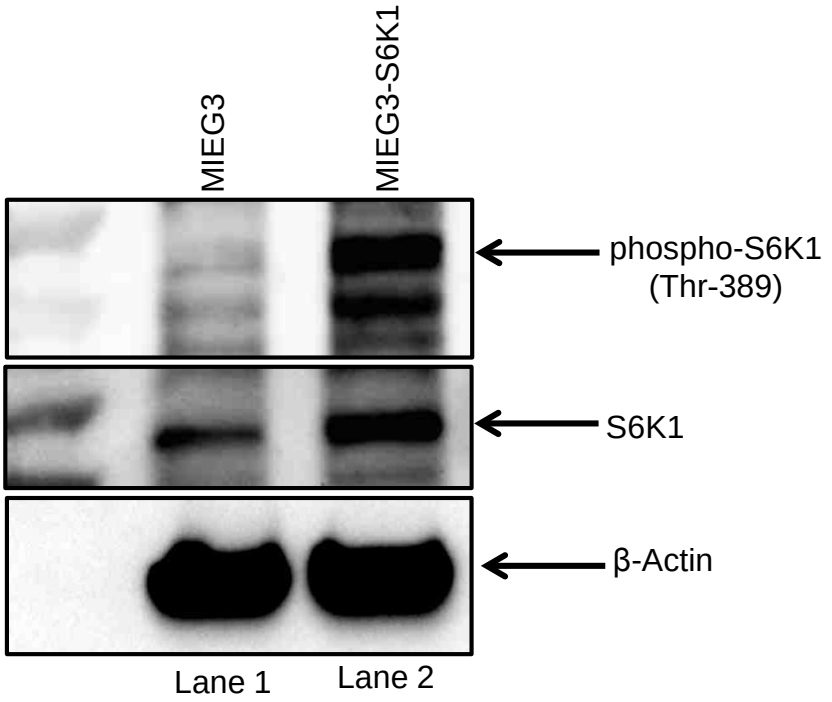
MIEG3
MIEG3-S6K1
phospho-S6K1
(Thr-389)
S6K1
β-Actin
Lane 1
Lane 2

B

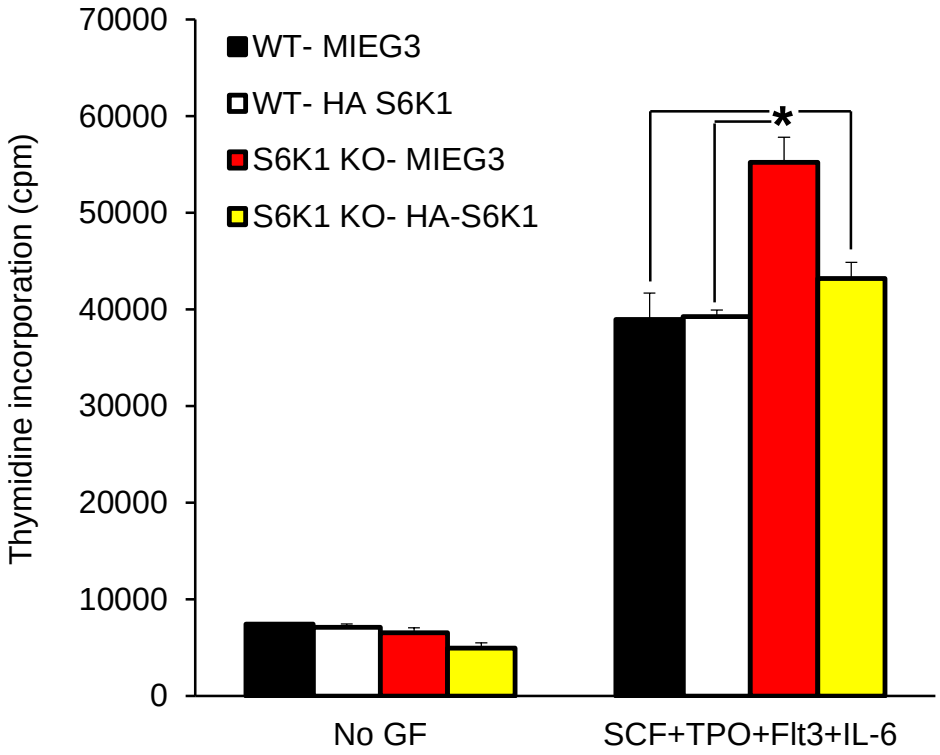
70000
60000
50000
40000
30000
20000
10000
0
Thymidine incorporation (cpm)
WT- MIEG3
WT- HA S6K1
S6K1 KO- MIEG3
S6K1 KO- HA-S6K1
*
No GF
SCF+TPO+Flt3+IL-6

Figure 32: Overexpression of S6K1 in HSC/Ps.

(A) Expression level of phospho-S6K1 and S6K1 in WT HSC/Ps transduced with either MIEG3 or MIEG3-S6K1. ß-Actin was used as a loading control. (B) Thymidine incorporation assay with WT and *S6K1-/-* HSC/Ps transduced with MIEG3 or MIEG3-S6K1. WT and *S6K1-/-* HSC/Ps were transduced with either MIEG3 or MIEG3-S6K1 and sorted to homogeneity based on GFP expression. Cells were serum starved and plated in absence of growth factors (No GF) or in presence of growth factors (SCF, TPO, IL-6, Flt3). After 42 hours, cells were pulsed with thymidine and thymidine incorporation into cells were determined after 6 hours of pulse. Experiment was performed in quadruplicates. Data are expressed as mean ± SEM; *$p<0.05$.

Figure 33

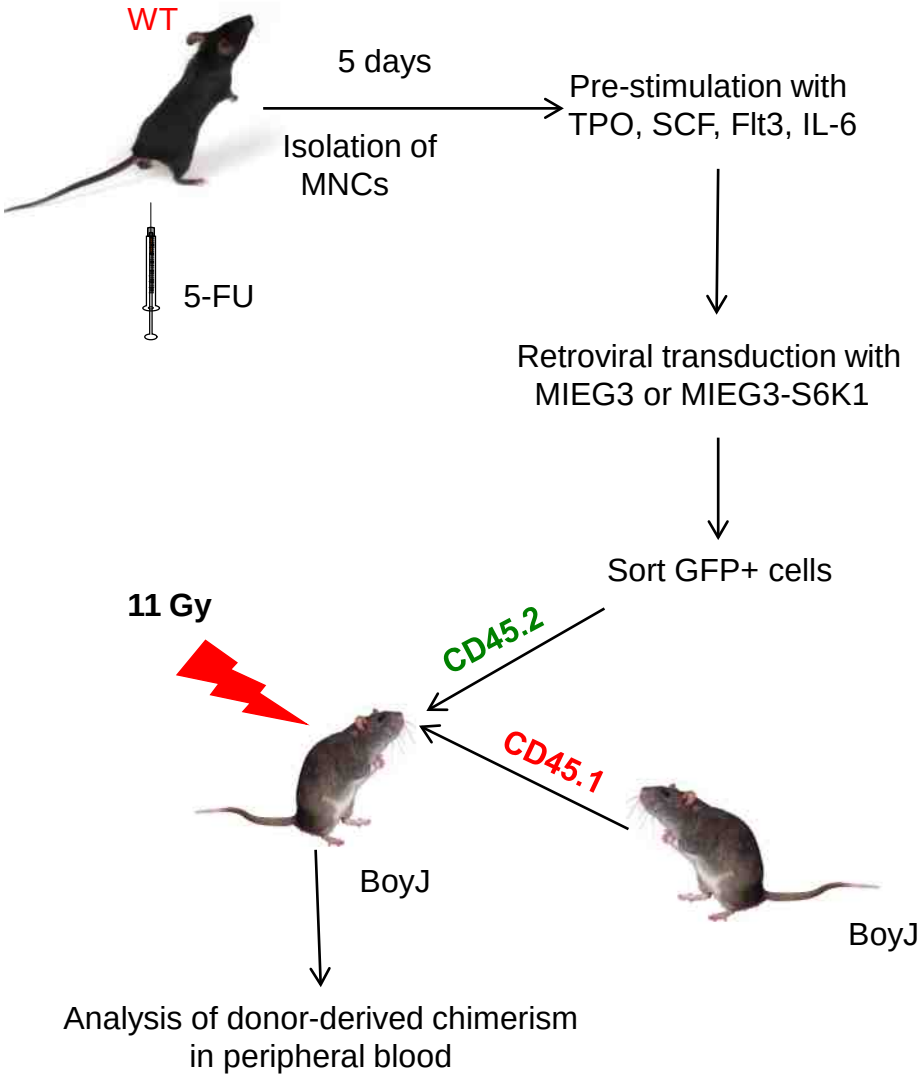
WT
5 days
Isolation of MNCs
5-FU
Pre-stimulation with TPO, SCF, Flt3, IL-6
Retroviral transduction with MIEG3 or MIEG3-S6K1
Sort GFP+ cells
11 Gy
CD45.2
CD45.1
BoyJ
BoyJ
Analysis of donor-derived chimerism in peripheral blood

Figure 33: Model of primary transplant using HSCs overexpressing S6K1.

$1.5X10^5$ MIEG3 or MIEG3-S6K1 HSCs (GFP+) were mixed with $3X10^5$ MNCs isolated from Boy/J mice and transplanted into lethally irradiated Boy/J recipients. Peripheral blood was obtained from the recipients at different time points and analyzed for engraftment of donor-derived cells (GFP+) by flow cytometry.

irradiated mice were transplanted with either WT expressing MIEG3 or MIEG3-S6K1. Mice transplanted with S6K1 overexpressing HSCs showed significantly decreased short-term and long-term engraftment in the peripheral blood of recipients compared to MIEG3 recipients that persisted up to 24 weeks after transplantation (Figure 34A and B).

To determine the effect of S6K1 overexpression and hyperactivation on self-renewal on HSCs, BM MNCs were isolated from primary recipients after 24 weeks post-transplant. GFP+ cells were sorted from BM MNCs derived from recipients of either MIEG3 or MIEG3-S6K1 expressing HSCs (Figure 35). Sorted cells were mixed with syngenic competitor cells and transplanted into lethally irradiated recipients for secondary transplant. Secondary recipients of S6K1 overexpressing cells had significantly reduced engraftment of GFP+ cells in the peripheral blood of recipients compared to controls. The difference in engraftment of S6K1 overexpressing cells persisted from week 4 to week 18 post-transplant (Figure 36A and B). We next analyzed the engraftment of GFP+ cells in the BM of the secondary recipients after 18 weeks post-transplant. The recipients of S6K1 overexpressing HSCs also showed significantly reduced GFP+ BM MNCs compared to controls (Figure 37A and B).

Previous studies have demonstrated that deficiency in Akt activity results in reduced engraftment and self-renewal of HSCs (Juntilla et al., 2010). As described previously, S6K1 is a regulator of Akt activation through a negative feedback loop in which S6K1 directly regulates mTORC2 activity (Julien et al., 2010). We determined the effect of S6K1 overexpression on Akt activity. We

Figure 34

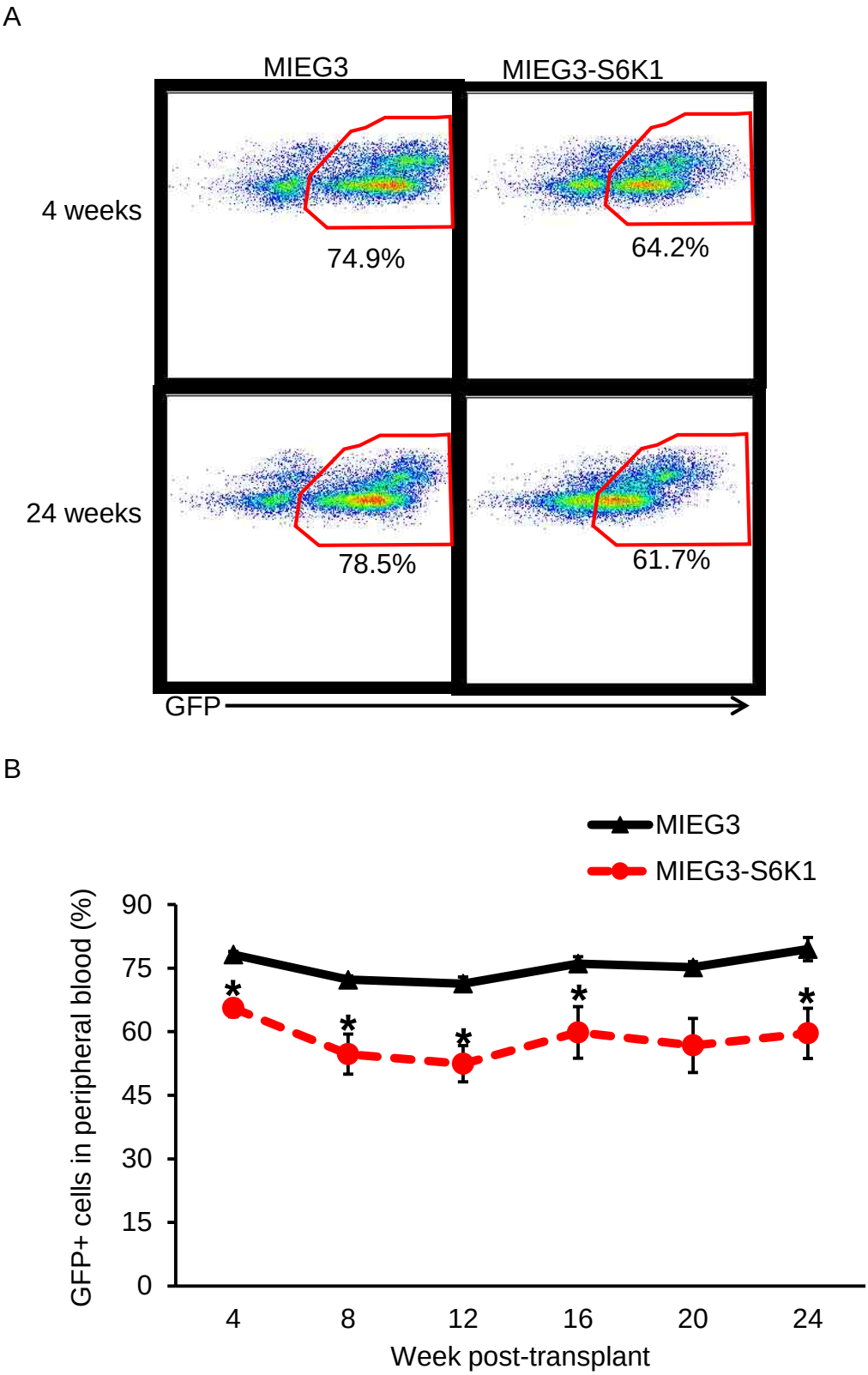
A
MIEG3
MIEG3-S6K1
4 weeks
24 weeks
74.9%
64.2%
78.5%
61.7%
GFP
B
MIEG3
MIEG3-S6K1
GFP+ cells in peripheral blood (%)
90
75
60
45
30
15
0
4
8
12
16
20
24
Week post-transplant

Figure 34: Hyperactivation of S6K1 causes reduced engraftment of HSCs in primary transplant recipients.

(A) Representative flow plot of peripheral blood of primary transplant recipients of either WT HSCs transduced with either MIEG3 or MIEG3-S6K1 at 4 and 24 weeks after transplantation. Peripheral blood was obtained from the recipients at different time points and analyzed for engraftment of donor-derived cells (GFP+) by flow cytometry. (B) Quantitative representation of donor-derived cells in peripheral blood of primary transplant recipients of WT HSCs transduced with either MIEG3 or MIEG3-S6K1; n=4-6 mice in each group. Data are expressed as mean ± SEM; *$p<0.05$.

Figure 35

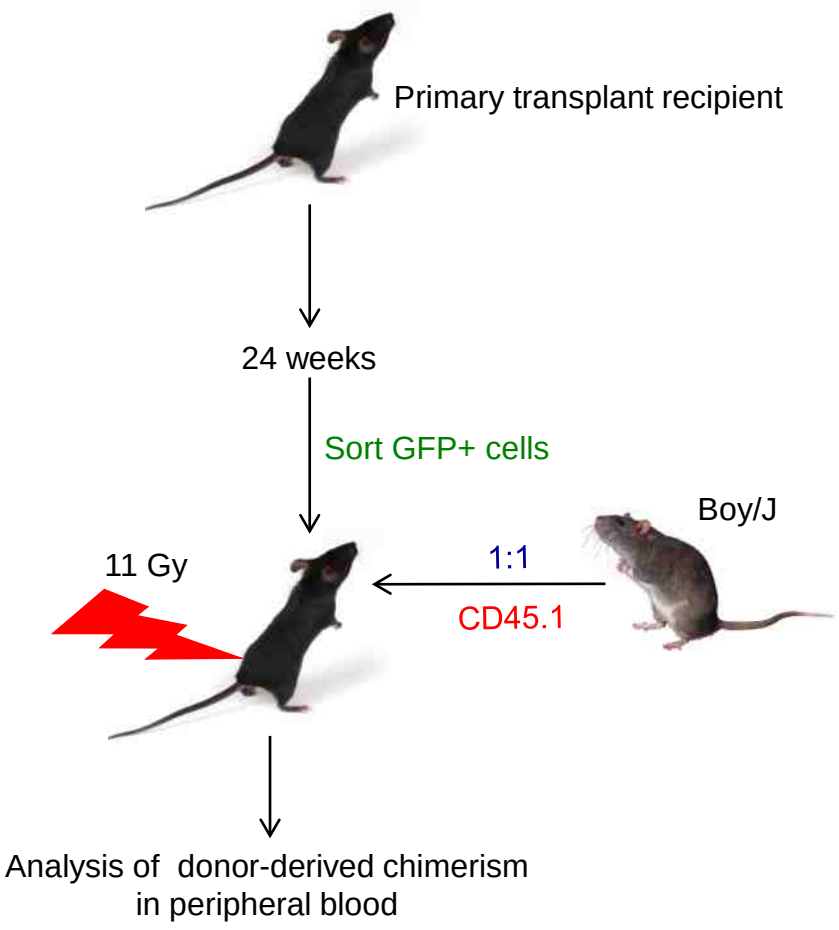
Primary transplant recipient
24 weeks
Sort GFP+ cells
Boy/J
1:1
CD45.1
11 Gy
Analysis of donor-derived chimerism
in peripheral blood

Figure 35: Model of secondary transplantation with HSCs overexpressing S6K1.

At 24 weeks after primary transplant, $5X10^5$ MIEG3 or MIEG3-S6K1 BM MNCs (GFP+) were sorted from primary transplant recipients, mixed with $5X10^5$ MNCs isolated from Boy/J mice and transplanted into lethally irradiated Boy/J recipients. Peripheral blood was obtained from the recipients at different time points and analyzed for engraftment of donor-derived cells by flow cytometry

Figure 36

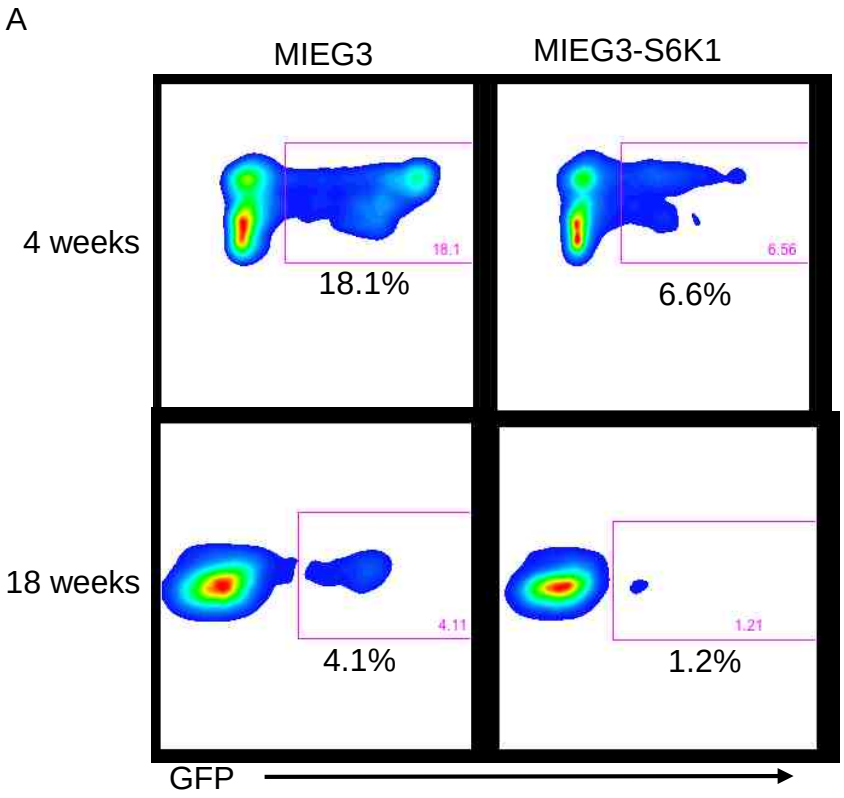
A
MIEG3
MIEG3-S6K1
4 weeks
18 weeks
18.1%
6.6%
4.1%
1.2%
GFP
B
GFP+ cells in peripheral blood (%)
MIEG3
MIEG3-S6K1
Weeks post-transplant
0
4
8
12
16
18
20

Figure 36: Hyperactivation of S6K1 causes reduced self-renewal of HSCs.

(A) Representative flow plot of peripheral blood of secondary transplant recipients of either WT HSCs transduced with either MIEG3 or MIEG3-S6K1 after 4 and 18 weeks of transplantation. At 24 weeks after primary transplant, $5X10^5$ MIEG3 or MIEG3-S6K1 HSCs (GFP+) were sorted from primary transplant recipients, mixed with $5X10^5$ MNCs isolated from Boy/J mice and transplanted into lethally irradiated Boy/J recipients. Peripheral blood was obtained from the recipients at different time points and analyzed for engraftment of donor-derived cells by flow cytometry. (B) Quantitative representation of donor-derived cells in peripheral blood of secondary transplant recipients of WT HSCs transduced with either MIEG3 or MIEG3-S6K1; n=7 mice in each group. Data are expressed as mean ± SEM; *$p<0.05$.

Figure 37

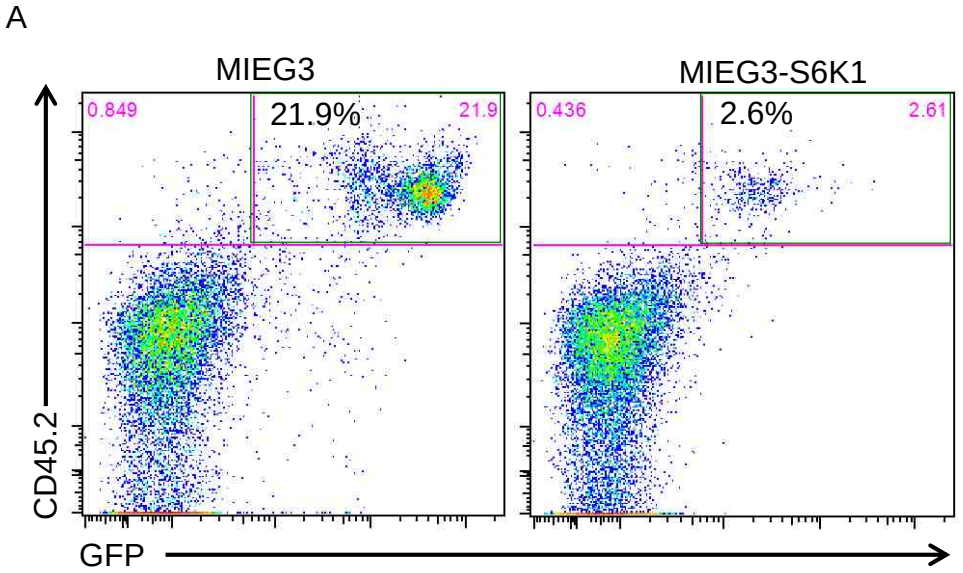
A
MIEG3
MIEG3-S6K1
0.849
21.9%
21.9
0.436
2.6%
2.61
CD45.2
GFP

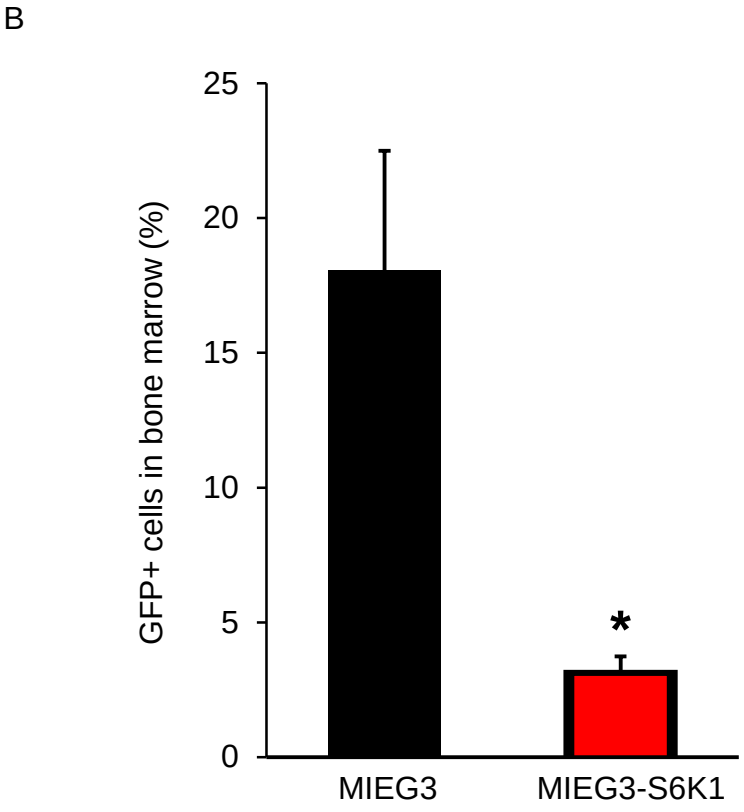
B
25
20
15
10
5
0
GFP+ cells in bone marrow (%)
*
MIEG3
MIEG3-S6K1

Figure 37: Hyperactivation of S6K1 causes reduced engraftment of HSCs in BM of secondary recipients.

(A) Representative flow plot of donor-derived cells (GFP+) in BM of secondary transplant recipients at 18 weeks after secondary transplant. (B) Quantitative representation of donor-derived cells in BM of secondary transplant recipients of WT HSCs transduced with either MIEG3 or MIEG3-S6K1; n=7 mice in each group. Data are expressed as mean ± SEM; *$p<0.05$.

transduced WT HSC/Ps with either empty vector or S6K1 and sorted the cells to homogeneity based on GFP expression and protein expression level was determined as described in the materials and methods section. Akt phosphorylation on Ser-473 was significantly reduced in HSC/Ps overexpressing S6K1 (Figure 38, Lane 2) as compared to controls (Figure 38, Lane 1). Overall, these data suggest that hyperactivation of S6K1 in HSCs results in reduced engraftment and self-renewal, which is associated with reduced activation of Akt in HSC/Ps.

Figure 38

A

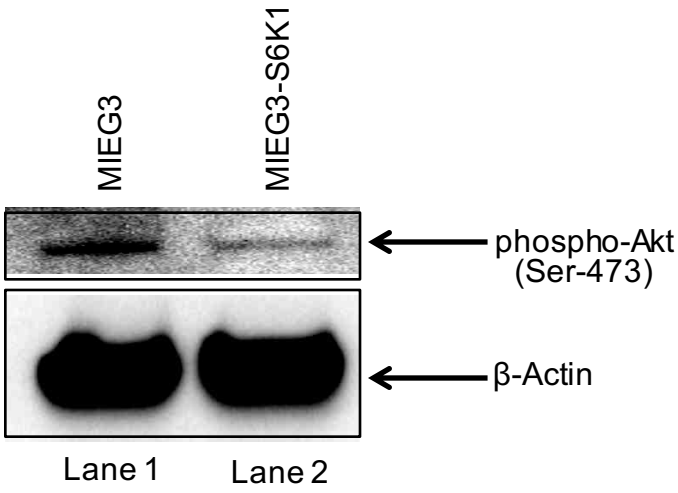
MIEG3
MIEG3-S6K1
phospho-Akt
(Ser-473)
β-Actin
Lane 1
Lane 2

B

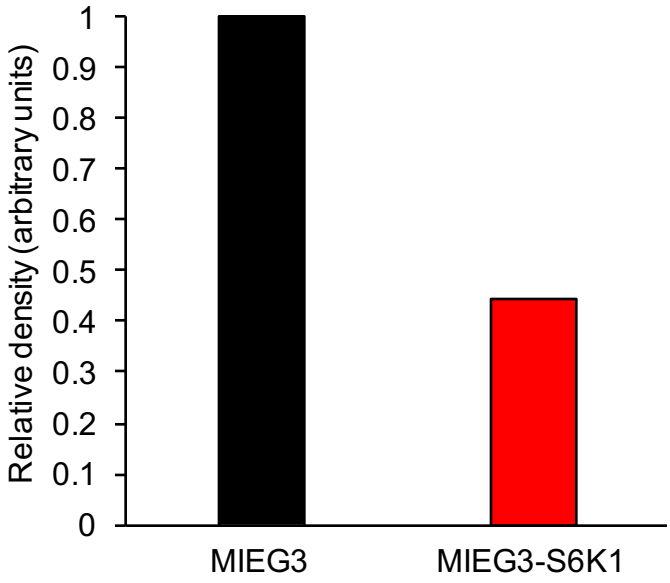
Relative density (arbitrary units)
1
0.9
0.8
0.7
0.6
0.5
0.4
0.3
0.2
0.1
0
MIEG3
MIEG3-S6K1

Figure 38: Hyperactivation of S6K1 results in increased Akt phosphorylation in HSC/Ps.

(A) Expression level of phospho-Akt in WT HSC/Ps transduced with either MIEG3 or MIEG3-S6K1. WT HSC/Ps were transduced with either MIEG3 or MIEG3-S6K1 and sorted based on GFP expression. Sorted cells were cultured *in vitro*. Ten million cells in each group were serum starved and protein was extracted. Proteins were separated by immunoblotting and probed with antibody against phosphorylated form of Akt. ß-Actin was used as a loading control. Data representative of two independent experiments. (B) Quantitative representation of relative density of phospho-Akt normalized to ß-Actin expression level.

Discussion:

The role of activators as well as inhibitors of S6K1 activity in regulation of HSC function have been studied in detail (Juntilla et al., 2010; Lee et al., 2010; Magee et al., 2012). However, the exact role of S6K1 expression and activity level in regulation of HSC function has not been studied before. Our data establishes that the level of S6K1 activation is critical for the self-renewal of HSCs. In the primary transplant, the engraftment potential of HSCs can be evaluated in a competitive setting, while in secondary transplant the self-renewal potential of HSCs can be determined. We found no significant differences in the homing and long-term engraftment of *S6K1-/-* HSCs in primary recipients. These data suggest that S6K1 does not regulate homing and long-term engraftment of HSCs in primary recipients. Our studies also show that S6K1 does not regulate short-term engraftment of HSCs when highly purified HSCs were used as test cells in a competitive assay. However, there were significant differences in engraftment of donor-derived cells in secondary transplant recipients as well as tertiary transplant recipients. This indicates that S6K1 is a positive regulator of self-renewal of HSCs. This defect in self-renewal could arise from reduced cell cycling or homing of S6K1-defcient HSCs derived from primary recipients. Further studies on homing and cell-cycle status of cells derived from primary recipients are required to identify the exact physiological mechanisms responsible for reduced self-renewal of *S6K1-/-* HSCs.

Previous studies have shown that deletion of mTOR results in reduced engraftment of HSCs in primary transplant recipients (Guo et al., 2013). Similarly,

Akt1 and Akt2 deficient HSCs have decreased engraftment in primary transplant recipients (Juntilla et al., 2010). As activation of mTORC1 results in inactivation of 4E-BP1 and activation of S6K1, it could be possible that both events are required for engraftment of HSCs in primary recipients. However, loss of expression of S6K1 does not affect long-term engraftment in primary recipients, but results in reduced self-renewal of HSCs following serial transplantation. By using genetic models, it has been established that loss of mTORC1 activity results in reduced engraftment and self-renewal of HSCs in mice (Guo et al., 2013; Haneline et al., 2006; Juntilla et al., 2010). However, inhibition of mTORC1 activity in HSCs by using pharmacological inhibitors in human and murine HSCs has yielded contradictory results. In ex-vivo culture of murine HSC enriched population, treatment with rapamycin results in expansion of phenotypically defined HSC enriched population (Luo et al., 2014). Furthermore, rapamycin treatment increases long-term engraftment of murine HSCs (Luo et al., 2014). Treatment of human UCB CD34+ cells with rapamycin results in increased engraftment and self-renewal following serial transplantation (Rohrabaugh et al., 2011). This difference in functional outcome could also be due to differential regulation of *p21* in different models. In our study, we show that expression level of *p21* was significantly down-regulated in *S6K1-/-* LSK cells isolated from BM of secondary recipients. Cheng et al. have demonstrated that *p21* deficient HSCs displays reduced self-renewal potential and exhaust upon serial transplant and from quaternary transplant have significantly reduced repopulating ability, which indicates a decline in self-renewal (Cheng et al., 2000). On the other hand,

previous studies have shown that rapamycin increases *p21* expression. Rapamycin treatment results in increased *p21* expression level in response to TGF-ß (Law et al., 2002). TGF-ß1 is a positive regulator of quiescence and previous studies have demonstrated its inhibitory effect on HSC and HPC proliferation (Ohta et al., 1987; Ottmann and Pelus, 1988; Yamazaki et al., 2009). TGF-ß1 treatment of human UCB CD34+ cells upregulates *p21* mRNA expression level (Ducos et al., 2000). It is possible that rapamycin treatment increases *p21* expression level in HSCs that results in increased self-renewal potential of HSCs. Lee et al. have demonstrated that peroxisome proliferator-activated receptor (PPAR)-γ and retinoic acid X receptor (RXR)-α heterodimer represses TGF-ß1 expression level by inhibiting S6K1 activation (Lee et al., 2006). Loss of S6K1 expression in HSCs could result in decreased TGF-ß1 expression, which in turn downregulates p21 expression in *S6K1-/-* HSCs. The increase in long-term engraftment following rapamycin treatment could be also due to increased expression level of Bmi1 in HSCs following rapamycin treatment (Luo et al., 2014). Bmi1 represses p16 expression level thus decreasing cellular senescence in HSCs (Park et al., 2003) and inhibition of p16 activity has been associated with increase in HSC function (Janzen et al., 2006).

Interestingly, our studies also provide evidence that expression and activation level of S6K1 is critical for engraftment and self-renewal of HSCs. In this study, we have shown that loss of expression of S6K1 in HSCs as well as overexpression and hyperactivation of S6K1 in HSCs results in reduced engraftment and self-renewal of HSCs. We also show that Akt activity is

diminished following overexpression of S6K1 in HSC/Ps. As loss of Akt activity results in decreased engraftment of HSCs, the reduction in engraftment of HSCs following overexpression of S6K1 could be due to reduced Akt activity (Juntilla et al., 2010). S6K1 has been identified as a negative regulator of mTORC2-dependent activation of Akt. SIN1 and Rictor are two components of mTORC2 complex and both are required for mTORC2-dependent phosphorylation of Akt (Yang et al., 2006). In MEF, S6K1 phosphorylates SIN1 at Thr-86 and Thr-398 thus impairing mTORC2 activity (Figure 39A) (Liu et al., 2013). In MEFs, following mTORC1-dependent activation, S6K1 also phosphorylates Rictor, another component of mTORC2, at Thr-1135 (Figure 39A) (Julien et al., 2010). Phosphorylation of Rictor at Thr-1135 by S6K1 results in inhibition of Akt activity (Julien et al., 2010). It is probable that following overexpression of S6K1 in HSC/Ps, the reduction in Akt activation could be due to inhibition of mTORC2 activity by hyperactivated S6K1 (Figure 39B).

It has been shown previously that either hyperactivation or loss of function of PI3K-mTORC1 pathway negatively regulates the functions of HSCs (Campbell et al., 2009; Chen et al., 2008; Guo et al., 2013; Haneline et al., 2006; Juntilla et al., 2010; Kharas et al., 2010; Lee et al., 2010; Yilmaz et al., 2006b). However, these studies involved a single approach involving either loss of expression or overexpression of a single component of the PI3K-mTORC1 pathway. In our studies, we provide compelling evidence that both loss of expression and gain of expression of a single component of PI3K-mTORC1 pathway have the same impact on the functional potential of HSCs. The dependency of HSCs on a

Figure 39

A

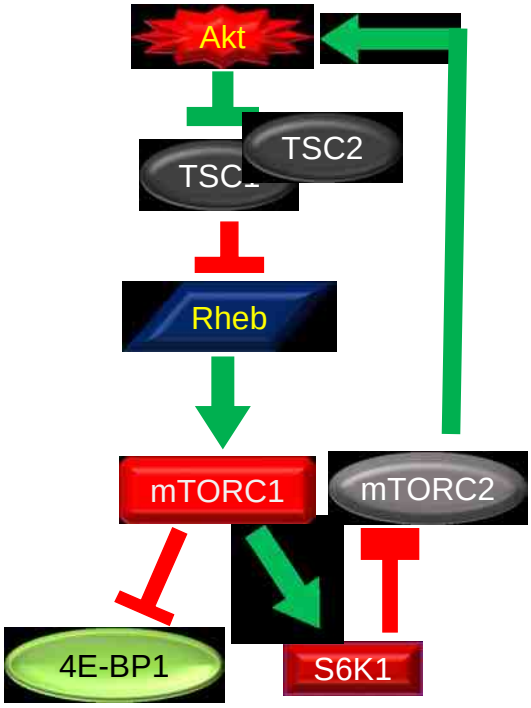
Akt
TSC2
Rheb
mTORC1
mTORC2
4E-BP1
S6K1

B

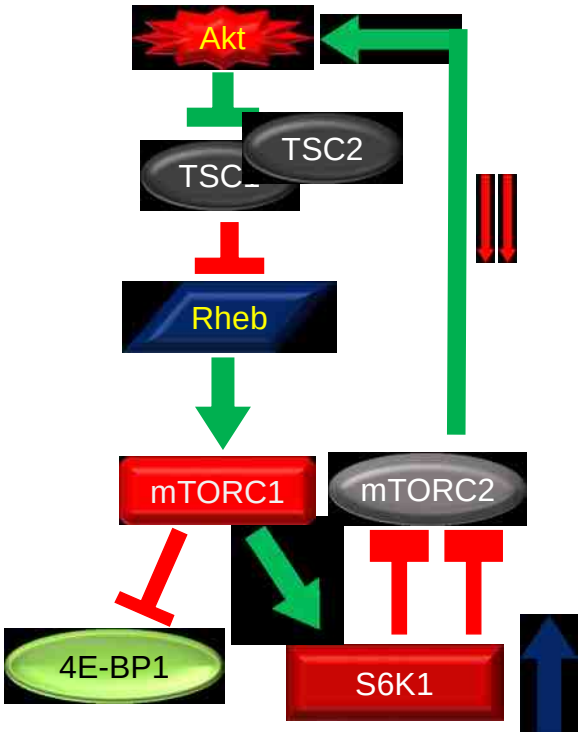
Akt
TSC2
Rheb
mTORC1
mTORC2
4E-BP1
S6K1

Figure 39: Proposed mechanism of effect of S6K1 overexpression on Akt-mTORC activity in HSCs.

A schematic model of potential signaling pathways that could affect Akt activity based on the evidence provided in our studies as well as current literature. (A) In normal HSCs, mTORC2 acts an activator of Akt. S6K1 exerts an inhibitory effect on mTORC2 thus negatively regulating Akt phosphorylation. (B) Following overexpression of S6K1, S6K1-mediated inhibition of mTORC2 is increased which results in downregulation of Akt activity in HSCs.

threshold level of a single factor have been described before. HSCs deficient in both Akt1 and Akt2 displayed significantly reduced differentiation compared to controls along with reduced ROS level (Juntilla et al., 2010). However, the differentiation of Akt1 and Akt2 deficient HSCs significantly increased following increase in ROS level (Juntilla et al., 2010). On the other hand, in Foxo or Atm deficient mice, HSCs display an increase in ROS level, which causes exhaustion of HSC pool (Ito et al., 2004; Tothova et al., 2007). Treatment with N-acetyl-Lcysteine, an antioxidative agent, which decreases cellular ROS level, reverses the phenotype of Atm or Foxo deficient HSCs (Ito et al., 2004; Tothova et al., 2007). Zhou et al. have demonstrated that rotenone inhibits S6K1 activity and increases the ROS level in neurons. In astrocytes, ischemia induced by oxygen and glucose deprivation causes increased ROS level, which was associated with decreased S6K1 activity (Zhou et al., 2015). It is probable that S6K1 activity regulates the critical ROS level that is required for proper functioning of HSCs. Additionally, the importance of critical S6K1 level has been described before. A study by Yang et al. has shown that in PTEN deficient neurons, both overexpression or loss of expression of S6K1 results in reduced axon regeneration (Yang et al., 2014). It is probable that in HSCs too, a critical level of S6K1 is required to maintain self-renewal.

In summary, we have defined the role of S6K1 in self-renewal, engraftment and differentiation of HSCs. Following serial transplantation, *S6K1-/-* HSCs had significantly decreased engraftment in the recipients. However, hyperactivation of S6K1 in HSCs also results in reduced engraftment in

recipients upon serial transplantation. Taken together, these data suggest that activation level of S6K1 is critical for maintenance of self-renewal potential of HSCs. Previous studies have shown that hyperactivation of mTORC1 or loss of function of mTORC1 causes reduced engraftment of HSCs. Our data indicate S6K1 could be the key regulator of mTORC1 functions in regulation of self-renewal of HSCs. Our study also establishes that S6K1 deficiency does not affect differentiation or homing of HSCs in primary transplant recipients. We have showed that *p21* expression is reduced in *S6K1-/-* HSCs derived from secondary recipients. We also provide evidence that hyperactivation of S6K1 results in reduced activation of Akt in HSC/Ps. We hypothesize that this reduction in Akt activation could be due to reduced mTORC2 activity in HSCs overexpressing S6K1 (Figure 39B).

Chapter 6: S6K1 is a positive regulator of propagation of acute myeloid leukemia

Introduction:

Previous studies from our group and others have established that PI3K-mTORC1 pathway, of which S6K1 is a part of, plays an essential role in regulating myeloproliferative neoplasms. Pharmacological inhibition of PI3K, Akt or mTORC1 results in reduced S6K1 activity (Boulay et al., 2004; Liu et al., 2014a; Xin et al., 2014). Furthermore, PI3K, Akt and mTORC1, the upstream regulators of S6K1 activation, have been identified as critical mediators of myeloproliferative neoplasms. Previous studies from our lab have shown that p85 regulatory subunit of PI3K regulates c-Kit D814V mutation induced transformation in murine cells. We have also demonstrated that inhibition of p85α activity in oncogenic c-Kit expressing cells is sufficient to suppress growth and leukemogenesis (Munugalavadla et al., 2007; Munugalavadla et al., 2008). Consistently, pharmacologic inhibition of mTORC1 activity is sufficient to inhibit the growth of oncogenic c-Kit expressing cells (Munugalavadla et al., 2007). The p110δ catalytic subunit of PI3K, is the primarily upregulated PI3-K isoform in AML cells (Sujobert et al., 2005). Combined inhibition of p110δ activity and mTORC1 activity results in increased apoptosis and reduced survival of AML cells compared to individual inhibition of either mTORC1 or p110α (Colamonici et al., 2015).

Deletion of PTEN, a negative regulator of S6K1 activation, results in leukemogenesis in mice (Yilmaz, 2006). Pharmacological inactivation of mTORC1 activity in PTEN-deficient mice prolongs their survival, which suggests that PTEN-deficient AML cells require S6K1 for leukemogenesis (Yilmaz et al., 2006b). Dysregulated PTEN transcript level in AML patients have been associated with increased activation of Akt and poor prognosis in AML patients (Cheong et al., 2003). Older AML patients who are negative for or lack PTEN expression but are positive for the expression of CD44 demonstrate poor overall survival (Huang et al., 2015). As S6K1 and mTORC1 remains hyperactive in PTEN deficient hematopoietic cells (Magee et al., 2012), it is important to understand the role of S6K1 in AML to determine if S6K1 is critical for leukemogenesis.

Akt is phosphorylated at Thr-308 and Ser-473 in 50-72% of AML patients (Tamburini, 2007; Min, 2003). Phosphorylation on either of the residues of Akt is associated with poor overall survival in AML patients. The PI3-K pathway in AML cells can also be hyperactivated because of activation of the IGF-1/IGF-1R autocrine loop (Chapuis et al., 2010a). Deletion of Raptor, a component of mTORC1, results in delayed AML progression in vivo (Hoshii et al., 2012). Deficiency of Raptor induces apoptosis selectively in differentiated AML cells, but not in undifferentiated AML cells, which might result in delayed AML progression in mice (Hoshii et al., 2012). Furthermore, S6K1 phosphorylation level is decreased in Raptor-deficient AML cells (Hoshii et al., 2012). There is evidence suggesting that oncogenes could regulate mTORC1 activation bypassing Akt.

Cells bearing FMS-like tyrosine kinase-3 internal tandem duplication (FLT3-ITD) activates Stat5, which results in mTORC1 activation, rendering the cells resistant to PI3K-Akt inhibitor (Nogami et al., 2015). This study suggests mTORC1 can be activated in AML cells by oncogenic receptors through a mechanism that is independent of Akt activation. This evidence emphasizes the fact that the detailed study of S6K1, a downstream effector of mTORC1, is required to understand the role of mTORC1 activation in AML.

In this chapter, we show that S6K1 delays the propagation of AML inn secondary recipients, but does not play a role in leukemia initiation and progression. Furthermore, mTORC1 activity is reduced in S6K1 deficient AML cells. We also demonstrate that PF-4708671, a specific inhibitor of S6K1, can inhibit the growth of human leukemic cells *in vitro* and inhibits mTORC1 activity.

Results:

Deficiency of S6K1 in HSC/Ps does not affect leukemia initiation and progression:

Based on previous studies demonstrating the importance of mTORC1 activation in AML, we hypothesized that S6K1 is a regulator of leukemia initiation, progression and propagation by serial transplantation. We used a well-defined model of AML due to translocation in the MLL gene (Goyama et al., 2013; Harris et al., 2012; Neff et al., 2012). Previous studies have demonstrated that transplantation of WT HSC/Ps expressing MLL-AF9 result in myeloid expansion of HSC/Ps and recipient mice develops AML characterized by increased WBC count in peripheral blood along with splenomegaly (Goyama et al., 2013; Harris et al., 2012; Neff et al., 2012). To test our hypothesis, WT and *S6K1-/-* HSC/Ps were transduced with MLL-AF9 and transplanted into lethally irradiated mice. We monitored the transplant recipients for WBC counts in the peripheral blood and engraftment of donor cells. At 28 days post-transplant, both groups of mice had increased WBC count in the peripheral blood (Figure 40A). Furthermore, there were no differences in the engraftment of donor cells in the peripheral blood of the recipients of WT and *S6K1-/-* HSC/Ps bearing MLL-AF9 (Figure 40B, left panel; Figure 40C). We analyzed peripheral blood of the recipients of WT and *S6K1-/-* HSC/Ps bearing MLL-AF9 for differentiation of cells into myeloid cells. In peripheral blood of WT and *S6K1-/-* HSC/Ps bearing MLL-AF9, GFP+ cells were of myeloid lineage as determined by the expression of Gr1 and Mac1 on the cell surface (Figure 40B, right panel; Figure 40D). The primary transplant recipients

Figure 40

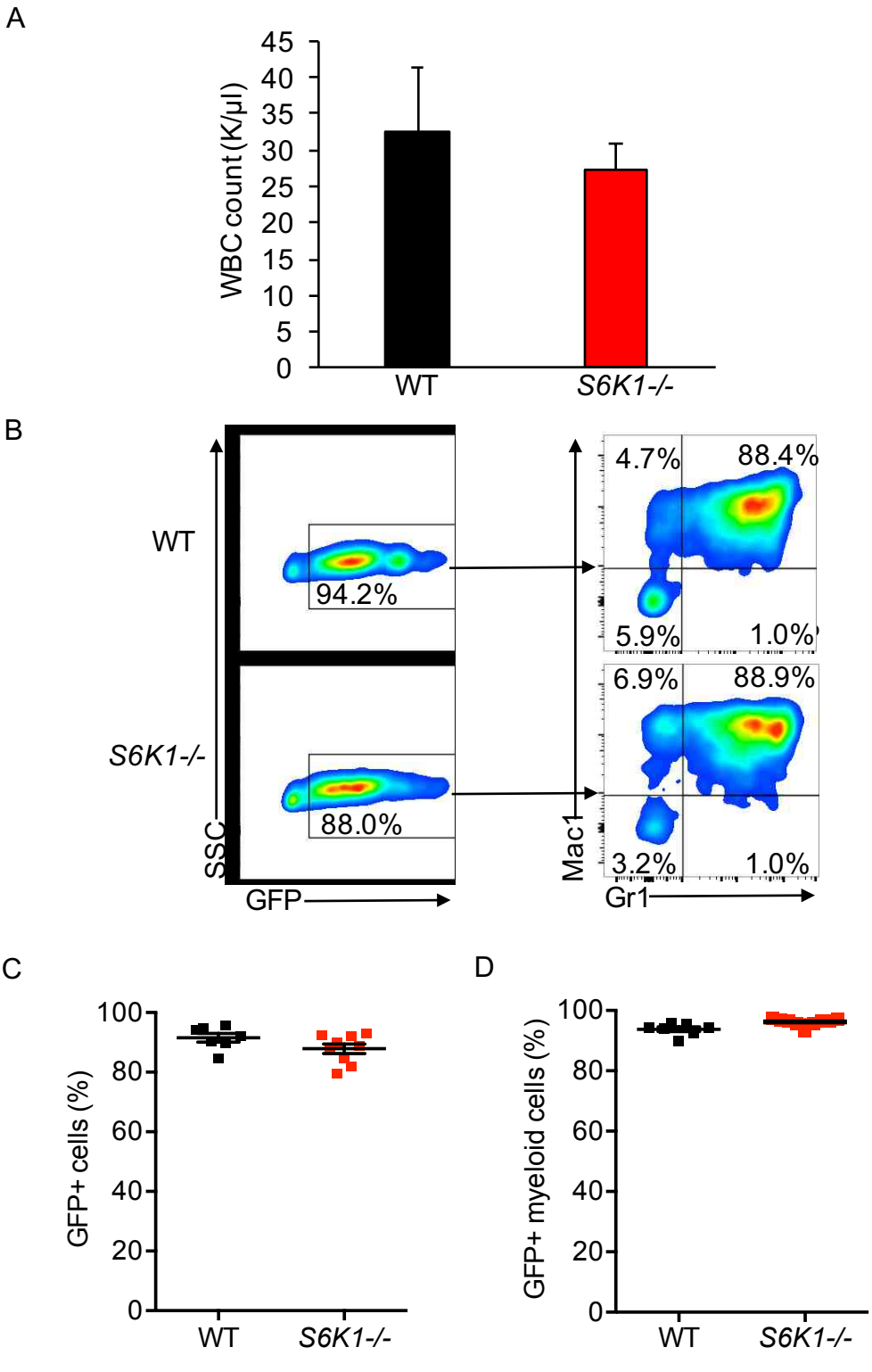
A
WBC count (K/µl)
45
40
35
30
25
20
15
10
5
0
WT
S6K1-/-
B
WT
S6K1-/-
94.2%
88.0%
SSC
GFP
4.7%
88.4%
5.9%
1.0%
6.9%
88.9%
3.2%
1.0%
Mac1
Gr1
C
GFP+ cells (%)
100
80
60
40
20
0
WT
S6K1-/-
D
GFP+ myeloid cells (%)
100
80
60
40
20
0
WT
S6K1-/-

Figure 40: Increased WBC counts and expansion of myeloid cells in primary transplant recipients of HSC/Ps expressing MLL-AF9.

(A) Quantitative representation of WBC count in primary transplant recipients of WT and *S6K1-/-* HSC/Ps expressing MLL-AF9. (B) Representative flow plot of GFP+ cells and GFP+ myeloid cells in peripheral blood of primary recipients of WT and *S6K1-/-* HSC/Ps expressing MLL-AF9. (C) Quantitative representation of GFP+ cells in peripheral blood of primary recipients. (D) Quantitative representation of GFP+ myeloid cells (Gr1+, Mac1+, Gr1+Mac1+) in peripheral blood of primary recipients. Data are expressed as mean ± SEM; n=11-12 mice in each group.

in both groups developed myeloid leukemia around day 40 (Figure 41A) and developed splenomegaly (Figure 41B). There was no difference in the median survival of both groups bearing MLL-AF9 (Figure 41A). We analyzed the bone marrow of mice with AML to determine the engraftment of donor-derived cells. There was no difference in the engraftment of GFP+ cells within the bone marrow of WT and *S6K1-/-* groups that developed AML (Figure 41C, top panel). When we further analyzed the differentiation of GFP+ cells, most of the cells in the GFP+ fraction were myeloid cells (Gr1+, Mac1+) in both groups of recipients (Figure 41C, bottom panel).

Deficiency of S6K1 delays propagation of leukemia by AML cells:

Previous studies have demonstrated that cells bearing MLL-AF9 fusion gene isolated from primary recipients who have developed AML, can propagate AML in secondary recipients (Harris et al., 2012; Neff et al., 2012). To determine the role of S6K1 in leukemia propagation, we transplanted lethally irradiated mice with splenocytes derived from primary transplant recipients who developed AML (Goyama et al., 2013). The engraftment of GFP+ Mac1+ cells in splenocytes of primary recipients were similar in two groups (Figure 42A and B). Following transplantation, the survival of secondary transplant recipients of cells derived from *S6K1-/-* primary transplant recipients was prolonged significantly compared to controls (Figure 42C). The median survival time of *S6K1-/-* recipients was 24 days compared to median survival of 7 days in WT controls (Figure 42C). We analyzed the peripheral blood and bone marrow of secondary transplant recipients to determine the engraftment of donor cells. The engraftment of GFP+

Figure 41

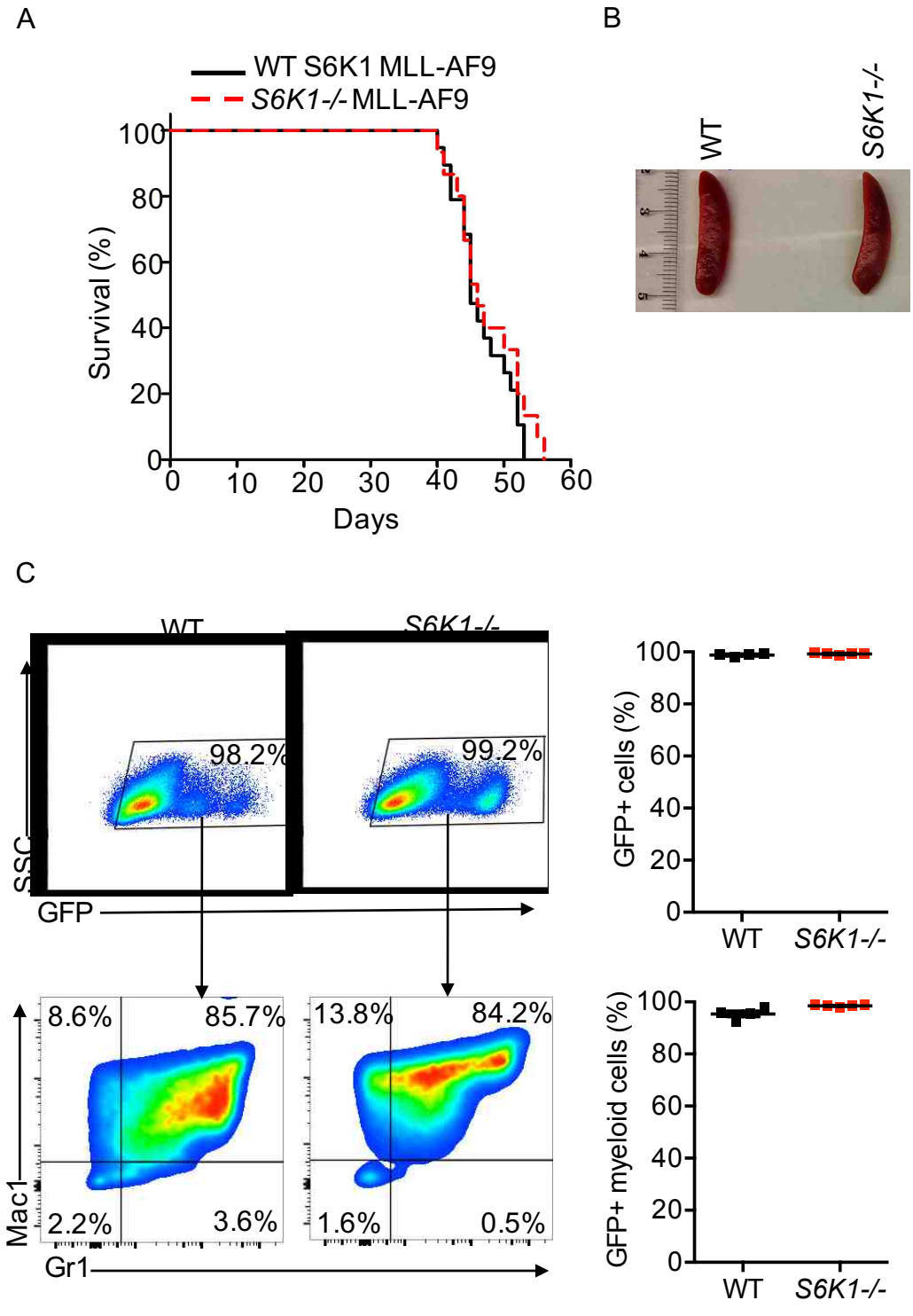
A
WT S6K1 MLL-AF9
S6K1-/- MLL-AF9
Survival (%)
Days
B
WT
S6K1-/-
C
WT
S6K1-/-
98.2%
99.2%
SSC
GFP
8.6%
85.7%
2.2%
3.6%
13.8%
84.2%
1.6%
0.5%
Mac1
Gr1
GFP+ cells (%)
GFP+ myeloid cells (%)

Figure 41: S6K1 does not affect leukemia initiation and progression in primary recipients.

(A) Kaplan-Meier survival curve of primary recipients of WT and *S6K1-/-* HSC/Ps expressing MLL-AF9. Statistical significance between the survival of two groups was analyzed by the log-rank (Mantel-Cox) test. n=15-19 mice in each group. (B) Spleens isolated from WT and *S6K1-/-* primary recipients. (C) Representative flow plot and quantitative representation of GFP+ cells in BM of primary recipients of WT and *S6K1-/-* HSC/Ps expressing MLL-AF9 (top panel). Representative flow plot and quantitative representation of GFP+ myeloid cells (Gr1+, Mac1+, Gr1+Mac1+) in BM of primary recipients of WT and *S6K1-/-* HSC/Ps expressing MLL-AF9 (bottom panel). Data are expressed as mean ± SEM; n=5 mice in each group.

Figure 42

A

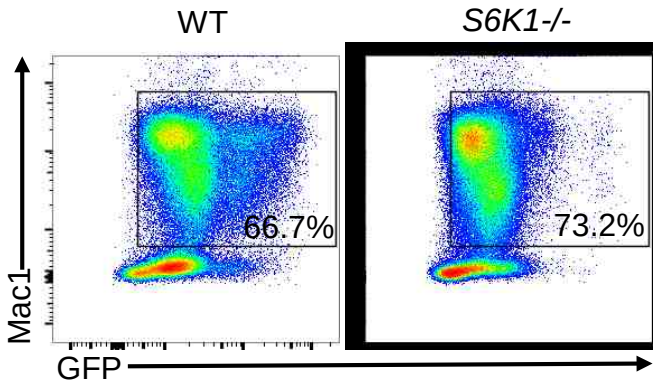

B

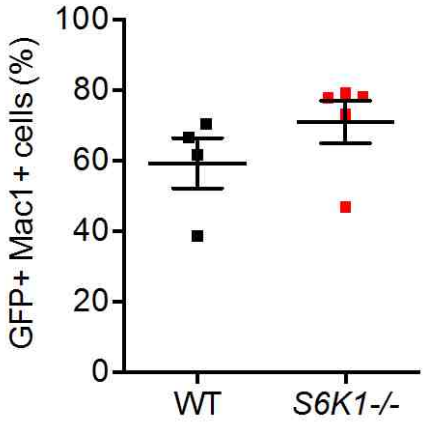

C

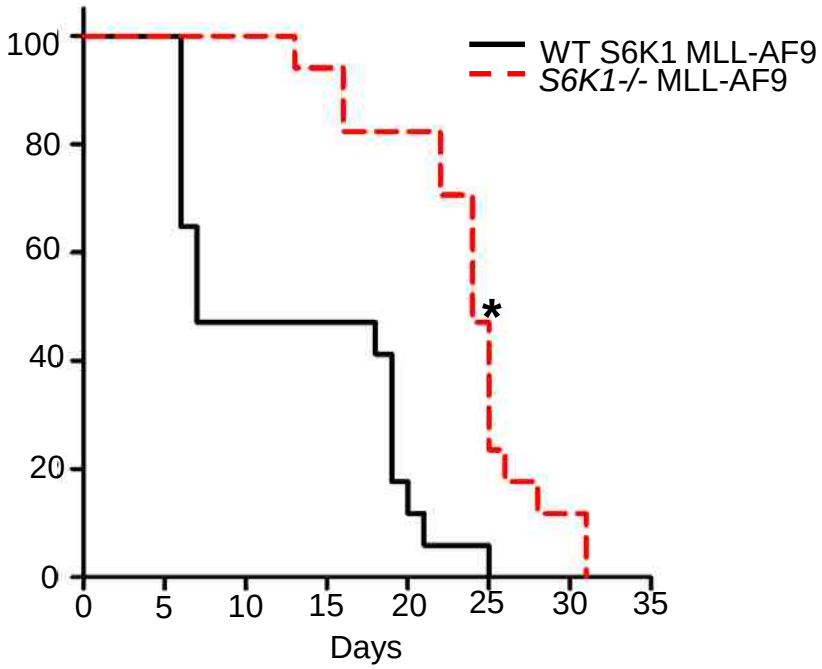

Figure 42: S6K1 deficiency delays propagation of leukemia.

(A) Representative flow plot of GFP+ Mac1+ cells in spleen of primary recipients of WT and *S6K1-/-* HSC/Ps expressing MLL-AF9. (B) Quantitative representation of GFP+ Mac1+ cells in spleen of primary recipients of WT and *S6K1-/-* HSC/Ps expressing MLL-AF9. n=5 mice in each group. (C) Kaplan-Meier survival curve of secondary transplant recipients of WT and *S6K1-/-* HSC/Ps expressing MLL-AF9. Statistical significance between the survival of two groups was analyzed by the log-rank (Mantel-Cox) test; n=17 mice in each group; *$p<0.01$.

cells in peripheral blood of secondary recipients was similar in two groups (Figure 43A, top panel and B, left panel). Additionally, the GFP+ cells in both groups demonstrated expression of Gr1 and Mac1, which indicates expansion of myeloid cells (Figure 43A, bottom panel and B, right panel). Furthermore, the engraftment of GFP+ cells in bone marrow of secondary recipients was similar in two groups (Figure 44A, top panel and B). Additionally, the GFP+ cells in both groups demonstrated expression of Gr1 and Mac1 to a similar level, which indicates expansion of myeloid cells (Figure 44A, bottom panel and C). Overall, these data suggest that deficiency of S6K1 does not affect leukemia initiation and progression in primary recipients, but delays the propagation of leukemia through serial transplantation.

S6K1 deficiency reduces Akt activation in MLL-AF9 bearing cells:

S6K1 has been identified as a negative regulator of Akt activation (Treins et al., 2010; Um et al., 2004) and previous studies have demonstrated that Akt is hyperactivated in MLL-AF9 bearing cells (Chapuis et al., 2010b; Hoshii et al., 2012). MOLM-13 cells, a human cell line expressing MLL-AF9, show constitutive activation of Akt, which is inhibited upon treatment with rapamycin or BEZ-235, a dual PI3K/mTORC1/C2 inhibitor (Chapuis et al., 2010b). To assess if S6K1 induced transformation in the context of MLL is in part mediated via hyperactive Akt, we analyzed phosphorylation level of Akt in the presence or absence of SK61. We expressed MLL-AF9 in WT and *S6K1-/-* HSC/Ps and sorted the cells to homogeneity based on GFP expression. Cells were analyzed for expression and activation of Akt. In WT HSC/Ps expressing MLL-AF9 (Figure 45A, Lane 1),

Figure 43

A

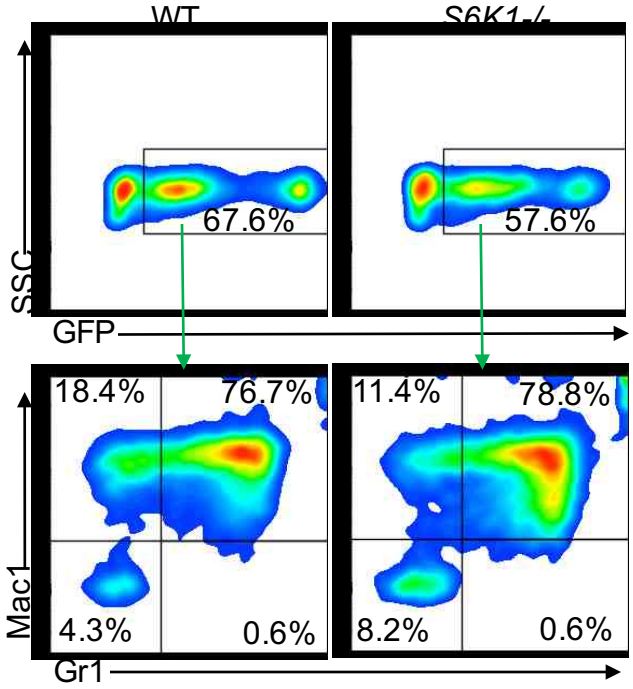
WT
S6K1-/-
67.6%
57.6%
SSC
GFP
18.4%
76.7%
11.4%
78.8%
4.3%
0.6%
8.2%
0.6%
Mac1
Gr1

B

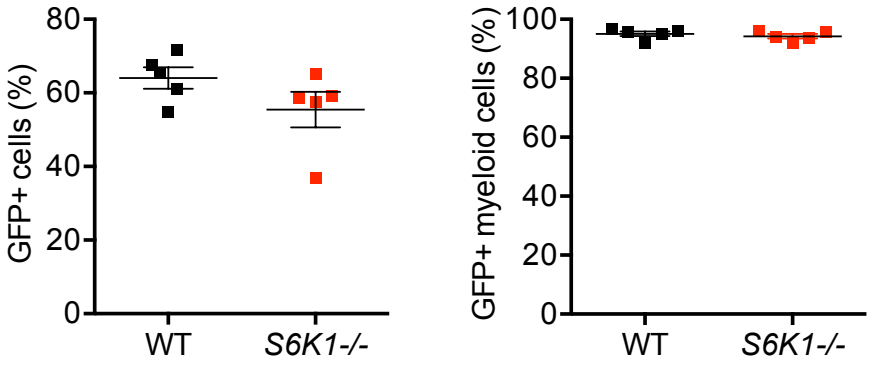
GFP+ cells (%)
80
60
40
20
0
WT
S6K1-/-
GFP+ myeloid cells (%)
100
80
60
40
20
0
WT
S6K1-/-

Figure 43: Engraftment of donor cells in peripheral blood of secondary transplant recipients.

(A) Representative flow plot of GFP+ cells in peripheral blood of secondary recipients of WT and *S6K1-/-* HSC/Ps expressing MLL-AF9 (top panel). Representative flow plot of GFP+ myeloid cells (Gr1+, Mac1+, Gr1+Mac1+) in peripheral blood of secondary recipients of WT and *S6K1-/-* HSC/Ps expressing MLL-AF9 (bottom panel). (B) Quantitative representation of GFP+ cells in peripheral blood of secondary recipients of WT and *S6K1-/-* HSC/Ps expressing MLL-AF9 (left panel). Quantitative representation of GFP+ myeloid cells (Gr1+, Mac1+, Gr1+Mac1+) in peripheral blood of secondary recipients of WT and *S6K1-/-* HSC/Ps expressing MLL-AF9 (right panel). Data are expressed as mean ± SEM; n=5 mice in each group.

Figure 43

A

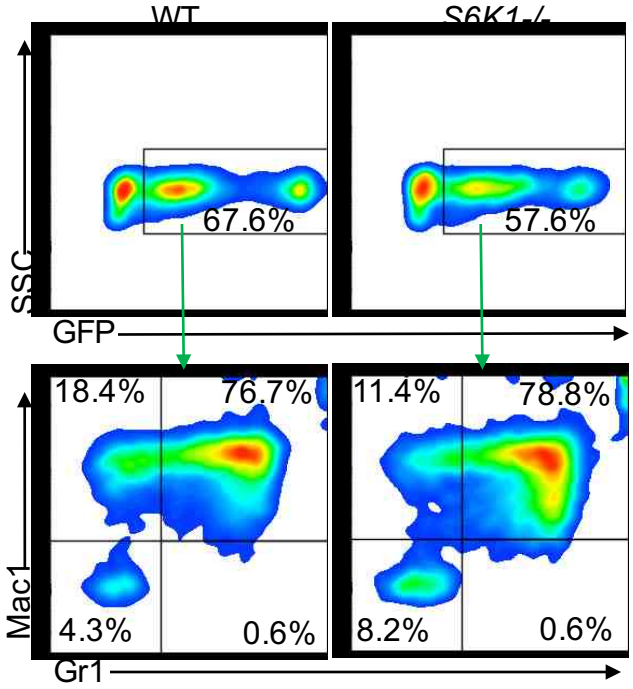
WT
S6K1-/-
67.6%
57.6%
SSC
GFP
18.4%
76.7%
11.4%
78.8%
Mac1
4.3%
0.6%
8.2%
0.6%
Gr1

B

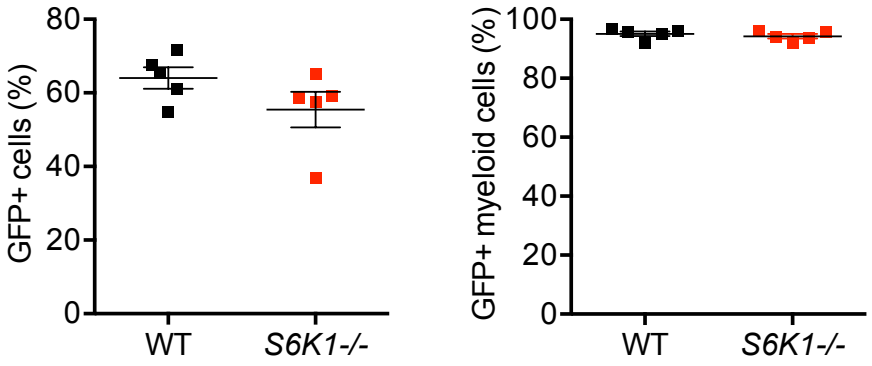
GFP+ cells (%)
80
60
40
20
0
WT
S6K1-/-
GFP+ myeloid cells (%)
100
80
60
40
20
0
WT
S6K1-/-

Figure 44: Engraftment of donor cells in bone marrow of secondary transplant recipients.

(A) Representative flow plot of GFP+ cells in BM of secondary recipients of WT and *S6K1-/-* HSC/Ps expressing MLL-AF9 (top panel). Representative flow plot of GFP+ myeloid cells (Gr1+, Mac1+, Gr1+Mac1+) in BM of secondary recipients of WT and *S6K1-/-* HSC/Ps expressing MLL-AF9 (bottom panel). (B) Quantitative representation of GFP+ cells in BM of secondary recipients of WT and *S6K1-/-* HSC/Ps expressing MLL-AF9. (C) Quantitative representation of GFP+ myeloid cells (Gr1+, Mac1+, Gr1+Mac1+) in BM of secondary recipients of WT and *S6K1- /-* HSC/Ps expressing MLL-AF9. Data are expressed as mean ± SEM; n=5 mice in each group.

Figure 45

A

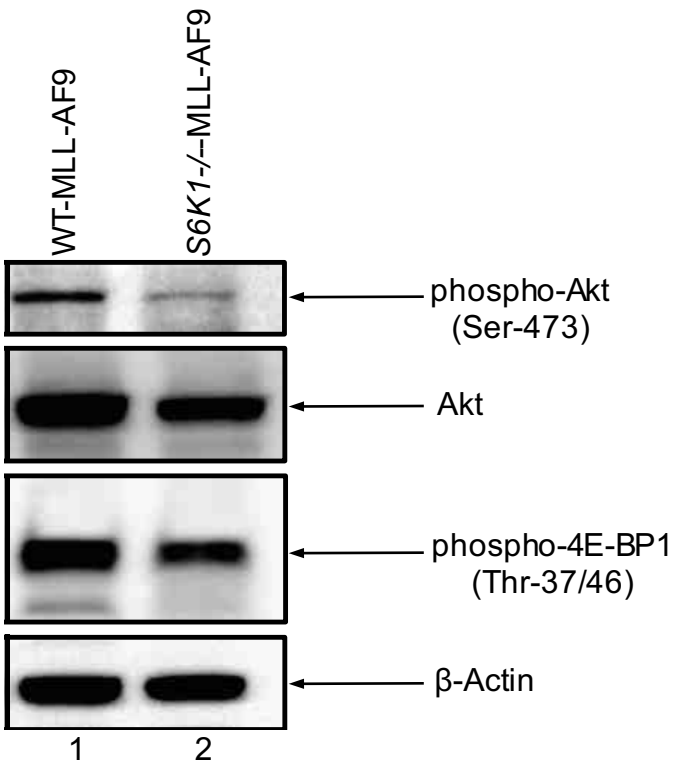
WT-MLL-AF9
S6K1-/--MLL-AF9
phospho-Akt
(Ser-473)
Akt
phospho-4E-BP1
(Thr-37/46)
β-Actin
1
2

B

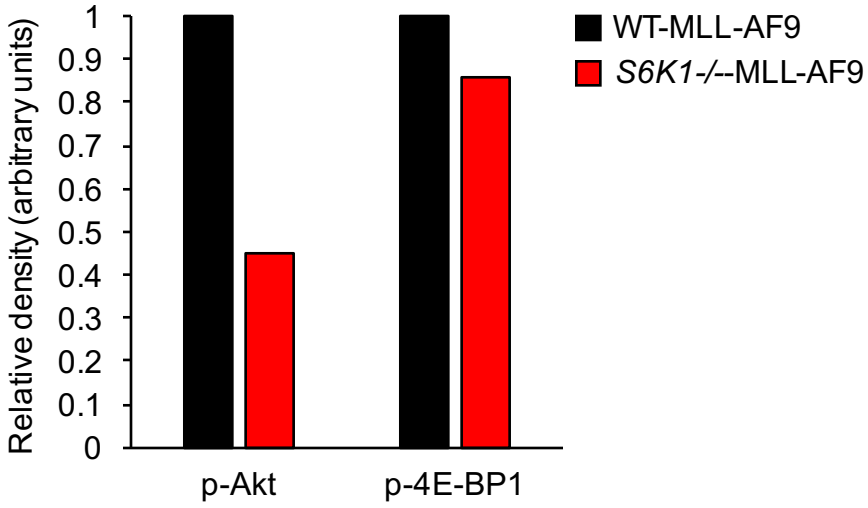
Relative density (arbitrary units)
1
0.9
0.8
0.7
0.6
0.5
0.4
0.3
0.2
0.1
0
p-Akt
p-4E-BP1
WT-MLL-AF9
S6K1-/--MLL-AF9

Figure 45: S6K1 deficiency causes reduction in Akt and mTORC1 activation in MLL-AF9 expressing cells.

(A) WT and *S6K1-/-* HSC/Ps were transduced with MLL-AF9 fusion oncogene. Cells were sorted based on GFP expression and expanded *in vitro*. Cells were serum-starved for 6 hours and protein was extracted. Phosphorylation level of Akt and 4E-BP1 was detected by immunoblotting. Akt and β-Actin was used as loading control. Data representative of three independent experiments. (B) Quantitative analysis of relative density of phospho-Akt and phospho-4E-BP1.

we observed phosphorylation of AKt, which was significantly reduced in MLL-AF9 cells in the absence of S6K1 (Figure 45A, Lane 2; Figure 45B). As Akt is an upstream positive regulator of mTORC1 activity, we next analyzed the phosphorylation of 4E-BP1, which is a downstream substrate of mTORC1. 4E-BP1 is phosphorylated and inactivated following activation of mTORC1. Previous studies have shown that 4E-BP1 remains hyperphosphorylated in AML cells, which indicates increased Akt-mTORC1 activity. *S6K1-/-* HSC/Ps bearing MLL-AF9 (Figure 45A, Lane 2; Figure 45B) showed reduced 4E-BP1 phosphorylation compared to WT HSC/Ps expressing MLL-AF9 (Figure 45A, Lane 1; Figure 45B). These data suggest that following loss of S6K1 expression in HSC/Ps bearing MLL-AF9, the mTORC1 activity is decreased which might delay leukemia propagation seen in our studies.

Inhibition of S6K1 activity results in decreased proliferation of human leukemic cells bearing the MLL-AF9 translocation:

Activation of mTORC1 and mTORC2 plays a critical role in regulation of growth of human leukemic cells (Tamburini et al., 2009). Pharmacological inhibition of mTORC activity in cells derived from AML patients results in cell death. Moreover, S6K1 has been shown to be constitutively active in cells obtained from AML patients (Sujobert et al., 2015). We therefore evaluated if inhibition of S6K1 in human cell lines bearing MLL-AF9 can inhibit the proliferation of leukemic cells. We have used PF-4708671, a cell permeable compound that specifically inhibits S6K1 activity, (Pearce et al., 2010) and UCB CD34+ cells expressing MLL-AF9 fusion oncoprotein for our studies. PF-

4708671 is a piperazinyl-pyrimidine analogue that specifically inhibits S6K1 activity without significantly inhibiting activity of other AGC kinases (Pearce et al., 2010). Furthermore, in HEK-294 cells, PF-4708671 does not inhibit Akt or mTORC1 activity (Pearce et al., 2010). MA9-3 cells are human UCB CD34+ cells transformed and immortalized by expressing MLL-AF9 (Wei et al., 2008). These cells display a myeloid phenotype and can initiate leukemia *in vivo* (Wei et al., 2008). We serum starved the cells and performed thymidine incorporation assay with different concentration of PF-4708671 in presence or absence of growth factors. We observed a dose-dependent decrease in proliferation of MA9-3 cells following treatment with PF-4708671 (Figure 46). To determine the possible mechanism for growth repression of human AML cells following S6K1 inhibition, we analyzed activation level of mTOR and 4E-BP1 following S6K1 inhibition. In presence of S6K1 inhibitor, the phosphorylation level of mTOR was significantly downregulated compared to vehicle treated cells (Figure 47A and C). Phosphorylation level of 4E-BP1, a downstream substrate of mTORC1, was also downregulated (Figure 47B and C). These data suggest that inhibition of S6K1 results in reduced mTORC1 activity and attenuates proliferation of human leukemic cells.

Figure 46

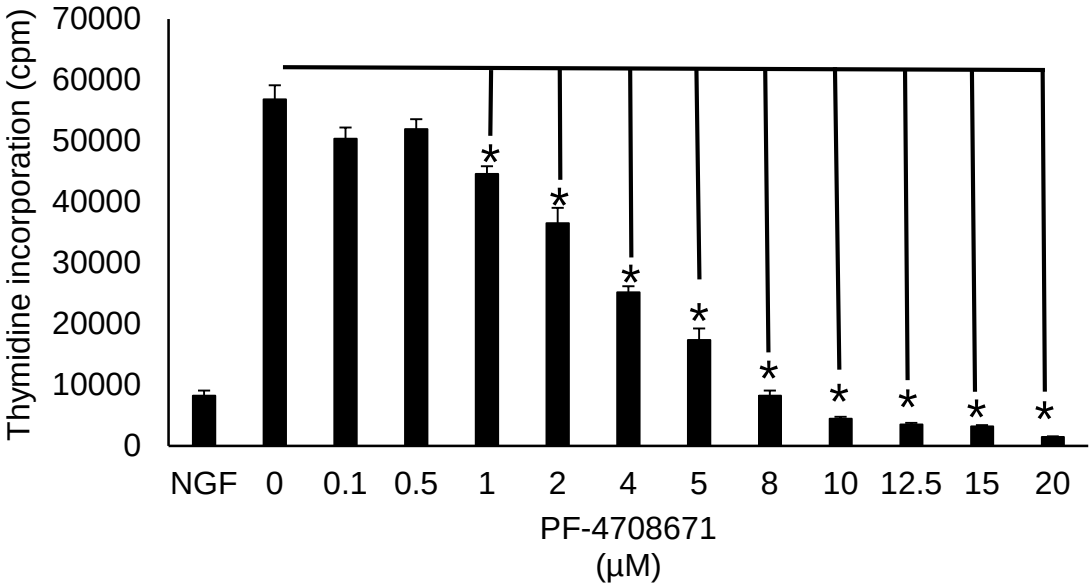
Thymidine incorporation (cpm)
70000
60000
50000
40000
30000
20000
10000
0
NGF
0
0.1
0.5
1
2
4
5
8
10
12.5
15
20
PF-4708671
(μM)

Figure 46: Inhibition of S6K1 activity results in reduced proliferation of MLL-AF9 expressing human cells.

Thymidine incorporation assay was performed with MA9-3 cells in absence or presence of PF-4708671. Cells were serum starved and plated in absence of growth factors (NGF) or in presence of growth factors along with increasing concentration of PF-4708671. After 42 hours, cells were pulsed with thymidine and thymidine incorporation into cells were determined after 6 hours of pulse. Experiment was performed in quadruplicates. Data are expressed as mean ± SEM; *$p<0.05$.

Figure 47

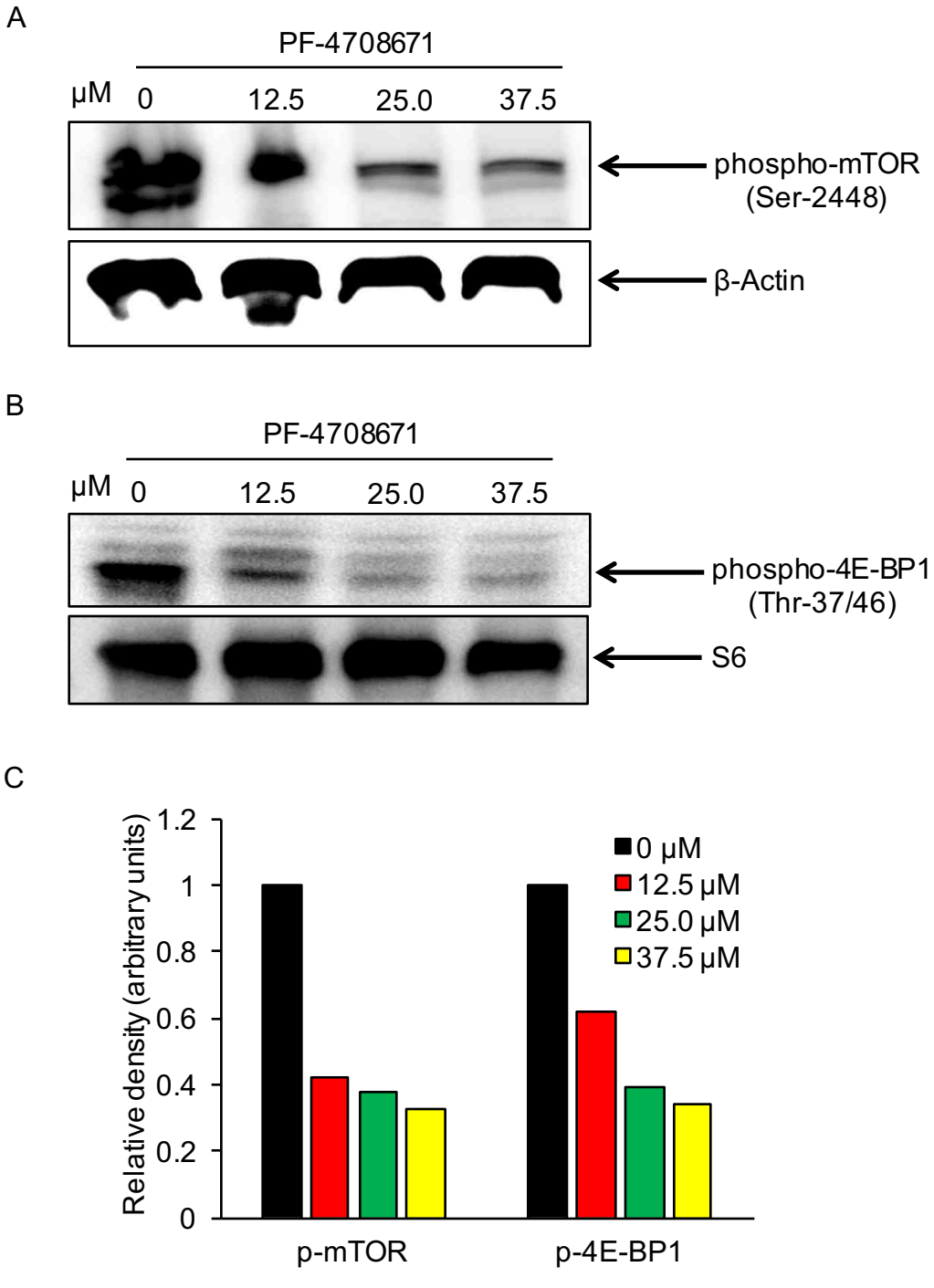
A
PF-4708671
μM 0 12.5 25.0 37.5
phospho-mTOR
(Ser-2448)
β-Actin
B
PF-4708671
μM 0 12.5 25.0 37.5
phospho-4E-BP1
(Thr-37/46)
S6
C
Relative density (arbitrary units)
1.2
1
0.8
0.6
0.4
0.2
0
0 μM
12.5 μM
25.0 μM
37.5 μM
p-mTOR
p-4E-BP1

Figure 47: Inhibition of S6K1 activity results in reduced mTORC1 activation in MLL-AF9 expressing human cells.

(A) MA9-3 cells were treated with increasing doses of PF-4708671 and phospho-mTOR level was analyzed by immunoblotting. β-Actin was used as loading control. (B) MA9-3 cells were treated with increasing doses of PF-4708671 and phospho-4E-BP1 level was analyzed by immunoblotting. S6 was used as loading control. Data representative of three independent experiments. (C) Quantitative analysis of relative density of phospho-mTOR and phospho-4E-BP1.

Discussion:

While previous studies have established that PI3K-mTORC1 axis regulates leukemia initiation and progression (Lee et al., 2010; Magee et al., 2012), the specific role of S6K1, a downstream substrate of mTORC1, has not been studied in detail. The PI3K-mTORC1 pathway is hyperactivated in a large section of AML patients (Chapuis et al., 2010a; Chapuis et al., 2010b; Chow et al., 2006; Kubota et al., 2004; Xu et al., 2003). However, the prognostic value of PI3K-mTORC1 pathway in AML remains contradictory. AML patients with increased level of phosphorylated Akt in peripheral blood and bone marrow cells have significantly shorter median survival time compared to patients with reduced phosphorylated Akt (Kornblau et al., 2006). In patients who are older than 60 years, lack of response to chemotherapy has been associated with hyperactive Akt (Kornblau et al., 2010). In another study, Tamburini et al. showed that AML patients with hyperactive Akt have an increased overall survival and increased relapse free survival compared to patients with reduced Akt phosphorylation at Ser473 (Tamburini et al., 2007). They hypothesized that increased PI3K activity in immature leukemic cells results in increased number of cells in S phase, which make the cells more susceptible to chemotherapeutic agents (Tamburini et al., 2007). In a CML model of Bcr-Abl driven leukemia, Naka et al. have demonstrated that in LICs, Akt activity is suppressed which results in nuclear localization of Foxo3a (Naka et al., 2010). LICs are able to evade stress-induced depletion in a Foxo3a dependent manner (Naka et al., 2010). Contrarily, in non-LIC population in CML, inactivation of Akt results in increased Foxo3a activity,

which causes cell cycle arrest and apoptosis (Naka et al., 2010). These findings are further corroborated in AML caused by translocation of AF9 within MLL. In MLL-AF9 expressing AML cells, constitutive activation of Akt results in growth arrest of cells and causes increased maturation of cells towards myeloid lineage (Sykes et al., 2011). Furthermore, depletion of Foxo1, Foxo3 and Foxo4, which act downstream of Akt, result in diminished LIC activity (Sykes et al., 2011). Proliferation of myeloid cells is associated with increased intracellular ROS level (Saito et al., 2015). Increased ROS level have been associated with acquisition of DNA damage and cellular apoptosis (Huang et al., 2003). AML cells expressing MLL-AF9 maintain a reduced ROS level (Naka et al., 2010; Saito et al., 2015). Increased ROS level in MLL-AF9 expressing cells results in DNA damage, which was associated with downregulation of antioxidant genes by Foxo group of proteins (Naka et al., 2010; Santos et al., 2014). However, Akt driven Foxo3a activity could also regulate self-renewal potential of LICs differentially. Although Foxo3a regulates self-renewal of LICs in CML, it does not regulate the self-renewal of LICs in blast crisis model of CML (Naka et al., 2010).

Previous studies suggest that Foxo group of proteins are a key regulator of propagation of CML and AML and this group of proteins are regulated by mTORC1 (Naka et al., 2010; Sykes et al., 2011). Inhibition of mTORC1 activity in colon cancer cells results in increased translocation of Foxo1 from nucleus to cytoplasm (Abdelnour-Berchtold et al., 2010). In this study, we provided evidence that S6K1 deficiency results in reduced mTORC1 activity as phosphorylation of 4E-BP1, a downstream substrate of mTORC1, was reduced

in MLL-AF9 cells deficient in S6K1. It could be possible that MLL-AF9 expressing cells have increased cytoplasmic Foxo1 level due to diminished mTORC1 activity following inhibition of S6K1.

AML cells are also highly dependent on glycolysis for cellular metabolism (Herst et al., 2011). Herst et al. have demonstrated that AML blast cells with high glycolysis rate are resistant to chemotherapeutic agent induced apoptosis (Herst et al., 2011). Recent study by Saito et al. has shown that MLL-AF9 expressing cells are dependent on glucose metabolism (Saito et al., 2015). Disruption of glucose metabolism by metabolic stress diminishes the activity of LICs (Saito et al., 2015). S6K1 has been established as a positive regulator of glycolysis in leukemic cells. In PTEN-deficient hematopoietic cells, inhibition of S6K1 activity results in decreased glycolysis and induced apoptosis (Tandon et al., 2011). S6K1 is also a positive regulator of glycolysis in Bcr-Abl expressing cells (Barger et al., 2013). However, inhibition of S6K1 activity in Bcr-Abl expressing cells did not result in induction of apoptosis in the cells (Barger et al., 2013). It is possible that MLL-AF9 expressing cells that are deficient in S6K1 have dysregulated glucose metabolism, which delayed the propagation of the disease in vivo.

In this chapter, we provide evidence that S6K1 regulates the propagation of MLL-AF9 expressing AML through serial transplantation. We also demonstrate that genetic disruption of S6K1 expression results in reduced mTORC1 and mTORC2 activity as both activation of 4E-BP1 and Akt was diminished in S6K1 deficient AML cells. Our studies also demonstrate that inhibition of S6K1 activity using a specific inhibitor against S6K1 results in

reduced growth of human leukemic cells and inhibits mTORC1 activity. We propose that in AML cells, S6K1 phosphorylates and activates mTOR, which is a common catalytic subunit of both mTORC1 and mTORC2 (Figure 48A). mTORC2 further activates Akt which contributes to subsequent hyperactivation of mTORC1 in AML cells (Figure 48A). In *S6K1-/-* AML cells, S6K1-dependent phosphorylation of mTOR is withdrawn (Figure 48B). Subsequently, mTORC2 driven hyperphosphorylation of Akt is decreased which causes downregulation of mTORC1 activity (Figure 48B).

Figure 48

A

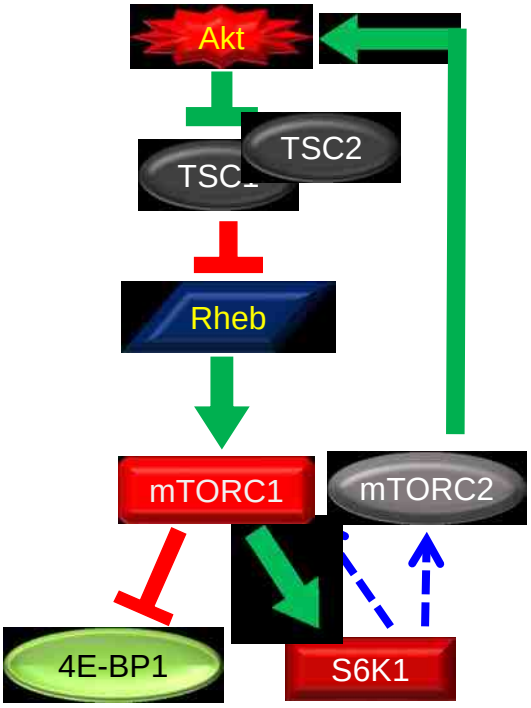
Akt
TSC2
Rheb
mTORC1
mTORC2
4E-BP1
S6K1

B

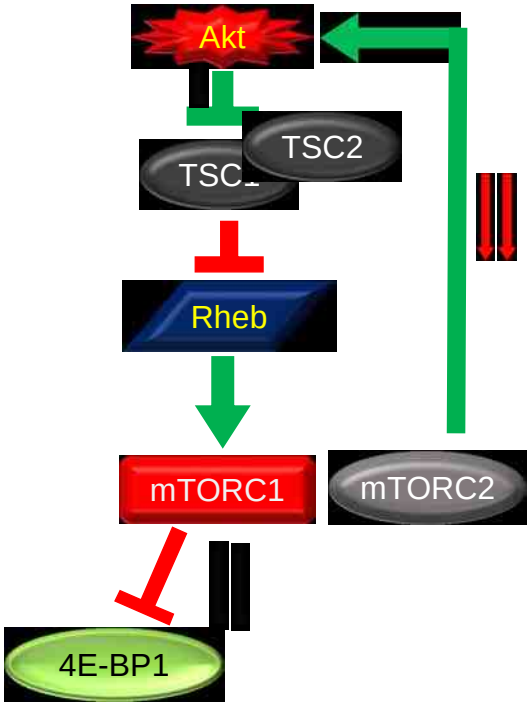
Akt
TSC2
Rheb
mTORC1
mTORC2
4E-BP1

Figure 48: Proposed schematic model of S6K1 signaling in AML cells expressing MLL-AF9.

(A) S6K1 phosphorylates and activates mTOR, which is a common catalytic subunit of both mTORC1 and mTORC2. mTORC2 further activates Akt, which contributes to subsequent hyperactivation of mTORC1 in AML cells. (B) In S6K1-deficient AML cells expressing MLL-AF9, S6K1-dependent phosphorylation of mTOR is withdrawn. Subsequently, mTORC2-driven hyperphosphorylation of Akt is decreased, which causes downregulation of mTORC1 activity.

Chapter 7: Future Directions

Determining the mechanism of reduced self-renewal of HSCs following modulation of S6K1 expression level:

In the current study, we have demonstrated that *S6K1-/-* HSCs have reduced self-renewal ability when they undergo serial transplant. We have also shown that *p21* expression is significantly downregulated in *S6K1-/-* HSCs. Although in our studies, *S6K1-/-* HSCs demonstrate similar functional abilities as *p21-/-* HSCs, the exact physiological mechanism that causes reduced self-renewal and engraftment of *S6K1-/-* HSCs has not been identified. It is probable that S6K1 deficiency results in a decrease in functional HSCs. Further analysis is required to determine the frequency of HSCs in *S6K1-/-* mice by performing limiting dilution assay with different cell doses with WT and *S6K1-/-* HSCs. In our CRA studies, we have used purified HSCs from test groups (WT and *S6K1-/-*) and performed a head-to-head competitive assay with unfractionated BM MNCs derived from competitor (Boy/J). However, a more stringent assay could be performed by using sorted HSCs as competitor cells instead of BM MNCs. This will allow us to determine the functional potential of *S6K1-/-* HSCs in a head-to-head setting with WT HSCs.

Loss of expression of S6K1 does not affect homing and long-term engraftment of HSCs in primary recipients. However, it could be possible there is a homing or cell cycle defect in *S6K1-/-* HSCs derived from primary transplant recipients, which contributes to reduced engraftment in secondary recipients. To

determine the effect of S6K1 deficiency on homing and cell cycle state of HSCs derived from primary recipients, further studies are required. To further strengthen our data that S6K1 is a positive regulator of *p21* expression in HSCs, we propose to determine whether restoration of S6K1 expression in *S6K1-/-* HSCs results in upregulation of *p21* expression. WT and *S6K1-/-* HSCs will be transduced with either empty vector or retroviral vector encoding S6K1. Following sorting of transduced cells based on GFP expression, we will examine the expression of *p21*. As TGF-ß1 regulates p21 expression level following inhibition of mTORC1 activity, it is required to determine TGF-ß1 level in response to S6K1 deficiency (Law et al., 2002). Furthermore, S6K1 has been shown to be a negative regulator of mTORC2 and Akt activity in HEK293 cells (Julien et al., 2010). However, whether this negative feedback loop exists in HSCs or not, is unknown. Studies to determine the activation level of mTORC2 and Akt could be critical to determine the signaling pathways that cause dysfunction in *S6K1-/-* HSCs.

Our studies also provide evidence that overexpression of S6K1 results in reduced engraftment of HSCs in primary recipients. The decrease in engraftment of HSCs overexpressing HSCs could be due to reduced homing or cell cycle status of these cells. Further studies are required to determine the effect of S6K1 overexpression on homing and cell cycle progression of HSCs. Previous studies have established that S6K1 negatively regulates Akt phosphorylation through repressing mTORC2 activity (Julien et al., 2010). In our studies, overexpression of S6K1 in HSCs results in reduced phosphorylation of Akt. Further biochemical

analysis is required to determine the mTORC2 activity in HSCs overexpressing S6K1.

Determining the effect of inhibition of S6K1 activity on human AML cells:

S6K1 has been shown to be hyperactivated in in various cancer cells including AML (Khotskaya et al., 2014; Sujobert et al., 2015). The studies in this thesis have established that S6K1 is a critical regulator of MLL propagation. However, the precise cellular processes that are dysregulated in S6K1-deficient AML cells are not known. Recent studies have demonstrated the importance of glucose metabolism in AML cells. Chen et al. have demonstrated that increased glycolysis in AML cells results in resistance to chemotherapeutic agents (Chen et al., 2014). Furthermore, inhibition of glycolysis in human AML cells renders them susceptible to chemotherapy (Chen et al., 2014). Previous studies have shown that S6K1 positively regulates glycolysis in different cell types including leukemic cells (Barger et al., 2013; Tandon et al., 2011). However, how specific inhibition of S6K1 activity will affect the progression of human AML cells are unknown. Our preliminary studies indicate that PF-4708671, a specific inhibitor of S6K1, can cause growth arrest in human AML cells. Moreover, our preliminary studies indicate that inhibition of S6K1 also results in apoptosis in human AML cells in a dose-dependent manner (Figure 49). The effect of S6K1 inhibition on human AML cells could be further studied in vivo using established xenograft models for AML. NOD/LtSz-scid IL2RG–SGM3 (NSGS) mice have been identified as a better host for AML xenografts as they constitutively express three human cytokines (hSCF, hIL-3, hGM-CSF) (Wunderlich et al., 2010). After

Figure 49

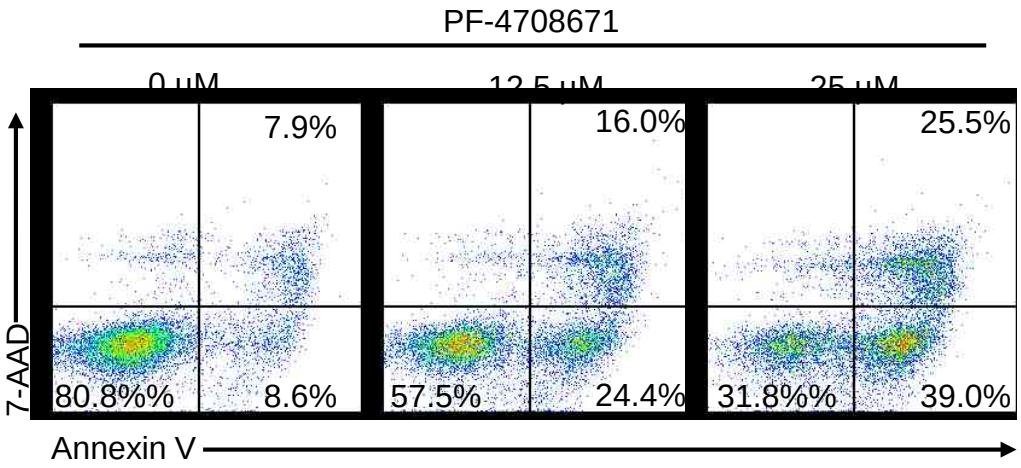
PF-4708671
0 μM
12.5 μM
25 μM
7.9%
16.0%
25.5%
80.8%%
8.6%
57.5%
24.4%
31.8%%
39.0%
7-AAD
Annexin V

Figure 49: Pharmacological inhibition of S6K1 activity results in increased apoptosis of human AML cells expressing MLL-AF9.

MA9-3 cells were treated with increasing doses of PF-4708671 for 18 hours and apoptotic cells were determined by staining with Annexin-V and 7-AAD.

transplantation of MA9-3 cells, NSGS mice could be treated with PF-4708671 to determine if S6K1 inhibition affects development of human AML cells *in vivo*. This would further define the role of S6K1 in initiation and progression of AML.

Determining the effect of inhibition of S6K1 activity on human HSCs:

In this study, we have provided compelling evidence that activity level of S6K1 is key for self-renewal of murine HSCs. Both loss of expression and gain of expression of S6K1 result in reduced self-renewal of murine HSCs. However, previous studies have shown that pharmacological inhibition of mTORC1-S6K1 activity in ex vivo cultured human HSCs result in increased engraftment and self-renewal in irradiated hosts (Rohrabaugh et al., 2011). There is a possibility that mTORC1-S6K1 differentially regulates the HSC functions in mouse and human. Our preliminary studies showed that inhibition of S6K1 activity in human UCB CD34+ cells results in enrichment of phenotypically defined HSC-enriched population (CD34+CD38-). We performed *in vitr*o culture of human UCB derived CD34+ cells in presence or absence of S6K1 inhibitor, PF-4708671. After 5 days of culture, the frequency of CD34+CD38- cells were significantly increased in cells treated with PF-4708671 (Figure 50A and B). This data suggests that inhibition of S6K1 activity in ex vivo cultured human HSCs could expand the phenotypically defined HSC-enriched population. The expansion of phenotypic HSCs might result in increased engraftment and self-renewal of HSCs. However, our study also demonstrated that S6K1 is a positive regulator of HSC quiescence. It is also possible that inhibition of S6K1 in human HSCs could result in decreased quiescence of HSCs, which forced them to cycle and expand.

Figure 50

A

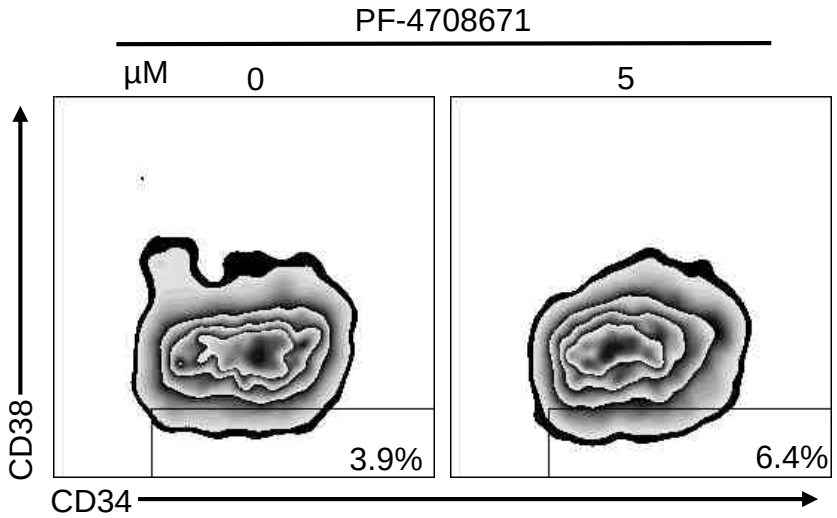
PF-4708671
μM
0
5
CD38
3.9%
6.4%
CD34

B

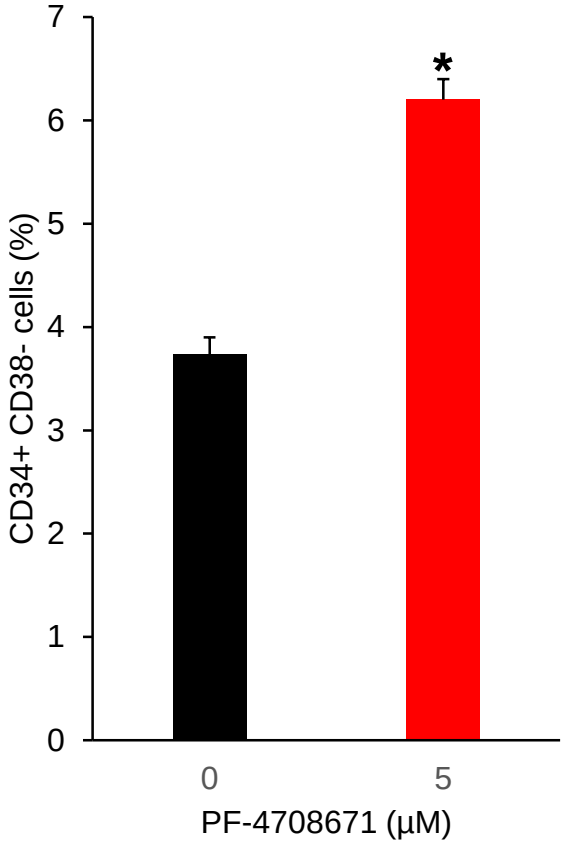
7
6
5
4
3
2
1
0
*
CD34+ CD38- cells (%)
0
5
PF-4708671 (μM)

Figure 50: Pharmacological inhibition of S6K1 activity results in increased HSC frequency in human CD34+ cells.

(A) Representative flow plot of UCB CD34+ cells following treatment with PF-4708671. UCB CD34+ cells were treated with either vehicle or 5 μM of PF-4708671 for 5 days and frequency of CD34+ CD38- cells was determined by FACS. (B) Quantitative representation of CD34+ CD38- cells in UCB CD34+ cells in presence or absence of PF-4708671 for 5 days. Experiment was performed in triplicates. Data are expressed as mean ± SEM; *$p<0.05$.

Previous studies have shown that increased cycling of HSCs contribute to functional defects (Jetmore et al., 2002; Srour and Jordan, 2002). To determine the effect of S6K1 inhibition on HSCs, NSG mice could be transplanted with UCB CD34+ cells following treatment with S6K1 inhibitor. If S6K1 inhibition increases engraftment of ex vivo cultured HSCs that would suggest S6K1 inhibition might be a potential therapeutic tool for areas such as gene transduction that requires preservation of HSC function while being cultured ex vivo and enhancing donor HSC function. Furthermore, inhibition of S6K1 in human HSC could be used as a tool to enhance efficiency of bone marrow transplantation if it increases expansion of functional HSCs. In bone marrow transplantation, total body irradiation (TBI) has been used as a conditioning regimen. However, TBI causes radiation-induced injury, which is partly mediated by generation of ROS within the cells (Bianco et al., 1991; Holler et al., 1990; Riley, 1994). Previously, it has been showed that mTORC1 is a positive regulator of ROS production in HSCs (Chen et al., 2008). In this study, we have shown that inhibition of S6K1 results in reduced mTORC1 activity. Based on this, administration of PF-4708671 could be explored as a probable therapeutic tool to mitigate cellular damages following TBI.

Moreover, as inhibition of S6K1 results in increased HSC-enriched population in human UCB cells, it could be explored as a probable therapeutic target to enhance radiomitigation. Following a radiation accident, especially involving a significantly large number of affected individuals, hematopoietic transplantation might not be the practical approach given the logistics and timing

required. A more practical and ideal approach would be administration of drugs targeting molecules, inhibition of which will enhance HSC function *in vivo*. Further studies are required to determine the effects of PF-4708671 on physiological systems. If PF-4708671 does not has any adverse effect on physiological systems, and can enhance hematopoietic recovery and survival following exposure to irradiation, it can be considered for use as a potential radiomitigation agent.

References

Abdelnour-Berchtold, E., Cerantola, Y., Roulin, D., Dormond-Meuwly, A., Demartines, N., and Dormond, O. (2010). Rapamycin-mediated FOXO1 inactivation reduces the anticancer efficacy of rapamycin. Anticancer Res *30*, 799-804.

Abkowitz, J.L., Golinelli, D., Harrison, D.E., and Guttorp, P. (2000). In vivo kinetics of murine hemopoietic stem cells. Blood *96*, 3399-3405.

Adolfsson, J., Borge, O.J., Bryder, D., Theilgaard-Monch, K., Astrand-Grundstrom, I., Sitnicka, E., Sasaki, Y., and Jacobsen, S.E. (2001). Upregulation of Flt3 expression within the bone marrow Lin(-)Sca1(+)c-kit(+) stem cell compartment is accompanied by loss of self-renewal capacity. Immunity *15*, 659-669.

Akashi, K., Traver, D., Miyamoto, T., and Weissman, I.L. (2000). A clonogenic common myeloid progenitor that gives rise to all myeloid lineages. Nature *404*, 193-197.

Akiyama, T., Ohuchi, T., Sumida, S., Matsumoto, K., and Toyoshima, K. (1992). Phosphorylation of the retinoblastoma protein by cdk2. Proc Natl Acad Sci U S A *89*, 7900-7904.

Alessi, D.R. (1997). The protein kinase C inhibitors Ro 318220 and GF 109203X are equally potent inhibitors of MAPKAP kinase-1beta (Rsk-2) and p70 S6 kinase. FEBS Lett *402*, 121-123.

Alessi, D.R., Deak, M., Casamayor, A., Caudwell, F.B., Morrice, N., Norman, D.G., Gaffney, P., Reese, C.B., MacDougall, C.N., Harbison, D.*, et al.* (1997). 3-Phosphoinositide-dependent protein kinase-1 (PDK1): structural and functional homology with the Drosophila DSTPK61 kinase. Curr Biol *7*, 776-789.

Aoki, Y., Watanabe, T., Saito, Y., Kuroki, Y., Hijikata, A., Takagi, M., Tomizawa, D., Eguchi, M., Eguchi-Ishimae, M., Kaneko, A.*, et al.* (2015). Identification of CD34+ and CD34- leukemia-initiating cells in MLL-rearranged human acute lymphoblastic leukemia. Blood *125*, 967-980.

Banerjee, P., Ahmad, M.F., Grove, J.R., Kozlosky, C., Price, D.J., and Avruch, J. (1990). Molecular structure of a major insulin/mitogen-activated 70-kDa S6 protein kinase. Proceedings of the National Academy of Sciences of the United States of America *87*, 8550-8554.

Barger, J.F., Gallo, C.A., Tandon, P., Liu, H., Sullivan, A., Grimes, H.L., and Plas, D.R. (2013). S6K1 determines the metabolic requirements for BCR-ABL survival. Oncogene *32*, 453-461.

Basu, S. (2014). A complex interplay between PGC-1 co-activators and mTORC1 regulates hematopoietic recovery following 5-fluorouracil treatment. Stem cell research *12*, 178-193.

Baum, C.M., Weissman, I.L., Tsukamoto, A.S., Buckle, A.M., and Peault, B. (1992). Isolation of a candidate human hematopoietic stem-cell population. Proceedings of the National Academy of Sciences of the United States of America *89*, 2804-2808.

Becker, A.J., Mc, C.E., and Till, J.E. (1963). Cytological demonstration of the clonal nature of spleen colonies derived from transplanted mouse marrow cells. Nature *197*, 452-454.

Benveniste, P., Frelin, C., Janmohamed, S., Barbara, M., Herrington, R., Hyam, D., and Iscove, N.N. (2010). Intermediate-term hematopoietic stem cells with extended but time-limited reconstitution potential. Cell stem cell *6*, 48-58.

Bersenev, A., Wu, C., Balcerek, J., and Tong, W. (2008). Lnk controls mouse hematopoietic stem cell self-renewal and quiescence through direct interactions with JAK2. The Journal of clinical investigation *118*, 2832-2844.

Bianco, J.A., Appelbaum, F.R., Nemunaitis, J., Almgren, J., Andrews, F., Kettner, P., Shields, A., and Singer, J.W. (1991). Phase I-II trial of pentoxifylline for the prevention of transplant-related toxicities following bone marrow transplantation. Blood *78*, 1205-1211.

Boulay, A., Zumstein-Mecker, S., Stephan, C., Beuvink, I., Zilbermann, F., Haller, R., Tobler, S., Heusser, C., O'Reilly, T., Stolz, B*., et al.* (2004). Antitumor efficacy of intermittent treatment schedules with the rapamycin derivative RAD001 correlates with prolonged inactivation of ribosomal protein S6 kinase 1 in peripheral blood mononuclear cells. Cancer research *64*, 252-261.

Broeker, P.L., Harden, A., Rowley, J.D., and Zeleznik-Le, N. (1996a). The mixed lineage leukemia (MLL) protein involved in 11q23 translocations contains a domain that binds cruciform DNA and scaffold attachment region (SAR) DNA. Curr Top Microbiol Immunol *211*, 259-268.

Broeker, P.L., Super, H.G., Thirman, M.J., Pomykala, H., Yonebayashi, Y., Tanabe, S., Zeleznik-Le, N., and Rowley, J.D. (1996b). Distribution of 11q23 breakpoints within the MLL breakpoint cluster region in de novo acute leukemia

and in treatment-related acute myeloid leukemia: correlation with scaffold attachment regions and topoisomerase II consensus binding sites. Blood *87*, 1912-1922.

Brugarolas, J., Bronson, R.T., and Jacks, T. (1998). p21 is a critical CDK2 regulator essential for proliferation control in Rb-deficient cells. J Cell Biol *141*, 503-514.

Brugarolas, J., Moberg, K., Boyd, S.D., Taya, Y., Jacks, T., and Lees, J.A. (1999). Inhibition of cyclin-dependent kinase 2 by p21 is necessary for retinoblastoma protein-mediated G1 arrest after gamma-irradiation. Proc Natl Acad Sci U S A *96*, 1002-1007.

Buchner, T., Schlenk, R.F., Schaich, M., Dohner, K., Krahl, R., Krauter, J., Heil, G., Krug, U., Sauerland, M.C., Heinecke, A.*, et al.* (2012). Acute Myeloid Leukemia (AML): different treatment strategies versus a common standard arm--combined prospective analysis by the German AML Intergroup. J Clin Oncol *30*, 3604-3610.

Burnett, P.E., Barrow, R.K., Cohen, N.A., Snyder, S.H., and Sabatini, D.M. (1998a). RAFT1 phosphorylation of the translational regulators p70 S6 kinase and 4E-BP1. Proceedings of the National Academy of Sciences of the United States of America *95*, 1432-1437.

Burnett, P.E., Blackshaw, S., Lai, M.M., Qureshi, I.A., Burnett, A.F., Sabatini, D.M., and Snyder, S.H. (1998b). Neurabin is a synaptic protein linking p70 S6 kinase and the neuronal cytoskeleton. Proceedings of the National Academy of Sciences of the United States of America *95*, 8351-8356.

Busch, K., Klapproth, K., Barile, M., Flossdorf, M., Holland-Letz, T., Schlenner, S.M., Reth, M., Hofer, T., and Rodewald, H.R. (2015). Fundamental properties of unperturbed haematopoiesis from stem cells in vivo. Nature *518*, 542-546.

Campbell, T.B., Basu, S., Hangoc, G., Tao, W., and Broxmeyer, H.E. (2009). Overexpression of Rheb2 enhances mouse hematopoietic progenitor cell growth while impairing stem cell repopulation. Blood *114*, 3392-3401.

Challen, G.A., Boles, N.C., Chambers, S.M., and Goodell, M.A. (2010). Distinct hematopoietic stem cell subtypes are differentially regulated by TGF-beta1. Cell stem cell *6*, 265-278.

Chapuis, N., Tamburini, J., Cornillet-Lefebvre, P., Gillot, L., Bardet, V., Willems, L., Park, S., Green, A.S., Ifrah, N., Dreyfus, F.*, et al.* (2010a). Autocrine IGF-1/IGF-1R signaling is responsible for constitutive PI3K/Akt activation in acute

myeloid leukemia: therapeutic value of neutralizing anti-IGF-1R antibody. Haematologica *95*, 415-423.

Chapuis, N., Tamburini, J., Green, A.S., Vignon, C., Bardet, V., Neyret, A., Pannetier, M., Willems, L., Park, S., Macone, A.*, et al.* (2010b). Dual inhibition of PI3K and mTORC1/2 signaling by NVP-BEZ235 as a new therapeutic strategy for acute myeloid leukemia. Clinical cancer research : an official journal of the American Association for Cancer Research *16*, 5424-5435.

Chauvin, C., Koka, V., Nouschi, A., Mieulet, V., Hoareau-Aveilla, C., Dreazen, A., Cagnard, N., Carpentier, W., Kiss, T., Meyuhas, O.*, et al.* (2014). Ribosomal protein S6 kinase activity controls the ribosome biogenesis transcriptional program. Oncogene *33*, 474-483.

Chen, C., Liu, Y., Liu, R., Ikenoue, T., Guan, K.L., Liu, Y., and Zheng, P. (2008). TSC-mTOR maintains quiescence and function of hematopoietic stem cells by repressing mitochondrial biogenesis and reactive oxygen species. The Journal of experimental medicine *205*, 2397-2408.

Chen, C., Liu, Y., Liu, Y., and Zheng, P. (2009). mTOR regulation and therapeutic rejuvenation of aging hematopoietic stem cells. Sci Signal *2*, ra75.

Chen, C., Liu, Y., Liu, Y., and Zheng, P. (2010). Mammalian target of rapamycin activation underlies HSC defects in autoimmune disease and inflammation in mice. The Journal of clinical investigation *120*, 4091-4101.

Chen, W.L., Wang, J.H., Zhao, A.H., Xu, X., Wang, Y.H., Chen, T.L., Li, J.M., Mi, J.Q., Zhu, Y.M., Liu, Y.F.*, et al.* (2014). A distinct glucose metabolism signature of acute myeloid leukemia with prognostic value. Blood *124*, 1645-1654.

Cheng, J.Q., Godwin, A.K., Bellacosa, A., Taguchi, T., Franke, T.F., Hamilton, T.C., Tsichlis, P.N., and Testa, J.R. (1992). AKT2, a putative oncogene encoding a member of a subfamily of protein-serine/threonine kinases, is amplified in human ovarian carcinomas. Proceedings of the National Academy of Sciences of the United States of America *89*, 9267-9271.

Cheng, T., Rodrigues, N., Shen, H., Yang, Y., Dombkowski, D., Sykes, M., and Scadden, D.T. (2000). Hematopoietic stem cell quiescence maintained by p21cip1/waf1. Science *287*, 1804-1808.

Cheong, J.W., Eom, J.I., Maeng, H.Y., Lee, S.T., Hahn, J.S., Ko, Y.W., and Min, Y.H. (2003). Phosphatase and tensin homologue phosphorylation in the C-terminal regulatory domain is frequently observed in acute myeloid leukaemia and associated with poor clinical outcome. Br J Haematol *122*, 454-456.

Cheshier, S.H., Morrison, S.J., Liao, X., and Weissman, I.L. (1999). In vivo proliferation and cell cycle kinetics of long-term self-renewing hematopoietic stem cells. Proceedings of the National Academy of Sciences of the United States of America *96*, 3120-3125.

Chessells, J.M., Harrison, C.J., Kempski, H., Webb, D.K., Wheatley, K., Hann, I.M., Stevens, R.F., Harrison, G., Gibson, B.E., and party, M.R.C.C.L.w. (2002). Clinical features, cytogenetics and outcome in acute lymphoblastic and myeloid leukaemia of infancy: report from the MRC Childhood Leukaemia working party. Leukemia *16*, 776-784.

Chou, M.M., and Blenis, J. (1996). The 70 kDa S6 kinase complexes with and is activated by the Rho family G proteins Cdc42 and Rac1. Cell *85*, 573-583.

Chow, S., Minden, M.D., and Hedley, D.W. (2006). Constitutive phosphorylation of the S6 ribosomal protein via mTOR and ERK signaling in the peripheral blasts of acute leukemia patients. Experimental hematology *34*, 1183-1191.

Civin, C.I., Strauss, L.C., Brovall, C., Fackler, M.J., Schwartz, J.F., and Shaper, J.H. (1984). Antigenic analysis of hematopoiesis. III. A hematopoietic progenitor cell surface antigen defined by a monoclonal antibody raised against KG-1a cells. Journal of immunology *133*, 157-165.

Colamonici, M., Blyth, G., Saleiro, D., Szilard, A., Bliss-Moreau, M., Giles, F.J., Altman, J.K., Beauchamp, E.M., and Platanias, L.C. (2015). Dual targeting of acute myeloid leukemia progenitors by catalytic mTOR inhibition and blockade of the p110alpha subunit of PI3 kinase. Oncotarget *6*, 8062-8070.

Dancey, J.T., Deubelbeiss, K.A., Harker, L.A., and Finch, C.A. (1976). Neutrophil kinetics in man. The Journal of clinical investigation *58*, 705-715.

Das, S., Dixon, J.E., and Cho, W. (2003). Membrane-binding and activation mechanism of PTEN. Proceedings of the National Academy of Sciences of the United States of America *100*, 7491-7496.

Dennis, P.B., Pullen, N., Pearson, R.B., Kozma, S.C., and Thomas, G. (1998). Phosphorylation sites in the autoinhibitory domain participate in p70(s6k) activation loop phosphorylation. The Journal of biological chemistry *273*, 14845-14852.

Devgan, V., Mammucari, C., Millar, S.E., Brisken, C., and Dotto, G.P. (2005). p21WAF1/Cip1 is a negative transcriptional regulator of Wnt4 expression downstream of Notch1 activation. Genes Dev *19*, 1485-1495.

DeYoung, M.P., Horak, P., Sofer, A., Sgroi, D., and Ellisen, L.W. (2008). Hypoxia regulates TSC1/2-mTOR signaling and tumor suppression through REDD1-mediated 14-3-3 shuttling. Genes Dev *22*, 239-251.

DiGiusto, D., Chen, S., Combs, J., Webb, S., Namikawa, R., Tsukamoto, A., Chen, B.P., and Galy, A.H. (1994). Human fetal bone marrow early progenitors for T, B, and myeloid cells are found exclusively in the population expressing high levels of CD34. Blood *84*, 421-432.

Dimri, G.P., Nakanishi, M., Desprez, P.Y., Smith, J.R., and Campisi, J. (1996). Inhibition of E2F activity by the cyclin-dependent protein kinase inhibitor p21 in cells expressing or lacking a functional retinoblastoma protein. Mol Cell Biol *16*, 2987-2997.

Duan, Z., and Horwitz, M. (2003). Targets of the transcriptional repressor oncoprotein Gfi-1. Proceedings of the National Academy of Sciences of the United States of America *100*, 5932-5937.

Ducos, K., Panterne, B., Fortunel, N., Hatzfeld, A., Monier, M.N., and Hatzfeld, J. (2000). p21(cip1) mRNA is controlled by endogenous transforming growth factor-beta1 in quiescent human hematopoietic stem/progenitor cells. Journal of cellular physiology *184*, 80-85.

Eguchi, M., Eguchi-Ishimae, M., and Greaves, M. (2003). The role of the MLL gene in infant leukemia. Int J Hematol *78*, 390-401.

Ema, H., Sudo, K., Seita, J., Matsubara, A., Morita, Y., Osawa, M., Takatsu, K., Takaki, S., and Nakauchi, H. (2005). Quantification of self-renewal capacity in single hematopoietic stem cells from normal and Lnk-deficient mice. Developmental cell *8*, 907-914.

Essers, M.A., Offner, S., Blanco-Bose, W.E., Waibler, Z., Kalinke, U., Duchosal, M.A., and Trumpp, A. (2009). IFNalpha activates dormant haematopoietic stem cells in vivo. Nature *458*, 904-908.

Fang, Y., Park, I.H., Wu, A.L., Du, G., Huang, P., Frohman, M.A., Walker, S.J., Brown, H.A., and Chen, J. (2003). PLD1 regulates mTOR signaling and mediates Cdc42 activation of S6K1. Curr Biol *13*, 2037-2044.

Ferrari, S., Bannwarth, W., Morley, S.J., Totty, N.F., and Thomas, G. (1992). Activation of p70s6k is associated with phosphorylation of four clustered sites displaying Ser/Thr-Pro motifs. Proceedings of the National Academy of Sciences of the United States of America *89*, 7282-7286.

Fleming, W.H., Alpern, E.J., Uchida, N., Ikuta, K., Spangrude, G.J., and Weissman, I.L. (1993). Functional heterogeneity is associated with the cell cycle status of murine hematopoietic stem cells. The Journal of cell biology *122*, 897-902.

Garelick, M.G., Mackay, V.L., Yanagida, A., Academia, E.C., Schreiber, K.H., Ladiges, W.C., and Kennedy, B.K. (2013). Chronic rapamycin treatment or lack of S6K1 does not reduce ribosome activity in vivo. Cell cycle *12*, 2493-2504.

Gerdes, J., Lemke, H., Baisch, H., Wacker, H.H., Schwab, U., and Stein, H. (1984). Cell cycle analysis of a cell proliferation-associated human nuclear antigen defined by the monoclonal antibody Ki-67. Journal of immunology *133*, 1710-1715.

Gerdes, J., Li, L., Schlueter, C., Duchrow, M., Wohlenberg, C., Gerlach, C., Stahmer, I., Kloth, S., Brandt, E., and Flad, H.D. (1991). Immunobiochemical and molecular biologic characterization of the cell proliferation-associated nuclear antigen that is defined by monoclonal antibody Ki-67. The American journal of pathology *138*, 867-873.

Gonzalez-Rodriguez, A., Alba, J., Zimmerman, V., Kozma, S.C., and Valverde, A.M. (2009). S6K1 deficiency protects against apoptosis in hepatocytes. Hepatology *50*, 216-229.

Goodell, M.A., Brose, K., Paradis, G., Conner, A.S., and Mulligan, R.C. (1996). Isolation and functional properties of murine hematopoietic stem cells that are replicating in vivo. The Journal of experimental medicine *183*, 1797-1806.

Gottifredi, V., Karni-Schmidt, O., Shieh, S.S., and Prives, C. (2001). p53 down-regulates CHK1 through p21 and the retinoblastoma protein. Mol Cell Biol *21*, 1066-1076.

Goyama, S., Schibler, J., Cunningham, L., Zhang, Y., Rao, Y., Nishimoto, N., Nakagawa, M., Olsson, A., Wunderlich, M., Link, K.A.*, et al.* (2013). Transcription factor RUNX1 promotes survival of acute myeloid leukemia cells. The Journal of clinical investigation *123*, 3876-3888.

Greenberg, P.L., Lee, S.J., Advani, R., Tallman, M.S., Sikic, B.I., Letendre, L., Dugan, K., Lum, B., Chin, D.L., Dewald, G.*, et al.* (2004). Mitoxantrone, etoposide, and cytarabine with or without valspodar in patients with relapsed or refractory acute myeloid leukemia and high-risk myelodysplastic syndrome: a phase III trial (E2995). J Clin Oncol *22*, 1078-1086.

Grove, J.R., Banerjee, P., Balasubramanyam, A., Coffer, P.J., Price, D.J., Avruch, J., and Woodgett, J.R. (1991). Cloning and expression of two human p70 S6 kinase polypeptides differing only at their amino termini. Molecular and cellular biology *11*, 5541-5550.

Gu, Y., Rosenblatt, J., and Morgan, D.O. (1992). Cell cycle regulation of CDK2 activity by phosphorylation of Thr160 and Tyr15. EMBO J *11*, 3995-4005.

Guo, F., Zhang, S., Grogg, M., Cancelas, J.A., Varney, M.E., Starczynowski, D.T., Du, W., Yang, J.Q., Liu, W., Thomas, G.*, et al.* (2013). Mouse gene targeting reveals an essential role of mTOR in hematopoietic stem cell engraftment and hematopoiesis. Haematologica *98*, 1353-1358.

Hac, A., Domachowska, A., Narajczyk, M., Cyske, K., Pawlik, A., and Herman-Antosiewicz, A. (2015). S6K1 controls autophagosome maturation in autophagy induced by sulforaphane or serum deprivation. European journal of cell biology *94*, 470-481.

Haneline, L.S., White, H., Yang, F.C., Chen, S., Orschell, C., Kapur, R., and Ingram, D.A. (2006). Genetic reduction of class IA PI-3 kinase activity alters fetal hematopoiesis and competitive repopulating ability of hematopoietic stem cells in vivo. Blood *107*, 1375-1382.

Hao, Q.L., Thiemann, F.T., Petersen, D., Smogorzewska, E.M., and Crooks, G.M. (1996). Extended long-term culture reveals a highly quiescent and primitive human hematopoietic progenitor population. Blood *88*, 3306-3313.

Harper, J.W., Adami, G.R., Wei, N., Keyomarsi, K., and Elledge, S.J. (1993). The p21 Cdk-interacting protein Cip1 is a potent inhibitor of G1 cyclin-dependent kinases. Cell *75*, 805-816.

Harris, W.J., Huang, X., Lynch, J.T., Spencer, G.J., Hitchin, J.R., Li, Y., Ciceri, F., Blaser, J.G., Greystoke, B.F., Jordan, A.M.*, et al.* (2012). The histone demethylase KDM1A sustains the oncogenic potential of MLL-AF9 leukemia stem cells. Cancer Cell *21*, 473-487.

Harrison, D.E. (1980). Competitive repopulation: a new assay for long-term stem cell functional capacity. Blood *55*, 77-81.

Harrison, D.E., and Lerner, C.P. (1991). Most primitive hematopoietic stem cells are stimulated to cycle rapidly after treatment with 5-fluorouracil. Blood *78*, 1237-1240.

Henriques, R., Magyar, Z., and Bogre, L. (2013). S6K1 and E2FB are in mutually antagonistic regulatory links controlling cell growth and proliferation in Arabidopsis. Plant signaling & behavior *8*, e24367.

Herst, P.M., Howman, R.A., Neeson, P.J., Berridge, M.V., and Ritchie, D.S. (2011). The level of glycolytic metabolism in acute myeloid leukemia blasts at diagnosis is prognostic for clinical outcome. J Leukoc Biol *89*, 51-55.

Holler, E., Kolb, H.J., Moller, A., Kempeni, J., Liesenfeld, S., Pechumer, H., Lehmacher, W., Ruckdeschel, G., Gleixner, B., Riedner, C*., et al.* (1990). Increased serum levels of tumor necrosis factor alpha precede major complications of bone marrow transplantation. Blood *75*, 1011-1016.

Hong, S.E., Kim, E.K., Jin, H.O., Kim, H.A., Lee, J.K., Koh, J.S., Seol, H., Kim, J.I., Park, I.C., and Noh, W.C. (2013). S6K1 inhibition enhances tamoxifen-induced cell death in MCF-7 cells through translational inhibition of Mcl-1 and survivin. Cell Biol Toxicol *29*, 273-282.

Hoshii, T., Tadokoro, Y., Naka, K., Ooshio, T., Muraguchi, T., Sugiyama, N., Soga, T., Araki, K., Yamamura, K., and Hirao, A. (2012). mTORC1 is essential for leukemia propagation but not stem cell self-renewal. The Journal of clinical investigation *122*, 2114-2129.

Hu, B., Mitra, J., van den Heuvel, S., and Enders, G.H. (2001). S and G2 phase roles for Cdk2 revealed by inducible expression of a dominant-negative mutant in human cells. Mol Cell Biol *21*, 2755-2766.

Huang, H.L., Fang, L.W., Lu, S.P., Chou, C.K., Luh, T.Y., and Lai, M.Z. (2003). DNA-damaging reagents induce apoptosis through reactive oxygen species-dependent Fas aggregation. Oncogene *22*, 8168-8177.

Huang, X., Li, D., Li, T., Zhao, B.O., and Chen, X. (2015). Prognostic value of the expression of phosphatase and tensin homolog and CD44 in elderly patients with refractory acute myeloid leukemia. Oncol Lett *10*, 103-110.

Inoki, K., Li, Y., Xu, T., and Guan, K.L. (2003). Rheb GTPase is a direct target of TSC2 GAP activity and regulates mTOR signaling. Genes Dev *17*, 1829-1834.

Inoki, K., Li, Y., Zhu, T., Wu, J., and Guan, K.L. (2002). TSC2 is phosphorylated and inhibited by Akt and suppresses mTOR signalling. Nature cell biology *4*, 648-657.

Ip, C.K., Cheung, A.N., Ngan, H.Y., and Wong, A.S. (2011). p70 S6 kinase in the control of actin cytoskeleton dynamics and directed migration of ovarian cancer cells. Oncogene *30*, 2420-2432.

Ishikawa, F., Yoshida, S., Saito, Y., Hijikata, A., Kitamura, H., Tanaka, S., Nakamura, R., Tanaka, T., Tomiyama, H., Saito, N.*, et al.* (2007). Chemotherapy-resistant human AML stem cells home to and engraft within the bone-marrow endosteal region. Nat Biotechnol *25*, 1315-1321.

Isotani, S., Hara, K., Tokunaga, C., Inoue, H., Avruch, J., and Yonezawa, K. (1999). Immunopurified mammalian target of rapamycin phosphorylates and activates p70 S6 kinase alpha in vitro. The Journal of biological chemistry *274*, 34493-34498.

Ito, K., Hirao, A., Arai, F., Matsuoka, S., Takubo, K., Hamaguchi, I., Nomiyama, K., Hosokawa, K., Sakurada, K., Nakagata, N.*, et al.* (2004). Regulation of oxidative stress by ATM is required for self-renewal of haematopoietic stem cells. Nature *431*, 997-1002.

Jacobson, L.O., Simmons, E.L., and Bethard, W.F. (1950a). Studies on hematopoietic recovery from radiation injury. The Journal of clinical investigation *29*, 825.

Jacobson, L.O., Simmons, E.L., Marks, E.K., Robson, M.J., Bethard, W.F., and Gaston, E.O. (1950b). The role of the spleen in radiation injury and recovery. J Lab Clin Med *35*, 746-770.

Janzen, V., Forkert, R., Fleming, H.E., Saito, Y., Waring, M.T., Dombkowski, D.M., Cheng, T., DePinho, R.A., Sharpless, N.E., and Scadden, D.T. (2006). Stem-cell ageing modified by the cyclin-dependent kinase inhibitor p16INK4a. Nature *443*, 421-426.

Jetmore, A., Plett, P.A., Tong, X., Wolber, F.M., Breese, R., Abonour, R., Orschell-Traycoff, C.M., and Srour, E.F. (2002). Homing efficiency, cell cycle kinetics, and survival of quiescent and cycling human CD34(+) cells transplanted into conditioned NOD/SCID recipients. Blood *99*, 1585-1593.

Jia, Y., Subramanian, K.K., Erneux, C., Pouillon, V., Hattori, H., Jo, H., You, J., Zhu, D., Schurmans, S., and Luo, H.R. (2007). Inositol 1,3,4,5-tetrakisphosphate negatively regulates phosphatidylinositol-3,4,5- trisphosphate signaling in neutrophils. Immunity *27*, 453-467.

Johnson, D.G., Schwarz, J.K., Cress, W.D., and Nevins, J.R. (1993). Expression of transcription factor E2F1 induces quiescent cells to enter S phase. Nature *365*, 349-352.

Jones, P.F., Jakubowicz, T., Pitossi, F.J., Maurer, F., and Hemmings, B.A. (1991). Molecular cloning and identification of a serine/threonine protein kinase of the second-messenger subfamily. Proceedings of the National Academy of Sciences of the United States of America *88*, 4171-4175.

Jude, C.D., Climer, L., Xu, D., Artinger, E., Fisher, J.K., and Ernst, P. (2007). Unique and independent roles for MLL in adult hematopoietic stem cells and progenitors. Cell stem cell *1*, 324-337.

Julien, L.A., Carriere, A., Moreau, J., and Roux, P.P. (2010). mTORC1-activated S6K1 phosphorylates Rictor on threonine 1135 and regulates mTORC2 signaling. Molecular and cellular biology *30*, 908-921.

Juntilla, M.M., Patil, V.D., Calamito, M., Joshi, R.P., Birnbaum, M.J., and Koretzky, G.A. (2010). AKT1 and AKT2 maintain hematopoietic stem cell function by regulating reactive oxygen species. Blood *115*, 4030-4038.

Kaizuka, T., Hara, T., Oshiro, N., Kikkawa, U., Yonezawa, K., Takehana, K., Iemura, S., Natsume, T., and Mizushima, N. (2010). Tti1 and Tel2 are critical factors in mammalian target of rapamycin complex assembly. The Journal of biological chemistry *285*, 20109-20116.

Kandel, E.S., and Hay, N. (1999). The regulation and activities of the multifunctional serine/threonine kinase Akt/PKB. Experimental cell research *253*, 210-229.

Keshwani, M.M., von Daake, S., Newton, A.C., Harris, T.K., and Taylor, S.S. (2011). Hydrophobic motif phosphorylation is not required for activation loop phosphorylation of p70 ribosomal protein S6 kinase 1 (S6K1). The Journal of biological chemistry *286*, 23552-23558.

Kharas, M.G., Okabe, R., Ganis, J.J., Gozo, M., Khandan, T., Paktinat, M., Gilliland, D.G., and Gritsman, K. (2010). Constitutively active AKT depletes hematopoietic stem cells and induces leukemia in mice. Blood *115*, 1406-1415.

Khotskaya, Y.B., Goverdhan, A., Shen, J., Ponz-Sarvise, M., Chang, S.S., Hsu, M.C., Wei, Y., Xia, W., Yu, D., and Hung, M.C. (2014). S6K1 promotes invasiveness of breast cancer cells in a model of metastasis of triple-negative breast cancer. Am J Transl Res *6*, 361-376.

Kiel, M.J., Yilmaz, O.H., Iwashita, T., Yilmaz, O.H., Terhorst, C., and Morrison, S.J. (2005). SLAM family receptors distinguish hematopoietic stem and progenitor cells and reveal endothelial niches for stem cells. Cell *121*, 1109-1121.

Koh, P.O. (2013). Ferulic acid attenuates focal cerebral ischemia-induced decreases in p70S6 kinase and S6 phosphorylation. Neuroscience letters *555*, 7-11.

Kornblau, S.M., Minden, M.D., Rosen, D.B., Putta, S., Cohen, A., Covey, T., Spellmeyer, D.C., Fantl, W.J., Gayko, U., and Cesano, A. (2010). Dynamic single-cell network profiles in acute myelogenous leukemia are associated with patient response to standard induction therapy. Clinical cancer research : an official journal of the American Association for Cancer Research *16*, 3721-3733.

Kornblau, S.M., Womble, M., Qiu, Y.H., Jackson, C.E., Chen, W., Konopleva, M., Estey, E.H., and Andreeff, M. (2006). Simultaneous activation of multiple signal transduction pathways confers poor prognosis in acute myelogenous leukemia. Blood *108*, 2358-2365.

Krause, D.S., Fackler, M.J., Civin, C.I., and May, W.S. (1996). CD34: structure, biology, and clinical utility. Blood *87*, 1-13.

Kubota, Y., Ohnishi, H., Kitanaka, A., Ishida, T., and Tanaka, T. (2004). Constitutive activation of PI3K is involved in the spontaneous proliferation of primary acute myeloid leukemia cells: direct evidence of PI3K activation. Leukemia *18*, 1438-1440.

Kultz, D. (2005). Molecular and evolutionary basis of the cellular stress response. Annu Rev Physiol *67*, 225-257.

Lacorazza, H.D., Yamada, T., Liu, Y., Miyata, Y., Sivina, M., Nunes, J., and Nimer, S.D. (2006). The transcription factor MEF/ELF4 regulates the quiescence of primitive hematopoietic cells. Cancer Cell *9*, 175-187.

Lai, K.P., Leong, W.F., Chau, J.F., Jia, D., Zeng, L., Liu, H., He, L., Hao, A., Zhang, H., Meek, D.*, et al.* (2010). S6K1 is a multifaceted regulator of Mdm2 that connects nutrient status and DNA damage response. The EMBO journal *29*, 2994-3006.

Lapidot, T., Dar, A., and Kollet, O. (2005). How do stem cells find their way home? Blood *106*, 1901-1910.

Lapidot, T., Sirard, C., Vormoor, J., Murdoch, B., Hoang, T., Caceres-Cortes, J., Minden, M., Paterson, B., Caligiuri, M.A., and Dick, J.E. (1994). A cell initiating human acute myeloid leukaemia after transplantation into SCID mice. Nature *367*, 645-648.

Law, B.K., Chytil, A., Dumont, N., Hamilton, E.G., Waltner-Law, M.E., Aakre, M.E., Covington, C., and Moses, H.L. (2002). Rapamycin potentiates transforming growth factor beta-induced growth arrest in nontransformed, oncogene-transformed, and human cancer cells. Molecular and cellular biology *22*, 8184-8198.

Lee, J.Y., Nakada, D., Yilmaz, O.H., Tothova, Z., Joseph, N.M., Lim, M.S., Gilliland, D.G., and Morrison, S.J. (2010). mTOR activation induces tumor suppressors that inhibit leukemogenesis and deplete hematopoietic stem cells after Pten deletion. Cell stem cell *7*, 593-605.

Lee, S.J., Yang, E.K., and Kim, S.G. (2006). Peroxisome proliferator-activated receptor-gamma and retinoic acid X receptor alpha represses the TGFbeta1 gene via PTEN-mediated p70 ribosomal S6 kinase-1 inhibition: role for Zf9 dephosphorylation. Molecular pharmacology *70*, 415-425.

Lerner, C., and Harrison, D.E. (1990). 5-Fluorouracil spares hemopoietic stem cells responsible for long-term repopulation. Experimental hematology *18*, 114-118.

Li, J., Hou, N., Faried, A., Tsutsumi, S., and Kuwano, H. (2010). Inhibition of autophagy augments 5-fluorouracil chemotherapy in human colon cancer in vitro and in vivo model. European journal of cancer *46*, 1900-1909.

Li, Y., Inoki, K., Yeung, R., and Guan, K.L. (2002). Regulation of TSC2 by 14-3-3 binding. The Journal of biological chemistry *277*, 44593-44596.

Lin, K.K., Rossi, L., Boles, N.C., Hall, B.E., George, T.C., and Goodell, M.A. (2011). CD81 is essential for the re-entry of hematopoietic stem cells to quiescence following stress-induced proliferation via deactivation of the Akt pathway. PLoS biology *9*, e1001148.

Liu, J.L., Gao, G.R., Zhang, X., Cao, S.F., Guo, C.L., Wang, X., Tong, L.J., Ding, J., Duan, W.H., and Meng, L.H. (2014a). DW09849, a selective phosphatidylinositol 3-kinase (PI3K) inhibitor, prevents PI3K signaling and preferentially inhibits proliferation of cells containing the oncogenic mutation p110alpha (H1047R). The Journal of pharmacology and experimental therapeutics *348*, 432-441.

Liu, P., Gan, W., Inuzuka, H., Lazorchak, A.S., Gao, D., Arojo, O., Liu, D., Wan, L., Zhai, B., Yu, Y.*, et al.* (2013). Sin1 phosphorylation impairs mTORC2 complex integrity and inhibits downstream Akt signalling to suppress tumorigenesis. Nature cell biology *15*, 1340-1350.

Liu, Z., Chen, X., Wang, Y., Peng, H., Wang, Y., Jing, Y., and Zhang, H. (2014b). PDK4 protein promotes tumorigenesis through activation of cAMP-response element-binding protein (CREB)-Ras homolog enriched in brain (RHEB)-mTORC1 signaling cascade. The Journal of biological chemistry *289*, 29739-29749.

Lohr, K., Moritz, C., Contente, A., and Dobbelstein, M. (2003). p21/CDKN1A mediates negative regulation of transcription by p53. J Biol Chem *278*, 32507-32516.

Lorenz, E., Uphoff, D., Reid, T.R., and Shelton, E. (1951). Modification of irradiation injury in mice and guinea pigs by bone marrow injections. J Natl Cancer Inst *12*, 197-201.

Lowenberg, B., Downing, J.R., and Burnett, A. (1999). Acute myeloid leukemia. N Engl J Med *341*, 1051-1062.

Lukas, J., Petersen, B.O., Holm, K., Bartek, J., and Helin, K. (1996). Deregulated expression of E2F family members induces S-phase entry and overcomes p16INK4A-mediated growth suppression. Mol Cell Biol *16*, 1047-1057.

Luo, Y., Li, L., Zou, P., Wang, J., Shao, L., Zhou, D., and Liu, L. (2014). Rapamycin enhances long-term hematopoietic reconstitution of ex vivo expanded mouse hematopoietic stem cells by inhibiting senescence. Transplantation *97*, 20-29.

MacDonald, A.S., and Group, R.G.S. (2001). A worldwide, phase III, randomized, controlled, safety and efficacy study of a sirolimus/cyclosporine regimen for prevention of acute rejection in recipients of primary mismatched renal allografts. Transplantation *71*, 271-280.

Magee, J.A., Ikenoue, T., Nakada, D., Lee, J.Y., Guan, K.L., and Morrison, S.J. (2012). Temporal changes in PTEN and mTORC2 regulation of hematopoietic stem cell self-renewal and leukemia suppression. Cell stem cell *11*, 415-428.

Manning, G., Whyte, D.B., Martinez, R., Hunter, T., and Sudarsanam, S. (2002). The protein kinase complement of the human genome. Science *298*, 1912-1934.

Martin, K.A., Schalm, S.S., Richardson, C., Romanelli, A., Keon, K.L., and Blenis, J. (2001). Regulation of ribosomal S6 kinase 2 by effectors of the phosphoinositide 3-kinase pathway. The Journal of biological chemistry *276*, 7884-7891.

Masure, S., Haefner, B., Wesselink, J.J., Hoefnagel, E., Mortier, E., Verhasselt, P., Tuytelaars, A., Gordon, R., and Richardson, A. (1999). Molecular cloning, expression and characterization of the human serine/threonine kinase Akt-3. Eur J Biochem *265*, 353-360.

Maximow, A.A. (1909). Der Lymphozyt als gemeinsame Stammzelle der verschiedenen Blutelemente in der embryonalen Entwicklung und im postfetalen Leben der Säugetiere. Folia Haematol. (Frankf.) 8, 125–134.

Miyamoto, K., Araki, K.Y., Naka, K., Arai, F., Takubo, K., Yamazaki, S., Matsuoka, S., Miyamoto, T., Ito, K., Ohmura, M.*, et al.* (2007). Foxo3a is essential for maintenance of the hematopoietic stem cell pool. Cell stem cell *1*, 101-112.

Momparler, R.L. (1974). A model for the chemotherapy of acute leukemia with 1-beta-D-arabinofuranosylcytosine. Cancer research *34*, 1775-1787.

Muller-Sieburg, C.E., Cho, R.H., Karlsson, L., Huang, J.F., and Sieburg, H.B. (2004). Myeloid-biased hematopoietic stem cells have extensive self-renewal capacity but generate diminished lymphoid progeny with impaired IL-7 responsiveness. Blood *103*, 4111-4118.

Muntean, A.G., and Hess, J.L. (2012). The pathogenesis of mixed-lineage leukemia. Annu Rev Pathol *7*, 283-301.

Munugalavadla, V., Sims, E.C., Borneo, J., Chan, R.J., and Kapur, R. (2007). Genetic and pharmacologic evidence implicating the p85 alpha, but not p85 beta, regulatory subunit of PI3K and Rac2 GTPase in regulating oncogenic KIT-induced transformation in acute myeloid leukemia and systemic mastocytosis. Blood *110*, 1612-1620.

Munugalavadla, V., Sims, E.C., Chan, R.J., Lenz, S.D., and Kapur, R. (2008). Requirement for p85alpha regulatory subunit of class IA PI3K in myeloproliferative disease driven by an activation loop mutant of KIT. Experimental hematology *36*, 301-308.

Naka, K., Hoshii, T., Muraguchi, T., Tadokoro, Y., Ooshio, T., Kondo, Y., Nakao, S., Motoyama, N., and Hirao, A. (2010). TGF-beta-FOXO signalling maintains leukaemia-initiating cells in chronic myeloid leukaemia. Nature *463*, 676-680.

Nakorn, T.N., Miyamoto, T., and Weissman, I.L. (2003). Characterization of mouse clonogenic megakaryocyte progenitors. Proceedings of the National Academy of Sciences of the United States of America *100*, 205-210.

Neff, T., Sinha, A.U., Kluk, M.J., Zhu, N., Khattab, M.H., Stein, L., Xie, H., Orkin, S.H., and Armstrong, S.A. (2012). Polycomb repressive complex 2 is required for MLL-AF9 leukemia. Proceedings of the National Academy of Sciences of the United States of America *109*, 5028-5033.

Nogami, A., Oshikawa, G., Okada, K., Fukutake, S., Umezawa, Y., Nagao, T., Kurosu, T., and Miura, O. (2015). FLT3-ITD confers resistance to the PI3K/Akt pathway inhibitors by protecting the mTOR/4EBP1/Mcl-1 pathway through STAT5 activation in acute myeloid leukemia. Oncotarget *6*, 9189-9205.

Notta, F., Doulatov, S., Laurenti, E., Poeppl, A., Jurisica, I., and Dick, J.E. (2011). Isolation of single human hematopoietic stem cells capable of long-term multilineage engraftment. Science *333*, 218-221.

Nowakowski, R.S., Lewin, S.B., and Miller, M.W. (1989). Bromodeoxyuridine immunohistochemical determination of the lengths of the cell cycle and the DNA-synthetic phase for an anatomically defined population. J Neurocytol *18*, 311-318.

Ogawa, M. (1993). Differentiation and proliferation of hematopoietic stem cells. Blood *81*, 2844-2853.

Ogden, D.A., and Mickliem, H.S. (1976). The fate of serially transplanted bone marrow cell populations from young and old donors. Transplantation *22*, 287-293.

Oguro, H., Ding, L., and Morrison, S.J. (2013). SLAM family markers resolve functionally distinct subpopulations of hematopoietic stem cells and multipotent progenitors. Cell stem cell *13*, 102-116.

Ohta, M., Greenberger, J.S., Anklesaria, P., Bassols, A., and Massague, J. (1987). Two forms of transforming growth factor-beta distinguished by multipotential haematopoietic progenitor cells. Nature *329*, 539-541.

Okada, S., Nakauchi, H., Nagayoshi, K., Nishikawa, S., Miura, Y., and Suda, T. (1992). In vivo and in vitro stem cell function of c-kit- and Sca-1-positive murine hematopoietic cells. Blood *80*, 3044-3050.

Orschell-Traycoff, C.M., Hiatt, K., Dagher, R.N., Rice, S., Yoder, M.C., and Srour, E.F. (2000). Homing and engraftment potential of Sca-1(+)lin(-) cells fractionated on the basis of adhesion molecule expression and position in cell cycle. Blood *96*, 1380-1387.

Osawa, M., Hanada, K., Hamada, H., and Nakauchi, H. (1996). Long-term lymphohematopoietic reconstitution by a single CD34-low/negative hematopoietic stem cell. Science *273*, 242-245.

Ottmann, O.G., and Pelus, L.M. (1988). Differential proliferative effects of transforming growth factor-beta on human hematopoietic progenitor cells. Journal of immunology *140*, 2661-2665.

Pardo, V., Gonzalez-Rodriguez, A., Muntane, J., Kozma, S.C., and Valverde, A.M. (2015). Role of hepatocyte S6K1 in palmitic acid-induced endoplasmic reticulum stress, lipotoxicity, insulin resistance and in oleic acid-induced protection. Food and chemical toxicology : an international journal published for the British Industrial Biological Research Association *80*, 298-309.

Park, I.K., Qian, D., Kiel, M., Becker, M.W., Pihalja, M., Weissman, I.L., Morrison, S.J., and Clarke, M.F. (2003). Bmi-1 is required for maintenance of adult self-renewing haematopoietic stem cells. Nature *423*, 302-305.

Pearce, L.R., Alton, G.R., Richter, D.T., Kath, J.C., Lingardo, L., Chapman, J., Hwang, C., and Alessi, D.R. (2010). Characterization of PF-4708671, a novel and highly specific inhibitor of p70 ribosomal S6 kinase (S6K1). Biochem J *431*, 245-255.

Pende, M., Um, S.H., Mieulet, V., Sticker, M., Goss, V.L., Mestan, J., Mueller, M., Fumagalli, S., Kozma, S.C., and Thomas, G. (2004). S6K1(-/-)/S6K2(-/-) mice exhibit perinatal lethality and rapamycin-sensitive 5'-terminal oligopyrimidine mRNA translation and reveal a mitogen-activated protein kinase-dependent S6 kinase pathway. Molecular and cellular biology *24*, 3112-3124.

Petzer, A.L., Hogge, D.E., Landsdorp, P.M., Reid, D.S., and Eaves, C.J. (1996). Self-renewal of primitive human hematopoietic cells (long-term-culture-initiating cells) in vitro and their expansion in defined medium. Proceedings of the National Academy of Sciences of the United States of America *93*, 1470-1474.

Piacibello, W., Gammaitoni, L., and Pignochino, Y. (2005). Proliferative senescence in hematopoietic stem cells during ex-vivo expansion. Folia Histochem Cytobiol *43*, 197-202.

Price, D.J., Mukhopadhyay, N.K., and Avruch, J. (1991). Insulin-activated protein kinases phosphorylate a pseudosubstrate synthetic peptide inhibitor of the p70 S6 kinase. The Journal of biological chemistry *266*, 16281-16284.

Pronk, C.J., Rossi, D.J., Mansson, R., Attema, J.L., Norddahl, G.L., Chan, C.K., Sigvardsson, M., Weissman, I.L., and Bryder, D. (2007). Elucidation of the phenotypic, functional, and molecular topography of a myeloerythroid progenitor cell hierarchy. Cell stem cell *1*, 428-442.

Pullen, N., Dennis, P.B., Andjelkovic, M., Dufner, A., Kozma, S.C., Hemmings, B.A., and Thomas, G. (1998). Phosphorylation and activation of p70s6k by PDK1. Science *279*, 707-710.

Purton, L.E., and Scadden, D.T. (2007). Limiting factors in murine hematopoietic stem cell assays. Cell stem cell *1*, 263-270.

Qin, X.Q., Livingston, D.M., Kaelin, W.G., Jr., and Adams, P.D. (1994). Deregulated transcription factor E2F-1 expression leads to S-phase entry and p53-mediated apoptosis. Proc Natl Acad Sci U S A *91*, 10918-10922.

Raimondi, S.C., Chang, M.N., Ravindranath, Y., Behm, F.G., Gresik, M.V., Steuber, C.P., Weinstein, H.J., and Carroll, A.J. (1999). Chromosomal abnormalities in 478 children with acute myeloid leukemia: clinical characteristics and treatment outcome in a cooperative pediatric oncology group study-POG 8821. Blood *94*, 3707-3716.

Randall, T.D., and Weissman, I.L. (1997). Phenotypic and functional changes induced at the clonal level in hematopoietic stem cells after 5-fluorouracil treatment. Blood *89*, 3596-3606.

Reese, N.D., and Schiller, G.J. (2013). High-dose cytarabine (HD araC) in the treatment of leukemias: a review. Curr Hematol Malig Rep *8*, 141-148.

Riley, P.A. (1994). Free radicals in biology: oxidative stress and the effects of ionizing radiation. International journal of radiation biology *65*, 27-33.

Rohrabaugh, S.L., Campbell, T.B., Hangoc, G., and Broxmeyer, H.E. (2011). Ex vivo rapamycin treatment of human cord blood CD34+ cells enhances their engraftment of NSG mice. Blood cells, molecules & diseases *46*, 318-320.

Rosner, M., and Hengstschlager, M. (2011). Nucleocytoplasmic localization of p70 S6K1, but not of its isoforms p85 and p31, is regulated by TSC2/mTOR. Oncogene *30*, 4509-4522.

Rosner, M., Schipany, K., and Hengstschlager, M. (2012). p70 S6K1 nuclear localization depends on its mTOR-mediated phosphorylation at T389, but not on its kinase activity towards S6. Amino acids *42*, 2251-2256.

Rossi, L., Lin, K.K., Boles, N.C., Yang, L., King, K.Y., Jeong, M., Mayle, A., and Goodell, M.A. (2012). Less is more: unveiling the functional core of hematopoietic stem cells through knockout mice. Cell stem cell *11*, 302-317.

Saito, Y., Chapple, R.H., Lin, A., Kitano, A., and Nakada, D. (2015). AMPK Protects Leukemia-Initiating Cells in Myeloid Leukemias from Metabolic Stress in the Bone Marrow. Cell stem cell *17*, 585-596.

Sancak, Y., Thoreen, C.C., Peterson, T.R., Lindquist, R.A., Kang, S.A., Spooner, E., Carr, S.A., and Sabatini, D.M. (2007). PRAS40 is an insulin-regulated inhibitor of the mTORC1 protein kinase. Molecular cell *25*, 903-915.

Santos, M.A., Faryabi, R.B., Ergen, A.V., Day, A.M., Malhowski, A., Canela, A., Onozawa, M., Lee, J.E., Callen, E., Gutierrez-Martinez, P.*, et al.* (2014). DNA-damage-induced differentiation of leukaemic cells as an anti-cancer barrier. Nature *514*, 107-111.

Satyanarayana, A., Hilton, M.B., and Kaldis, P. (2008). p21 Inhibits Cdk1 in the absence of Cdk2 to maintain the G1/S phase DNA damage checkpoint. Mol Biol Cell *19*, 65-77.

Saunders, R.N., Metcalfe, M.S., and Nicholson, M.L. (2001). Rapamycin in transplantation: a review of the evidence. Kidney Int *59*, 3-16.

Schalm, S.S., and Blenis, J. (2002). Identification of a conserved motif required for mTOR signaling. Curr Biol *12*, 632-639.

Selman, C., Tullet, J.M., Wieser, D., Irvine, E., Lingard, S.J., Choudhury, A.I., Claret, M., Al-Qassab, H., Carmignac, D., Ramadani, F.*, et al.* (2009). Ribosomal protein S6 kinase 1 signaling regulates mammalian life span. Science *326*, 140-144.

Shats, I., Milyavsky, M., Tang, X., Stambolsky, P., Erez, N., Brosh, R., Kogan, I., Braunstein, I., Tzukerman, M., Ginsberg, D.*, et al.* (2004). p53-dependent down-regulation of telomerase is mediated by p21waf1. J Biol Chem *279*, 50976-50985.

Shen, F.W., Tung, J.S., and Boyse, E.A. (1986). Further definition of the Ly-5 system. Immunogenetics *24*, 146-149.

Shiyanov, P., Bagchi, S., Adami, G., Kokontis, J., Hay, N., Arroyo, M., Morozov, A., and Raychaudhuri, P. (1996). p21 Disrupts the interaction between cdk2 and the E2F-p130 complex. Mol Cell Biol *16*, 737-744.

Siegemund, S., Rigaud, S., Conche, C., Broaten, B., Schaffer, L., Westernberg, L., Head, S.R., and Sauer, K. (2015). IP3 3-kinase B controls hematopoietic stem cell homeostasis and prevents lethal hematopoietic failure in mice. Blood *125*, 2786-2797.

Siminovitch, L., McCulloch, E.A., and Till, J.E. (1963). The Distribution of Colony-Forming Cells among Spleen Colonies. Journal of cellular physiology *62*, 327-336.

Sipkins, D.A., Wei, X., Wu, J.W., Runnels, J.M., Cote, D., Means, T.K., Luster, A.D., Scadden, D.T., and Lin, C.P. (2005). In vivo imaging of specialized bone marrow endothelial microdomains for tumour engraftment. Nature *435*, 969-973.

Song, X., Dilly, A.K., Kim, S.Y., Choudry, H.A., and Lee, Y.J. (2014). Rapamycin-enhanced mitomycin C-induced apoptotic death is mediated through the S6K1-Bad-Bak pathway in peritoneal carcinomatosis. Cell death & disease *5*, e1281.

Spangrude, G.J., Heimfeld, S., and Weissman, I.L. (1988). Purification and characterization of mouse hematopoietic stem cells. Science *241*, 58-62.

Srour, E.F., and Jordan, C.T. (2002). Isolation and characterization of primitive hematopoietic cells based on their position in the cell cycle. Methods Mol Med *63*, 93-111.

Stark, B., Jeison, M., Gabay, L.G., Mardoukh, J., Luria, D., Bar-Am, I., Avrahami, G., Kapeliushnik, Y., Sthoeger, D., Herzel, G*., et al.* (2004). Classical and molecular cytogenetic abnormalities and outcome of childhood acute myeloid leukaemia: report from a referral centre in Israel. British journal of haematology *126*, 320-337.

Sujobert, P., Bardet, V., Cornillet-Lefebvre, P., Hayflick, J.S., Prie, N., Verdier, F., Vanhaesebroeck, B., Muller, O., Pesce, F., Ifrah, N*., et al.* (2005). Essential role for the p110delta isoform in phosphoinositide 3-kinase activation and cell proliferation in acute myeloid leukemia. Blood *106*, 1063-1066.

Sujobert, P., Poulain, L., Paubelle, E., Zylbersztejn, F., Grenier, A., Lambert, M., Townsend, E.C., Brusq, J.M., Nicodeme, E., Decrooqc, J*., et al.* (2015). Co-activation of AMPK and mTORC1 Induces Cytotoxicity in Acute Myeloid Leukemia. Cell Rep *11*, 1446-1457.

Sutton, E.J., Henning, T.D., Pichler, B.J., Bremer, C., and Daldrup-Link, H.E. (2008). Cell tracking with optical imaging. Eur Radiol *18*, 2021-2032.

Sykes, S.M., Lane, S.W., Bullinger, L., Kalaitzidis, D., Yusuf, R., Saez, B., Ferraro, F., Mercier, F., Singh, H., Brumme, K.M.*, et al.* (2011). AKT/FOXO signaling enforces reversible differentiation blockade in myeloid leukemias. Cell *146*, 697-708.

Szilvassy, S.J., Humphries, R.K., Lansdorp, P.M., Eaves, A.C., and Eaves, C.J. (1990). Quantitative assay for totipotent reconstituting hematopoietic stem cells by a competitive repopulation strategy. Proceedings of the National Academy of Sciences of the United States of America *87*, 8736-8740.

Takubo, K., Nagamatsu, G., Kobayashi, C.I., Nakamura-Ishizu, A., Kobayashi, H., Ikeda, E., Goda, N., Rahimi, Y., Johnson, R.S., Soga, T.*, et al.* (2013). Regulation of glycolysis by Pdk functions as a metabolic checkpoint for cell cycle quiescence in hematopoietic stem cells. Cell stem cell *12*, 49-61.

Tallman, M.S., Lee, S., Sikic, B.I., Paietta, E., Wiernik, P.H., Bennett, J.M., and Rowe, J.M. (1999). Mitoxantrone, etoposide, and cytarabine plus cyclosporine for patients with relapsed or refractory acute myeloid leukemia: an Eastern Cooperative Oncology Group pilot study. Cancer *85*, 358-367.

Tamburini, J., Elie, C., Bardet, V., Chapuis, N., Park, S., Broet, P., Cornillet-Lefebvre, P., Lioure, B., Ugo, V., Blanchet, O.*, et al.* (2007). Constitutive phosphoinositide 3-kinase/Akt activation represents a favorable prognostic factor in de novo acute myelogenous leukemia patients. Blood *110*, 1025-1028.

Tamburini, J., Green, A.S., Bardet, V., Chapuis, N., Park, S., Willems, L., Uzunov, M., Ifrah, N., Dreyfus, F., Lacombe, C.*, et al.* (2009). Protein synthesis is resistant to rapamycin and constitutes a promising therapeutic target in acute myeloid leukemia. Blood *114*, 1618-1627.

Tandon, P., Gallo, C.A., Khatri, S., Barger, J.F., Yepiskoposyan, H., and Plas, D.R. (2011). Requirement for ribosomal protein S6 kinase 1 to mediate glycolysis and apoptosis resistance induced by Pten deficiency. Proceedings of the National Academy of Sciences of the United States of America *108*, 2361-2365.

Till, J.E., and Mc, C.E. (1961). A direct measurement of the radiation sensitivity of normal mouse bone marrow cells. Radiation research *14*, 213-222.

Tothova, Z., Kollipara, R., Huntly, B.J., Lee, B.H., Castrillon, D.H., Cullen, D.E., McDowell, E.P., Lazo-Kallanian, S., Williams, I.R., Sears, C.*, et al.* (2007). FoxOs

are critical mediators of hematopoietic stem cell resistance to physiologic oxidative stress. Cell *128*, 325-339.

Treins, C., Warne, P.H., Magnuson, M.A., Pende, M., and Downward, J. (2010). Rictor is a novel target of p70 S6 kinase-1. Oncogene *29*, 1003-1016.

Uchida, N., Aguila, H.L., Fleming, W.H., Jerabek, L., and Weissman, I.L. (1994). Rapid and sustained hematopoietic recovery in lethally irradiated mice transplanted with purified Thy-1.1lo Lin-Sca-1+ hematopoietic stem cells. Blood *83*, 3758-3779.

Uchida, N., Sutton, R.E., Friera, A.M., He, D., Reitsma, M.J., Chang, W.C., Veres, G., Scollay, R., and Weissman, I.L. (1998). HIV, but not murine leukemia virus, vectors mediate high efficiency gene transfer into freshly isolated G0/G1 human hematopoietic stem cells. Proceedings of the National Academy of Sciences of the United States of America *95*, 11939-11944.

Um, S.H., Frigerio, F., Watanabe, M., Picard, F., Joaquin, M., Sticker, M., Fumagalli, S., Allegrini, P.R., Kozma, S.C., Auwerx, J.*, et al.* (2004). Absence of S6K1 protects against age- and diet-induced obesity while enhancing insulin sensitivity. Nature *431*, 200-205.

Vazquez, F., and Devreotes, P. (2006). Regulation of PTEN function as a PIP3 gatekeeper through membrane interaction. Cell cycle *5*, 1523-1527.

Vazquez, F., Matsuoka, S., Sellers, W.R., Yanagida, T., Ueda, M., and Devreotes, P.N. (2006). Tumor suppressor PTEN acts through dynamic interaction with the plasma membrane. Proceedings of the National Academy of Sciences of the United States of America *103*, 3633-3638.

Venezia, T.A., Merchant, A.A., Ramos, C.A., Whitehouse, N.L., Young, A.S., Shaw, C.A., and Goodell, M.A. (2004). Molecular signatures of proliferation and quiescence in hematopoietic stem cells. PLoS biology *2*, e301.

Walter, D., Lier, A., Geiselhart, A., Thalheimer, F.B., Huntscha, S., Sobotta, M.C., Moehrle, B., Brocks, D., Bayindir, I., Kaschutnig, P.*, et al.* (2015). Exit from dormancy provokes DNA-damage-induced attrition in haematopoietic stem cells. Nature *520*, 549-552.

Wei, J., Wunderlich, M., Fox, C., Alvarez, S., Cigudosa, J.C., Wilhelm, J.S., Zheng, Y., Cancelas, J.A., Gu, Y., Jansen, M.*, et al.* (2008). Microenvironment determines lineage fate in a human model of MLL-AF9 leukemia. Cancer Cell *13*, 483-495.

Weng, Q.P., Kozlowski, M., Belham, C., Zhang, A., Comb, M.J., and Avruch, J. (1998). Regulation of the p70 S6 kinase by phosphorylation in vivo. Analysis using site-specific anti-phosphopeptide antibodies. The Journal of biological chemistry *273*, 16621-16629.

Williams, M.R., Arthur, J.S., Balendran, A., van der Kaay, J., Poli, V., Cohen, P., and Alessi, D.R. (2000). The role of 3-phosphoinositide-dependent protein kinase 1 in activating AGC kinases defined in embryonic stem cells. Curr Biol *10*, 439-448.

Woo, M.S., Sanchez, I., and Dynlacht, B.D. (1997). p130 and p107 use a conserved domain to inhibit cellular cyclin-dependent kinase activity. Mol Cell Biol *17*, 3566-3579.

Wu, H.M., Lewis, J.P., Sky-Peck, H.H., and Trobaugh, F.E., Jr. (1968). Biochemical studies of spleens of heavily irradiated mice transfused with bone marrow. Radiation research *33*, 50-65.

Wunderlich, M., Chou, F.S., Link, K.A., Mizukawa, B., Perry, R.L., Carroll, M., and Mulloy, J.C. (2010). AML xenograft efficiency is significantly improved in NOD/SCID-IL2RG mice constitutively expressing human SCF, GM-CSF and IL-3. Leukemia *24*, 1785-1788.

Xin, Y., Shen, X.D., Cheng, L., Hong, D.F., and Chen, B. (2014). Perifosine inhibits S6K1-Gli1 signaling and enhances gemcitabine-induced anti-pancreatic cancer efficiency. Cancer Chemother Pharmacol *73*, 711-719.

Xu, Q., Simpson, S.E., Scialla, T.J., Bagg, A., and Carroll, M. (2003). Survival of acute myeloid leukemia cells requires PI3 kinase activation. Blood *102*, 972-980.

Yamazaki, S., Iwama, A., Takayanagi, S., Eto, K., Ema, H., and Nakauchi, H. (2009). TGF-beta as a candidate bone marrow niche signal to induce hematopoietic stem cell hibernation. Blood *113*, 1250-1256.

Yang, L., Bryder, D., Adolfsson, J., Nygren, J., Mansson, R., Sigvardsson, M., and Jacobsen, S.E. (2005). Identification of Lin(-)Sca1(+)kit(+)CD34(+)Flt3-short-term hematopoietic stem cells capable of rapidly reconstituting and rescuing myeloablated transplant recipients. Blood *105*, 2717-2723.

Yang, L., Miao, L., Liang, F., Huang, H., Teng, X., Li, S., Nuriddinov, J., Selzer, M.E., and Hu, Y. (2014). The mTORC1 effectors S6K1 and 4E-BP play different roles in CNS axon regeneration. Nat Commun *5*, 5416.

Yang, Q., Inoki, K., Ikenoue, T., and Guan, K.L. (2006). Identification of Sin1 as an essential TORC2 component required for complex formation and kinase activity. Genes Dev *20*, 2820-2832.

Yilmaz, O.H., Kiel, M.J., and Morrison, S.J. (2006a). SLAM family markers are conserved among hematopoietic stem cells from old and reconstituted mice and markedly increase their purity. Blood *107*, 924-930.

Yilmaz, O.H., Valdez, R., Theisen, B.K., Guo, W., Ferguson, D.O., Wu, H., and Morrison, S.J. (2006b). Pten dependence distinguishes haematopoietic stem cells from leukaemia-initiating cells. Nature *441*, 475-482.

Yokoyama, A., Wang, Z., Wysocka, J., Sanyal, M., Aufiero, D.J., Kitabayashi, I., Herr, W., and Cleary, M.L. (2004). Leukemia proto-oncoprotein MLL forms a SET1-like histone methyltransferase complex with menin to regulate Hox gene expression. Molecular and cellular biology *24*, 5639-5649.

Yoon, M.S., Rosenberger, C.L., Wu, C., Truong, N., Sweedler, J.V., and Chen, J. (2015). Rapid mitogenic regulation of the mTORC1 inhibitor, DEPTOR, by phosphatidic acid. Molecular cell *58*, 549-556.

Yu, H., Yuan, Y., Shen, H., and Cheng, T. (2006). Hematopoietic stem cell exhaustion impacted by p18 INK4C and p21 Cip1/Waf1 in opposite manners. Blood *107*, 1200-1206.

Yuan, Y., Shen, H., Franklin, D.S., Scadden, D.T., and Cheng, T. (2004). In vivo self-renewing divisions of haematopoietic stem cells are increased in the absence of the early G1-phase inhibitor, p18INK4C. Nature cell biology *6*, 436-442.

Zeng, H., Yucel, R., Kosan, C., Klein-Hitpass, L., and Moroy, T. (2004). Transcription factor Gfi1 regulates self-renewal and engraftment of hematopoietic stem cells. The EMBO journal *23*, 4116-4125.

Zeng, Z., Shi, Y.X., Tsao, T., Qiu, Y., Kornblau, S.M., Baggerly, K.A., Liu, W., Jessen, K., Liu, Y., Kantarjian, H.*, et al.* (2012). Targeting of mTORC1/2 by the mTOR kinase inhibitor PP242 induces apoptosis in AML cells under conditions mimicking the bone marrow microenvironment. Blood *120*, 2679-2689.

Zhang, J., Grindley, J.C., Yin, T., Jayasinghe, S., He, X.C., Ross, J.T., Haug, J.S., Rupp, D., Porter-Westpfahl, K.S., Wiedemann, L.M.*, et al.* (2006). PTEN maintains haematopoietic stem cells and acts in lineage choice and leukaemia prevention. Nature *441*, 518-522.

Zhao, L., and Vogt, P.K. (2008). Class I PI3K in oncogenic cellular transformation. Oncogene *27*, 5486-5496.

Zhou, Q., Liu, C., Liu, W., Zhang, H., Zhang, R., Liu, J., Zhang, J., Xu, C., Liu, L., Huang, S.*, et al.* (2015). Rotenone induction of hydrogen peroxide inhibits mTOR-mediated S6K1 and 4E-BP1/eIF4E pathways, leading to neuronal apoptosis. Toxicological sciences : an official journal of the Society of Toxicology *143*, 81-96.

Zhu, L., Harlow, E., and Dynlacht, B.D. (1995). p107 uses a p21CIP1-related domain to bind cyclin/cdk2 and regulate interactions with E2F. Genes Dev *9*, 1740-1752.

Curriculum Vitae

Joydeep Ghosh

Education

2004	**B.S.** in Physiology University of Calcutta, Calcutta, India.
2006	**M.S.** in Physiology University of Calcutta, Calcutta, India.
2016	**Ph.D.** in Microbiology & Immunology Indiana University, Indianapolis, IN, USA.

Honors

2015- American Society of Hematology Abstract Achievement Award.
2014- American Society of Hematology Abstract Achievement Award.
2013- Midwest Blood Club Oral Presentation Award.
2008- Indiana University School of Medicine Travel Fellowship.

Teaching Experience

Teaching Assistant for Undergraduate Microbiology Laboratory (J210), Fall 2011.
Indiana University, Indianapolis, IN, USA

Work Experience

2006-2008:	Project assistant. National Brain Research Centre, India.

Publications

1. **Ghosh J,** Kobayashi M, Ramdas B, Chatterjee A, Ma P, Mali RS, Carlesso N, Liu Y, Plas DR, Chan RJ, Kapur R. S6K1 regulates hematopoietic stem cell self-renewal and leukemia maintenance. **The Journal of Clinical Investigation.** (Accepted)**.**

2. Kapur R, Shi J, **Ghosh J**, Munugalavadla V, Sims E, Martin H, Wei L, Mali RS. **(2016**). ROCK1 via LIM kinase regulates growth, maturation and actin based functions in mast cells. **Oncotarget.** DOI: 10.18632/oncotarget.7851.

3. Chatterjee A, **Ghosh J**, Kapur R. **(2015)**. Mastocytosis: a mutated KIT receptor induced myeloproliferative disorder. **Oncotarget.** 6(21):18250-18264.

4. Chatterjee A, **Ghosh J**, Ramdas B, Mali RS, Martin H, Kobayashi M, Vemula S, Visconte V, Tiu RV, Smith CC, Shah N, Bunting KD, Boswell HS, Liu Y, Chan RJ, Kapur R. **(2014)**. Regulation of Stat5 by FAK and PAK1 in oncogenic FLT3 and KIT driven leukemia. **Cell Reports.** 9(4): 1333-1348.

5. Martin H, Mali RS, Ma P, Chatterjee A, Ramdas B, Sims E, Munugalavadla V, **Ghosh J**, Mattingly RR, Visconte V, Tiu RV, Vlaar CP, Dharmawardhane S, Kapur R. **(2013)**. Pak and Rac GTPases promote oncogenic KIT-induced neoplasms. **The Journal of Clinical Investigation.** 123(10):4449–4463.

6. Mali RS, Ma P, Zeng LF, Martin H, Ramdas B, He Y, Sims E, Nabinger S, **Ghosh J**, Sharma N, Munugalavadla V, Chatterjee A, Li S, Sandusky G, Craig AW, Bunting KD, Feng GS, Chan RJ, Zhang ZY, Kapur R. **(2012)**. Role of SHP2 phosphatase in KIT-induced transformation: identification of SHP2 as a druggable target in diseases involving oncogenic KIT. **Blood.** 120(13):2669-2678.

7. Krishnan S, Mali RS, Ramdas B, Sims E, Ma P, **Ghosh J**, Munugalavadla V, Hanneman P, Beane JD, Kapur R. **(2012)**. p85β regulatory subunit of class IA PI3 kinase negatively regulates mast cell growth, maturation, and leukemogenesis. **Blood.** 119 (17): 3951-3961.

8. Krishnan S, Mali RS, Koehler KR, Vemula S, Chatterjee A, **Ghosh J**, Ramdas B, Ma P, Hashino E, Kapur R. **(2012).** Class I(A) PI3Kinase regulatory subunit, p85α, mediates mast cell development through regulation of growth and survival related genes. **PLoS ONE.** 7(1): e28979. doi:10.1371/journal.pone.0028979.

9. Ma P, Mali RS, Munugalavadla V, Krishnan S, Ramdas B. Sims E, Martin H, **Ghosh J**, Li S, Chan RJ, Krystal G, Craig AW, Takemoto C, Kapur R. **(2011).** The PI3K pathway via micropthalmia transcription factor drives the maturation of mast cells. **Blood.** 118(13): 3459-3469.

10. **Ghosh J**, Swarup V, Saxena A, Das S, Hazra A, Paira P, Banerjee S, Mondal NB, Basu A. **(2008)**. Therapeutic effect of a novel anilidoquinoline derivative- 2-(2-methylquinoline-4ylamino)-N-(2-chlorophenyl)-acetamide in Japanese encephalitis: Correlation with in vitro neuroprotection. **International Journal of Antimicrobial Agents.** 32(4): 349-354.

11. Swarup V, **Ghosh J**[*], Das S, Basu A. **(2008)**. Tumor necrosis factor receptor associated death domain mediated neuronal death contributes to the glial activation and subsequent neuroinflammation in Japanese encephalitis. **Neurochemistry International.** 52(7): 1310-1321. (*****Co First Author).

12. Swarup V, **Ghosh J**[*], Mishra MK, Basu A. **(2008).** Novel strategy for treatment of Japanese encephalitis using Arctigenin, a plant lignan. **Journal of Antimicrobial Chemotherapy.** 61(3): 679-688 (*****Co First Author).

13. Das S, Mishra MK, **Ghosh J**, Basu A. **(2008)**. Japanese encephalitis virus infection induces IL-18 and IL-1 in microglia and astrocytes: Correlation with in vitro cytokine responsiveness of glial cells and subsequent neuronal death. **Journal of Neuroimmunology.** 195: 60-72.

14. Swarup V, **Ghosh J**, Ghosh S, Saxena A, Basu A. **(2007)**. Anti viral and anti inflammatory effect of rosmarinic acid in an experimental murine model of Japanese Encephalitis. **Antimicrobial Agents and Chemotherapy.** 51(9): 3367-3370.

15. Swarup V, **Ghosh J**, Duseja R, Ghosh S, Basu A. **(2007)**. Japanese encephalitis virus infection decrease endogenous IL-10 production: Correlation with microglial activation and neuronal death. **Neuroscience Letters.** 420(2): 144-149

Abstracts

1. **Ghosh J**, Chatterjee A, Ramdas B, Kobayashi M, Ma P, Liu Y, Plas DR, Kapur R. S6K1 regulates self-renewal of leukemia initiating cells and normal hematopoietic stem cells. Oral presentation at the 57th ASH Annual Meeting, Orlando, FL, USA; December 5-8, 2015.

2. **Ghosh J**, Chatterjee A, Kobayashi M, Ramdas B, Ma P, Liu Y, Plas DR, Kapur R. p70 ribosomal protein S6 kinase regulates self-renewal of hematopoietic stem cells and propagation of leukemia by leukemia initiating cells. Oral presentation at the 12th Annual Midwest Blood Club Symposium, French Lick, IN, USA; October 9-11, 2015.

3. **Ghosh J**, Ramdas B, Chatterjee A, Ma P, Kobayashi M, Mali RS, Liu Y, Plas DR, Kapur R. Modulation in the expression of p70S6 kinase impairs the engraftment and self-renewal of hematopoietic stem cells. Oral presentation at the 56th ASH Annual Meeting, San Francisco, CA, USA; December 6-9, 2014.

4. **Ghosh J**, Ramdas B, Chatterjee A, Ma P, Kobayashi M, Mali RS, Liu Y, Plas DR, Kapur R. Modulation in the expression of p70S6 kinase impairs the engraftment and self-renewal of hematopoietic stem cells. Poster presentation at the ISEH 43rd Annual Scientific Meeting, Montréal, Canada; August 21-24, 2014.

5. **Ghosh J**, Ramdas B, Chatterjee A, Ma P, Mali RS, Plas DR, Kapur R. Modulation in the expression of p70S6 kinase impairs the engraftment and self-renewal of hematopoietic stem cells. Oral presentation at the 11th Annual Midwest Blood Club Symposium, Cincinnati, OH, USA; September 19-23, 2013.

6. **Ghosh J**, Ramdas B, Chatterjee A, Ma P, Mali RS, Kapur R. Role of p70s6 kinase in regulation of normal and stress hematopoiesis. 42nd ISEH Annual Scientific Meeting, Vienna, Austria; 2013.